DIPARTIMENTO DI INGEGNERIA PER L'AMBIENTE E IL TERRITORIO E INGEGNERIA CHIMICA
UNIVERSITA' DELLA CALABRIA

Dottorato di Ricerca in Ingegneria Chimica e dei Materiali

CICLO XXVII

Erasmus Mundus Doctorate in Membrane Engineering – EUDIME

in co-supervisione con:

Université Toulouse 3 Paul Sabatier (FRANCE)

KU Leuven (BELGIUM)

TESI

Bio-Hybrid Membrane Process for Food-based Wastewater Valorisation: a pathway to an efficient integrated membrane process design

Settore Scientifico Disciplinare: CHIM/07- Fondamenti Chimici delle Tecnologie

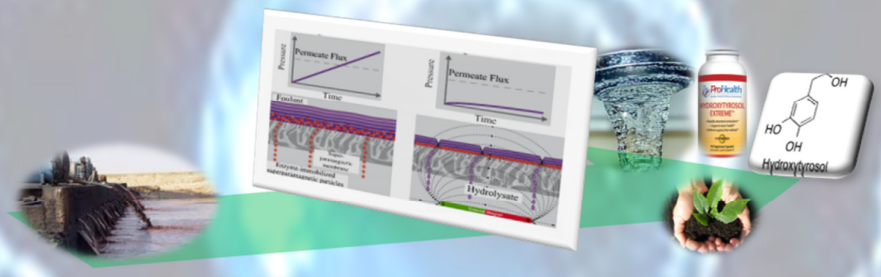

I supervisori

Dr. Pierre Aimar

Dr. Lidietta Giorno

Prof. Dr. Ivo F.J. Vankelecom

Dr.Eng. Efrem Curcio

La dottoranda

Abaynesh Yihdego Gebreyohannes

Il Coordinatore del Dottorato di Ricerca in Ingegneria Chimica e dei Materiali

Ch.mo Prof. Raffaele MOLINARI

ANNO ACCADEMICO 2013-2014

DIPARTIMENTO DI INGEGNERIA PER L'AMBIENTE E IL TERRITORIO E INGEGNERIA CHIMICA
UNIVERSITA' DELLA CALABRIA

Dottorato di Ricerca in Ingegneria Chimica e dei Materiali

CICLO XXVII

Erasmus Mundus Doctorate in Membrane Engineering – EUDIME

in co-supervisione con:

Université Toulouse 3 Paul Sabatier (FRANCE)

KU Leuven (BELGIUM)

TESI

Bio-Hybrid Membrane Process for Food-based Wastewater Valorisation: a pathway to an efficient integrated membrane process design

Settore Scientifico Disciplinare: CHIM/07- Fondamenti Chimici delle Tecnologie

I supervisori

Dr. Pierre Aimar

Dr. Lidietta Giorno

Prof. Dr. Ivo F.J. Vankelecom

Dr.Eng. Efrem Curcio

La dottoranda

Abaynesh Yihdego Gebreyohannes

Il Coordinatore del Dottorato di Ricerca in Ingegneria Chimica e dei Materiali

Ch.mo Prof. Raffaele MOLINARI

ACKNOWLEDGEMENT

The financial support of The Education, Audiovisual and Culture Executive Agency – EACEA/European Commission within the "Erasmus Mundus Doctorate in Membrane Engineering – EUDIME" (ERASMUS MUNDUS Programme 2009-2013, FPA n. 2011-0014, SGA n. 2011-1599) is kindly acknowledged.

CO-AUTHORSHIP STATEMENT

Chapters 1 and 2 entitled “Introduction” and “Vegetation wastewater treatment/valorization and challenges”, respectively, were written by A. Y. Gebreyohannes and Dr. L. Giorno of Institute on Membrane Technology ITM-CNR, Italy with suggestions of Dr. Pierre Aimar and Prof. Ivo Vankelecom.

Chapter 3 entitled “A study on the in-situ enzymatic self-cleansing of microfiltration membrane for valorization of olive mill wastewater” is adapted from Gebreyohannes *et al*., 2013. Ind. Eng & Chem. Res, 2013, 52 (31), pp 10396–10405. Experiments were carried out by A.Y. Gebreyohannes with assistance from R. Mazzei and T. Poerio under the supervision of Dr. Lidietta Giorno and Dr. Eng. Efrem Curcio in the laboratory of Institute on Membrane Technology ITM-CNR and Department of Environmental and Chemical Engineering, University of Calabria (DIATIC-UNICAL), Italy. The publication was written by A.Y. Gebreyohannes, R. Mazzei, E. Curcio, T. Poerio, E. Drioli and L. Giorno.

Chapter 4 entitled “Nanoscale Tuning of Enzyme Localization for Enhanced Reactor Performance in a Novel Magnetic Responsive Biocatalytic Membrane Reactor” is adapted from a manuscript submitted to Journal of Membrane science as Gebreyohannes *et al.* Experiments were performed by A.Y. Gebreyohannes with assistance from M. R. Bilad under the supervision of Prof. Ivo Vankelecome and were carried out in the laboratory of Centrum voor Oppervlaktechemie en Katalyse Dept. M²S, Faculteit Bio ingenieurswetenschappen KU Leuven, Belguim. Magnetic nanoparticle were prepared by Professor Thierry Verbiest at the laboratory of Molecular Imaging and Photonics, Faculty of Bioengineering Sciences, KU Leuven, Belgium and xylanase activity were measured by A.Y. Gebreyohannes and Dr. Emmie Dornez under the supervision of Prof. Christophe M. Courtin at the Laboratory of Food Chemistry and Biochemistry & Leuven Food Science and Nutrition Research Centre (LFoRCe), Faculty of Bioengineering Sciences, KU Leuven, Belgium. Chapter was written by A.Y. Gebreyohannes, Prof. Ivo Vankelecome, Dr. M. R. Bilad, Prof. Thierry Verbiest, Dr. Emmie Dornez, Prof. Christophe Courtin, Dr. Lidietta Giorno and Dr. Efrem Curcio.

Chapter 5 entitled “Effect of operational parameters on the efficiency of magnetic responsive biocatalytic membrane reactor” is adapted from a manuscript under preparation as Gebreyohannes *et al.* Experiments were performed by A.Y. Gebreyohannes under the supervision of Dr. Pierre Aimar University of Paul sabatier and an assistance from Dr. Lidietta Giorno of ITM-CNR, Italy. Experiments were carried out in the laboratory of De Génie Chimique de Toulouse, University of Paula Sabatier III, France. Magnetic nanoparticles were prepared by Professor Thierry Verbiest at the laboratory of Molecular Imaging and Photonics, Faculty of Bioengineering Sciences, KU Leuven, Belgium. Membrane was prepared by A.Y. Gebreyohannes under the supervision of Prof. Ivo Vankelecom at the Laboratory of Centrum voor Oppervlaktechemie en Katalyse Dept. M²S, Faculteit Bio ingenieurswetenschappen KU Leuven, Belguim. Chapter was written by A.Y. Gebreyohannes and Dr. Pierre Aimar.

Chapter 6 entitled “Challenging the chemical stability of magnetic responsive organic-inorganic hybrid membrane during cleaning” is adapted from a manuscript prepared as Gebreyohannes *et al.* Experiments were performed by A.Y. Gebreyohannes under the supervision of Dr. Pierre Aimar and Prof. Christel

Causserand with assistance from Dr. Lidietta Giorno of ITM-CNR, Italy and Prof. Ivo Vankelecom of KU Leuven, Belgium. Experiments were carried out in the laboratory of De Génie Chimique de Toulouse, University of Paula Sabatier III, France. Membrane was prepared by A.Y. Gebreyohannes under the supervision of Prof. Ivo Vankelecom at the Laboratory of Centrum voor Oppervlaktechemie en Katalyse Dept. M²S, Faculteit Bio ingenieurswetenschappen KU Leuven, Belguim. Chapter was written by A.Y. Gebreyohannes, Dr. Pierre Aimar and Prof. Christel Causserand.

Chapter 7 entitled "Treatment of Olive Mill wastewater using Forward Osmosis process" is adapted from a manuscript prepared as Gebreyohannes et al. Experiments were performed by A.Y. Gebreyohannes under the supervision of Dr. Eng. Efrem Curcio and Dr. Lidietta Giorno with assistance from Dr. R. Mazzei and T. Poerio of ITM-CNR, Italy. Experiments were carried out in the laboratory of Institute on Membrane Technology ITM-CNR and Department of Environmental and Chemical Engineering, University of Calabria (DIATIC-UNICAL), Italy. Chapter was written by A.Y. Gebreyohannes, Dr. Eng. Efrem Curcio, Dr. Lidietta Giorno, Dr. R. Mazzei, and Dr. T. Poerio.

Chapter 8 entitled "Comparison between enzyme & chemical cleaning, Summary & Conclusion, New developments and Future research perspective" was written by A. Y. Gebreyohannes and Dr. L. Giorno of Institute on Membrane Technology ITM-CNR, Italy.

Part or all chapters of the thesis are read and edited by Dr. Pierre Aimar, Dr. Lidietta Giorn, Dr. Eng. Efrem Curcio and Prof. Ivo Vankelecome.

Abstract

The food industry is by far the largest potable water consuming industry that releases about 500 million m^3 of wastewater per annum with very high organic loading. Simple treatment of this stream using conventional technologies often fails due to cost factors overriding their pollution abating capacity. Hence, recently the focus has been largely centered on valorization through combinatorial recovery of valuable components and reclaiming good quality water using integrated membrane process. Membrane processes practically cover all existing and needed unit operations that are used in wastewater treatment facilities. They often come with advantages like simplicity, modularity, process or product novelty, improved competitiveness, and environmental friendliness.

Thus, the main focus of this PhD thesis is development of integrated membrane process comprising microfiltration (MF), forward osmosis (FO), ultrafiltration (UF) and nanofiltration (NF) for valorization of food based wastewater within the logic of zero liquid discharge. As a case study, vegetation wastewater coming from olive oil production was taken. Challenges associated with the treatment of vegetation wastewater are: absence of unique hydraulic or organic loadings, presence of biophenolic compounds, sever membrane fouling and periodic release of large volume of wastewater. Especially presence of biophenolic compounds makes the wastewater detrimental to the environment. However, recovering these phytotoxic compounds can also add economic benefit to the simple treatment since they have interesting bioactivities that can be exploited in the food, pharmaceutical and cosmetic industries.

The first part of the experimental work gives special emphasis on the development of biohybrid membranes used to control membrane fouling during MF. Regardless of 99% TSS removal with rough filtration, continuous MF of vegetation wastewater using 0.4 µm polyethelene membrane over 24 h resulted in continuous flux decline. This is due to sever membrane fouling mainly caused by macromolecules like pectins.

To overcome the problem of membrane fouling, biocatalytic membrane reactors with covalently immobilized pectinase were used to develop *self-cleaning* MF membrane. The biocatalytic membrane with pectinase on its surface gave a 50% higher flux compared to its counterpart inert

membrane. This better performance was attributed to simultaneous *in-situ* degradation of foulants and removal of hydrolysis products from reaction site that overcome enzyme product inhibition.

Although the biocatalytic membrane gave a better performance, its fate is disposal once the covalently immobilized enzyme gets deactivated or oversaturated with foulants. To surmount this problem a new class of superparamagnetic biochemical membrane reactor was developed, verified and optimized. This development is novel for its use of superparamagnetic nanoparticles both as support for the immobilized enzyme and as agent to render the membrane magnetized. This reversible immobilization method was designed to facilitate the removal of enzyme during membrane cleaning using an external magnet. Hence PVDF based organic-inorganic (O/I) hybrid membrane was prepared using superparamagnetic nanoparticles (NP^{SP}) as inorganic filler. In parallel, superparamagnetic biocatalytic nanocomposites were prepared by covalently immobilizing pectinase on to the surface of NP^{SP} dispersed in aqueous media. The synergetic magnetic responsiveness of both the O/I hybrid membrane and the biocatalytic particle to an external magnetic field was later on used to physically immobilize the biocatalytic particles on the membrane. This magnetically controlled dynamic layer of biocatalytic particles prevented direct membrane-foulant interaction, allowed *in-situ* degradation, easy magnetic recovery of the enzyme from the surface of the membrane, use of both membrane and immobilized enzyme over multiple cycles and possibility of fresh enzyme make up. The system gave stable performance over broad range of experimental condition: 0.01-3 mg/mL foulant concentration, 1-9 g per m^2 of membrane area bionanocomposites, 5- 45 $L/m^2.h$ flux and different filtration temperatures. Under condition of mass transfer rate prevailing reaction rate, the system gave upto 75% reduction in filtration resistance. After optimization of the different operational parameters, it also revealed no visible loss in enzyme activity or overall system performance, when 0.3 mg/mL pectin solution was continuously filtered for over two weeks.

In addition, the chemical cleaning stability of the O/I hybrid membrane was studied under accelerated ageing and accelerated fouling conditions. The ageing caused change in the physico-chemical characteristics and enhanced fouling propensity of the membrane due to step-by-step degradation of the polymeric coating layer of used NP^{SP}. But 400 ppm NaOCl solution at pH 12 was found compatible; henceforth it was used to clean the membrane.

Second major limitation identified during the treatment of vegetation wastewater is presence of large volume of wastewater that comes in short period following the harvest of olive fruit. To alleviate this problem, FO was investigated to concentrate the wastewater. This process is believed to be less energy demanding, suppose that draw solution does need to be regenerated, and with low foul propensity. By operating at 3.7 molal $MgCl_2$ draw solution and 6 cm/s crossflow velocity, single-step FO resulted in an average flux of 5.2 kg/m^2.h. and 71% volume concentration factor with almost complete retention of all the pollutants. Moreover, the system gave a stable performance over ten days when operated continuously. After FO, both NF and UF were used to fractionate the recovered biophenols from the concentrate streams of FO. Compared to polymeric UF membrane, ceramic NF gave better flux of 27 kg/m^2.h at 200 L/h feed flow rate and 7 bar TMP. Finally, when FO was used as a final polishing step to recover highly concentrated biophenols from permeate of the UF; it gave an average flux of 5 kg/m^2.h and VCF of 64%.

In conclusion, a great success has been made in tackling the two most important challenges of vegetation wastewater valorisation using the concept of biohybridization and FO. The bio-inspired NP^{SP} provides strong evidence that magnetically controlled enzyme immobilization have an immense potential in membrane fouling prevention and paves a potential breakthrough for continuous wastewater filtration. By setting bio-inspired NP^{SP} biocatalytic membrane reactor at the heart, it is possible to successfully use integrated membrane process for continuous valorisation of food based wastewater. In addition to fouling prevention, they open a new horizon for applications in localized biocatalysis to intensify performance in industrial production, processing, environmental remediation or bio-energy generation.

KEYWORDS: vegetation wastewater, bio-hybrid membrane, biocatalytic reactors, biophenols, forward osmosis, fouling, *in-situ* self-cleaning, chemical ageing, magnetically controlled enzyme reversible immobilization

Sommario

L'industria alimentare è la più grande industria che consuma acqua potabile e scarica circa 500 milioni di m^3 di acque all'anno con elevato carico organico. Semplici trattamenti utilizzando tecnologie convenzionali non sono adatti a causa del costo che spesso supera l'efficienza dei trattamenti. Per cui, recentemente lo sforzo è stato focalizzato sulla valorizzazione attraverso la simultanea separazione di componenti di valore e purificazione dell'acqua mediante processi integrati a membrana.

I processi a membrana praticamente coprono tutte le esistenti e necessarie operazioni usate nel trattamento delle acque. Essi spesso hanno il vantaggio di essere semplici, modulari, rappresentano processi e prodotti innovativi, hanno migliore competitività e sono ecosostenibili.

Sulla base di quanto detto, il principale obiettivo della presente tesi di dottorato è stato lo sviluppo di un sistema integrato a membrana che comprende microfiltrazione (MF), "forward osmosi" (FO), ultrafiltrazione (UF) e nanofiltrazione (NF) per la valorizzazione di acque provenienti dall'industria alimentare, nell'ambito della logica dello "zero liquid discharge".

Le acque di vegetazione provenienti dalla produzione di olio d'oliva sono state prese come modello per lo svolgimento dello studio e della ricerca.

Sfide associate con il trattamento delle acque di vegetazione includono: presenza di più componenti organiche, presenze di composti biofenolici, severo sporcamento delle membrane, presenza di grandi quantità di acque di scarico in ristretti periodi dell'anno.

In particolare, la presenza di composti biofenolici rende queste acque nocive per l'ambiente. D'altra parte, recuperare questi composti fitotossici può essere un beneficio economico rispetto al semplice trattamento, poiché essi hanno interessanti bioattività che possono essere impiegate nell'industria alimentare, farmaceutica e cosmetica.

La prima parte del lavoro sperimentale ha dato speciale enfasi allo sviluppo di membrane bioibride usate per il controllo del "fouling" durante la microfiltrazione. Nonostante la rimozione del 99% dei solidi sospesi totali (TSS) mediante una filtrazione grossolana, le acque di vegetazione sottoposte a microfiltrazione utilizzando membrane in polietilene con pori da 0,4 μm hanno causato un declino severo del flusso in 24 ore di operazione. Questo è dovuto a sporcamento principalmente causato da pectine.

Per superare il problema dello sporcamento è stato sviluppato un reattore con membrane biocatalitiche contenenti pectinasi immobilizzata, per fornire proprietà autopulenti alle membrane da MF. Il reattore biocatalitico a membrane contenente pectinasi sulla superficie ha promosso un miglioramento del 50% del flusso di permeato rispetto alla membrana da MF inerte (senza enzima immbilizzato).

Questa migliore efficienza è da attribuire alla simultanea degradazione in situ delle pectine, a mano a mano che si depositano sulla membrana ed alla rimozione dei prodotti di idrolisi dall'ambiente di reazione, che evita l'inibizione dell'enzima.

Sebbene il reattore biocatalitico abbia fornito una migliore performance del processo, il suo destino, una volta che la membrana si sarà prima o poi sporcata, sarà la dismissione.

Per evitare questo problema, è stata sviluppata una nuova classe di reattori biochimici a membrana con proprietà superparamagnetiche. Il processo è stato anche sperimentato ed ottimizzato. Questo sviluppo è innovativo per l'uso di nanoparticelle superparamagnetiche sia come supporto per l'immobilizzazione dell'enzima sia per rendere le membrane magnetiche.

È stato quindi progettato un metodo di immobilizzazione reversibile, usando un magnete esterno per facilitare l'allontanamento dell'enzima dalla membrana quando è necessario sottoporre la membrana a lavaggio con reagenti chimici aggressivi, che altrimenti denaturebbero l'enzima. Quinidi, sono state preparate membrane organiche/inorganiche (O/I) in PVDF contenenti nanoparticelle superparamagnetiche (NP^{sp}) legando covalentemente la pectinasi sulla superficie di NP^{sp} disperse in fase acquosa. La risposta magnetica sinergica di entrambe membrane O/I ibrida e nanoparticelle biocatalitiche al campo magnetico esterno è stata utilizzata per immobilizzare le nanoparticelle biocatalitiche sulla membrana.

Questo strato dinamico di nanoparticelle biocatalitiche controllato da un campo magnetico consente

i. di prevenire il contatto diretto tra foulant e membrana;
ii. la degradazione in situ del foulant;
iii. il facile recupero dell'enzima dalla superficie della membrana;
iv. l'uso di entrambi membrana ed enzima per cicli multipli. Il sistema ha mostrato performance stabile nell'arco di un ampio range di condizioni sperimentali: 0,01 - 3

mg/ml concentrazione del foulant 1 - 9 grammi di nanobiocompositi per m^2 di area di membrana, 5-45 L/hm^2 di flusso e varie temperature.

In condizioni di trasporto di massa maggiore della velocità di reazione, il sistema ha promosso fino al 75% di riduzione della resistenza idraulica durante la filtrazione.

A seguito della ottimizzazione di diversi parametri operativi, non si è osservata perdita dell'attività dell'enzima o in generale perdita di performance del sistema complessivo durante la filtrazione di pectine alla concentrazione di 0,3 mg/ml per due settimane.

Inoltre, è stata studiata la stabilità della membrana O/I a reagenti di lavaggio chimici, in condizioni di invecchiamento e di fouling accelerato. L'invecchiamento causa cambiamenti nelle caratteristiche chimico fisiche ed aumenta la propensione al fouling delle membrane a causa di degradazioni stadio dopo stadio del coating polimerico delle NP^{sp}. Le condizioni di lavaggio compatibili sono risultate: soluzioni di 400 ppm Na OCl a pH 12.

Il secondo maggiore limite identificato durante il trattamento di acque di vegetazione è la presenza di grandi volumi in un breve periodo, legati alla stagionalità della produzione dell'olio d'oliva.

Per alleviare questo problema, è stato investigato l'impiego di FO per concentrare le acque di scarto. Questo processo è considerato richiedere poca energia supposto che la soluzione di "drenaggio" non necessiti di essere rigenerata e le membrane abbiano bassa propensità al fouling.

In un unico step di FO è stato raggiunto un flusso medio pari a 5.2 kg/m^2h con un fattore di concentrazione del feed del 71% ed una quasi completa ritenzione degli inquinanti, utilizzando una soluzione madre di $MgCl_2$ con concentrazione molale di 3.7 e velocità di alimentazione di 6 cm/s. Le prestazioni del sistema sono state stabili per oltre 10 giorni di operazione in continuo.

Al processo di FO, sono state seguite operazioni di NF e UF al fine di ottenere il frazionamento dei polifenoli. Confrontandola con quella polimerica da UF, la membrana ceramica da NF ha dato un flusso di permeato pari a 27 kg/hm^2 utilizzando una portata di alimentazione di 200 L/h e una pressione transmembrana di 7 bar, ottenendo così il miglior risultato.

Nel caso in cui la FO è stata usata come step finale per concentrare il permeato proveniente dalla UF, è stato ottenuto un flusso pari a 5 kg/hm^2 con VCF del 64%.

In conclusione, un importante risultato è stato ottenuto attraverso bioibridazione e la FO che rappresentano le due più importanti sfide nella valorizzazione delle acque di vegetazione. La bioinspired NP^{SP} fornisce forti evidenze che l'immobilizzazione di enzimi magneticamente controllata ha un enorme potenziale nella prevenzione dello sporcamento delle membrane e fornisce una potenziale svolta per la filtrazione in continuo di acque reflue.
Una volta ottimizzato, il reattore biocatalitico a membrana (bioinspired NP^{SP}) può essere impiegato con successo in un processo integrato per valorizzare i reflui agroalimentari. Oltre alla prevenzione del fouling, i reattori biocatalitici a membrana possono essere applicati nella biocatalisi per intensificare le prestazioni nella produzione industriale, nel processamento, nella bonifica ambientale o nella generazione di bio-energia.

Parole chiavi: acque di vegetazione, membrane bio-ibride, reattore biocatalitico, biofenoli, forward osmosi, fouling, membrane autopulenti, invecchiamento chimico, immobilizzazione enzimatica reversibile controllata magneticamente

Résumé

L'industrie alimentaire est de loin l'industrie la plus grande consommatrice d'eau potable et elle rejette environ 500 millions de m^3 d'eaux usées par an contenant une charge organique très élevée. Un simple traitement de ce flux par des technologies conventionnelles échoue souvent en raison de facteurs de coûts. Aussi, récemment, l'accent a été largement mis sur la valorisation de ces effluents par récupération des éléments d'intérêt et la production d'eau de bonne qualité en utilisant des procédés à membrane intégrés. Les procédés membranaires couvrent pratiquement toutes les opérations unitaires utiles et nécessaires qui sont utilisés dans les usines de traitement des eaux usées. Ils apportent souvent des avantages comme la simplicité, la modularité, le caractère innovant, la compétitivité et le respect de l'environnement.

Ainsi, l'objectif principal de cette thèse est le développement d'un procédé à membrane intégré comprenant microfiltration (MF), osmose directe (FO), ultrafiltration (UF) et nanofiltration (NF) pour la valorisation des eaux usées d'origine agro-alimentaire dans une logique de « zéro effluent liquide ». Nous avons pris les eaux de végétation provenant de la production d'huile d'olive comme support d'étude. Les défis associés au traitement des eaux usées de végétation sont: la variabilité des charges hydrauliques ou organiques, la présence de composés bio phénoliques, le colmatage des membranes et le rejet périodique de grands volumes d'eaux usées. En particulier, la présence de composés bio phénoliques rend ces eaux usées nocives pour l'environnement. Toutefois, la récupération de ces composés phytotoxiques peut également apporter une valeur ajoutée, car ils ont des activités biologiques intéressantes qui peuvent être exploitées dans les industries cosmétique, alimentaire et pharmaceutique.

La première partie du travail expérimental porte en particulier sur le développement de membranes biohybrides utilisées pour contrôler le colmatage des membranes de MF. Malgré l'élimination de 99% des matières solides en suspension par une pré-filtration grossière, une diminution du flux est observée pendant plus de 24 h lors de la MF d'eaux de végétation sur membranes de polyéthylène 0,4 µm. Cela est dû à un colmatage sévère des membranes, principalement causé par des macromolécules comme les pectines.

Pour surmonter le problème du colmatage des membranes, des réacteurs à membrane biocatalytiques avec pectinase immobilisée de manière covalente ont été utilisés pour obtenir un effet auto-nettoyant. Cette membrane biocatalytique a un flux supérieur de 50% par rapport à son homologue non modifiée. Cette meilleure performance est attribuée à la dégradation simultanée in situ de dépôts et l'élimination des produits d'hydrolyse ce qui permet de réduire l'inhibition de l'enzyme.

Bien que la membrane biocatalytique ait donné de meilleurs résultats, son usage devient impossible une fois que l'enzyme immobilisé est désactivé ou couvert par un dépôt. Pour surmonter ce problème, une nouvelle classe de réacteur à membrane superparamagnétiques a été développée, mise au point et optimisée. Ce développement est innovant par l'utilisation de nanoparticules superparamagnétiques à la fois comme support de l'enzyme et comme agent conférant à la membrane des propriétés magnétiques. Le procédé d'immobilisation réversible a été conçu pour faciliter le déplacement de l'enzyme au cours du nettoyage de la membrane au moyen d'un aimant externe. Une membrane hybride donc à base de PVDF organique/inorganique (O / I) a été préparée en utilisant des nanoparticules superparamagnétiques (NP^{SP}) comme charge inorganique. En parallèle, les nanocomposites biocatalytiques superparamagnétiques ont été préparés par immobilisation covalente de la pectinase sur la surface de NP^{SP} dispersées dans des milieux aqueux. La réponse de la membrane hybride et des particules biocatalytiques grâce à un champ magnétique extérieur a été plus tard utilisée pour immobiliser physiquement les particules biocatalytiques sur la membrane. Cette couche dynamique de particules biocatalytiques commandée magnétiquement empêche les interactions directes agent colmatant-membrane, permet la dégradation in situ de protéines, la récupération magnétique aisée de l'enzyme et la ré utilisation de la membrane et de l'enzyme sur de multiples cycles. Le système a donné des performances stables sur une large gamme de conditions expérimentales: 0,01-3 mg de pectine / mL, 1-9 g de bionanocomposites /m^2 de membrane, pour des flux imposés de 5 à 45 L / m^2.h et des températures de filtration différentes. Lorsque la réaction enzymatique est plus rapide que le dépôt de matière par convection sur la membrane, on obtient une réduction de 75% de la résistance à la filtration. Après l'optimisation des différents paramètres de fonctionnement, on n'observe aucune perte de l'activité enzymatique ou de la performance globale du système traitant une solution de pectine à 0,3 mg/ mL en continu pendant plus de deux semaines.

En outre, la stabilité chimique de la membrane hybride a été étudiée sous conditions de vieillissement accéléré et en conditions de colmatage. Le vieillissement induit modifie les caractéristiques physico-chimiques et augmente la propension de la membrane à l'encrassement à la suite de la dégradation progressive de la couche de revêtement polymère utilisé sur les NP^{SP}. Cependant une solution de NaOCl 400 ppm à pH 12 a été jugée compatible avec un objectif de maintien des propriétés de la membrane et est désormais utilisée pour nettoyer la membrane.

Le deuxième obstacle majeur identifié lors du traitement des eaux de végétation est le rejet de grands volumes d'eaux usées sur de courtes périodes suivant la récolte des olives. Pour atténuer ce problème, la FO a été étudiée pour concentrer les eaux usées. Ce processus est censé être moins consommateur d'énergie, en supposant que la solution d'extraction n'a pas besoin d'être régénérée, et présenter une faible propension au colmatage. En fonctionnant à 3,7 molaire en $MgCl_2$ pour extraire la solution et à une vitesse tangentielle de 6 cm/s en une seule étape la FO a produit un flux moyen de 5,2 kg/m^2.h. et un facteur de concentration volumique de 71% avec une rétention presque totale de tous les polluants. En outre, le système a donné une performance stable pendant dix jours lorsqu'il est opéré en continu. Après la FO, tant la NF que l'UF ont été utilisées pour fractionner les biophénols récupérés dans le concentrat de FO. Une membrane en céramique de NF a donné une flux plus élevé qu'une membrane UF en polymère, à 27 L/m^2.h pour un débit d'alimentation de 200 L/h et 7 bars de pression transmembranaire (TMP). Enfin, lorsque la FO a été utilisée comme une étape de polissage final pour récupérer les biophénols très concentrés à partir du perméat d'UF; nous avons obtenu un flux moyen de 5 L/m^2.h et un facteur de concentration volumique de 64%.

En conclusion, de très bons résultats ont été obtenus dans la lutte contre les deux défis les plus importants de la valorisation des eaux de végétation en utilisant le concept de biohybridation et la FO. Les nanoparticules superparamagnétiques (NP^{SP}) bio-inspirées fournissent des preuves solides que le contrôle magnétique de l'immobilisation d'enzymes possède un immense potentiel dans la prévention du colmatage des membranes et ouvre une voie potentielle pour la filtration des eaux usées en continu. En fixant des NP^{SP} bio-inspirée au cœur d'un réacteur à membrane biocatalytique, il est possible de mettre en œuvre avec succès un procédé à membrane intégré pour la valorisation en continu d'eaux usées issues de l'industrie alimentaire. En plus de la prévention du colmatage, il ouvre un nouvel horizon à des applications de la biocatalyse pour

intensifier la performance de procédés industriels, la dépollution de l'environnement ou la production de bio-énergie.

Samenvatting

De voedingsindustrie is veruit de sector met het hoogste verbruik aan drinkbaar water, met een jaarlijkse productie van ongeveer 500 miljoen m³ afvalwater met een hoge organische belasting. Een eenvoudige behandeling van deze afvalstroom met behulp van conventionele technieken faalt dikwijks vanwege de kosten. Omwille van deze reden wordt tegenwoordig de klemtoon gelegd op valorisatie van de afvalstroom door middel van combinatoriële herwinning van kostbare componenten en de productie van water van goede kwaliteit, door gebruik te maken van geïntegreerde membraanprocessen. Membraanprocessen omvatten ongeveer alle bestaande eenheidsoperaties die gebruikt worden in afvalwaterzuiveringsinstallaties en gaan gepaard met voordelen als eenvoud, modulaire opbouw en een innoverend, competitief en milieuvriendelijk karakter.

Omwille hiervan ligt de klemtoon in deze doctoraatsthesis op de ontwikkeling van een geïntegreerd membraanproces met het oog op een gesloten waterketen, bestaande uit microfilatratie (MF), *forward osmosis* (FO), ultrafiltratie (UF) en nanofiltratie (NF). Het afvalwater dat hier werd geselecteerd is afkomstig van olijfolieproductie. De uitdagingen gepaard met dit afvalwater zijn: de afwezigheid van eenduidige organische belading, de aanwezigheid van biologische fenol-componenten, ernstige membraanvervuiling en de periodische vrijgave van grote volumes afvalwater. Voornamelijk de aanwezigheid van de biologische fenol-componenten is nadelig voor het milieu. Echter, het herwinnen van deze fytotoxische componenten, kan een economische meerwaarde betekenen omwille van toepassingen binnen de voedingsindustrie, evenals de farmaceutische en kosmetische sector.

In het eerste deel van het experimenteel werk lag de klemtoon voornamelijk op de ontwikkeling van biohybride membranen om membraanvervuiling tegen te gaan tijdens MF. Desalniettemin een TSS verwijdering van 99% door middel van een ruwe filtratie, werd tijdens een continue MF van het plantaardig afvalwater met behulp van een 0.4 µm polyethyleen membraan een continue daling vastgesteld van de waterflux gedurende 24u. De oorzaak van deze daling ligt bij de membraanvervuiling veroorzaakt door macromolecules als pectines.

Om dit probleem van membraanvervuiling te overwinnen werden zelfreinigende MF membranen ontwikkeld door middel van biocatalytische membraanreactoren met covalent gebonden

pectinase. Het biocatalytisch membraan met pectinase aan het oppervlak gaf een 50% hogere flux in vergelijking met het ongemodifieerd membraan. Deze verhoogde performantie werd toegekend aan de *in-situ* afbraak van afgezette componenten en de afvoer van de gehydrolyseerde producten, weg van de reactiesites en zodanig productinhibitie voorkomt.

Hoewel het biocatalytisch membraan een betere performantie gaf, wordt het gebruik hiervan onmogelijk eenmaal het covalent geïmmobiliseerde enzym gedesactiveerd wordt of oververzadigd geraakt aan vervuilende componenten. Om dit probleem te overkomen werd een nieuwe klasse van superparamagnetische, biochemische membraanreactoren ontwikkeld, gecontroleerd en geoptimaliseerd. Deze ontwikkeling is innoverend omwille van het gebruik van superparamagnetische nanopartikels als substraat en als magnetiserend agens van het membraan. De omkeerbare immobilisatiemethode werd ontworpen om de verwijdering van het enzym te vergemakkelijken tijdens de reiniging van het membraan, door gebruik te maken van een externe magneet. Hiervoor werd een organisch-anorganisch (O/A) hybride membraan gesynthetiseerd met superparamagnetische nanopartikels (NPSP) als anorganische vuller. Gelijktijdig werden superparamagnetische biocatalytische nanocomposieten ontwikkeld door pectinase covalent te immobiliseren aan het oppervlak van deze NPSP, gedispergeerd in waterig midden. Het synergetisch magnetisch reactievermogen van zowel de O/A hybride membranen en de biocatalytische partikels op een extern magnetisch veld, werd vervolgens gebruikt om de biocatalytische partikels fysisch te immobiliseren op het membraan. Deze magnetisch gecontroleerde, dynamische laag van biocatalytische partikels voorkwam directe membraan-contaminant interactie, liet *in-situ* afbraak toe, als ook een gemakkelijke recuperatie van het enzym uit het membraan, het gebruik van zowel membraan als geïmmobiliseerd enzym gedurende meerdere cycli en de mogelijkheid nieuw enzym toe te voegen. Het systeem gaf een stabiele performantie over een waaier aan experimentele condities: 0.01-3 mg/mL aan contiminant, 1-9 g bionanocomposieten per m² membraanoppervlak, flux van 5-45 L/m².h en verschillende temperaturen tijdens filtratie. Onder massatransport limiterende condities gaf dit systeem een tot 75% lagere filtratieweerstand. Na een optimalisatie van de verschillende operationele parameters, bleek er zich geen verlies voor te doen van enzymactiviteit of systeemperformantie tijdens een twee weken durende continue filtratietest van een 0.3 mg/mL pectine oplossing.

Bijkomend werd de stabiliteit nagegaan ten opzichte van de chemische reiniging van het O/A hybride membraan onder versnelde verouderings- en vervuilingscondities. De veroudering bracht een verandering teweeg binnen de fysico-chemische karakteristieken en een versterkte vervuilingsgevoeligheid van het membraan door de systematische afbraak van de polymeerlaag rond de NPSP. Echter, een 400 ppm NaOCl oplossing met pH 12 was compatiebel en werd als dusdanig gebruikt voor de reiniging van het membraan.

Een tweede groot probleem bij de behandeling van plantaardig afvalwater is het grote volume aan afvalwater dat op een korte periode geproduceerd wordt, volgend op de olijfoogst. Om dit probleem te stillen, werd FO onderzocht om het afvalwater op te concentreren. Dit proces wordt beschouwd als minder energie-intensief, in de veronderstelling dat de extractie-oplossing niet moet worden gerecupereerd en een lage vervuilingstendens bezit. Het gebruik van een éénstaps FO proces met een 3.7 molaal $MgCl_2$ extractie-oplossing en een tegenstroom-snelheid van 6 cm/s, resulteerde in een gemiddelde flux van 5.2 kg/m².h en een opconcentratie van 71% met een quasi gehele retentie van alle polluenten. Dit systeem vertoonde een stabiele performantie gedurende 10 dagen in continue modus. Na FO werden vervolgens NF en UF gebruikt om de biologische fenolen te recupereren uit de concentraatstroom van de FO stap. In vergelijking met een polymerisch UF membraan, gaf een keramisch NF membraan een betere flux, namelijk 27 kg/m².h bij een debiet van 200 L/h en een transmembranaire druk van 7 bar. Tot slot, het gebruik van FO als laatste stap voor de recuperatie van biofenolen uit het UF permeaat, gaf een gemiddelde flux van 5 kg/m².h en een opconcentratie van 64%.

Als algemene conclusie kan worden vastgesteld dat de twee grootste uitdagingen met betrekking tot de valorisering van plantaardig afvalwater succesvol werden aangepakt met behulp van het concept van biohybridisatie en FO. De biologisch geïnspireerde NPSP tonen aan dat magnetisch gecontrolleerde enzym-immobilisatie een immens potentieel bezit voor het voorkomen van membraanvervuiling en een potentiële doorbraak vertoont bij de continue filtratie van afvalwater. Door de biologisch-geïnspireerde NPSP biocatalytische membraanreactor in de kern te plaatsen, is een succesvol gebruik van een geïntegreerd membraanproces voor de continue valorisering van voedings-gebaseerd afvalwater mogelijk. Bovenop de preventie van membraanvervuiling, openen deze systemen de deur naar nieuwe toepassingen binnen de

biocatalyse om de performantie te versterken van industriële productie en verwerking, milieusanering en bio-energie productie.

Acknowledgments

First and foremost, I wish to thank the Almighty God for granting me the divine insight, grace and wisdom to accomplish this work.

I would like to express my appreciation to all my supervisors Dr. Lidietta Giorno, Dr. Eng. Efrem Curcio, Prof. dr. Ivo Vankelecom and Dr. Pierre Aimar for the enormous guidance and encouragement in general.

My most sincere exaltation goes to Dr. Lidietta Giorno for the kind gesture and unreserved support academically and beyond it. Her constructive criticism and optimism have been the source of inspiration for my work. She was always there to calm me down during the anxious moments. I have been benefited from her rich knowledge and experience in research.

My sincere appreciation is also extended to Dr.Eng. Efrem Curcio for the warm welcome and unreserved support with all the administration that paved a smooth way to the start of the PhD and for the kind assistance and contribution throughout this research. I learn a lot from him.

I would like to express my deep gratitude to Prof. dr. Ivo Vankelecom for the gear changing research ideas. His critical way of enlightening guidance and encouragements as well as occasional discouragement changed me to think critically and try new ways.

My sincere gratitude is extended to Dr. Pierre Aimar for the humble gesture, teaching without judging and unreserved support academically and morally during my mobility stay at Toulouse and afterwards. The meetings and discussions I had with him were the extra energy to move forward. The sense of responsibility he showed me as a supervisor was very unique and I enjoyed very much his humble and critical approach of commenting on all parts of my work.

I would also like to thank Prof. Enrico Drioli for the organization of the program and for his guidance in the beginning of my PhD project.

I am greatly indebted to Dr. Rosalinda Mazzei for shaping the start of my PhD path and for all the cooperations during my research work at ITM-CNR.

I am also grateful to Dr. Teresa Poerio for her unreserved technical support during the experimental work at ITM-CNR.

I am also thankful to Dr. Emmie Dornez, Prof. Christophe Courtin and Prof. Thiery Verbiest who helped in providing materials and developing the work at KU Leuven.

I also extend my sincere appreciation to Prof. Christel Causserand of University of Paul Sabatier for the interesting discussion we had and for the critical advices particularly during my work on membrane ageing

I wish to express my deep sense of gratitude to all collogues at ITM-CNR, KU Leuven and University of Paul Sabatier and for the smooth working environments at the respective labs.

I would also like to express my heartfelt thanks to all EUDIME students for the wonderful team spirit.

My mom is the beginning of all my inspiration for all my successes, Emayiye thank you for your constant Love and wisdom which I would cherish all my life. All my families were by my side during all my way, I was enjoying their blessings constantly. And hence I am thankful to my Fathers, my sisters, brothers and family members.

I have been the luckiest person ever walked on earth to get the closest care, support and love of my husband, which always kept me green. Aymere had it not been for your great love & support, kindness and incredible patience at the times of desperate; I would not have seen these fruits. I have relied so many times on your critical thinking when I got stacked somewhere. I love you Aymu.

Words are not strong enough in offering my thanks to my Indian families Sushumna and Lakshimisha. You were a surprise gift from EUDME. Sushu, you warmly provided me support as a family.

Lastly but not least all the co-authors of my work and all the authors of literatures used in this thesis and all others who on one or another way contributed to this work are greatly appreciated.

Table of contents

List of abbreviation

BCA	Bicichronic acid
BMR	Biocatalytic membrane reactor
BMR^{SP}	Superparamagnetic biocatalytic membrane reactor
BSA	Bovine serum albumin
CF	Cake Filtration
CPB	Complete Pore Blockage
CSTR	Continuously Stirred Tank Reactor
CTA	Cellulose triacetate
DMF	Dimethylfomamide
DS	Draw solution
ECP	External concentration polarization
EDX	Dispersive X-ray spectroscopy
Enz^{SP}	Superparamagnetic immobilized enzymes
GalA	Galacturonic acid
HA	Humic acid
HF	Hollow fiber
ICP	Internal concentration polarization
IPB	Intermediate Pore Blockage
MBR	Membrane Bioreactor
MF	Microfiltration
MFI	Modified Fouling Index
M^{SP}	Superparamagnetic mixed matrix membrane
NP^{SP}	Superparamagnetic nanoparticles
O/I	Organic-inorganic
OMWW	Olive mill wastewater
PE	Polyethylene
$Pect^{SP}$	Superparamagnetic immobilized pectinase
PVDF	Polyvinylidene fluoride
RTD	Residence Time Distribution

SEM	Scanning electron microscopy
SPB	Standard Pore Blockage
STR	Stirred Tank Reactor
TDS	Total Dissolved Solid
TMP	Transmembrane pressure
TS	Total Solid
TSS	Total Suspended Solid
VCF	Volume concentration factor
VRF	Volume Reduction Factor
Xyl^{SP}	Superparamagnetic immobilized xylanase

Chapter 1: General introduction

1.1. Overview

Food processing is one of the main industrial activities that consume huge volume of water at different production line and their supply chains [1]. For example in UK food and drink manufacturing contributed an estimated water consumption of 230 and 190 million m^3 in the year 2007 and 2010 respectively. Eventually 50% of the utilized water comes as wastewater with high organic load that need an end-of pipe treatment [2]. However, as the industrial practice is evolving from treat-or-pay' to 'treat-or-close [3], water and wastewater costs are becoming detrimental economic factor for small and medium-sized food enterprises.

One of the industrial activities that release such huge volume of wastewater is the production of olive oil. The BOD and COD value that this water represents is about 300 times higher than those of a typical municipal wastewater [4]. The effluent is also often rich in valuable compounds such as biophenols at concentration enough to encourage recovery [5-6]. In the last decade successive integration of membrane process in decreasing order of their molecular weight cutoff has gained a great deal of attention to recover these biophenolic compounds. Extraction and valorization of these compounds may lower the polluting load of the effluents and compensate partly for their discarding cost.

In order to obtain a concentrated biophenols, the wastewater's pollution load needs to be minimized first. Since huge parts of the organic pollutants are contained in the suspended solids, a reasonable reduction in the COD by removing suspended solid is important. Therefore, the successive integration usually begins with microfiltration (MF) and/or ultrafiltration (UF) for the removal of the suspended solids. In some cases these processes could be preceded by screening, centrifugation or enzymatic treatment. Since the polyphenols have low molecular weight, they will be recovered in the permeate of MF/UF after removal of the total suspended solids. Subsequently, nanofiltration (NF) and reverse osmosis (RO) will be applied to concentrate and fraction the recovered polyphenols. In some cases membrane contactors like membrane distillation (MD) or vacuum membrane distillation (VMD) can also be used for concentration.

Unfortunately, not a single successfully commercialized integrated membrane process for valorization of vegetation wastewater is available. The two major factors limiting the successful commercialization are:

1. The first and most important problem is severe membrane fouling that survives most of the commonly employed pre-treatment strategies. As a result, the productivity of MF situated at the early stage of the integrated scheme is limited. Moreover fouling modified rejection layer of fouled MF membrane restricts permeation of the biophenols, thereby hampering the target biophenol recovery.
2. The second challenge is seasonal discharge of huge volume of wastewater. This urges for huge onsite storage facilities, transportation to offsite treatment facilities, and huge storage at the offsite treatment facility, huge membrane area and possible oxidative loss of the most important biophenolic compounds.

Inorder to avoid oxidative loss of the high added value compounds that could arise from long term storage, it is necessary to process the wastewater shortly after its release. Presence of fouling driven delay time in processing such huge volume of wastewater makes the oxidative loss inevitable. This may negatively impact the claimed economic benefit through recovery of high added value compounds. Moreover, the periodic pause for cleaning, the water, energy and chemical consumed for cleaning, premature module replacement and ultimate disposal of a large quantity of concentrated solution may incur a considerable cost.

In recent years, the combination of biocatalysis with membrane separations and physically or covalently immobilized enzymes in biocatalytic membrane reactors has become an important avenue in the development fouling resistant membranes. The integrated operation offers potentials in further improving yield and kinetics, compartmentalization of enzymes within the system in their free soluble state, and reducing operating costs and capital investment. It also provides particular advantages in reactions with product inhibition or equilibrium limited conversion [7].

1.2. Thesis outline

In view of the above brief overview, the work presented in this thesis is about study and optimization of individual membrane operations for vegetation wastewater valorization. The

various aspects of the work carried out are summarized in this section while the overall strategy is exhibited in Figure 1. Based on the individual investigation, the ultimate aim is suggesting need based different successive hybridization of the individual membrane operations. The successive integration of MF, UF/NF and FO (Figure 2) is aimed to achieve step-by-step pollutant removal, recovery, fractionation and concentration of biophenols, reclaiming high quality water and a biophenol free sludge for composting or biogasification.

In Chapter 2, relevant literature review on the current state of scientific knowledge and the major missing gaps based on analysis of published articles and survey of patents over the last 20 years together with brief introduction of biochemical membrane reactors is provided. Chapter 3 describes the effect of free and immobilized pectinase to control membrane fouling during MF. After both kinetic and hydrodynamic characterization of reactor, results of filtration using free and covalently immobilized enzyme are presented using vegetation wastewater as feed. In Chapter 4, more technological advancement that is employed to the enzyme immobilization technique is discussed. Results obtained from first time application of superparamagnetism in immobilizing enzyme on membrane are presented. Results from further optimization of different operating parameters for the superparamagnetic enzyme membrane reactor described in chapter 4 are discussed in chapter 5. Chapter 6 deals with comprehensive study of the chemical cleaning stability of superparamagnetic organic/inorganic hybrid membrane. The results of the study on performance evaluation of ageing and cleaning are also presented and discussed in this chapter. In Chapter 7, forward osmosis (FO) process is investigated for concentration of vegetation wastewater. System efficiency is evaluated as standalone, or integrated with MF, where the MF acting as pre-treatment. Both UF and NF are also investigated to treat the FO concentrate with the aim of recovering high added value compounds. FO is also applied as a final polishing step to concentrate UF/NF recovered biophenols. Chapter 8 describes the advantages and disadvantages of the enzymatic cleaning employed from chapter 3 to 5 and chemical cleanings employed in chapter 6. This chapter also includes the summary and conclusion, significance and contributions of the studies comprised in this thesis together with suggestion of possible new integrated membrane flowsheet.

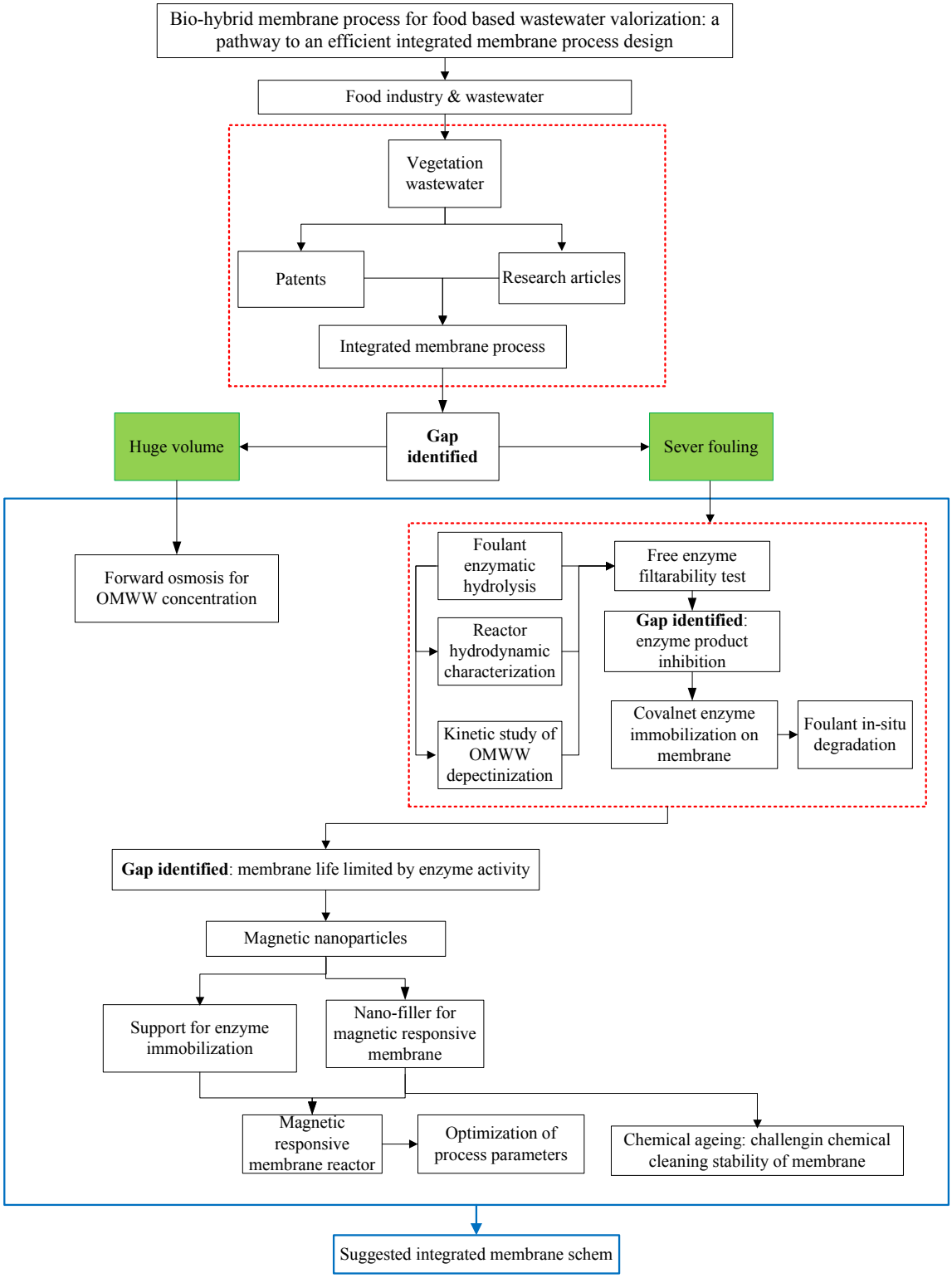

Figure 1: Schematic illustration of the overall strategy of the PhD work carried out.

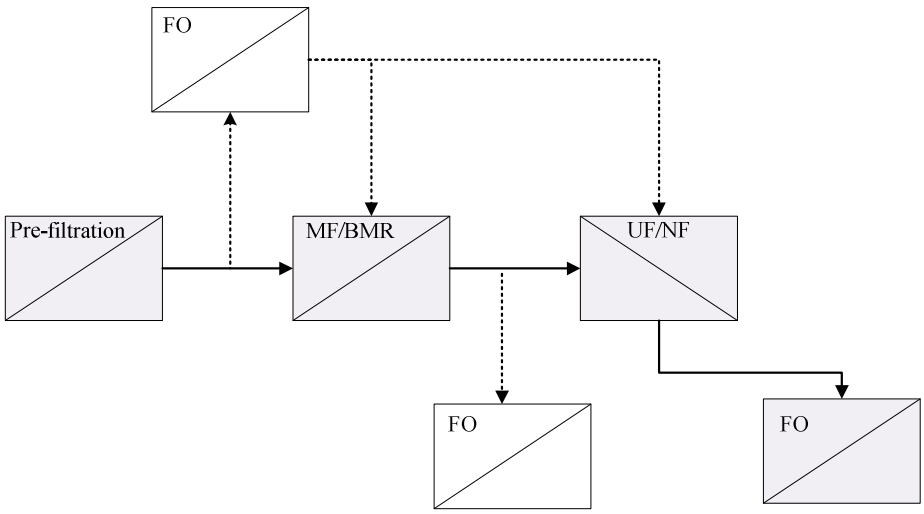

Figure 2: Illustration of successive integration of pre-filtration, microfiltration or biocatalytic MF, UF/NF and FO process for step-by-step pollutant removal and recovery, fractionation and concentration of biophenolic compounds from vegetation wastewater.

1.3. References

[1] C. Blöcher, M. Noronha, L. Fünfrocken, J. Dorda, V. Mavrov, H.D. Janke, H. Chmiel, Recycling of spent process water in the food industry by an integrated process of biological treatment and membrane separation, Desalination, 144 (2002) 143-150.
[2] A. Latif Ahmad, S. Ismail, S. Bhatia, Water recycling from palm oil mill effluent (POME) using membrane technology, Desalination, 157 (2003) 87-95.
[3] G. Daufin, J.P. Escudier, H. Carrère, S. Bérot, L. Fillaudeau, M. Decloux, Recent and Emerging Applications of Membrane Processes in the Food and Dairy Industry, Food and Bioproducts Processing, 79 (2001) 89-102.
[4] H. Dhaouadi, B. Marrot, Olive mill wastewater treatment in a membrane bioreactor: Process feasibility and performances, Chem Eng J, 145 (2008) 225-231.
[5] C.M. Galanakis, E. Tornberg, V. Gekas, Clarification of high-added value products from olive mill wastewater, Journal of Food Engineering, 99 (2010) 190-197.
[6] C.A. Paraskeva, V.G. Papadakis, E. Tsarouchi, D.G. Kanellopoulou, P.G. Koutsoukos, Membrane processing for olive mill wastewater fractionation, Desalination, 213 (2007) 218-229.
[7] L. Giorno, E. Drioli, Biocatalytic membrane reactors: applications and perspectives, Trends in Biotechnology, 18 (2000) 339-349.

Chapter 2: Vegetation wastewater treatment/valorization and challenges

2.1. Abstract

During olive oil extraction, a huge volume of environmentally detrimental wastewater is released. This vegetation wastewater is rich in biophenolic compounds with controversial behavior of phytotoxicity and interesting bioactivities in pharmacology. In this chapter, first a brief overview on the extent of water consumption, wastewater release, and suggested possible wastewater mitigation strategies on the whole food processing industries is provided. Subsequently, an overview of recent developments made in the treatment of vegetation wastewater through analysis of patents and published research works is provided. For better understanding, published research articles and patents related to vegetation wastewater over the last 20 years are classified chronologically and geographically. The paradigm shift from simple detoxification to valorization through analysis of used treatment strategies is illustrated. Special focus is given to the potential of integrated membrane process to treat this wastewater together with recovery of high added value compounds.

Progressive development and a significant rise in the use of integrated membrane process supported by quantitative analysis are also provided. This part is also supported with a number of examples that have investigated different integrated membrane schemes. Two major factors: huge volume of wastewater and severe membrane fouling, have been identified as the two major missing gaps that limited the success of membrane technology in this field. Thorough analysis is also given to the different pre-treatment strategies that have been followed to alleviate these chronic problems.

Finally, based on the detailed analysis of the literature, a clear time line in the main strategies followed to solve environmental pollution due to vegetation wastewater have been plotted. Indication to what a future strategy should follow is also highlighted.

This chapter is based on Review article to be submitted to Journal of Food Chemistry as:
Gebreyohannes A.Y., R. Mazzei and L. Giorno, Vegetation wastewater treatment/valorization and challenges.

2.2. Sensitization of the extent of wastewater problem in the food industry

Although water is a source of life and energy, millions of people worldwide are yet suffering from access to fresh and clean drinking water. Pressure on fresh water source and severe water pollution is also intensified by sudden urbanization, fast industrialization, climate change and population expansion [1]. One of the main sources of freshwater pollution is attributed to generation of huge volume of toxic industrial wastes and dumping of industrial effluents.

The food industry is by far the largest potable water consuming industrial activity per ton of food product [2]. Example breweries consume 4 to 11 m^3 water/m^3 beer produced [3]. To estimate the extent and magnitude of local business and consumers impact on global water cycle, the concept of water footprint has recently been introduced [4-5]. It gives the sum of all consumed water at different stages of production and introduced supply chain for a particular product. The water footprint to produce 1 L of e.g., wine is estimated to be as high as 870 L while for vegetable oils e.g. olive oil it could reach upto 14.5 million L per ton [6]. Water is involved in many steps and unit operations, e.g., soaking, washing, rinsing, fluming, blanching, scalding, heating, pasteurizing, chilling, cooling, steam production, as an ingredient, and for general cleaning, sanitation and disinfection purposes [7].

More than 50% of the utilized water eventually exits as a wastewater with high organic fraction that requires an end-of-pipe treatment [8]. Annually about 500 million m^3 of wastewater is discharged from the food processing industry alone. Of these, Cleaning-in-place (CIP) operations contribute 54-98% of the overall volume of discharged waste streams [9]. Typical amount of wastewater released are: 1.6-2.0 m^3 per m^3 wine produced [10], 25-35 L per ton of cassava processed [11], 3.5 tons of potato-juice per ton potato-starch produced, 5-7.5 tonne per ton of crude palm oil extracted [8] and 24-30 m^3 per batch of processed fruit juice [12]. According to Table 2.1, diary processing shows the largest specific water release while olive oil extraction gave by far the highest chemical oxygen demand (COD).

Table 2.1: List of food processing sectors, amount of wastewater released per ton of product and their polluting capacity in terms of COD. Adapted from [13].

Food processing	**Wastewater (m^3/ton of product)**	**COD (g O_2/L)**
Fruit juice general	3.1	2.5-11.2
Olive mills	5	200.0
Potato starch	1.1	5.4
Frozen carrot	30	5
Beer production	4.2	2.5
Fish industry	10	7
Dairy industry e.g. whey	90	50.0
Meat processing	0.9	8.3

2.2.1. Food industry water management

Approximately 50% of the total water used in the food industry is tap water, groundwater and part of surface water [2, 7]. Acquiring this water needs money and effort such as for pumping, purification and licensing [7, 9]. Eventually, the wastewater will often be a by-product of the main production process that urges treatment to meet discharge limits, hence incurring additional waste handling cost. Therefore, appropriate management of food industry wastewaters should follow two major strategies. The first strategy must be ascribed to reduction at source such as waste minimization, reuse, smart plant design etc. The next strategy must cover the use of best available technologies (BAT) as an end-of-pipe treatment to meet the effluent standards [14]. BAT for food wastewater treatment as its name implies is a technical and organizational measure that minimize overall environmental impact and are available at an acceptable cost [15].

2.2.2. Food wastewater valorization

Effluents resulting from food processing are often rich in valuable compounds including non commercial available high added value molecules at concentration enough to encourage recovery [16-17]. In wine industry product loss to wastewater is worth approximately $2.4–3.4 million per

annum. Extraction and valorization of these compounds may lower the polluting load of the effluents and compensate partly for their management cost. There are already several studies devoted to the recovery of β-carotene and lycopene, natural pigments with known antioxidant property, from by-products of tomato industry [18-19] and carotenoids from carrots, utilization of soybean oil by-products to produce antioxidants, e.g. vitamin E [20] and biogas production [21] or lactic acid [22]. There is also growing demand for functional foods like nutraceuticals that can be easily recovered from food wastewater [23-24].Therefore, utilizing the food wastewater as potentially cheap source of materials ensures sustainability in terms of material recovery, reduced new material consumption and prevention of environmental degradation through waste discharge prevention and new material use limitation.

2.2.3. Water reuse in the food industry

Driven by economic factors, environmental concern and availability of better purification processes, water reuse practices have also become more technically feasible [7]. Depending on the type of food sector, there is a potential of reducing 20 to 50% of fresh water use through schematizing water reuse/recycle strategies in the production line. Possibility of zero level waste discharged through combinatorial high added value product recovery and reclaiming good quality water for food processing effluents have already been demonstrated [25-26]. Considerable advances have already been made in developing better water treatment technologies.

2.2.4. Wastewater treatment technologies

A number of technologies with varying degree of success are available to abate food wastewater problems. These are flocculation-coagulation [27], biological treatment and bioremediation [28-29], filtration, adsorption, evaporation [30] and advanced oxidation processes [31]. However, most of them necessitate considerable financial input and often fail to take material resource efficiency into consideration. Hence, their use in most of the cases is restricted because of cost factors prevailing their treatment capacity [32]. In addition, they often end-up producing concentrated waste (sludge) that requires further handling steps.

2.2.5. Membrane technology in food processing

Membrane can be defined as a permselctive barrier between two phases [33]. The most commonly used membrane operations in wastewater treatment are microfiltration (MF), ultrafiltration (UF), nanofiltration (NF) and reverse osmosis (RO). MF is the oldest known porous membranes process that is used to separate suspended particles with diameters between 0.1 and 10 μm [34]. UF membrane process uses finely porous membrane (1 to 100 nm) to separate water and microsolutes from macromolecules and colloids [35]. Separation in both MF and UF is done mainly based on size exclusion. NF is a pressure-driven separation process that has ionisable membrane surface charge groups. Hence separation efficiency depends on steric (sieving) and charges (Donnan) exclusion [33]. Although NF is closely related to RO, it uses 21% less energy as compared to RO. RO is a unit operation for removing solutes such as dissolved ions from a solution using membranes that are permeable to water but essentially impermeable to salt [33, 36]. Separation in RO is mainly based on solution diffusion mechanism. There is no doubt that a consolidated membrane technology also holds a great potential to play a leading role in the treatment/valorization of food wastewater to limit its environmental impact [24]. It has been widely applied in the food industry since a breakthrough discovery of anisotropic cellulose acetate membranes by Sourirajan and Loeb in 1959. It also is in-line with the requirements of so called process intensification or BAT [15, 24]. As depicted in Table 2.2, it is mostly applied in hybrid with conventional system or successively integrated with one another [37].

Table 2.2: Hybrid membrane processes investigated for the treatment/valorization of streams exiting from different food processing plants.

Food processing plant	Implemented hybrid system	Reference
Tomato wastewater	Biological pre-treatment and NF	[38]
Artichoke wastewaters	UF and NF	[39]
Potato wastewater	Side stream MBR (UF)	[40]
Breweries wastewater		[41]
Winery wastewater	RO and solar photo-Fenton process	[42]
Olive mill wastewater	Enzymatic pre-treatment, centrifugation, MF, UF, NF, RO	[43]
Rapeseed oil mill wastewater	Side stream MBR (UF)	[44]
Palm oil mill wastewater	Anaerobic digestion, aerobic biodegradation, UF and RO	[45]

2.2.6. Integrated membrane process

The increased world-wide competitiveness in production has forced industries to reorganize present process designs and to develop new process designs using alternative technologies [37]. Driven by its simplicity, modularity, process or product novelty, improved competitiveness, and environmental friendliness, membrane technology has shown great potential towards replacing conventional flowsheet in the whole food industry [46-49]. It permits working under milder temperature and pressure while avoiding use of additives or solvents [33]. They practically cover all existing and needed unit operations that are used in process industries [24].

However, membrane processes have a range of inherent limitations e.g, a membrane system designed to treat wastewater may be limited by the water's high concentration of suspended

solids, viscosity, osmotic pressure, and temperature to attain a target quality. Therefore, the optimal separation process in many cases may be a membrane based hybrid processes.

The term hybrid or integrated membrane process is here used to refer integration of membrane with membrane or membrane with conventional unit operations. The integration is supposed to bring performance improvements depending on feed characteristics or desired product quality [50]. So it is a strategy designed to benefit from the synergy among the different unit operations [24]. Example Guo et al, [51] investigated hybridization of flocculation and activated carbon adsorption with MF. The MF benefited from the hybridization, owing to the removal of organics and phosphate by the pre-treatments. Hence, its critical flux was six times more than the critical flux measured for a none-pre-treated feed. Alternatively, integration of a UF unit into fermentation process for recycling a distillery waste enabled a zero discharge for an alcohol fermentation system [25].

The integration or the substitution of some traditional operations with membrane process may also permit the rationalization of improvements in indirect and direct energy consumption. An RO-evaporator hybrid process for example is designed to minimize the energy needed to concentrate corn steep water [52]. The water contains approximately 6 w/w % solids and the target concentration is 50 w/w% using minimal energy. The solution is dehydrated via RO to 15 w/w%. The RO concentrated solids is further concentrated to 50 w/w% solids in the evaporator. It is reported that the energy requirement of the hybrid RO-evaporator process was about one third of the energy requirements of an evaporator alone.

It also comes with reduced capital cost, equipment size, environmental pollution, footprint and ease of fractionation [24]. So it can be claimed as one of the key factors that have contributed to the successful widespread use of membrane [50]. There are a number of membrane-conventional unit hybridizations; with membrane bioreactors (MBR) taking the lead in wastewater treatment. But compared to integration of membrane with conventional processes, the available information regarding membrane-membrane integration is very limited [37]. Nevertheless, as the amount of research and industrial applications of membrane increase, recognition in the importance of tangential flow membrane integration in different field of water treatment is inevitable.

Of the broad food based wastewater, in the following sections special emphasis is given to vegetation wastewater.

2.3. Vegetation wastewater

Vegetation wastewater is one among the numerous food based wastewaters discussed earlier very well known for its significant negative impact on the environment [43]. It is basically the huge volume of foul smelling acidic dark liquid generated during the extraction of olive oil. It is mostly named as olive mill wastewaters (OMWW) [53]. There are three basic olive oil production methodologies: i) press olive oil extraction, ii) two-phase centrifugal olive oil extraction and iii) three-phase centrifugal olive oil extraction [54-55]. Especially the later two methods produce a very huge amount of wastewater compared to the first one [55]. The estimated amount of OMWW produced are about 60-65% and 90-120% of the processed olives for the traditional and continuous press method respectively [56]. Annually there is upto 30 million m^3 wastewater discharge into the environment [53]. These effluents result from the mixture of "vegetation water" coming from the olives and water added during the basic stage of olive process like washing, grinding, beating and the extraction itself. The characteristics and amount of pollutants present in the OMWW vary depending on place, age, season, year of growth, method of extraction, etc [57]. In general, it is composed of water (83-92 wt %), organic matter (4-16 wt %) and minerals (1-2 wt%). Presences of water soluble biophenolic compounds, which are partitioned to water from the olive fruit during the oil extraction, represent the highest polluting capacity [55-56, 58-59].

The continuous illegal damping of OMWW generated by both traditional and the three-phase system to the soil or into a nearby aquatic system for many years have brought about serious environmental problems [57]. The negative environmental and socioeconomic impacts of this industrial activity are more than obvious since a large number of processing facilities are located close to sea resorts and places of high tourist interest [60]. Treatment and disposal of such a huge volume of wastewater is a very critical problem [56, 60].

2.3.1. Present state of scientific knowledge on vegetation wastewater

An environmental law has been enforced for olive producing companies either to treat or eliminate their wastes to reduce the subsequent environmental degradation. In the Mediterranean countries, the most practical means of reducing the OMWW is by evaporation in storage ponds in the open because of the low investment required and the favorable climatic conditions.

However, the disadvantages associated with this method are larger area requirement together with the production of black foul smelling sludge difficult to remove, pollutant infiltration to ground water and insect proliferation [54, 57]. Many researchers have also applied OMWW directly on soil and have tested its beneficial effects related to its high nutrient concentration, especially potassium, and its potential for mobilizing soil ions. But application to soil have also revealed negative effects of OMWW associated with its high mineral salt content and low pH [57]. Especially OMWW is characterized by presence of more than 30 different types of biophenols and related compounds that are phytotoxic with strong antibacterial effects [61-62]. Therefore, excessive application into the soil may pass the toxicity tolerance of soil microorganisms.

In recent years, many other management options have been proposed for the treatment and valorization of OMWW. Most of these methods aim at the reduction of the phytotoxicity in order to reuse it for agricultural purposes [63] or to make the wastewater suitable to be treated in conventional treatment facilities e.g., activated sludge system [53].These includes physico-chemical treatments such as coagulation, precipitation biological treatments [54, 64] or use of advanced oxidation system for the destruction of dissolved organic compounds.

On the other hand, the phytotoxic biophenols have also interesting bioactivities that can be exploited in the food, pharmaceutical or cosmetic industries [54, 61]. The most important phenolic includes tyrosol, hydroxytyrosol (HT) and olueropein [57]. These compounds hardly contribute to the nutritional value of the olive. But they may play an important role in maintaining human health owing to their antioxidant or anti-carcinogenic activities. Hence, there is also a growing research activities towards recovering these biophenolic compounds to benefit from their pharmacologically interesting behaviors [65-66].

So in the following section, detailed discussion about the different treatment methods and strategies investigated so far will be provided. For better understanding, the analysis is based on chronological classification of published research articles and patents over the last 20 years.

2.3.2. Progresses made over the last 20 years in the treatment of vegetation wastewater

Analysis of published research articles over the last 20 years have been made to understand the progress made in the treatment of OMWW. Figure 1 exhibited total number of publications from 1995 to 2014 divided in chronological order (source: http://www.sciencedirect.com). The data

have also been classified into four main categories: simple treatment, biophenol recovery, other valorization and process that involve membrane technology. In the first time slot (1995-2000), 71% of published results are simple treatment, 24% valorization e.g. composting [67-69] with 5% involving membrane technology [70-71] and no polyphenol recovery. Both aerobic and anaerobic bioreactor with pre-treatments involving centrifugation, adsorption and/or settling are the main technologies investigated. Since the polyphenols have strong antibacterial activity, 40% of the studies have focused on developing mechanisms that can reduce the polyphenols content to make the feed water composition suitable for bioremediation. The most commonly utilized physico-chemical treatments for detoxification include enzymatic catalysis [72-73], electrochemical oxidation and mostly ozonation [74-75].

From 2001-2005, again the main focus (75%) remained treating the wastewater with aerobic-anaerobic treatment [76-79]. For example Fountoulakis *et al,* [64] studied the removal of phenolics using the white-rot fungus. Valorization in terms of biogasification and composting [80] reduced to 12% while a 4% activity is observed in polyphenol recovery. The use of membrane technology mainly UF hybridized with centrifugation [81] or UF with UV/H_2O_2 oxidation [82] increased to 9%. The physico-chemical treatments are: electro-coagulation [27, 83], electrochemical oxidation [84], advanced oxidation such as UV/H_2O_2 [82] H_2O_2/UV and O_3/UV [85]. Of these ozonation was the dominantly applied advanced oxidation method. A considerable effort was also observed in trying to acclimatize microorganisms to grow on polyphenols during bioremediation.

From 2006-2011, 136 papers were analyzed in total. Of which 27 focused on different types of valorization mostly composting while 11 are focused on polyphenol recovery solely. So now a considerable diversion from simple detoxification to recovery is observed [86]. Especially from 2009-2011, the no of publication related to phenolics recovery increased significantly [65, 87-89]. In parallel, the share of membrane technology in both simple treatment and valorization increased noticeably [90-92]. Yet the efforts of detoxifying the polyphenols have not stopped. But the technology for detoxification shifted from aerobic-anaerobic acclimatization to advanced oxidation. Electrochemical oxidation [93] photocatalysis [94], Fenton oxidation [95-97], O_3/UV [98] or H_2O_2 [99] are few to mention. But the advanced oxidation utilized in this era was mostly Fenton reaction.

The years 2012-2014 can be called the membrane bloom era covering about 30% of all the treatment strategies. It has been used as standalone comprising from MF to RO including membrane contactors like MD [100] and OD [101] or integrated with each other [102-104]. Out of the 84 papers examined, eight of them were solely focused on polyphenol recovery using different extraction mechanism such as solvent extraction, while 20 of them were used for different types of valorization. Among which 28 have used membrane as stand alone or in hybrid for either recovery or treatment.

Therefore, it is possible to draw a clear time line: evolution from simple remediation to acclimatization of microorganisms to degrade biophenols. Subsequently, a paradigm shift from simple detoxification to recovery of the biophenols. The advanced oxidation also transformed from ozonation to electro-chemical oxidation and later to Fenton led reactions. In addition, a clearly growing habit of use in membrane technology is observed. Especially in the last five years, a significantly rising successive integration of different membrane processes in decreasing order of their molecular weight cut-off for selective recovery, purification, fractionation and concentration of biophenols is observed.

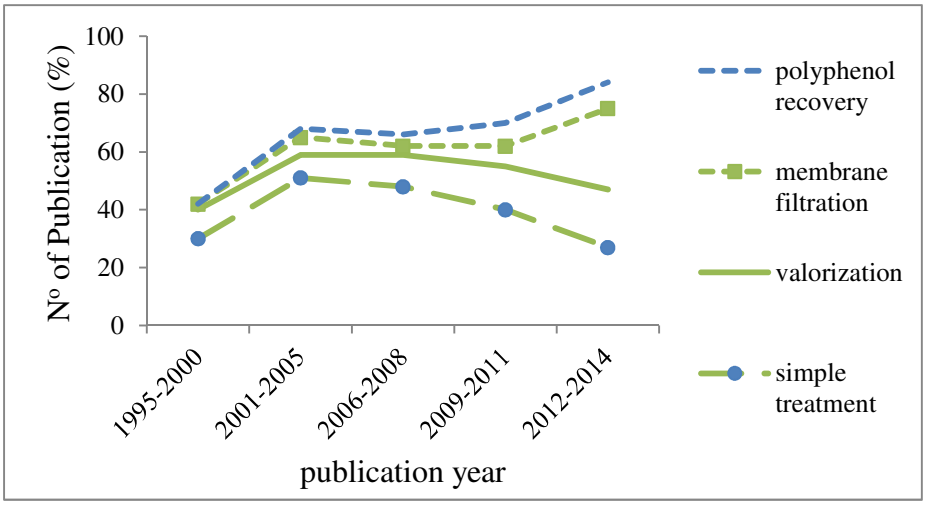

Figure 1: Time line in olive mill wastewater treatment obtained through analysis of published research articles (source: http://www.sciencedirect.com) from 1995 to August 2014.

Innovative works both in the treatment and valorization of vegetation wastewater is also analyzed in terms of patent publication from 1992 to 2013 (source: http://worldwide.espacenet.com.

Table A1 depicts list of OMWW related patents. As shown in Figure 2a, the highest patenting rate is registered from 2006 to 2010 with 40% of them published in 2007. Based on detailed

analysis of the published patents, 54% of them focused at recovery of biophenols particularly hydroxytyrosol (HT) and 5% biogasification (Figure 2b). The majority of them tend to use solvent extraction. But the use of membrane process in both recovery and remediation is also considerable (20%). Patents related to simple detoxification or treatments are dated back to late 90s to early 2000s. But the use of advanced oxidation based on O_3 is also observed in 2009. But the objective of this later detoxification was to make the wastewater suitable for irrigation and the sludge for composting WO2009101455 [105].

Geographical distribution of the patents (Figure 2c) shows that Spain took a lead in valorization followed by Italy. Often, OMWW is thought as a regional problem belonging to the Mediterranean where there is 97% of the world olive oil production. But fair distribution of the patents over the different continents indicates that the problem has a rather global concern.

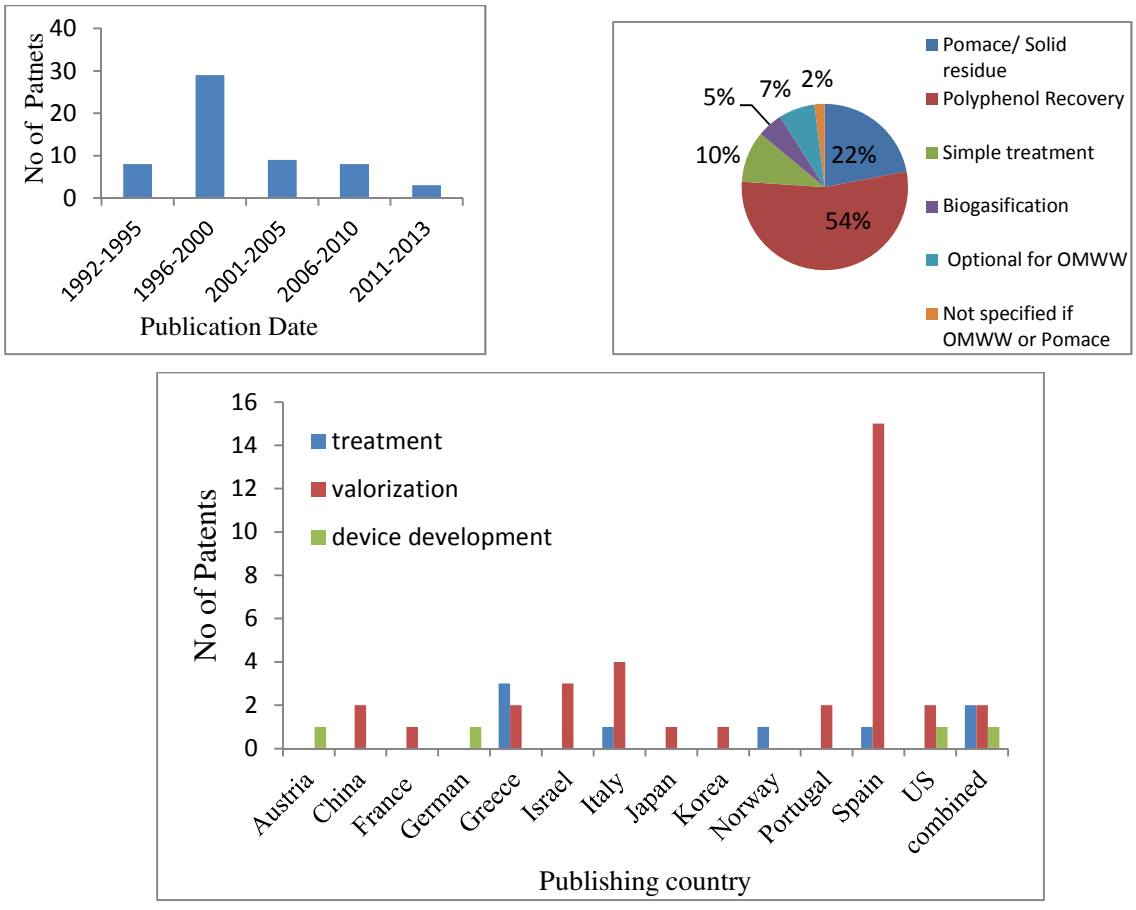

Figure 2: Analysis of patents related to OMW treatment

2.3.3. Integrated membrane process for vegetation wastewater

Careful analysis of both published research articles and innovative patents in the previous section revealed a noticeable rise in the use of membrane technology for OMWW treatment. There already are patents dated back to the 90s and early 2000s developed on the use of membrane techniques for OMWW treatment WO9521136 [106], EP1424122 [107] and WO2004064978 [108]. e.g. a patents released in 1995 comprises a method for purifying OMWW with processes containing: (i) an oxidizing agent; (ii) a coagulant; (iii) an anionic or cationic polyelectrolyte; and (iv) rough filtration followed by UF WO9521136 [106]. There was also a UF OMWW treatment facility installed in Lamezia (Italy), with a nominal capacity of 300 m^3 per day. The plant that started in November 1995, used polymeric (Polysulfone) UF membrane batteries [109].

In the eldest publication treated in this paper, membrane appeared first as a means of fractionating polyphenols to identify which molecular weights were most problematic for bioremediation [70]. Ever since, the number has increased very quickly for both remediation and valorization. Especially during the last five years, the major focus was the successive integration of different membrane operations for the recovery and concentration of biophenols. Table 2.3 lists different successive or hybrid membrane processes investigated/ patented for both treatment and valorization of OMWW.

The successive integration is observed to benefits from step-by-step pollutant removal, fractionation and concentration of the recovered biophenols. For example Garcia-castelo *et al*, [89] have used an integrated membrane system composed of MF, NF as pre-treatment and OD or VMD for concentration of recovered biophenols. A tubular Al_2O_3 MF membrane reduced the total solid from 18 g/kg to 1.6 g/kg while the TOC reduced to 15 g/L from 20 g/L at 0.72 bar and 760 L/h feed flowrate. A subsequent NF process using Nadir N30F PES spiral-wound membrane reduced the TOC further down to 6 g/L at 8 bar and 20°C. The NF permeate with 160 ppm total biophenols is subjected to OD containing a microporous hollow-fibers polypropylene membrane. The OD process achieved a polyphenolic concentration of 493.01 ppm in the OD retentate.

In another cases, a novel method was developed and patented by ENEA and Verdiana Company using tangential flow membrane filtration for selective separation and total recovery of HT, water and organic substances [43]. MF retained all the suspended solids and showed a rejection of total nitrogen and sugars of 40% and minerals 25%. The inventors have also observed an

increased concentration of polyphenols in the permeate of MF (349.18 ppm) than it was in the feed (55.38 ppm) [26]. They have ascribed this lateral increase in the permeate to the rupture and release of agglomerated polypehonols that are attached to organic substances due to mechanical stress during MF. Subsequently, NF and RO are applied to concentrate the obtained polyphenols. The inventors claimed that the MF and UF concentrates, devoid of the polyphenols, can be used as fertilizers or in the production of biogas in anaerobic reactors. Concentrated and purified low molecular weight polyphenols of RO concentrate, is the principal product for food, pharmaceutical or cosmetic industries. About 50–60% of the initial feed volume obtained as RO permeate, is vegetable water suitable e.g., for beverage formulations [26].

Table 2.3: List of hybrid membrane process for treatment/ valorization of OMWW

Hybrid membrane	**Objective**	**Ref.**
Sieving-centrifugation-UF	Treatment	[110]
Acid treatment-cartidge filtration-UF	"	[90]
UF-NF-RO/ UF-RO	"	[62]
WO2004064978	"	[108]
Ceramic MBR with acclimatized biomass	"	[53]
Settling-UF – biological system	"	[109]
UF-NF	"	[111]
OD and osmotic membrane distillation	"	[101]
Centrifugation-UF-NF-RO	"	[91]
UF-NF-RO	"	[103]
Flocculation-UF-NFO_3/H_2O_2 oxidation-RO-evaporation basin (EP20080105026)	"	
Successive 3MF-2 UF -3NF	"	[104]

Micelar formation with Soduim Dodecyl sulfate salt-UF	valorization	[112]
MF-DCMD	“	[113]
Enzyme treatment-centrifugation-MF-UF-NF-RO (WO2005123603)	“	[43]
MF-UF-RO with no centrifugation	“	[26]
4UF-NF	“	[65]
4UF	“	[114]
2UF-NF	“	[102]
Pectinase treatment-MF-UF-RO	“	[115]
MF-NF-OD/ MF-NF-VMD	“	[89]
Screen-press cylinder-MF/UF-RO (EP 1424122)	“	[107]
Extraction-reaction-adsorption -desorption-RO-evaporators (WO2012ES70491)	“	[116]
• Pre-dilution-centrifugation-membrane filtration-adsorption for biophenols recovery • Aerobic and anaerobic treatment for biogas and fertilizer (WO2009IT00246)	“	[117]

2.4. Membrane performance in treating vegetation wastewater

Membrane treatment of OMWW is also highly dependent on concentration polarization and membrane fouling [60]. Concentration polarization is a reversible phenomena caused by increased transport resistance in the boundary layer. Whereas, membrane fouling is an irreversible phenomenon including the effects of surface fouling, adsorption, gel layer formation, pore radius reduction, pore blockage, cake formation, and adhesion of particles on the membrane (Figure 3). The causes of fouling vary depending on the nature of the solute and solute-

membrane interactions. Fouling causes a loss in water flux and quality reduced operating efficiency, lost service time and premature membrane replacement. In addition, fouling limited lower productivity may raise the need for large membrane surface area resulting in higher capital and operating costs [33]. Permeate flux profiles under fouling typically shows an initial stage sudden drop followed by a smoother but continuous decay. A study by Tsagaraki and Lazarides [60] revealed that during the UF of OMWW the permeate flux decreased by 60-65% of its initial value within the first 15-20 minutes. Many authors have also agreed that, fouling during OMWW filtration restricted its lifetime to a single working life cycle. It also makes the process highly expensive owing to repeated operational periodic pause for membrane cleaning. In some cases, even an extensive cleaning may not guarantee full recovery of permeability. For example Garcia-Castello *et al*, [89] cleaned a ceramic MF membrane with 20 g/L NaOH solution at 40°C for 30 minutes followed by rinsing with tap water for another 30 minutes. However, the authors stated that the initial permeate flux decreased due to an irreversible fouling despite the membrane cleaning done among different run. In another study Claudio and the coworkers found MF, situated at the very early stage of the integrated membrane process; as the critical step due to severe membrane fouling. It is worth noting that, fouling modified rejection layer of MF or UF during integrated membrane process may restrict passage of low molecular weight polyphenols interfering with their recovery. Besides, membrane fouling during filtration of OMWW involves more technological difficulties related to the presence of gelling substances, e.g., pectins [118].

Therefore proper implementation of any of the above mentioned hybrid membrane operations, at an industrial scale are strictly limited by lack of either economical or technical feasibility. Particularly, reduction in membrane permselectivity and overall productivity due to fouling is a major bottleneck. The problem of fouling is also augmented by periodic release of huge volume of OMWW in a short time.

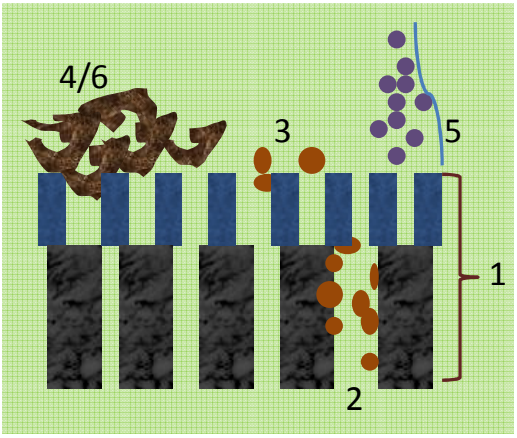

1. Membrane
2. 2. Adsorption/ Scaling
3. Pore blocking/ Plugging
4. Cake deposition/ formation
5. Concentration polarization
6. Bio-fouling:biofilms/ EPS

Figure 3: Illustration of the different types of membrane fouling.

The main parameters affecting fouling in membrane process are feed flow rate, temperature, and transmembrane pressure. Optimizing operating conditions to limit fouling may involve limiting transmembrane pressure, controlling temperature and maintaining a high cross-flow velocity. In addition to operational conditions, the magnitude of membrane fouling is determined by membrane property and feed water characteristics.

2.4.1. Effect of membrane property on process performance

There is no specific membrane that is universally suitable for every fluid stream owing to factors like nature of feed, target product qualities or process design. Thus, fouling by OMWW is also highly dependent on type and characteristics of the membrane such as membrane material, pore size, porosity etc. Cassano *et al,* [114] made a comparative study on the effect of fouling on two polymeric membranes (UF regenerated cellulose and UF PES membranes). Results showed that regenerated cellulose membranes exhibited lower rejections towards phenolic compounds; higher permeate fluxes and lower fouling index compared to PES membranes. In another study, a 0.45 µm ceramic membrane and 500 kDa polymeric membranes are compared [26]. After acid pre-treatment of OMWW to avoid oxidative polyphenol loss, MF of OMWW through 500 kDa polymeric membrane resulted in more than 70% decreased permeate flux shortly after the onset of filtration without even attaining steady state. On the other hand working on ceramic membrane gave a volume concentration ratio of 3 with a steady flux of 50 $L/m^2.h$. Again, the fouling index for polymeric MF (0.0476) was much greater than fouling index of 0.45 µm ceramic MF (0.0017). Moreover, the ceramic membrane showed a 100% recoverable permeability through alternate washings with alkaline and acid solutions (NaOH and HNO_3), at

high concentrations (0.5–1 M) and at high temperatures (50–70°C). In contrast for polymeric MF, washing with alkaline and acid solutions 0.1–0.2 M, was difficult and the membrane resulted in recovery of only 40% of the initial permeability. Nonetheless, the superior 100% permeability recovery attained for ceramic membrane in this study is not a universal truth. In a study conducted by Garcia-Castello *et al* [89], there was a continuous permeability loss among six different runs regardless of a chemical cleaning done with concentrated basic solution among each run while using ceramic membrane. Moreover, for the same membrane material and pore size, different performance could also be inevitable. In the same study mentioned earlier [26], use of a 0.45 µm isoflux ceramic membrane, specially designed to treat food wastewater gave a constant flux of ~ 75 $L/m^2.h$ compared to the 50 $L/m^2.h$ for the normal ceramic membrane. The fouling index for the isoflux ceramic membrane (0.0009) was also much lower.

2.4.2. Pre-treatments during the filtration of vegetation wastewater

Different pre-treatment strategies have been tested to alleviate the problem of fouling during OMWW filtration. Centrifugation [81, 119], screening [62], sieving and centrifugation [110], acid treatment and rough filtration [90] settling of suspended solids [109] and enzymatic treatment [115] are few of them. Tsagaraki and Lazarides [60] observed a rapid flux decline regardless of a 93% removal of total solid content by centrifugation prior to UF. To enhance the performance of direct contact membrane distillation (DCMD), El Abbassi *et a*, [113] removed larger particles through acid cracking by adding concentrated H_2SO_4 until pH 2. This was followed by coagulation/ flocculation with 5 g/L of $FeCl_3$ using flash mixing under magnetic stirring (1200 rpm) during 2 min, followed by 30 min of moderate mixing. As an alternative, MF using pre-ethanol wetted TF200 membrane is also tested. The DCMD permeate fluxes of crude and pre-treated OMWW indicated that MF gave relatively higher flux (7.7 $L/m^2.h$) than coagulation/flocculation (6.9 $L/m^2.h$) or use of crude OMWW as feed (5.6 $L/m^2.h$) [113]. MF also reduced total solid by 30%. The coagulation/flocculation is also mentioned to reduce the total phenols by 20%, in addition to a 23% reduction in total solids.

A pH adjustment to 2 using H_2SO_4 followed by cartridge filtration and a final pH adjustment to 6 using $Ca(OH)_2$ were also applied by Akdemir and Ozer [90] prior to UF. A COD removal efficiency of 63% was reported after only pH adjustment and cartridge filtration. Stable flux during UF is also reported possibly linked to the pre-treatment. However, an important increase

in the COD and TOC retention coefficients took place in the first minutes of the operation. This may be correlated to the presence of foulants that have survived the implemented pre-treatment. Regardless of removal of particles greater than 80 µm with screening, the water permeability decreased drastically when the OMWW was fed into UF process by Paraskeva *at al*, [62]. Attributed to severe fouling, quick reduction of flux to 51% of its initial value for volume reduction value of 3 using regenerated cellulose membrane is also reported by Cassano *et al*, [114]. The authors have stated that the severe fouling occurred regardless of the feed water pre-treatment with MF.

Therefore, the clear message that can be withdrawn from all these examples is the impossibility of preventing fouling or reducing its magnitude by using most of the available traditional pre-treatment strategies.

2.4.3. Feed water characteristics

OMWW is characterized by presence of high organic loading and colloids that can lead to problems during the filtration process. The polluting load is determined by presence of large amount of organic substances (sugars, oil, pectin, tannins, nitrogen substances, polyphenols, polyalcohols, organic acids). The COD ranges between 80 to 210 g/L of O_2 and BOD between 50 and 150 g/L of O_2 [26]. The COD to BOD ratio, indicator for degree of biodegradability, may reach upto 7 indicating the hardly biodegradability of the wastewater [110]. It is also characterized by solid contents as high as 109 g/L [113]. Pectins are natural hydrocolloids found in all higher plants. The water soluble gel-forming pectin mostly ends up in the vegetation water during olive oil extraction. Pectins obtained from OMWW have already shown a very good gelling capacity [120]. Therefore, presence of pectin in OMWW may also impede membrane filtration. The typical concentration of pectin and colloids present in OMWW is up to 0.5 g/L [118].

2.5. Biochemical membrane reactors

In recent year, the investigation of integrated biochemical processes in membrane bioreactor (MBR) gained high popularity in the treatment of wastewater [121-123]. The integrated operation offers potentials in further improving yield and kinetics, compartmentalization of enzymes within the system in their free soluble state, and reducing operating costs and capital

investment. It also provides particular advantages in reactions with product inhibition or equilibrium limited conversion [122]. The combination also helps to achieve process intensification [124]. It opens the channel to continuously operate a system resulting in considerable reduction of the capital cost. The plant size needed for continuous process is two orders of magnitude smaller than that required for the batch process using free enzymes.

The aforementioned pectins that occur in OMWW are explained to have good jelling capacity [120]. Presence of these gel forming macromolecules is the primary cause of severe membrane fouling that occurs during MF of OMWW situated at the onset of the integrated membrane process. The enzymes pectinase are responsible for the hydrolysis of pectin. These enzymes have been extensively studied because of their applications in food technology, e.g., in the extraction and clarification processes during the manufacturing of juice and wine [125-126]. These enzymes have also resulted in a 1.3 fold increased flux compared to free pectinase during clarification of fruit juices[127]. Another study has also shown the possibility of maintaining stable flux for longer period without cleaning when pectinase is immobilized on membrane [128]. The commercial enzyme cocktail used for the manufacture of fruit juices contains three different pectinases: pectinlyase, polygalacturonase and pectinesterase to make pectic complexes soluble to complete the sedimentation and clarification of the juice. Pectinase have also been used to pre-treat OMWW in order to avoid the fouling of the membranes [43]. In addition to fouling reduction, enzymatic treatment of OMWW helps to increase the biophenolic yield since some of the biophenols are bound to pectin [43]. Therefore, OMWW pectin hydrolysis using the enzyme pectinase in biochemical membrane reactors can also be used as a clean biotechnological process to reduce fouling and enhance flux during MF of OMWW.

2.5.1. Biochemical membrane reactor configuration

The biocatalysts can be used either as a free enzyme suspended in the reaction mixture or could be immobilized on the membrane physically or chemically [123]. The choice depends on the properties of the reaction system. For example, bioconversions for which the homogeneous catalyst distribution is particularly important are optimally performed in a reactor with the biocatalyst compartmentalized by the membrane in the reaction vessel. The membrane is used to retain large components, such as the enzyme and the substrate while allowing small molecules (e.g., the reaction product) to pass through. Since enzymes are biological catalysts that are not

consumed in the reactions in which they participate, they may be used repeatedly for as long as they remain active. However, in most applications enzymes are mixed in a solution with substrates and cannot be economically recovered. This single use is obviously uneconomical when the cost of enzymes is considered. Thus, immobilization of enzyme in a biochemical reactor configuration may help to retain them for use over multiple cycles. Immobilized enzyme also allow continuous operation of a reactor which eventually give better reactor stability and productivity, improved product purity and quality, waste reduction and prevent reaction inhibition by products [122]. Moreover in batch reactor both substrate and enzyme have equal residence time. In contrast, in continuous flow reactor configurations, the average substrate residence time within the reactor is far shorter than that of the immobilized enzyme catalyst. Hence for a fixed amount of enzyme, the continuous flow reactor has a better productivity [129]. Numerous methods exist for enzyme immobilization to create bio-hybrid matrices. The principal strategies for enzyme immobilization on MF membrane are chemical grafting or molecular recognition. This may be based on ionic binding, crosslinking or covalent linking. The sites involved in this chemistry are generally carboxylic acid, hydroxyls, amino or quaternary ammonium groups, which are created on the membrane by various methods such as direct chemical surface modification or plasma or UV activation. The reactive sites thus created allow the immobilization of the enzyme by using coupling reagents such as glutaraldehyde.

2.5.2. Mixing and flow pattern

In a continuous flow system, the Residence Time Distribution (RTD) is defined as the probability distribution of time that reactants stay inside the reactor. It is a vital index in understanding the material flow pattern, and is widely used in many industrial processes, such as the continuous manufacturing of chemicals, plastics, polymers, food, catalysts, and pharmaceutical products. In order to achieve satisfactory yield from a specific membrane bioreactor, substrate are designed to stay inside the reactor under specific operating conditions for a specified period of time. This residence time information is usually compared with the time necessary to complete the reaction or process within the same unit operation. If the time required to achieve a desired degree of conversion is longer than the actual residence time the substrate stay in the system, the process cannot provide a complete conversion, and it fails to meet its design requirements. Therefore, the characterization of the RTD in different continuous unit

operations is the first step in the design, improvement, and scale-up of many membrane bioreactors [130].

Early fluid reactor models assumed PFR in a tubular-shape reactor, or complete mixing in CSTR that two extreme RTD profiles in the reactor. But in actual continuous flow systems, experimental RTD profiles lies between the two extremes. To describe the deviation from ideality of the RTD profile, different combinations of CSTR and PFR were introduced in modeling practical cases. CSTR in a series model is one commonly used model [130]:

$$\tau = \frac{NV_i}{F} \quad (1)$$

$$E(\theta) = \frac{NN(\theta)^{N-1}}{N-1}\exp(-N\theta) \quad (2)$$

where τ is the mean residence time, N the number of CSTR tanks, V_i is the volume of each tank, and F the volumetric flow rate. $E(\theta)$ represents the dimensionless RTD where $\theta = t/\tau$ the dimensionless time. As a one-parameter model, the idealness of the RTD is represented by the number of CSTR tanks used. Large number of tanks indicates a PFR-like reactor ($N \rightarrow \infty$), and a small number leads to a CSTR-like reactor ($N=1$).

The most employed method of RTD measurement is the stimulus-response test using inert tracer such as salt. This tracer should hold similar properties to the bulk stream to avoid hydrodynamic flow disturbances. The inlet and outlet boundaries are assumed to be closed to avoid boundary dispersion, hence unidirectional. Pulse injection or step change of a tracer is performed at the inlet of a continuous flow system where steady state of bulk flow is achieved, and response of the tracer profile at the outlet is recorded [130-131].

2.5.3. Challenges of enzyme immobilization direct onto membrane

Although immobilization of enzymes onto membrane generally enhances their stability, it also is mostly accompanied by significant loss in enzyme activity relative to the free enzyme activity [124]. This may be due to active site blocked from substrate accessibility, occurrence of multiple-point binding, or enzyme denaturation [31]. The amount of immobilized enzyme is an important parameter and strongly affects the reactor performance. A highly cross-linked enzyme may eventually reduce the intrinsic membrane permeability.

Another very critical limitation of direct onto membrane immobilization is the limited membrane life cycle by the enzyme activity. For example, when a covalently linked enzyme is denatured, removing the denatured enzyme to reuse the membrane is practically difficult. In addition to deactivation, the enzyme may get covered with excess substrate particularly when mass transfer rate is prevailing reaction rate, which is the case for most biochemical membrane reactors. Thus even in the absence of loss in apparent enzyme activity, there is a need to apply membrane cleaning to remove the over accumulated foulants without affecting the enzyme activity. This overfouled membrane first of all cause in reduce membrane water productivity. At the same time, the diffusion resistance encountered by the product molecules can sometimes cause the product to accumulate near the immobilized enzyme to an undesirable high level, leading to product inhibition for some enzymes e.g., pectinase. Moreover, cleaning may poses another difficulty since enzymes are highly sensitive to the change in the microenvironment that may be induced by the applied cleaning strategy. In addition, because an immobilized enzyme preparation is intended for a prolonged period of operation, there is also a gradual, but noticeable, loss in the apparent enzyme activity. This will eventually, raise the demand for fresh enzyme make-up or need for replacement of the entire immobilized enzyme layer.

Alternatively, large sized retainable carrier particles are available to perform important biocatalysis in biochemical membrane reactors. These include alginate beads or surface functionalized biopolymers. They give better degree of freedom for reutilization compared to direct integration of enzyme onto membrane. But the problem with such carrier particles is: first of all the retention of the biocatalytic particles on the membrane is based on size exclusion. This will imply the need for membrane molecular weight cutoff dictated choice of enzyme carrier particle or vice versa. But the main drawback of these particles for extensive use as industrial biocatalysts is that they exhibit similar particle sizes with other retainable components of the wastewater by the membrane. As a result separation based on size exclusion from the rest of the mixture for reutilizing the enzyme is a great challenge. Therefore, successful application of biochemical membrane reactors at larger scale should overcome all the aforementioned limitations.

2.5.4. Magnetically guided materials

Superparamagnetic nanoparticles (NP^{SP}) are most often superparamagnetic iron oxide Fe_3O_4 or γ-Fe_2O_3, or "soft" metallic iron and "hard" magnetic materials *e.g.* Co, Ni, FeN, FePt, FePd etc [132]. Since they have zero reminance of their magnetic property in the absence of an external magnetic field, they can be well dispersed in a reaction mixture [133]. Coating with polymers are approaches aiming at creating biocompatible environments for this nanoparticles [134]. In addition introducing surface functional groups to assist the chemical immobilization of enzyme on the surface of these nanosized particles is a well demonstrated science [135-137]. The resulting materials represent an important tool for biotechnology because they can be used in a large variety of processes e.g. food industry, waste treatment, and production of chemicals, drug delivery, cell transplantation or cell immobilization. In particular the biocompatibility of magnetic nanoparticles and the high surface to volume ratio they can provide makes them interesting hosts for enzyme. Enzymes can be easily incorporated into or grafted to ferric based magnetic nanoparticles to form biohybrids. These biohybrids are indeed bionanocomposites that hold versatile interesting properties like mechanical, optical, electrical, ionic, sensors, bio-sensors, catalysts properties. These properties can also be modified via control of their microstructure. Since the first introduction of enzyme immobilization on iron oxide particles support in the 1970s [138], NP^{SP}s have got numerous applications as magnetically separable high-performance supporters for biocatalysis when they are dispersed in a reaction mixture [139].

In parallel, producing smart magnetic-responsive materials by mixing polymeric materials with superparamagnetic nanoparticles (NP^{SP}) has become more interesting and efficient strategy [140]. Indeed, the magnetic moment of these membranes containing small amount of the NP^{SP} is much larger than those of molecular magnets[132]. This allows the membrane to respond to weak stimuli of permanent or alternating magnetic field. The incorporation of superparamagnetic nanoparticles in the polymers offers not only new possibilities but also the chance for improvement of already established systems with respect to a better control [141].

In an attempt to fill the gap of permanent loss of both enzyme and membrane in the cases of enzyme deactivation and membrane oversaturation, one could envisage on spatial and temporal control of physical immobilization of enzyme triggered by reversible forces. In this case

magnetic guidance of the bionanocomposites and the hybrid membranes provided by an external magnetic field may offer the key strategy.

2.6. Conclusion and future trend

A great deal has been learned from studies focused on the use of integrated membrane process for treatment or valorization of OMWW. The successive integration is observed to benefits from step-by-step pollutant removal, fractionation and concentration of the recovered biophenols. But successful implementation of these processes actually needs controlling fouling. Especially since fouling occurs at the very beginning of the integrated scheme, the primary step should be identification of the most responsible foulants at this stage e.g during MF. It will also be necessary to develop a much more detailed understanding of the submolecular mechanism involved in macrofoulnats-membrane interaction and how this interaction influence the needed condition to prevent fouling, feed pre-treatment strategies and membrane cleaning mechanisms. Pre-treatment strategies focused at removal of course particles gave only a limited success. Even with extensive chemical cleaning, least probability of recovering the original membrane performance is reported. On the contrary, exposing membrane to high concentrations of chemical cleaning agents may simply lead to lost in the intrinsic property of the membrane. Hence, the main strategy of future work should be on the development of preventive mechanisms. This may give a high degree of freedom to deal with seasonal flow of huge volume of wastewater without facing chronic fouling, need for large storage facilities and possible loss of some of the bioactive compounds through bacterial fermentation and fouling modified rejection layer. So special focus should be given to careful examination of the feed water characteristics that could dictate the type of preventive action one can implement.

2.7. Hypothesis and objectives of the study

The overlying hypothesis of this work is that biohybrid system consisting of biochemical membrane reactors will overcome the limitations associated with membrane fouling, in turn; they will have improved productivity, high biophenol recovery and ultimately secure environmental protection and economical benefit. It is also hypothesized that FO process using dense membrane provides a low energy demanding way to reduce the large volumes with eventually low fouling propensity and possible retention of all pollutants. It is further

hypothesized that combined O/I superparamagnetic membrane and superparamagnetic biocatalytic particles (bionanocomposites) prepared by including magnetic nanoparticles in both the enzyme and the membrane will potentially mimic the micro-nano architecture of the covalent enzyme immobilization on the membrane and become a suitable platform for reversible enzyme immobilization. The final hypothesis is studying individual units will provide solid ground to select the best flowsheet of the integrated membrane process depending on feed water characteristics and desired quality. In order to test the above hypotheses, the following objectives are formulated:

General objectives

To assess the individual performance of different membrane processes with special emphasis on fouling prevention and total processable volume reduction aiming at the development of efficient integrated membrane process for wastewater valorization.

Specific objectives

1. To determine the extent of reduction in fouling propensity during MF by using biochemical membrane reactors (free or immobilized).
2. To develop and evaluate magnetically guided enzyme immobilization technique so as to give a degree of freedom to immobilize enzyme on membrane using reversible force.
3. To investigate effects of different operating parameters on the superparamagnetic biocatalytic membrane reactor with hetroginized pectinase.
4. To compare set enzymatic membrane cleaning with traditional membrane cleaning strategies e.g. chemical cleaning.
5. To investigate the total processable volume reduction and biophenol recovery efficiency of FO process.
6. To recommend possible integrated membrane processes that can valorize vegetation wastewater based on the individually studied membrane processes.

2.8. References

[1] B.G. Ridoutt, S. Pfister, A revised approach to water footprinting to make transparent the impacts of consumption and production on global freshwater scarcity, Global Environmental Change, 20 (2010) 113-120.

[2] M. Poretti, Quality control of water as raw material in the food industry, Food Control, 1 (1990) 79-83.
[3] L. Fillaudeau, P. Blanpain-Avet, G. Daufin, Water, wastewater and waste management in brewing industries, Journal of Cleaner Production, 14 (2006) 463-471.
[4] A.K. Chapagain, A.Y. Hoekstra, The water footprint of coffee and tea consumption in the Netherlands, Ecological Economics, 64 (2007) 109-118.
[5] A.Y. Hoekstra, A.K. Chapagain, M.M. Aldaya, M.M. Mekonnen, The Water Footprint Assessment Manual, in, Earthscan, 2011.
[6] M.M. Mekonnen, A.Y. Hoekstra, The green, blue and grey water footprint of crops and derived crop products, Hydrol. Earth Syst. Sci., 15 (2011) 1577-1600.
[7] S. Casani, M. Rouhany, S. Knøchel, A discussion paper on challenges and limitations to water reuse and hygiene in the food industry, Water Research, 39 (2005) 1134-1146.
[8] A. Latif Ahmad, S. Ismail, S. Bhatia, Water recycling from palm oil mill effluent (POME) using membrane technology, Desalination, 157 (2003) 87-95.
[9] G. Daufin, J.P. Escudier, H. Carrère, S. Bérot, L. Fillaudeau, M. Decloux, Recent and Emerging Applications of Membrane Processes in the Food and Dairy Industry, Food and Bioproducts Processing, 79 (2001) 89-102.
[10] B. Fernandez, I. Seijo, G. Ruiz-Filippi, E. Roca, L. Tarenzi, J.M. Lema, Characterization, management and treatment of wastewater from white wine production, Water Sci Technol, 56 (2007) 121-128.
[11] D. Peters, N. DD., A. DT., Agro-processing wastewater assessment in periurban Hanoi, in, CIP Program 2000, pp. 451-457.
[12] H. El-Kamah, A. Tawfik, M. Mahmoud, H. Abdel-Halim, Treatment of high strength wastewater from fruit juice industry using integrated anaerobic/aerobic system, Desalination, 253 (2010) 158-163.
[13] C. Muro, F. Riera, M.a.d.C. Díaz, Membrane Separation Process in Wastewater Treatment of Food Industry, Food Industrial Processes - Methods and Equipment,
, in: B. Valde (Ed.) food-industrial-processes-methods-and-equipment, InTech, 2012.
[14] S. Oktay, G. Iskender, F. Germirli Babuna, G. Kutluay, D. Orhon, Improving the wastewater management for a beverage industry with in-plant control, Desalination, 211 (2007) 138-143.
[15] A. Derden, P. Vercaemst, R. Dijkmans, Best available techniques (BAT) for the fruit and vegetable processing industry, Resources, Conservation and Recycling, 34 (2002) 261-271.
[16] R. Mazzei, E. Drioli, L. Giorno, Enzyme membrane reactor with heterogenized β-glucosidase to obtain phytotherapic compound: Optimization study, Journal of Membrane Science, 390–391 (2012) 121-129.
[17] A. Schieber, F.C. Stintzing, R. Carle, By-products of plant food processing as a source of functional compounds — recent developments, Trends in Food Science & Technology, 12 (2001) 401-413.

[18] T. Baysal, S. Ersus, D.A.J. Starmans, Supercritical CO2 Extraction of β-Carotene and Lycopene from Tomato Paste Waste, Journal of Agricultural and Food Chemistry, 48 (2000) 5507-5511.
[19] N.L. Rozzi, R.K. Singh, R.A. Vierling, B.A. Watkins, Supercritical Fluid Extraction of Lycopene from Tomato Processing Byproducts, Journal of Agricultural and Food Chemistry, 50 (2002) 2638-2643.
[20] M.F. Mendes, F.L.P. Pessoa, A.M.C. Uller, An economic evaluation based on an experimental study of the vitamin E concentration present in deodorizer distillate of soybean oil using supercritical CO2, The Journal of Supercritical Fluids, 23 (2002) 257-265.
[21] C. Fang, K. Boe, I. Angelidaki, Biogas production from potato-juice, a by-product from potato-starch processing, in upflow anaerobic sludge blanket (UASB) and expanded granular sludge bed (EGSB) reactors, Bioresource Technology, 102 (2011) 5734-5741.
[22] L.P. Huang, B. Jin, P. Lant, J. Zhou, Biotechnological production of lactic acid integrated with potato wastewater treatment by Rhizopus arrhizus, Journal of chemical technology and biotechnology, 78 (2003) 899-906.
[23] M. Herrero, A. Cifuentes, E. Ibañez, Sub- and supercritical fluid extraction of functional ingredients from different natural sources: Plants, food-by-products, algae and microalgae: A review, Food Chemistry, 98 (2006) 136-148.
[24] E. Drioli, M. Romano, Progress and New Perspectives on Integrated Membrane Operations for Sustainable Industrial Growth, Industrial & Engineering Chemistry Research, 40 (2001) 1277-1300.
[25] J.-S. Kim, B.-G. Kim, C.-H. Lee, S.-W. Kim, H.-S. Jee, J.-H. Koh, A.G. Fane, Development of clean technology in alcohol fermentation industry, Journal of Cleaner Production, 5 (1997) 263-267.
[26] C. Russo, A new membrane process for the selective fractionation and total recovery of polyphenols, water and organic substances from vegetation waters (VW), Journal of Membrane Science, 288 (2007) 239-246.
[27] H. Inan, A. Dimoglo, H. Şimşek, M. Karpuzcu, Olive oil mill wastewater treatment by means of electro-coagulation, Separation and Purification Technology, 36 (2004) 23-31.
[28] A. Gohil, G. Nakhla, Treatment of tomato processing wastewater by an upflow anaerobic sludge blanket–anoxic–aerobic system, Bioresource Technology, 97 (2006) 2141-2152.
[29] M. Petruccioli, J. Duarte, F. Federici, High-rate aerobic treatment of winery wastewater using bioreactors with free and immobilized activated sludge, Journal of Bioscience and Bioengineering, 90 (2000) 381-386.
[30] T. Colin, A. Bories, Y. Sire, R. Perrin, Treatment and valorisation of winery wastewater by a new biophysical process(ECCF (R)), Water Science & Technology, 51 (2005) 99-106.
[31] G.O. Sigge, J. Britz, P.C. Fourie, C.A. Barnardt, R. Strydom, Combining UASB technology and advanced oxidation processes (AOPs) to treat food processing wastewaters, Water Sci Technol, 45 (2002) 329-334.

[32] A. Bhatnagar, M. Sillanpää, Utilization of agro-industrial and municipal waste materials as potential adsorbents for water treatment—A review, Chemical Engineering Journal, 157 (2010) 277-296.
[33] M. Mulder, Basic Principles of Membrane Technology, 1996.
[34] R.W. Baker, Microfiltration, in: Membrane Technology and Applications, John Wiley & Sons, Ltd, 2004, pp. 275-300.
[35] R.W. Baker, Ultrafiltration, in: Membrane Technology and Applications, John Wiley & Sons, Ltd, 2004, pp. 237-274.
[36] R.W. Baker, Reverse Osmosis, in: Membrane Technology and Applications, John Wiley & Sons, Ltd, 2004, pp. 191-235.
[37] D. Eumine Suk, T. Matsuura, Membrane-Based Hybrid Processes: A Review, Separation Science and Technology, 41 (2006) 595-626.
[38] M. Iaquinta, M. Stoller, C. Merli, Optimization of a nanofiltration membrane process for tomato industry wastewater effluent treatment, Desalination, 245 (2009) 314-320.
[39] C. Conidi, A. Cassano, E. Garcia-Castello, Valorization of artichoke wastewaters by integrated membrane process, Water Research, 48 (2014) 363-374.
[40] S. Sayed, K. El-Ezaby, L. Groendijk, Treatment of potato processing wastewater using a membrane bioreactor, in: Proceedings of the 9th International Water Technology Conference, IWTC9-2005, Sharm El-Sheikh, Egypt, 2005.
[41] E.R. Cornelissen, W. Janse, J. Koning, Wastewater treatment with the internal MEMBIOR, Meded Rijksuniv Gent Fak Landbouwkd Toegep Biol Wet, 66 (2001) 139-143.
[42] L.A. Ioannou, C. Michael, N. Vakondios, K. Drosou, N.P. Xekoukoulotakis, E. Diamadopoulos, D. Fatta-Kassinos, Winery wastewater purification by reverse osmosis and oxidation of the concentrate by solar photo-Fenton, Separation and Purification Technology, 118 (2013) 659-669.
[43] M. Pizzichini, C. Russo, Process for recovering the components of olive mill wastewater with membrane technologies, in, Google Patents, 2005.
[44] E. Łobos-Moysa, M. Dudziak, Z. Zoń, Biodegradation of rapeseed oil by activated sludge method in the hybrid system, Desalination, 241 (2009) 43-48.
[45] Y. Zhang, L. Yan, X. Qiao, L. Chi, X. Niu, Z. Mei, Z. Zhang, Integration of biological method and membrane technology in treating palm oil mill effluent, J Environ Sci (China), 20 (2008) 558-564.
[46] A. Cassano, B. Jiao, E. Drioli, Production of concentrated kiwifruit juice by integrated membrane process, Food Research International, 37 (2004) 139-148.
[47] S. Álvarez, F.A. Riera, R. Álvarez, J. Coca, F.P. Cuperus, S. Th Bouwer, G. Boswinkel, R.W. van Gemert, J.W. Veldsink, L. Giorno, L. Donato, S. Todisco, E. Drioli, J. Olsson, G. Trägårdh, S.N. Gaeta, L. Panyor, A new integrated membrane process for producing clarified apple juice and apple juice aroma concentrate, Journal of Food Engineering, 46 (2000) 109-125.

[48] G. Galaverna, G. Di Silvestro, A. Cassano, S. Sforza, A. Dossena, E. Drioli, R. Marchelli, A new integrated membrane process for the production of concentrated blood orange juice: Effect on bioactive compounds and antioxidant activity, Food Chemistry, 106 (2008) 1021-1030.
[49] A. Cassano, E. Drioli, G. Galaverna, R. Marchelli, G. Di Silvestro, P. Cagnasso, Clarification and concentration of citrus and carrot juices by integrated membrane processes, Journal of Food Engineering, 57 (2003) 153-163.
[50] R. Singh, Hybrid membrane systems - applications and case studies, in: Hybrid Membrane Systems for Water Purification
Technology, Systems Design and Operations, 2005, pp. 131-196.
[51] W.S. Guo, S. Vigneswaran, H.H. Ngo, H. Chapman, Experimental investigation of adsorption–flocculation–microfiltration hybrid system in wastewater reuse, Journal of Membrane Science, 242 (2004) 27-35.
[52] R.J. Ray, J. Kucera-Gienger, S. Retzlaff, Membrane-based hybrid processes for energy-efficient waste-water treatment, Journal of Membrane Science, 28 (1986) 87-106.
[53] H. Dhaouadi, B. Marrot, Olive mill wastewater treatment in a membrane bioreactor: Process feasibility and performances, Chem Eng J, 145 (2008) 225-231.
[54] C. Gonçalves, M. Lopes, J.P. Ferreira, I. Belo, Biological treatment of olive mill wastewater by non-conventional yeasts, Bioresource Technology, 100 (2009) 3759-3763.
[55] S. Takaç, * , A. Karakaya, Recovery of Phenolic Antioxidants from Olive Mill Wastewater, Recent Patents on Chemical Engineering, 2 (2009) 230-237.
[56] R. Claudio, A new membrane process for the selective fractionation and total recovery of polyphenols, water and organic substances from vegetation waters (VW), Journal of Membrane Science, 288 (2007) 239-246.
[57] A. Roig, M.L. Cayuela, M.A. Sánchez-Monedero, An overview on olive mill wastes and their valorisation methods, Waste Management, 26 (2006) 960-969.
[58] S. Khoufi, M. Hamza, S. Sayadi, Enzymatic hydrolysis of olive wastewater for hydroxytyrosol enrichment, Bioresource Technology, 102 (2011) 9050-9058.
[59] R. Casa, A. D'Annibale, F. Pieruccetti, S.R. Stazi, G. Giovannozzi Sermanni, B. Lo Cascio, Reduction of the phenolic components in olive-mill wastewater by an enzymatic treatment and its impact on durum wheat (Triticum durum Desf.) germinability, Chemosphere, 50 (2003) 959-966.
[60] E. Tsagaraki, H. Lazarides, Fouling Analysis and Performance of Tubular Ultrafiltration on Pretreated Olive Mill Waste Water, Food and Bioprocess Technology, (2010) 1-9.
[61] A. Agalias, P. Magiatis, A.-L. Skaltsounis, E. Mikros, A. Tsarbopoulos, E. Gikas, I. Spanos, T. Manios, A New Process for the Management of Olive Oil Mill Waste Water and Recovery of Natural Antioxidants, J Agr Food Chem, 55 (2007) 2671-2676.
[62] C.A. Paraskeva, V.G. Papadakis, E. Tsarouchi, D.G. Kanellopoulou, P.G. Koutsoukos, Membrane processing for olive mill wastewater fractionation, Desalination, 213 (2007) 218-229.
[63] A. El-Abbassi, M. Khayet, A. Hafidi, Micellar enhanced ultrafiltration process for the treatment of olive mill wastewater, Water Res, 45 (2011) 4522-4530.

[64] M. S Fountoulakis, S.N. Dokianakis, M.E. Kornaros, G.G. Aggelis, G. Lyberatos, Removal of phenolics in olive mill wastewaters using the white-rot fungus Pleurotus ostreatus, Water Res, 36 (2002) 4735-4744.
[65] C.M. Galanakis, E. Tornberg, V. Gekas, Clarification of high-added value products from olive mill wastewater, Journal of Food Engineering, 99 (2010) 190-197.
[66] A. Cassano, C. Conidi, L. Giorno, E. Drioli, Fractionation of olive mill wastewaters by membrane separation techniques, Journal of Hazardous Materials, 248 (2013) 185-193.
[67] A.G. Vlyssides, D.L. Bouranis, M. Loizidou, G. Karvouni, Study of a demonstration plant for the co-composting of olive-oil-processing wastewater and solid residue, Bioresource Technology, 56 (1996) 187-193.
[68] I. Chatjipavlidis, M. Antonakou, D. Demou, F. Flouri, C. Balis, Bio-fertilization of olive oil mills liquid wastes. The pilot plant in Messinia, Greece, International Biodeterioration & Biodegradation, 38 (1996) 183-187.
[69] E. Galli, L. Pasetti, F. Fiorelli, U. Tomati, OLIVE-MILL WASTEWATER COMPOSTING: MICROBIOLOGICAL ASPECTS, Waste Management & Research, 15 (1997) 323-330.
[70] S. Sayadi, N. Allouche, M. Jaoua, F. Aloui, Detrimental effects of high molecular-mass polyphenols on olive mill wastewater biotreatment, Process Biochemistry, 35 (2000) 725-735.
[71] M. Beccari, M. Majone, C. Riccardi, F. Savarese, L. Torrisi, Integrated treatment of olive oil mill effluents: Effect of chemical and physical pretreatment on anaerobic treatability, Water Science and Technology, 40 (1999) 347-355.
[72] Alessandro, S. Rita Stazi, V. Vinciguerra, E. Di Mattia, G. Giovannozzi Sermanni, Characterization of immobilized laccase from Lentinula edodes and its use in olive-mill wastewater treatment, Process Biochemistry, 34 (1999) 697-706.
[73] A. D'Annibale, S.R. Stazi, V. Vinciguerra, G. Giovannozzi Sermanni, Oxirane-immobilized Lentinula edodes laccase: stability and phenolics removal efficiency in olive mill wastewater, Journal of Biotechnology, 77 (2000) 265-273.
[74] R. Andreozzi, G. Longo, M. Majone, G. Modesti, Integrated treatment of olive oil mill effluents (OME): Study of ozonation coupled with anaerobic digestion, Water Research, 32 (1998) 2357-2364.
[75] J. Beltran-Heredia, J. Torregrosa, J.R. Dominguez, J. Garcia, Treatment of black-olive wastewaters by ozonation and aerobic biological degradation, Water Research, 34 (2000) 3515-3522.
[76] I.P. Marques, Anaerobic digestion treatment of olive mill wastewater for effluent re-use in irrigation, Desalination, 137 (2001) 233-239.
[77] K. Fadil, A. Chahlaoui, A. Ouahbi, A. Zaid, R. Borja, Aerobic biodegradation and detoxification of wastewaters from the olive oil industry, International Biodeterioration & Biodegradation, 51 (2003) 37-41.
[78] F. Raposo, R. Borja, E. Sánchez, M.A. Martín, A. Martin, Inhibition kinetics of overall substrate and phenolics removals during the anaerobic digestion of two-phase olive mill effluents

(TPOME) in suspended and immobilized cell reactors, Process Biochemistry, 39 (2003) 425-435.
[79] L. Bertin, S. Berselli, F. Fava, M. Petrangeli-Papini, L. Marchetti, Anaerobic digestion of olive mill wastewaters in biofilm reactors packed with granular activated carbon and “Manville” silica beads, Water Research, 38 (2004) 3167-3178.
[80] A. García-Gómez, A. Roig, M.P. Bernal, Composting of the solid fraction of olive mill wastewater with olive leaves: organic matter degradation and biological activity, Bioresource Technology, 86 (2003) 59-64.
[81] E. Turano, S. Curcio, M.G. De Paola, V. Calabrò, G. Iorio, An integrated centrifugation–ultrafiltration system in the treatment of olive mill wastewater, Journal of Membrane Science, 209 (2002) 519-531.
[82] M. Drouiche, V. Le Mignot, H. Lounici, D. Belhocine, H. Grib, A. Pauss, N. Mameri, A compact process for the treatment of olive mill wastewater by combining OF and UV/H2O2 techniques, Desalination, 169 (2004) 81-88.
[83] N. Adhoum, L. Monser, Decolourization and removal of phenolic compounds from olive mill wastewater by electrocoagulation, Chemical Engineering and Processing: Process Intensification, 43 (2004) 1281-1287.
[84] M. Gotsi, N. Kalogerakis, E. Psillakis, P. Samaras, D. Mantzavinos, Electrochemical oxidation of olive oil mill wastewaters, Water Research, 39 (2005) 4177-4187.
[85] K. Kestioğlu, T. Yonar, N. Azbar, Feasibility of physico-chemical treatment and Advanced Oxidation Processes (AOPs) as a means of pretreatment of olive mill effluent (OME), Process Biochemistry, 40 (2005) 2409-2416.
[86] J.A. de la Casa, M. Lorite, J. Jiménez, E. Castro, Valorisation of wastewater from two-phase olive oil extraction in fired clay brick production, Journal of Hazardous Materials, 169 (2009) 271-278.
[87] T. Yangui, A. Dhouib, A. Rhouma, S. Sayadi, Potential of hydroxytyrosol-rich composition from olive mill wastewater as a natural disinfectant and its effect on seeds vigour response, Food Chemistry, 117 (2009) 1-8.
[88] A. Ena, C. Pintucci, P. Carlozzi, Recovery of the phenolic fraction of olive mill wastewater, Journal of Biotechnology, 150, Supplement (2010) 279.
[89] E. Garcia-Castello, A. Cassano, A. Criscuoli, C. Conidi, E. Drioli, Recovery and concentration of polyphenols from olive mill wastewaters by integrated membrane system, Water Res, 44 (2010) 3883-3892.
[90] E.O. Akdemir, A. Ozer, Investigation of two ultrafiltration membranes for treatment of olive oil mill wastewater, Desalination, 249 (2009) 660-666.
[91] T. Coskun, E. Debik, N.M. Demir, Treatment of olive mill wastewaters by nanofiltration and reverse osmosis membranes, Desalination, 259 (2010) 65-70.
[92] M. Stoller, Effective fouling inhibition by critical flux based optimization methods on a NF membrane module for olive mill wastewater treatment, Chemical Engineering Journal, 168 (2011) 1140-1148.

[93] E. Chatzisymeon, A. Dimou, D. Mantzavinos, A. Katsaounis, Electrochemical oxidation of model compounds and olive mill wastewater over DSA electrodes: 1. The case of Ti/IrO2 anode, Journal of Hazardous Materials, 167 (2009) 268-274.
[94] E. Chatzisymeon, N.P. Xekoukoulotakis, D. Mantzavinos, Determination of key operating conditions for the photocatalytic treatment of olive mill wastewaters, Catalysis Today, 144 (2009) 143-148.
[95] M. Kallel, C. Belaid, R. Boussahel, M. Ksibi, A. Montiel, B. Elleuch, Olive mill wastewater degradation by Fenton oxidation with zero-valent iron and hydrogen peroxide, Journal of Hazardous Materials, 163 (2009) 550-554.
[96] S. Dogruel, T. Olmez-Hanci, Z. Kartal, I. Arslan-Alaton, D. Orhon, Effect of Fenton's oxidation on the particle size distribution of organic carbon in olive mill wastewater, Water Research, 43 (2009) 3974-3983.
[97] F.A. El-Gohary, M.I. Badawy, M.A. El-Khateeb, A.S. El-Kalliny, Integrated treatment of olive mill wastewater (OMW) by the combination of Fenton's reaction and anaerobic treatment, Journal of Hazardous Materials, 162 (2009) 1536-1541.
[98] W.K. Lafi, B. Shannak, M. Al-Shannag, Z. Al-Anber, M. Al-Hasan, Treatment of olive mill wastewater by combined advanced oxidation and biodegradation, Separation and Purification Technology, 70 (2009) 141-146.
[99] W. Najjar, S. Azabou, S. Sayadi, A. Ghorbel, Screening of Fe–BEA catalysts for wet hydrogen peroxide oxidation of crude olive mill wastewater under mild conditions, Applied Catalysis B: Environmental, 88 (2009) 299-304.
[100] A. El-Abbassi, H. Kiai, A. Hafidi, M.C. García-Payo, M. Khayet, Treatment of olive mill wastewater by membrane distillation using polytetrafluoroethylene membranes, Separation and Purification Technology, 98 (2012) 55-61.
[101] A. El-Abbassi, M. Khayet, H. Kiai, A. Hafidi, M.C. García-Payo, Treatment of crude olive mill wastewaters by osmotic distillation and osmotic membrane distillation, Separation and Purification Technology, 104 (2013) 327-332.
[102] A. Cassano, C. Conidi, L. Giorno, E. Drioli, Fractionation of olive mill wastewaters by membrane separation techniques, Journal of Hazardous Materials, 248–249 (2013) 185-193.
[103] J.M. Ochando-Pulido, M. Stoller, M. Bravi, A. Martinez-Ferez, A. Chianese, Batch membrane treatment of olive vegetation wastewater from two-phase olive oil production process by threshold flux based methods, Separation and Purification Technology, 101 (2012) 34-41.
[104] A. Zirehpour, M. Jahanshahi, A. Rahimpour, Unique membrane process integration for olive oil mill wastewater purification, Separation and Purification Technology, 96 (2012) 124-131.
[105] P. Xynogalas, Procédé physico-chimique de traitement de déchets liquides et semi-solides d'huileries d'olive utilisant de l'ozone (o3), in, Google Patents, 2009.
[106] Y. Pescher, J.P. Raes, S. Danda, B. Castelas, F. Rabatel, J. Morales, J. Bonfill, Method for purifying an organic waste-containing medium, in, Google Patents, 1995.

[107] J.A. Thomassen, Installation for recycling agricultural waste and similar waste, in, Google Patents, 2004.
[108] M.R. Lobban, S.E.C. Lobban, A filter system, in, Google Patents, 2004.
[109] R. Borsani, B. Ferrando, Ultrafiltration plant for olive vegetation waters by polymeric membrane batteries, Desalination, 108 (1997) 281-286.
[110] E. Tsagaraki, H. Lazarides, Fouling Analysis and Performance of Tubular Ultrafiltration on Pretreated Olive Mill Waste Water, Food Bioprocess Technol, 5 (2012) 584-592.
[111] M. Stoller, Technical optimization of a dual ultrafiltration and nanofiltration pilot plant in batch operation by means of the critical flux theory: A case study, Chemical Engineering and Processing: Process Intensification, 47 (2008) 1165-1170.
[112] A. El-Abbassi, M. Khayet, A. Hafidi, Micellar enhanced ultrafiltration process for the treatment of olive mill wastewater, Water Res, 45 (2011) 4522-4530.
[113] A. El-Abbassi, A. Hafidi, M. Khayet, M.C. García-Payo, Integrated direct contact membrane distillation for olive mill wastewater treatment, Desalination, 323 (2013) 31-38.
[114] A. Cassano, C. Conidi, E. Drioli, Comparison of the performance of UF membranes in olive mill wastewaters treatment, Water Research, 45 (2011) 3197-3204.
[115] M. Servili, S. Esposto, G. Veneziani, S. Urbani, A. Taticchi, I. Di Maio, R. Selvaggini, B. Sordini, G. Montedoro, Improvement of bioactive phenol content in virgin olive oil with an olive-vegetation water concentrate produced by membrane treatment, Food Chemistry, 124 (2011) 1308-1315.
[116] G.J. FERNÁNDEZ-BOLAÑOS, G.G. RODRÍGUEZ, M.A. LAMA, R.F. SENENT, G.J.M. FERNÁNDEZ-BOLAÑOS, C.I. MAYA, L.Ó. LÓPEZ, C.A. MARSET, Method for obtaining hydroxytyrosol extract, mixture of hydroxytyrosol and 3,4-dihydroxyphenylglycol extract, and hydroxytyrosyl acetate extract, from by-products of the olive tree, and the purification thereof, in, Google Patents, 2014.
[117] A.M. Domnanovich, Cleaning of olive oil waste waster with mechanical, chemical and biological methods, in, Google Patents, 2009.
[118] A.Y. Gebreyohannes, R. Mazzei, E. Curcio, T. Poerio, E. Drioli, L. Giorno, Study on the in Situ Enzymatic Self-Cleansing of Microfiltration Membrane for Valorization of Olive Mill Wastewater, Industrial & Engineering Chemistry Research, 52 (2013) 10396-10405.
[119] N. Mameri, F. Halet, M. Drouiche, H. Grib, H. Lounici, D. Belhocine, A. Pauss, D. Piron, Treatment of olive mill washing water by ultrafiltration, The Canadian Journal of Chemical Engineering, 78 (2000) 590-595.
[120] E. Vierhuis, M. Korver, H.A. Schols, A.G.J. Voragen, Structural characteristics of pectic polysaccharides from olive fruit (Olea europaea cv moraiolo) in relation to processing for oil extraction, Carbohydrate Polymers, 51 (2003) 135-148.
[121] J.-y. Tian, H. Liang, J. Nan, Y.-l. Yang, S.-j. You, G.-b. Li, Submerged membrane bioreactor (sMBR) for the treatment of contaminated raw water, Chemical Engineering Journal, 148 (2009) 296-305.

[122] L. Giorno, E. Drioli, Biocatalytic membrane reactors: applications and perspectives, Trends in Biotechnology, 18 (2000) 339-349.
[123] R. Mazzei, E. Drioli, L. Giorno, 3.08 - Biocatalytic Membranes and Membrane Bioreactors, in: D. Editor-in-Chief: Enrico, G. Lidietta (Eds.) Comprehensive Membrane Science and Engineering, Elsevier, Oxford, 2010, pp. 195-212.
[124] P. Jochems, Y. Satyawali, L. Diels, W. Dejonghe, Enzyme immobilization on/in polymeric membranes: status, challenges and perspectives in biocatalytic membrane reactors (BMRs), Green Chemistry, 13 (2011) 1609-1623.
[125] J.M. Rodriguez-Nogales, N. Ortega, M. Perez-Mateos, M.D. Busto, Pectin hydrolysis in a free enzyme membrane reactor: An approach to the wine and juice clarification, Food Chemistry, 107 (2008) 112-119.
[126] A.P. Echavarría, A. Ibarz, J. Conde, J. Pagán, Enzyme recovery and effluents generated in the enzymatic elimination of clogging of pectin cake in filtration process, Journal of Food Engineering, 111 (2012) 52-56.
[127] L. Giorno, L. Donato, S. Todisco, E. Drioli, Study of fouling phenomena in apple juice clarification by enzyme membrane reactor, Separation Science and Technology, 33 (1998) 739-756.
[128] M.E. Carrin, L. Ceci, J.E. Lozano, EFFECTS OF PECTINASE IMMOBILIZATION DURING HOLLOW FIBER ULTRAFILTRATION OF APPLE JUICE, Journal of Food Process Engineering, 23 (2000) 281-298.
[129] M.F. Chaplin, C.Bucke, Enzyme technology, Cambridge University Press, 1990.
[130] O. Levenspiel, Chemical Reaction Engineering, 3rd ed., John Wiley & Sons Inc, New York, 1999.
[131] J.E. Bailey, D.F. Ollis, Biochemical Engineering Fundamentals, McGraw-Hill, New York, 1986.
[132] J. Thevenot, H. Oliveira, O. Sandre, S. Lecommandoux, Magnetic responsive polymer composite materials, Chemical Society Reviews, 42 (2013) 7099-7116.
[133] K.M. Yeon, C.H. Lee, J. Kim, Magnetic enzyme carrier for effective biofouling control in the membrane bioreactor based on enzymatic quorum quenching, Environ Sci Technol, 43 (2009) 7403-7409.
[134] N. Miguel-Sancho, O. Bomatí-Miguel, G. Colom, J.P. Salvador, M.P. Marco, J. Santamaría, Development of Stable, Water-Dispersible, and Biofunctionalizable Superparamagnetic Iron Oxide Nanoparticles, Chemistry of Materials, 23 (2011) 2795-2802.
[135] N. Miguel-Sancho, O. Bomati-Miguel, A.G. Roca, G. Martinez, M. Arruebo, J. Santamaria, Synthesis of Magnetic Nanocrystals by Thermal Decomposition in Glycol Media: Effect of Process Variables and Mechanistic Study, Industrial & Engineering Chemistry Research, 51 (2012) 8348-8357.
[136] W. Brullot, N.K. Reddy, J. Wouters, V.K. Valev, B. Goderis, J. Vermant, T. Verbiest, Versatile ferrofluids based on polyethylene glycol coated iron oxide nanoparticles, Journal of Magnetism and Magnetic Materials, 324 (2012) 1919-1925.

[137] Z. Xiao-Ming, I.W. Wainer, On-line determination of lipase activity and enantioselectivity using an immobilized enzyme reactor coupled to a chiral stationary phase, Tetrahedron Letters, 34 (1993) 4731-4734.
[138] P.J. Robinson, P. Dunnill, M.D. Lilly, The properties of magnetic supports in relation to immobilized enzyme reactors, Biotechnology and bioengineering, 15 (1973) 603-606.
[139] J. Lee, Y. Lee, J.K. Youn, H.B. Na, T. Yu, H. Kim, S.-M. Lee, Y.-M. Koo, J.H. Kwak, H.G. Park, H.N. Chang, M. Hwang, J.-G. Park, J. Kim, T. Hyeon, Simple Synthesis of Functionalized Superparamagnetic Magnetite/Silica Core/Shell Nanoparticles and their Application as Magnetically Separable High-Performance Biocatalysts, Small, 4 (2008) 143-152.
[140] P. Daraei, S.S. Madaeni, N. Ghaemi, M.A. Khadivi, B. Astinchap, R. Moradian, Fouling resistant mixed matrix polyethersulfone membranes blended with magnetic nanoparticles: Study of magnetic field induced casting, Separation and Purification Technology, 109 (2013) 111-121.
[141] Z.-Q. Huang, F. Zheng, Z. Zhang, H.-T. Xu, K.-M. Zhou, The performance of the PVDF-Fe3O4 ultrafiltration membrane and the effect of a parallel magnetic field used during the membrane formation, Desalination, 292 (2012) 64-72.

Chapter 3: A study on the *in-situ* enzymatic self-cleansing of microfiltration membrane for valorization of olive mill wastewater

3.1. Abstract

In this study intensified removal of pectins was integrated with microfiltration step to develop *in-situ* self-cleansing biocatalytically active membranes. This method was developed to reduce the severe fouling that occurred during microfiltration (MF) of olive mill wastewater (OMWW) for the recovery of bioactive compounds using integrated membrane processes.

As a proof-of-concept, pectinase has been immobilized on the MF membrane surface and flux performances as a function of time has been monitored and compared with inert membrane. For the experiments real OMWW has been used. The steady state flux through the enzyme immobilized on the membrane surface solo was 50% higher than inert membrane. The mechanism for the better performance of the biocatalytically active on the surface has been explained as based on both degradation of deposited pectins (*in-situ* self-cleansing) and overcome of product inhibition as it is continuously removed from the reaction site. The inhibitory effect has been clearly identified from kinetic study of pectinase.

For all types of used membrane systems, analysis of cake resistance, membrane resistance and membrane fouling index indicated surface bio-functionalized membranes with the least fouling tendency and significantly improved flux.

This chapter is published as**: Gebreyohannes A. Y**., R. Mazzei, E. Curcio, T. Poerio, E. Drioli and L. Giorno, "Study on the in Situ Enzymatic Self-Cleansing of Microfiltration Membrane for Valorization of Olive Mill Wastewater. *Ind. Eng. Chem. Res.*, **2013**, 52 (31), pp 10396–10405 **DOI:** 10.1021/ie400291w. (2013).

3.2. Introduction

Olive oil production generates dark acid wastewater with more than 300 times polluting capacity compared to that of municipal sewage. This wastewater called olive mill wastewater (OMWW) comes from the large amounts of water added during the basic stage of olive process. The annual environmental release is estimated to be about 30 million m^3/year with a very high organic load especially rich in more than 30 different types of biophenolic compounds [1-3]. These compounds are phytotoxic with strong antibacterial effect [2, 4-6]. Serious environmental damages have been caused over the years due to the continuous damping of OMWW reach in the environmentally toxic biophenolic compounds [7]. As a matter of fact, most of the processing facilities are located close to sea resorts and places of high tourist interest. This situation makes the negative socioeconomic and environmental impacts of this industrial activity more than obvious. Now a days expansion of olive oil production from Mediterranean to other part of the world as evidenced by emerging olive oil producers like US, Australia and South America transfer the environmental concern related to this process from a regional to an international concern. Especially increased awareness on the health preventing capacity of the olive oil raised the world wide consumption abruptly. In recent years many management options have been proposed for the treatment of OMWW; mostly aimed at reducing phytotoxic nature of the biophenols in order to reuse OMWW for agricultural purposes [8]. On the other hand the biophenolic compounds existing in OMWW though recalcitrant they are also compound of interest in the food, pharmaceutical or cosmetic industries due to their high antioxidant and other important bioactivities [1, 6]. Therefore focusing on the recovery of these high added value compounds has the potential to increase the material resource efficiency of handling such environmentally detrimental waste stream. This in turn would result in significant economic value increase of OMWW that otherwise could represent only a disposal cost in the mill industry.

Recently, there is a growing research activity in the use of integrated membrane system for valorization of olive mill wastewater [9-13]. Rationalizing industrial wastewater treatment by the use of integrated membrane process can benefit from the synergistic effect of individual units in terms of product quality, plant compactness, environmental impact, and energy consumption [14]. However until now none of the membrane process for treatment of OMWW is yet industrialized due to huge fouling phenomena that reduced the economical feasibility.

All the integrated membrane process for valorization of OMWW involve sequence of pretreatment steps like acidification, enzymatic treatment, centrifugation or classical filtration [10-12]to make the wastewater easily processable with the subsequent membrane process. But not all the foulants can be removed using the mentioned pre-treatment. Indeed the pectins are one of the strong foulants present in the wastewater that survives the traditional pre-treatment. Hence membrane treatment of olive mill wastewater is highly restricted by accumulation of these pectic and other extracellular materials on the surface and/or inside the pores of the membrane. Therefore improvement of the traditional pre-treatment in order to remove pectins necessitate for an additional process units. This will further increase the operational cost related to periodic pausing, cleaning chemicals, cleaning water, energy and time. Unfortunately, mostly the cleaning procedure never reverted the initial membrane permeability [9-10, 12, 15]. Hence to make the OMWW treatment both economically and ecologically feasible, it is important to use the concept of process intensification. Ultimately, an engineered method to control such fast flux decline and limited working life cycle is mandatory for the sustainable use of the integrated membrane process at large scale.

Here, an alternative strategy was proposed for an intensified removal of pectins by immobilized enzyme membrane reactor from OMWW. In most cases the enzyme pectinase was found effective in breaking down the pectins to easily permeable polygalacturonic subunits [16-18]. These enzymes have been extensively studied because of their depectinizing capacity, e.g., in the extraction and clarification processes during the manufacturing of juice and wine [18-19] or to improve flux[20].To the best of our knowledge, immobilized fungal enzymes were not used to hydrolyze the pectin in OMWW with the objective of controlling membrane fouling in OMWW. Hence coupling of membrane separation with pectinase hydrolysis of the core foulants may open the channel for continuous treatment of OMWW. This intensified strategy also permit to enhance the onsite use of integrated membrane process. Because intensification of OMWW treatment may also benefit from smaller foot print; removal of sole foulants, prevents loss of quality of microbially or enzymatically unstable high added value compounds and the necessity of storing facilities and transportation to offsite treatment facilities.

Therefore, the general objective of the present work is improving the self cleansing capacity of membrane using the enzyme pectinase as a clean biotechnological strategy. Thus, a case-by-case investigation of hydrodynamic mixing, reactor configuration, enzyme attachment and the

resulting flux improvements are presented. In the results sections, residence time distribution analyses (RTD) for a side stream configurations are reported. The kinetic and flux data obtained from stirred tank reactor, free enzyme membrane bioreactor and biocatalytic membrane reactor are presented. This includes investigations conducted with the aim of identifying the optimal configuration for the best performance of the system. Finally the comparison of the different configurations based on theoretical analysis of the sole fouling mechanism, cake resistance and membrane fouling index was considered

3.3. Materials and Method

3.3.1. Chemicals

OMWW (Total Suspended Solid TSS = 4.13 %, pectin = 0.3-0.46 mg/mL) was taken from three-phase local olive oil producer (Calabria, Italy) in January 2012. Sodium Chloride, commercial pectolytic enzyme from Aspergillus species, pectinex 3XL, Bicinchoninic Acid Kit (BCA) kit, galacturonic acid and 25% Grade I glutaraldehyde (G004) were purchased from Sigma Aldrich (Italy).

3.3.2. OMWW screening

A 40µm mesh size stainless steel was used before microfiltration to reduce TSS of OMWW. Screening resulted in a TSS removal efficiency of about 70% and 80% liquid recovery.

3.3.3. Membranes and modules

Lab-made modules were prepared by potting hollow fiber (HF) membranes in a glass vessel with epoxy resin Emerson & Cuming (Belgium). Each module contains 7 polyethylene (PE) HF membranes with 0.4µm pore size and internal/external diameter of 0.41/0.65 mm, kindly provided by Econity (South Korea). Hollow fibers have asymmetric structure with selective layer on the shell side and sponge layer on the lumen side.

Prior to use, membranes were extensively washed in pure water to remove preservatives at TMP of 0.1 bar for an hour. The removal of preservatives was monitored by spectrophotometric analysis of both permeate and retentate streams (Perkin Elmer, Lambda EZ201).

3.3.4. Experimental setup

The membrane module was fed by peristaltic pump General Control S.p.a (Milan, Italy). Two pressure gauges mounted before and after the module read the corresponding hydrodynamic pressure drop across the membrane. Permeate was collected using a separate beaker placed on an electronic balance Gibertini S.r.l (Milan, Italy) interfaced to a personal computer for recording the mass collected per unit time. A Pulse Dampener Masterflex General Control S.p.a (Milan, Italy) was used to reduce the unstable reading on the trans-membrane pressure (TMP) arising from the pulsating mode of the peristaltic pump. Figure 1 shows the schematic representation of the experimental set up. The system was operated in four different configurations:

a. inert membrane without enzyme;
b. inert membrane with free enzyme (free enzyme MBR);
c. biocatalytically active membrane with immobilized enzyme only on the surface (immobilized enzyme MBR);
d. biocatalytically active membrane with immobilized enzyme on both surface and within pores (immobilized enzyme MBR)

In configuration a), the pre-filtered OMWW was microfiltered at room temperature, cross flow velocities of 21 and 36 cm/s, in two different operational modes: complete recirculation (stepwise increasing TMP from 0.05 to 2.5 bar) and batch concentration (fixed TMP, recycling the retentate stream and collecting permeate separately).

At the end of the first run, standard cleaning procedure [9] of membranes resulted in a only 60% recovery of pure water permeability; therefore, all experiments were carried out using virgin membranes.

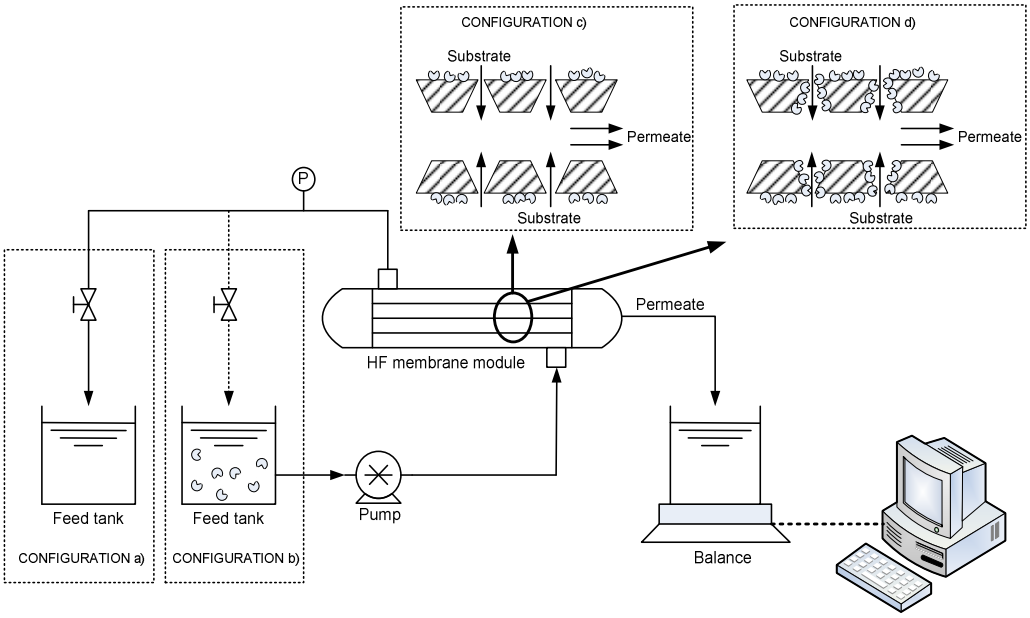

Figure 1: Schematic representation of simple microfiltration (a), free enzyme membrane bioreactor (b), solo surface activated biocatalytically active membrane reactor (c) and surface plus pore activated biocatalytically active membrane reactor (d).

3.3.5. Fluid-dynamics characterization

The fluid-dynamics of the lab-scale side stream was characterized by Residence Time Distribution (RTD) analysis. A tracer, consisting in an aqueous solution of NaCl, was fed (step-input) to the shell-side of the reactor with flowrate (Q) of 20.5 mL/min by a peristaltic pump General Control S.p.a, (Italy), and its concentration recorded as a function of time at the outlet of PE hollow fibers by conductivity meter (YSI 3200 Conductivity Instrument) with a 1.5 L system volume.

The cumulative RTD curve F(t) was experimentally determined as [21]:

$$F(t) = \frac{c_{out}(t)}{c_0} \qquad 1.a$$

where t is the time, c_{out} and c_0 the tracer concentration at the outlet and inlet of the bioreactor, respectively. The theoretical mean retention time τ was calculated as:

$$\tau = \frac{Q}{V} \qquad 1.b$$

The function E_θ, representing the age distribution of the non-ideal flow in the reactor expressed as a function of the dimensionless variable θ (where $\theta = t/\tau$), was mathematically derived as:

$$E(\theta) = \tau \cdot E(t) = \tau \cdot \frac{dF(t)}{dt} \quad \text{1.c}$$

E(θ) function allows easy comparison of RTD for reactors having different volumes and configurations.

3.3.6. Analytical methods

Before and after filtration tests, samples were collected and stored at -20°C for further analysis.

3.3.6.1. Procedure of Pectins Concentration Measurements.

The enzyme activity was determined by measuring unreacted pectin as a function of time. A sample of OMWW (0.2 mL) was mixed with 1.2 mL of sulfuric acid. The obtained solution is refrigerated in crushed ice. The mixture was shaken in a vortex mixer and then heated in an oil bath at 100 °C for 5 min. After cooling in a water-ice bath, 20 μL of 0.15% solution of mhydroxydiphenyl in 0.5% NaOH was added. The final solution was shaken, and, within 5 min, the absorbance of a pink complex of galacturonic acid was read at 520 nm in a Perkin- Elmer spectrophotometer using water as a background. The galacturonic acid is formed from the hydrolysis reaction of pectins with sulfuric acid. A standard solution of galacturonic acid was used for the preparation of the calibration curve (0−1 g/100 mL water).
The hydrolyzed OMWW were used to study the microfiltration performance in configuration b).
The conversion of the hydrolysis reaction was calculated as the percent ratio of the amount of galaturonic acid produced after hydrolysis over the amount of pectins in the initial reaction mixture.

3.3.6.2. Protein Quantification Assay.

The initial pectinex 3XL enzyme concentration was 18.4 mg/mL. The protein analysis was carried out using the bicinchoninic acid (BCA) assay (Sigma-Aldrich). The BCA assay primarily relies on two reactions, redox and complexation reactions:

1) In the redox reaction the peptide bonds present in the pectinex 3XL reduce Cu^{2+} ions from the cupric sulfate to Cu^{+}. The amount of Cu^{2+} reduced is proportional to the amount pectinex 3XL of present in the solution.

2) In the complexation reaction two molecules of bicinchoninic acid chelate with each Cu^{+} ion, forming a purple-colored product that strongly absorbs light at a wavelength of 562 nm. The amount of protein present in a solution can be quantified by measuring the absorption spectra and comparing with protein solutions of known concentration

The enzyme activity was determined by measuring the amount of unreacted pectin as a function of time [22]. Standard solutions of galacturonic acid (0-1 gm/100 mL water) were used for the preparation of the calibration curve. Colorimetric analysis was performed with UV/VIS Spectrophotometer (Perkin Elmer, Lambda EZ201). The hydrolyzed OMWW were used to study the microfiltration performance in configuration b).

3.3.7. Reaction rate and kinetic parameters determination

Hydrolysis reactions catalyzed by free pectinex 3XL were carried out by mixing in a 200 mL flask different concentration of enzyme and substrate with 100 mL OMWW. In order to achieve a Stirred Tank Reactor (STR) configuration, the flask was kept in thermostatic bath at 40°C and pH 4.2 under 40 rpm magnetic stirring. Every 15 seconds, 2.5 mL of sample was withdrawn from the reaction mixture for residual pectin quantification. Addition of 40µL of 37% HCl allowed a fast deactivation of the enzyme and the instantaneous termination of the reaction [23].

For free enzyme configuration, batch hydrolysis reactions catalyzed by free pectinex 3XL was carried out by mixing different concentrations of enzyme with 500 mL of pre-filtered OMWW at 40°C and pH 4.2.

For an optimal pectinase function, the substrate concentration was set to 4 to 5 order of magnitude higher than the enzyme concentration [17]. In STR, in order to determine the kinetic parameters of OMWW pectin hydrolysis, reaction tests were carried out by mixing 50µL of 0.92 mg/mL enzyme with 100 mL of OMWW at 0.3, 0.2 and 0.1 mg/mL substrate concentration; the initial rate of product formation was then obtained for the three different substrate concentrations. Plots of the initial reaction rate (v_0) against substrate concentration [S] were fitted to Lineweaver–Burk equation for estimating K_m and v_{max} constants [24].

Mass balance equation for STR in batch mode is reported below:

$$v_r = \frac{1}{V}\frac{d(V \cdot c)}{dt} \qquad 2$$

where c is the concentration (mg/mL), v_r is the volumetric reaction rate (mg/mL.s), V is the reaction volume (mL) and t is the time (s). Hence, v_0 was derived from the linear section of c vs t plot.

3.3.8. Enzyme Immobilization

Covalent bond formed by multifunctional reagent glutaraldehyde was used to immobilize the enzyme on the membrane. HF membranes were kept in contact with 25% grade I glutaraldehyde solution for 2 hours at room temperature. Then, membranes were thoroughly rinsed with ultrapure water, monitoring the concentration of glutaraldehyde in the wash water spectrophotometrically. Afterwards, the membranes were kept in contact with 20 mL of 0.92 mg/mL pectinex 3XL enzyme solution in 0.1M acetate buffer at pH 5.5 for 16 hours at 4°C without permeation. In such treatment the enzyme was chemically crosslinked only to the surface of the membrane. Unbound proteins were removed by rinsing of the membrane with pure water. The amount of enzyme immobilized (P_i) was determined by mass balance based on reduction in protein content of the solution recovered after the 16 hours contact time and the subsequent rinsing (equation 3):

$$P_i = m_o - m_a - m_w \qquad 3$$

where m_0 is the initial mass of enzyme, m_a the mass of enzyme in the recovered solution after immobilization and m_w the enzyme mass in the washing water.

The amount of protein (enzyme) in the initial and recovered solutions and washing water are measured using the BCA method as detailed in section 3.3.6.2.

In configuration c) or d), where enzyme is immobilized both on the surface and inside the pores of the membrane, both the glutaraldehyde and the enzyme solutions were permeated across the HF membranes with flowrate of 50mL/min and TMP of 0.1 bar. The duration of permeations was one hour out of the two hours and sixteen hours of contact time for glutaraldehyde and enzyme respectively.

3.3.9. Theoretical analysis of fouling mechanism

Fouling in membrane process can be either due to gel/cake layer formations or through pollutant-membrane interactions [25]. For practical reasons, it is useful to have a method to identify the

prevailing fouling mechanism. According to Mondal *et al* [26], the different types of mechanisms are discriminated by analysis of the transmembrane flux (J) data versus time (t) in particular referring statistical analysis with an acceptable R^2 value of greater than 0.9:

(i) Complete Pore Blocking (CPB): if ln(J) vs t plot straight line;

(ii) Intermediate Pore Blocking (IPB): if 1/J vs t plot is straight line;

(iii)Standard Pore Blocking (SPB): if $1/\sqrt{J}$ vs t plot is straight line;

(iv)Cake Filtration (CF): if $1/J^2$ vs t plot is straight line.

Henceforth, filtration data from MF tests (configuration a) were plotted accordingly.

Additional theoretical analysis was also performed in order to evaluate the hydrodynamic resistance developed within the system for all types of configuration. Based on Darcy's law, the transmembrane flux during OMWW microfiltration can be modeled assuming two resistances in series: cake resistance (α) and membrane resistance (β). Both parameters are obtained from slope and intercept of first linear part of t/V versus V curve, respectively [27-28]:

$$\frac{t}{V} = \frac{\alpha\omega\eta}{2\Delta P\, A^2} V + \frac{\eta\beta}{A\,\Delta P} \qquad 4$$

According to Mulder [27], the slope of the second linear part of such plot could be used to interpolate the membrane filtration index (MFI), a widely used indicator for fouling tendency.

3.4. Results and Discussion

3.4.1. Residence time distribution (RTD) analysis

Figure 2 for E curve versus dimensionless time θ showed that experimental data deviate from the ideal RTD of a Continuous Stirred Tank Reactor (CSTR) [28]:

$$E(\theta) = exp(-\theta) \qquad 5$$

In order to mathematically characterize and explain the deviation of real MBR fluid-dynamics from ideality, a 2-parameters model consisting of a CSTR with by-pass stream was adopted (refers to Figure 2 for a schematic representation).

The response of this model in terms of E(θ) is[28]:

$$E(\theta) = \frac{v_a}{v_a+v_b} exp\left(-\frac{v_a}{v_a+v_b}\theta\right) \qquad 6$$

where v_a is flowrate of the stream entering the reactor, and v_b is the flowrate of the stream by-passing the CSTR.

Model predictions well agree with experimental data assuming a 1mL/min bypass flowrate (v_b) while experimentally measured v_a was 19.4 ml/min. In terms of reactor diagnosis, it can be assumed that the hand-made assembly of PE hollow fibers in the membrane module resulted in the formation of small and limited peripheral regions where fluid follows preferential pathways. However, under the selected operating conditions, the bioreactor appears well mixed in the 95% of its volume.

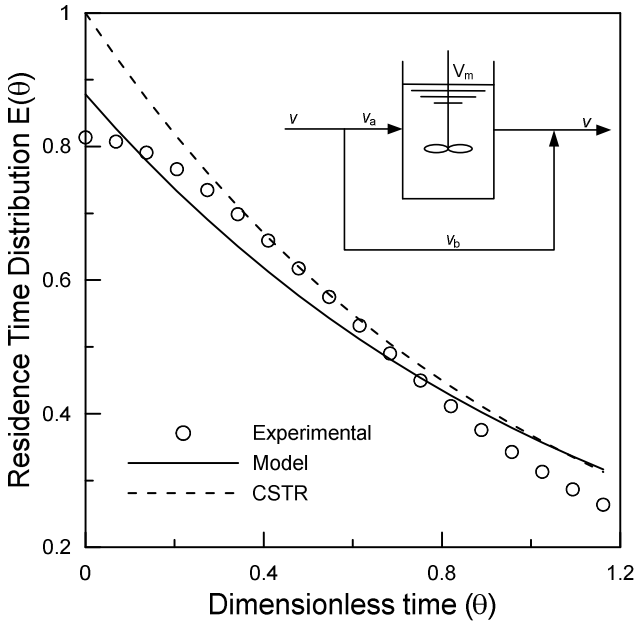

Figure 2: RTD of lab-scale side stream bioreactor (o: experimental points; solid line: 2-parameters bypass model; dotted line: ideal CSTR).

3.4.2. Microfiltration of OMWW with inert membrane

Microfiltration of OMWW was conducted on 0.40 μm pore size hydrophilic PE membrane in hollow fiber configuration, having a hydraulic membrane permeability of 360 L/m^2 h bar as determined from the slope of flux versus TMP curve. The flux reported in Figure 3 at each TMP, are average flux values after quasi steady state was achieved while operating the system in complete recirculation mode to avoid change in the feed water volume and concentration. Permeation data, recorded at different TMP once achieved a quasi steady value, illustrated that there was no increase in flux regardless for TMP higher than 1.2 bar, which clearly indicated an

early stage severe fouling. This is mainly attributed by the sensitivity of larger molecular weight cutoff (MWCO) membranes to internal pore blockage which offsets the enhanced driving force due to increased TMP [10, 26].

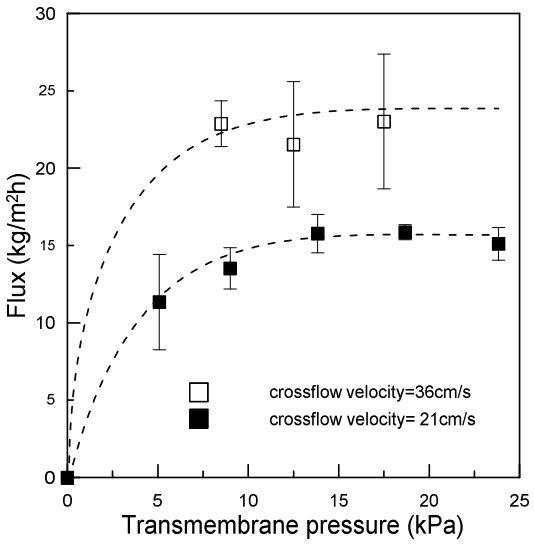

Figure 3: Influence of TMP and crossflow velocity during microfiltration of OMWW in a complete recirculation mode on PE membrane.

Figure 4 shows the dynamic response of permeate flux with time measured at crossflow velocities of 21 and 36 cm/s in a batch concentration mode. Filtration carried out at 36 cm/s lasted for 23 hours until a volume reduction factor (VRF), defined as the ratio of feed volume to retentate volume, of 2.4, beginning from 1000 mL feed volume. The experiments at 21cm/s lasted about six hours starting from 500 mL of feed volume. In Figure 3, due to recirculation of both concentrate and permeate to the feed tank, both constant volume and concentration were achieved. As a result it was possible to achieve a steady state flux after certain time for each TMP. On the contrary, for the experimental results shown in Figure 4, continuously reduced volume of the feed eventually increased the feed concentration. As a result continuously declining flux was observed.

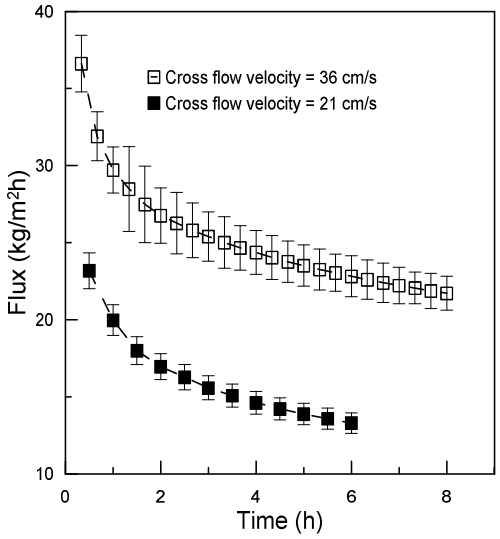

Figure 4: Influence of crossflow velocity at constant TMP of 0.1 bar during microfiltration of OMWW in batch concentration mode on PE membrane.

3.4.3. Microfiltration of OMWW hydrolyzed with free pectinase

A 500 mL of prefiltered OMWW was kept in contact with three different enzyme concentrations corresponding to enzyme-to-substrate ratio of 0.16, 0.08 and 0.04 (w/w), with a literature suggestion as the latter one being the optimal ratio [29]. The reaction proceeded at 40°C and pH 4.2 (optimal condition for the enzyme) under mild stirring for five hours [19, 30]. The whole mixture was then microfiltered at 36 cm/s and 0.1 bar. Based on Figure 5, the hydrolytic pre-treatment of OMWW with pectinase did not improve the process efficiency in terms transmembrane flux. Eventually, this was even reduced due to the enzymatic (protein) contribution to fouling process. Analysis of the unreacted pectin in the solution indicated that, after the release of the hydrolysis product at the initial stage, pectins were not converted. As a result, these pectins continued to accumulate on both surface and membrane pores, so limiting the flux in the subsequent MF of the enzyme treated solution. However, the relative decrease in flux up on use of excess enzyme-to-substrate ratio was mainly from the additional fouling layer attributed by the enzyme. The effect was more pronounced when an enzyme-to-substrate ratio of 0.16, which was for times higher than the optimal enzyme-to-substrate ratio was used.

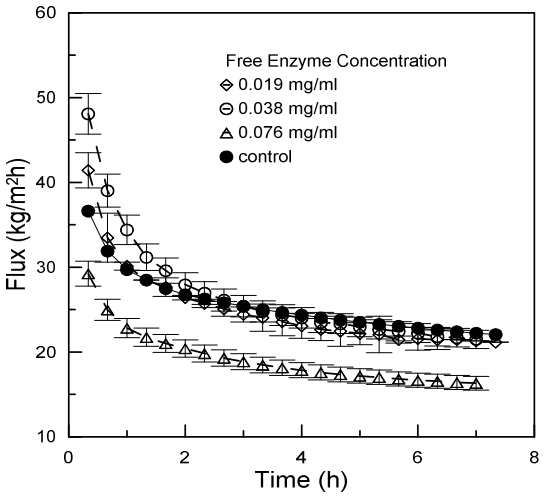

Figure 5: Effect of varying enzyme-to-substrate ratio on the permeate flux at 0.1 bar and 36cm/s crossflow velocity in batch concentration mode

3.4.4. Kinetic study of OMWW depectinization

To better understand the reason why there were unreacted pectins, kinetic studies have been performed in STR, which confirmed inhibition of the enzyme by the hydrolysis product. For the measurements of the kinetic parameters V_0, V_{max} and K_m, the STR was tested under three different substrate concentrations (0.1, 0.2, 0.3 mg/mL) keeping constant the enzyme concentration at 0.0092 mg/mL.

The STR bio-catalytic tests results, as reported in Figure 6, showed the concentration of galacturonic acid produced by pectins hydrolysis. Referring to the three curves presented, the concentration profile of galacturonic acid (Figure 6) in time, V_0 was calculated as the tangent to the curve in the linear range when the conversion is less than 5%, so that product concentration is negligible compared to substrate concentration.

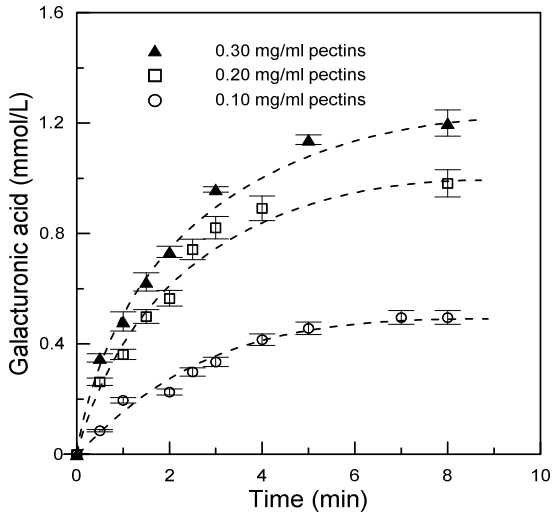

Figure 6: Evolution of galacturonic acid released from the hydrolysis of pectin as a function of time at 40°C reaction temperature, pH 4.2 and 0.0092 mg/mL enzyme concentration.

In the graph reported in Figure 7, the V_0 values and the corresponding conversion for different substrate concentrations are shown. Despite the higher reaction rate reached when the reactor was operated at the highest substrate concentration, the conversion revealed an opposite behavior. The overall conversions achieved were 63 %, 76 % and 83 % for 0.3, 0.2 and 0.1 mg/mL of substrate concentration, respectively. Therefore, additional experiments were carried out to study the effect of the product concentration on the reaction. For this purpose, two different galacturonic acid concentrations were initially added (0.2 and 0.3 mg/mL) to the reaction mixture containing 0.3 mg/mL substrate and 0.0092 mg/mL enzyme. Product formation was then monitored as a function of time. In Figure 8 it is clearly shown that the presence of galacturonic acid had a significant inhibition effect. This was more obvious looking at the decreasing trend of galacturonic acid released with increased amount of galacturonic acid added initially to the reaction mixture.

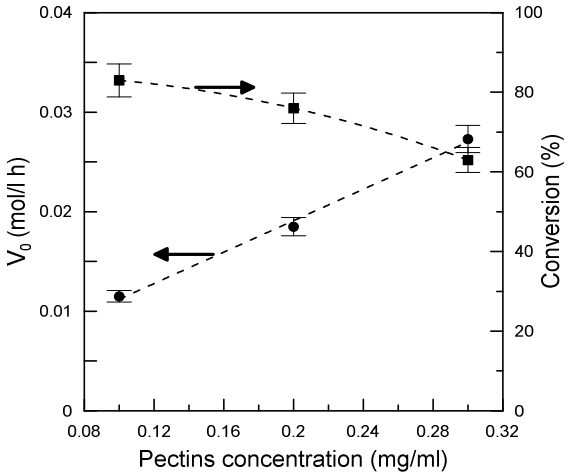

Figure 7: Initial reaction rate and degree of conversion for the three different substrate concentrations at 0.0092 mg/mL enzyme concentration, 40°C reaction temperature and pH 4.2.

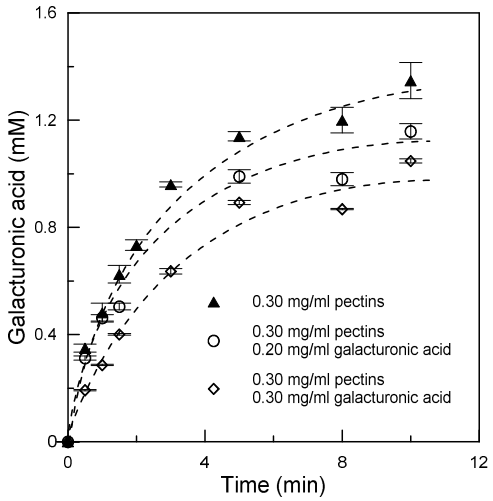

Figure 8 is inhibitory effect of galacturonic acid on the hydrolysis of pectin at 0.3 mg/mL substrate concentration and 0.0092 mg/mL enzyme concentration.

From the concentration profile of galacturonic acid produced, initial reaction rate was calculated and then plotted according to Lineweaver-Burk equation in Figure 9.

Figure 7 revealed that, with increased concentration of substrate, the degree of conversion decreased indicating a reaction limited by substrate or product coming from the hydrolysis of OMWW pectin [31]. It can be seen that the 1/V intercepts of all the lines in Figure 9 appeared convergent, which is typical for enzymatic reactions with product inhibitions. The calculated

inhibition constant (K_i= 0.33mg/mL) was less than K_m (0.51 mg/mL) indicating a high stability of enzyme-product complex. Similar behavior was also reported by Belafi-Bako and coworkers [17] using pure pectins as a substrate. The kinetic parameters K_m and V_{max} were 0.51 mg/mL and 0.07 M/h, respectively. These results were quite comparable with K_m and V_{max} found in literature [17, 29, 32]. For example the K_m obtained by Dinu and coworker [32] was 0.9 mg/mL at 40°C, pH 4.6 using enzyme pectinex on pure grade pectin as a substrate.

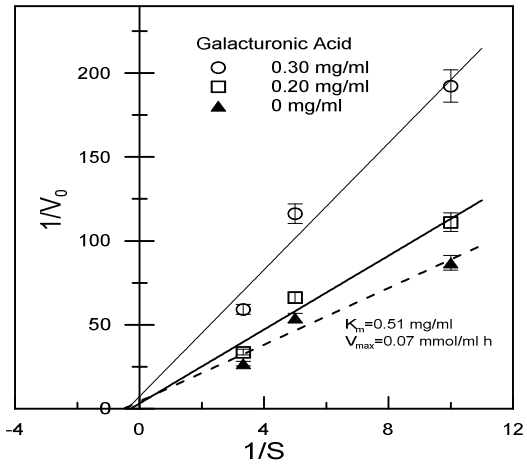

Figure 9: The Lineweaver-Burk plot for 0.3mg/mL pectin and galacturonic acid (0 mg/mL, 0.2 mg/mL, 0.3 mg/mL).

3.4.5. Microfiltration of OMWW through biocatalytically active membrane

Since the main reason for the worst performance with free enzyme membrane was due to enzyme product inhibition, the immobilization of the membrane is expected to improve the efficiency of the hydrolysis as a result of the continuous removal of product along with the permeate. Therefore, pectinase loaded membranes were prepared through covalent binding of the enzyme using glutaraldehyde as a bridge on the surface of PE HF membrane, which made the membrane itself biocatalytically active. In an alternative case (configuration d), instead of simple contact, permeation of the enzyme was also allowed to activate both the surface and pore of the membrane mimicking numerous micro-bioreactors working in parallel [33-34]. Amount of immobilized enzyme calculated based on equation (4) are reported on Table 5.1.

3.4.6. Surface immobilized biocatalytic membrane

After immobilizing a 0.54 g/m^2 enzyme on the surface of the membrane, it was possible to maintain 90% of the original pure water permeability. Then the prefiltered OMWW was permeated through the biocatalytic membrane at 0.1 bar TMP and 36 cm/s crossflow velocity in a batch concentration mode. Beginning from 300 mL feed solution, the VRF value was 3.3 while maintaining 60% of the initial permeate flux after 8 operating hours. In contrast to microfiltration of OMWW with free enzyme MBR or by inert membrane, the biocatalytically active membrane led to consistently greater permeate flux under the same hydrodynamic condition (Figure 10). The steady state flux value of the biocatalytically active membrane after 8 operating hours (30 kg /m^2 .h) was about 50% higher than the flux through the inert membrane. The degradation of pectins by the immobilized enzyme took place at the membrane-solution interface. This simultaneous conversion and selective permeation of product helped to limit inhibition and fouling, hence improving flux and overall membrane productivity. Since the early stage pore blockage made increasing TMP worthless during simple MF, experiments in the biocatalytically active membrane were conducted under the same TMP for fair comparison. This restricted the possibility of tuning the residence time of the immobilized enzyme MBR, which is highly determined by TMP.

Generally, membrane fouling and enzyme activity highly determine the efficiency of an enzymatic membrane reactor [33]. In the present case, the performance difference between the immobilized enzyme MBR and free enzyme MBR was mostly determined by enzyme product inhibition. According to Giorno and Drioli [35], combined selective mass transport with chemical reaction makes biocatalytic membrane reactors more interesting compared to conventional reactors for product-inhibited enzymatic reaction. Hence, the performance difference in terms of flux between immobilized enzyme MBR and free enzyme MBR has arised from the ability of immobilized enzyme MBR configuration to shield the enzyme from getting inhibited by the product.

In addition to flux, the different configuration has also resulted in different conversions (67% free enzyme MBR vs 34% immobilized enzyme MBR). The degree of conversion after 8 operating hours was calculated as the percentage difference between the initial feed and retentate pectin concentration. The value obtained in the free enzyme membrane reactor (67%) was close enough to the theoretical predicted degree of conversion based on the RTD analyses (73%)

according to method described in [21]. It is worth mentioning that, though not a general truth, there is always a tradeoff between stability and catalytic activity during enzyme immobilization. In addition, random covalent attachments have the disadvantage of reducing the active sites which were available for catalytic action. Therefore, the difference in degree of conversion obtained in STR and immobilized enzyme MBR might have arised from non-optimized amount of immobilized enzyme and non optimized residence time.

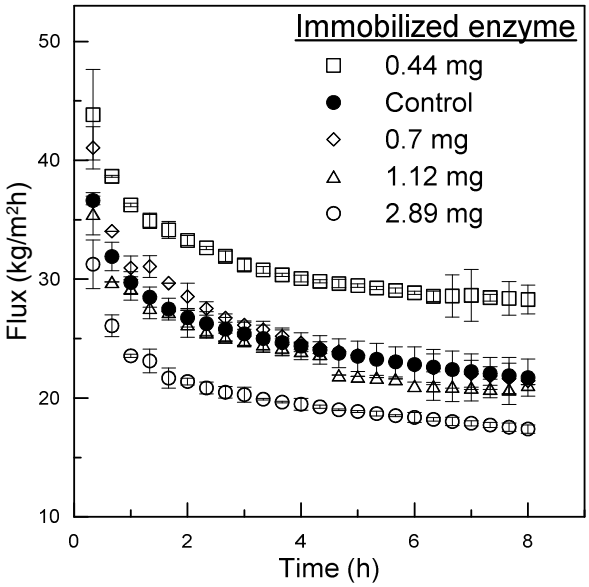

Figure 10: Flux trend over time for OMWW on inert membrane, surface activated membrane and both surface and pore activated membrane at 36 cm/s crossflow velocity and 0.1 bar TMP in a batch concentration mode.

3.4.7. Effect of enzyme concentration and site of immobilization

The maximum self cleansing capacity of the biocatalytically active membrane is greatly determined by the optimum enzyme concentration and site for immobilization. As previously observed, the highest extent of flux decline occurred at the beginning of the process, presumably due to early stage pore blockage. So, instead of immobilizing enzyme only on the surface of the membrane, both surface and pores were activated. This was done in order to check if activation of the membrane pores could enhance hydrolysis of pectins accumulating inside the pores. Therefore, three different initial enzyme concentrations (0.92, 1.23 and 1.84 mg/mL) were kept in contact with the surface and the pores of the membrane. As it was possible to verify through BCA test, the corresponding amount of immobilized enzymes were 0.91, 1.38 and 3.56 g/m^2,

respectively, for a constant volume of 21 mL enzyme solution. Figure 10 illustrates the profile of flux over time at 36 cm/s crossflow velocity and 0.1 bar for solo surface activated, surface plus pore activated and inert membranes. There was 40% difference in the amount of immobilized enzyme between the solo surface and surface plus pore activated membranes when starting from the same initial enzyme concentration and volume. Under any circumstance, the permeate flux dropped rapidly during the initial stage of the experiment, achieving the quasi steady-state flux value after about an hour. For the same initial enzyme concentration, compared to the surface plus pore activated membranes, the steady flux through solo surface activated membrane was higher by10 $kg.m^2.h$. The highest performance difference between the solo surface and surface plus pore activated membrane might have originated from the development of additional multilayer within the pores of the membrane apart from the surface [36].

Figure 10 also compares the flux measured at 36 cm/s and 0.1 bar through surface plus pore activated membrane under three different enzyme concentrations (0.91±0.05 g/m^2, 1.38±0.11 g/m^2 and 3.56±0.096 g/m^2). The pure water permeability loss after immobilization of 0.91, 1.38 and 3.56 g/m^2 of enzyme was 34%, 43.4±8.5%, 60.82±5.36% respectively.

According to Figure 10, fluxes were deteriorated by about 42, 53 and 48 %, respectively, before reaching a quasi steady state value; however, the quasi steady-state permeate flux for the highest enzyme concentration was 1.25 times lower than the one observed at the lowest enzyme concentration. The degree of conversion were found to be 44±10% for both 0.92 g/m^2 and 1.38 g/m^2 of enzyme loading, while decreasing to 16% for 3.56 g/m^2

3.4.8. Identification of major fouling mechanism

The impossibility of attaining a steady flux when system was operated in configuration a (Figures 3 and 4) proved that MF of OMWW was suffering from severe fouling. The 80% and 40% of pure water permeability loss after simple water wash and standard chemical cleaning, respectively, were also clear indicators of irreversible fouling. The presence of irreversible fouling during OMWW treatment was observed even on ceramic membrane at higher cross-flow rate [9, 12]. Time-variant linear regression analysis done at intervals of 0-1 hour, 2-7 hours, and 8-23 hours, resulted in an average R^2 value for CPB, IPB, SPB and CF of 0.95, 0.95, 0.96 and 0.95, respectively, thus confirming cake formation (CF) as the main fouling mechanism. Since more than 40% of the flux decline occurred in the first 40 minutes, it was imperative identifying

the dominating mechanism at this stage. The regression analysis on flux data of the first hour indicated that both CF and intermediate pore blocking (IPB) were equally responsible.

Table 3.1 summarizes the performance difference between inert and biocatalytic membranes based on cake resistance (α), membrane resistance (β) and MFI obtained from equation 1. The β value lied within a narrow range of variation as it is the membrane's intrinsic property. In the case of inert membrane, the cake resistance of the enzyme treated solution is approximately twice the value of the control solution. This result was in good agreement with the slightly lower permeate flux reported in MBR due to the additional fouling attributed by the enzyme itself. The enzyme treated solution gave 1.6 times higher MFI than the control solution on the inert membrane.

Table 3.1 also show a changing α and MFI value with different types of enzyme immobilization. The solo surface activated membrane's α value was 32% less than the inert membrane. Biocatalytically activated membrane with the lowest enzyme concentration gave the least MFI (0.007) for both solo surface and surface plus pore activated membranes. The overlying assumption of the cake resistance model, which α and MFI are derived from, is that performance is governed by cake filtration. In practice however, other factor could also affect the overall fouling resistance. The unexpected changing α and MFI with enzyme immobilization would therefore reinforce our earlier findings about fouling mechanism based on regression analysis that indicated flux decline was contributed by all kinds of fouling mechanisms. Hence, cake resistance model could be an oversimplification to represent the real scenario of the present BMR.

From the flux data given in the previous section and the different fouling mechanism analyses illustrated here, it can be generalized that membrane surface modification through immobilizing enzyme pectinase improved significantly the *in-situ* self cleaning capacity of the membrane. It is worth mentioning that all the experiments here were conducted considering the worst case scenario as a proof-of-concept: low TMP, laminar flow regime, random immobilization, and room temperature. These situations would suggest that the investigated system shows potential for further improvement and optimization to have better performance, especially in terms of transmembrane flux.

Table 3.1: Comparison of inert and differently activated biocatalytic membrane.

Membrane operation	Amount of free / immobilized enzyme (g/m^2)	X (%)	VRF	β	α	Membrane fouling index (MFI)
Biocatalytically active Membrane reactor	0.54 only surface	-	3.3	2.29	0.037 R^2= 0.96	0.007 R^2=0 .90
	0.91 surface plus pore	44	1.4	3.68	0.13 R^2= 0.93	0.007 R^2= 0.97
	1.38 surface plus pore	31	1.3	2.03	0.095 R^2= 0.98	0.022 R^2= 0.98
	3.56 surface plus pore	16	1.3	2.65	0.16 R^2= 0.97	0.020 R^2= 0.99
Membrane bioreactor	0.0092 mg/mL	63	1.6	2.08	0.09 R^2 = 0.96	0.024 R^2= 0.97
Simple microfiltration	OMWW without enzyme	-	1.4	2.78	0.054 R^2= 0.95	0.015 R^2= 0.99

3.5. Conclusion

The proposed process followed an engineered approach that combined both hydrodynamic and kinetic characterization of enzyme membrane bioreactor to handle the problem of fouling during the microfiltration of OMWW. Unlike the general trend observed in literature, the experiments took the bold step of realizing enzymatic membrane reactor on a real OMWW. The proposed intensified approach helped to develop an *in-situ* self-cleansing biocatalytically active membrane that control MF fouling promoted by pectins present in OMWW. The biocatalytically active membranes, functionalized with enzyme pectinase, gave 50% higher permeate flux compared to inert membrane. In conclusion, the concept of immobilized enzyme membrane reactor definitely paved the way to fouling free onsite integrated membrane process for valorization of olive mill wastewater.

3.6. References

[1] C. Gonçalves, M. Lopes, J.P. Ferreira, I. Belo, Biological treatment of olive mill wastewater by non-conventional yeasts, Bioresource Technology, 100 (2009) 3759-3763.
[2] S. Takaç, A. Karakaya Recovery of Phenolic Antioxidants from Olive Mill Wastewater, Recent Patents on Chemical Engineering, 2 (2009) 230-237.
[3] H. Dhaouadi, B. Marrot, Olive mill wastewater treatment in a membrane bioreactor: process stability and fouling aspects, Environmental Technology, 31 (2010) 761-770.
[4] S. Khoufi, M. Hamza, S. Sayadi, Enzymatic hydrolysis of olive wastewater for hydroxytyrosol enrichment, Bioresource Technology, 102 (2011) 9050-9058.
[5] R. Casa, A. D'Annibale, F. Pieruccetti, S.R. Stazi, G. Giovannozzi Sermanni, B. Lo Cascio, Reduction of the phenolic components in olive-mill wastewater by an enzymatic treatment and its impact on durum wheat (Triticum durum Desf.) germinability, Chemosphere, 50 (2003) 959-966.
[6] A. Agalias, P. Magiatis, A.-L. Skaltsounis, E. Mikros, A. Tsarbopoulos, E. Gikas, I. Spanos, T. Manios, A New Process for the Management of Olive Oil Mill Waste Water and Recovery of Natural Antioxidants, Journal of Agricultural and Food Chemistry, 55 (2007) 2671-2676.
[7] A. Roig, M.L. Cayuela, M.A. Sánchez-Monedero, An overview on olive mill wastes and their valorisation methods, Waste Management, 26 (2006) 960-969.
[8] A. El-Abbassi, M. Khayet, A. Hafidi, Micellar enhanced ultrafiltration process for the treatment of olive mill wastewater, Water Res, 45 (2011) 4522-4530.
[9] E. Garcia-Castello, A. Cassano, A. Criscuoli, C. Conidi, E. Drioli, Recovery and concentration of polyphenols from olive mill wastewaters by integrated membrane system, Water Res, 44 (2010) 3883-3892.

[10] E. Tsagaraki, H. Lazarides, Fouling Analysis and Performance of Tubular Ultrafiltration on Pretreated Olive Mill Waste Water, Food and Bioprocess Technology, 5 (2010) 584-592.
[11] C.A. Paraskeva, V.G. Papadakis, E. Tsarouchi, D.G. Kanellopoulou, P.G. Koutsoukos, Membrane processing for olive mill wastewater fractionation, Desalination, 213 (2007) 218-229.
[12] C. Russo, A new membrane process for the selective fractionation and total recovery of polyphenols, water and organic substances from vegetation waters (VW), Journal of Membrane Science, 288 (2007) 239-246.
[13] E.O. Akdemir, A. Ozer, Investigation of two ultrafiltration membranes for treatment of olive oil mill wastewater, Desalination, 249 (2009) 660-666.
[14] E. Drioli, M. Romano, Progress and New Perspectives on Integrated Membrane Operations for Sustainable Industrial Growth, Industrial & Engineering Chemistry Research, 40 (2001) 1277-1300.
[15] A. Cassano, C. Conidi, E. Drioli, Comparison of the performance of UF membranes in olive mill wastewaters treatment, Water Research, 45 (2011) 3197-3204.
[16] N. Demirel, I. Hakki Boyaci, M. Mutlu, Determination of kinetic parameters of pectolytic enzymes at low pectin concentrations by a simple method, European Food Research and Technology, 217 (2003) 39-42.
[17] K. Bélafi-Bakó, M. Eszterle, K. Kiss, N. Nemestóthy, L. Gubicza, Hydrolysis of pectin by Aspergillus niger polygalacturonase in a membrane bioreactor, Journal of Food Engineering, 78 (2007) 438-442.
[18] P. Lozano, A. Manjón, F. Romojaro, M. Canovas, J.L. Iborra, A cross-flow reactor with immobilized pectolytic enzymes for juice clarification, Biotechnology Letters, 9 (1987) 875-880.
[19] J.M. Rodriguez-Nogales, N. Ortega, M. Perez-Mateos, M.D. Busto, Pectin hydrolysis in a free enzyme membrane reactor: An approach to the wine and juice clarification, Food Chemistry, 107 (2008) 112-119.
[20] A.R. Szaniawski, H.G. Spencer, Effects of immobilized pectinase on the microfiltration of dilute pectin solutions by macroporous titania membranes: resistance model interpretation, Journal of Membrane Science, 127 (1997) 69-76.
[21] O. Levenspiel, Chemical Reaction Engineering, 3rd ed., John Wiley & Sons, Inc, New York, 1999.
[22] N. Blumenkrantz, G. Asboe-Hansen, New method for quantitative determination of uronic acids, Analytical Biochemistry, 54 (1973) 484-489.
[23] D. Demirel, I. Hakki Boyaci, M. Mutlu, Determination of kinetic parameters of pectolytic enzymes at low pectin concentrations by a simple method, European Food Research and Technology, 217 (2003) 39-42.
[24] J.E. Bailey, D.F. Ollis, Biochemical Engineering Fundamentals, McGraw-Hill, New York, 1986.
[25] H. Strathmann, L. Giorno, E. Drioli, An introduction to Membrane Science and Technology, Rende (CS), 2006.

[26] S. Mondal, C. Rai, S. De, Identification of Fouling Mechanism During Ultrafiltration of Stevia Extract, Food and Bioprocess Technology, (2011) 1-10.
[27] M. Mulder, Basic Principles of Membrane Technology Second Edition, Kluwer academic, 1996.
[28] K. Bélafi-Bakó, L. Gubicza, J. Mulder, Integration of Membrane Processes into Bioconversions, in, Kluwer Academic, 2000, pp. 252.
[29] N. Ortega, S. de Diego, M. Perez-Mateos, M.D. Busto, Kinetic properties and thermal behaviour of polygalacturonase used in fruit juice clarification, Food Chemistry, 88 (2004) 209-217.
[30] M. Pizzichini, C. RUSSO, Process for recovering the components of olive mill wastewater with membrane technologies in: E.P. Specification (Ed.), Italy, 2007.
[31] J.M. Rodríguez-Nogales, N. Ortega, M. Perez-Mateos, M.D. Busto, Operational Stability and Kinetic Study of a Membrane Reactor with Pectinases from Aspergillus niger, Journal of Food Science, 70 (2005) E104-E108.
[32] D. Dinu, M.T. Nechifor, G. Stoian, M. Costache, A. Dinischiotu, Enzymes with new biochemical properties in the pectinolytic complex produced by Aspergillus niger MIUG 16, Journal of Biotechnol, (2007).
[33] G.M. Rios, M.P. Belleville, D. Paolucci, J. Sanchez, Progress in enzymatic membrane reactors – a review, Journal of Membrane Science, 242 (2004) 189-196.
[34] K.F. Jensen, Microreaction engineering — is small better?, Chemical Engineering Science, 56 (2001) 293-303.
[35] L. Giorno, E. Drioli, Biocatalytic membrane reactors: applications and perspectives, Trends in Biotechnology, 18 (2000) 339-349.
[36] R. Mazzei, E. Drioli, G. Lidietta, Enzyme membrane reactor with hetrogenized beta glucosidase to obtain phytotherapic compund: Optimization study, Journal of Membrane Science, 390-391 (2012) 121-129.

Chapter 4: Nanoscale Tuning of Enzyme Localization for Enhanced Reactor Performance in a Novel Magnetic Responsive Biocatalytic Membrane Reactor

4.1. Abstract

The synergistic magnetic interaction between biofunctionalized magnetic nanoparticles and a hybrid membrane is exploited to develop a nano-inspired, magnetic-responsive enzyme membrane (micro)reactor. The novelty of the process lies in the use of superparamagnetic nanoparticles both as enzyme carrier to form bionanocomposites and as nanofiller to form organic inorganic (O/I) hybrid membrane to render both reversibly magnetizable. This reversible magnetic force facilitates dispersion of the enzymatically active magnetic nanoparticles (bionanocomposites) over the membrane surface, allows retention of the enzyme by a large pore, i.e. high-flux membrane and renders enzyme recovery after use very easy. The feasibility and versatility of the concept is demonstrated through 2 case studies, i.e. a pectin/polygalacturonase and an arabinoxylan/xylanase system, for membrane fouling prevention through in-situ enzymatic membrane cleaning. This robust multidisciplinary approach resulted in a 75% reduction in filtration resistance, thus realizing significant energy savings and high reactor productivity. The advantages of the novel approach include: i) absence of need for neither functionalized nor retentive membrane surfaces, ii) no leakage of nano-sized, high surface area immobilized enzymes through microporous membranes, iii) full recovery and re-usability of the enzymes, iv) possibility to apply enzyme cocktails to achieve optimal conversions, and v) use of the membrane beyond the enzyme life cycle.

This chapter is submitted to journal of membrane science as: **Gebreyohannes A. Y,** M. R. Bilad, T.Verbiest, C.Courtin, E.Dorenze, L.Gioro, E.Curcio, I.F.J. Vankelecom. Nanoscale Tuning of Enzyme Localization for Enhanced Reactor Performance in a Novel Magnetic Responsive Biocatalytic Membrane Reactor.

4.2. Introduction

Superparamagnetic Fe_2O_3 based nanoparticles (NP^{SP}) represent a versatile biocompatible nano-platform. Hence, colloidal dispersions of NP^{SP} surrounded by biocompatible coatings have attracted much interest for use in smart devices, sensors, catalysis, bio-separation, magnetic guidance, and targeted drug delivery [1-4]. When used for bio-magnetic separation after functionalization with for instance enzymes, they are often associated with long-term stability over multiple cycles and during storage, in addition to easy recovery from reaction mixtures [5].

The research on hybrid membranes, consisting of a polymeric matrix with incorporated NP^{SP}, holds many unexplored interesting avenues [6]. Their incorporation leads to stimuli-responsive "smart" polymeric membrane with magnetic properties that can be modulated in a reversible manner.

This study presents an innovative combination of these two NP^{SP} application fields to create a new type of efficient, magnetic-responsive enzyme membrane reactor. The NP^{SP} serves a dual purpose in the biocatalytic membrane (micro) reactors (BMRs) where super-paramagnetism is employed to tailor physical confinement of enzymes at the membrane surface, thus combining biocatalysis, superparamagnetic nanoparticles and superparamagnetic membranes during reaction.

Immobilization of enzymes on membranes to form BMRs is a typical example of process intensification which aims at hybridizing two or more traditional operations to make industrial production more efficient [7], since the coupling lowers chemicals and energy consumption, while increasing reaction yields and minimizing waste [8-10]. BMRs have been applied in different sectors e.g., in the pharmaceutical industry [11-12], in the production of bio-renewables [13], and in waste valorisation [14].

Similar approach was used in the previous chapter to alleviate the severe fouling occurred during MF of OMWW. By covalently immobilizing enzyme on PE MF membrane, upto 50% increase in quasi steady state transmembrane flux is achieved. However, in a prolonged run, membrane fouling and enzyme activity loss demand chemical cleaning of the membrane and enzyme make-up, respectively. Example in Figure a, the performance of the PE HF biocatalytic membrane of chapter 3 over three different cycles is illustrated. Although a stable performance was obtained

both in the 1st and 2nd cycles, the flux started to decrease continuously in the 3rd cycles possibly due to enzyme deactivation or oversaturation with foulants.

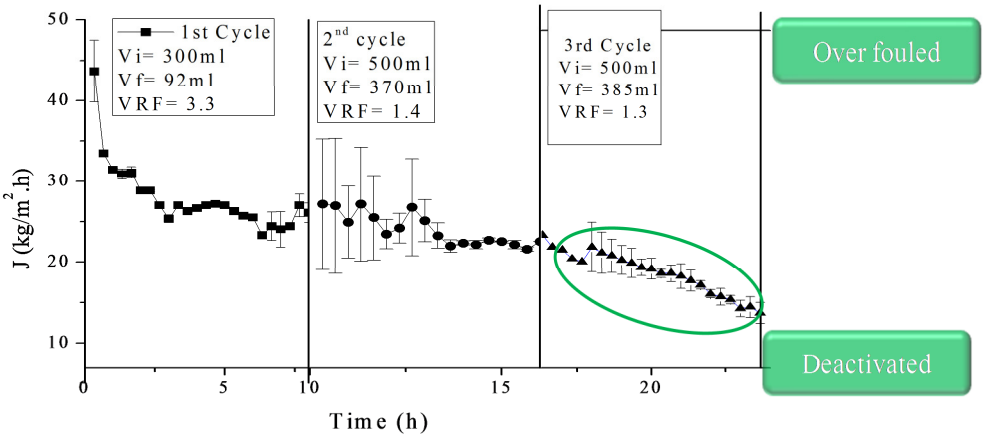

Figure a: Flux performance of biocatalytic PE HF membrane over three different cycles.

Since enzymes are loaded in conventional BMRs either by simple adsorption on the membrane or by covalent binding to the membrane, they are highly sensitive to chemical cleanings. In addition, when membrane immobilized enzymes get denatured or oversaturated, it is very difficult (if not impossible) to make-up fresh enzymes. Consequently, the ultimate fate of biocatalytic membranes is only disposal. Hence, a novel immobilization technique that fulfils the conditions of the BMRs, but still facilitates membrane chemical cleaning and enzyme make-up is urgently needed.

The aforementioned combination of enzyme functionalized superparamagnetic nanoparticles (bionanocomposites) and stimuli-responsive "smart" polymeric membrane is now suggested as the key to solve this bottleneck issue. Particularly, the appearance of the magnetic properties the NP^{SP} only in presence of an external magnetic field gives a high degree of freedom for reversible enzyme immobilization [15]. They can first be dispersed easily in a reactor in the absence of the magnetic field and readily moved to a desired location by switching the magnetic field on, while being removed later by switching it off again [6, 16].

Therefore, in this study, NP^{SP} are used as (1) support material for enzyme immobilization to form an enzyme immobilized superparamagnetic particles (Enz^{SP}) and (2) as filler in a hybrid membrane to form a superparamagnetic membrane (M^{SP}). Both the Enz^{SP} and the M^{SP} thus exhibit superparamagnetism which allows the Enz^{SP}, initially homogeneously dispersed in the bulk reaction mixture, to be attracted onto the M^{SP} surface. The synergies of the magnetic responsive M^{SP} and the Enz^{SP} enhance the formation of a dynamic layer of Enz^{SP} on the M^{SP}

surface. This Enz^{SP} layer can be considered as a specific reactor resulting from an array of microreactors formed by the voids between the NPs connected by magnetic forces. Their superparamagnetic properties can again be employed later on to recover the Enz^{SP} from the M^{SP} surface whenever the M^{SP} has for instance been severely fouled and needs chemical cleaning, or when the Enz^{SP} has been denatured, by simply switching off the external magnetic field. This novel approach, further referred as a superparamagnetic BMR (BMR^{SP}), offers a paradigm shift in addressing two of the most critical bottlenecks of BMRs currently hindering their widespread use: easy recycling of the enzyme, and extending the membrane working life cycle beyond the enzyme's active period.

As a proof-of-concept, the BMR^{SP} is applied in an *in-situ* enzymatic membrane cleaning for a pectin/polygalacturonase system, as encountered in a typical vegetation wastewater. The optimization of pectinase immobilization and the characterization of the M^{SP} were first carried out. The effectiveness of the BMR^{SP} system is then evaluated, including the effect of Enz^{SP} loading, reaction temperature, self-cleaning capacity, and Enz^{SP} reusability. In a second example, the BMR^{SP} is tested in an arabinoxylan/xylanase system, as typically used in bio-ethanol production or present in brewery and bakery wastewaters [17]. Ultimately, the effect of using a superparamagnetic enzyme cocktail is also evaluated.

4.3. Materials and methods

4.3.1. Materials

Dimethylformamide (DMF) was acquired from Arcos. Polyvinylidene fluoride (PVDF, 534 kDa), 2-cyanoacetamide, citrus fruit pectin (25-35% degree of esterification), polygalacturonase, galacturonic acid, sulfuric acid, sodium tetraborate, *m*-hydroxybiphenyl, and glycine were obtained from Sigma-Aldrich (Belgium); borate buffer solution (pH 9.2) from Fisher scientific; water extractable arabinoxylan (Mw= 300 kDa) and xylazyme AX tablets from Megazyme (Bray, Ireland), *Bacillus subtilis* XynA xylanase (Grindamyl H640) from Danisco (Copenhagen,Denmark),methoxy(polyethyleneoxy)-propyltrimethoxysilane (PEG Silane), (3-aminopropyl) trimethoxysilane (APTMS) from ABCR chemicals.

4.3.2. NP^{SP} synthesis

The NP^{SP} used as nanofillers during membrane preparation were PEG coated iron oxide nanoparticles with an average particle size of 8 nm. Analytical grade ferric chloride ($FeCl_3$) was

used as salt precursor, ethylene glycol as both solvent and reductant, and n-octylamine as capping agent. Typically, 37.5 mL ethylene glycol and 25 mL n-octylamine were transferred into a flask and heated to 150°C. In a beaker, 2.4 g $FeCl_3$ was dissolved in 10 mL ethylene glycol and 3.5 mL purified water. After dissolving the salt, the ferric iron solution was added slowly to the flask and further heated to reflux at 180°C for 24 h. The thermal decomposition of the $FeCl_3$ is frequently carried out in hot solvent containing surfactants e.g., n-octylamine, to control particles growth and prevent particle agglomeration [33-34]. A highly polar solvent, like ethylene glycol, is chosen since it can simultaneously serve as solvent and reducing agent, while it also provides enough hydrophilicity [18].

The n-octylamine coated nanoparticles 100 mg were then silanized by mixing with 1 mL methoxy(polyethyleneoxy)- propyltrimethoxy silane (PEG Silane) together with trace amounts of acetic acid to form dried PEG coated nanoparticles that can easily be redispersed in a desired solvent (e.g. water or DMF). The acetic acid acted as a catalyst for the hydrolysis and the condensation of silane groups on the particles surface and thus for the surface exchange reaction as a whole. The PEG silanized NP^{SP} that are dispersed in DMF were then used as nanofillers during membrane preparation (see section 4.4.3.2).

To enable the coupling of enzymes to the surfaces of NP^{SP}, instead of PEG, (3-aminopropyl) trimethoxysilane (APTMS) was used to introduce reactive amine groups on the surface of the NP^{SP}. This was achieved by reaction of 100 mg n-octylamine coated iron oxide nanoparticles that are dispersed in 100 mL methanol with 1 mL APTMS and 3 drops of acetic acid under sonication. A detailed description of the preparation and characterization of both the PEG coated and the aminated NP^{SP} is given elsewhere [19].

4.3.3. Membrane preparation and characterization

4.3.3.1. Reference membrane preparation

A flat sheet PVDF membrane was prepared on a polypropylene support (Novatex 2471, Freudenberg, Germany) using the phase inversion technique. A dope solution composed of (12%) PVDF in DMF was cast with a 0.25 mm wet thickness casting knife at 2.25 cm/s casting speed. After 30 s of evaporation, the cast film was immersed into coagulation bath containing demineralized water.

4.3.3.2. M^{SP} Preparation

To prepare the M^{SP}, dope solutions containing 12% PVDF in DMF were loaded with variable PEG coated NP^{SP} concentrations (0.08 to 0.5 w/w %). Before casting, sequential mechanical stirring using a custom-made mechanical rotator and a subsequent sonication were performed to uniformly mix and disperse the NP^{SP} in the dissolved polymer.

4.3.3.3. Clean water permeability and membrane rejection

The pure water permeability and the substrate rejection of the membranes were determined in a stirred ultrafiltration cell (Model 8050, Amicon) using a membrane coupon of 4.5 cm diameter (Figure 1a). A constant N_2 pressure was used to fix the transmembrane pressure (TMP) at 0.25 bar while stirring constantly at 275 rpm using a magnetic stirrer. An electronic balance recorded the amount of permeate collected per unit time. Both pectin and arabinoxylan retention capacities were determined by measuring their concentration in feed and permeate. Since the water flux measured between TMP of 0.25 to 5 bar increased linearly with an R^2 value of 0.9286, single pressure was then used to measure both water and pectin permeability. The permeability (L_p) and rejection (R) are defined as in Equation (1) and (2):

$$L_p = \frac{\Delta V}{A \Delta t TMP} \quad (1)$$

$$R = 1 - \frac{C_p}{C_f} \quad (2)$$

where ΔV is the filtration volume (L), A is membrane area (m^2), TMP is transmembrane pressure (bar), Δt the filtration time (h), C_f substrate concentration in the feed (g/L) and C_p substrate concentration in the permeate (g/L).

The pectin concentration both in the feed and permeate was measured according to the method proposed by Blumenkrantz and Asboe-Hansen [20]. This method, which involves acid hydrolysis of the pectin into galacturonic acid according to Ahmed and Labavitch [21], converts the uronic acid into a purple product with an absorbance at 520 nm. Detailed description of the method is provided in a previous work [22].

To quantify arabinoxylan, an acidic treatment was applied on the feed and permeates samples in order to hydrolyze arabinoxylan into its constituent monosaccharides, xylose and arabinose. These monosaccharides were then reduced and derivatized to alditol acetates according to the procedure of Englyst and Cummings and quantified using gas chromatography as described

previously [23].

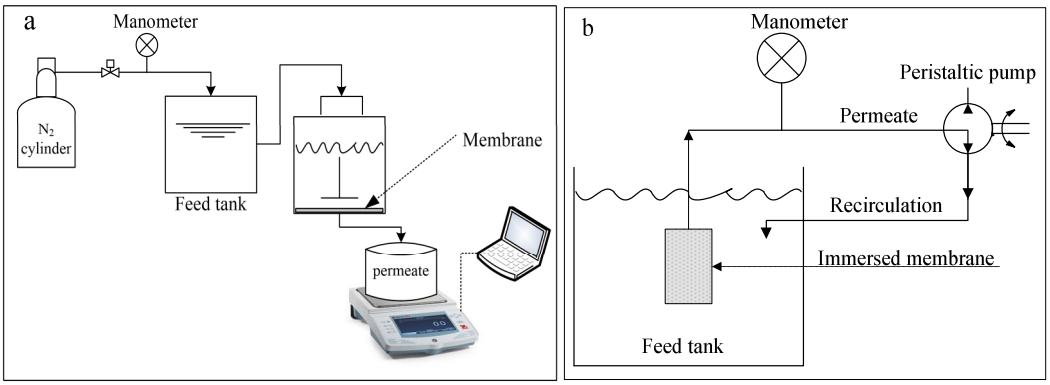

Figure 1: Schematic representation of a) a stirred dead-end filtration setup used to determine pure water permeability and substrate rejection capacity of membrane; and b) submerged membrane filtration system used for critical flux determination according to flux stepping experiment by immersing an envelope of membrane potted on an opposite side of a porous support in a 0.3 mg/mL pectin solution a step height of 2 L/m^2.h and step duration of 15 minutes were used.

4.3.3.4. SEM and EDX

The microstructures of plain membrane and the M^{SP} were observed by using scanning electron microscopy (SEM, Philips SEM XL30 FEG with Adax dx-4i system). The presence of NP^{SP} in the M^{SP} was analyzed further through energy dispersive X-ray spectroscopy via Fe/C ratio (EDX, integrated within the SEM apparatus).

4.3.3.5. Filtration tests

Fouling leads to a significant increase in the hydraulic resistance of membranes, manifested as a rise in TMP during constant flux operations. The critical flux, J_c, is therefore hypothesized as the flux below which a rise of TMP with time does not occur (subcritical flux), while above this value, the TMP rises significantly due to fouling [24]. Therefore, in the present case, constant flux experiments were conducted with a step height of 2 L/m^2.h and a step duration of 15 minutes to determine J_c. Constant flux experiment were chosen over constant TMP experiments, because the former one provides a better control over the material deposition on the membrane surface owing to the constant convective flow [25]. The constant flux was obtained by connecting a peristaltic pump to the outlet of permeate in a total permeate recycle mode (Figure 1b & Figure

3i). The test was performed using (0.3 mg/mL) of pectin solution dissolved in a sodium acetate buffer of pH 4.5 as feed. The TMP variations with step increments of flux were evaluated at each flux step using a manometer located along the permeate line.

4.3.4. Enzyme immobilization on aminated NP^{SP} to form Enz^{SP}

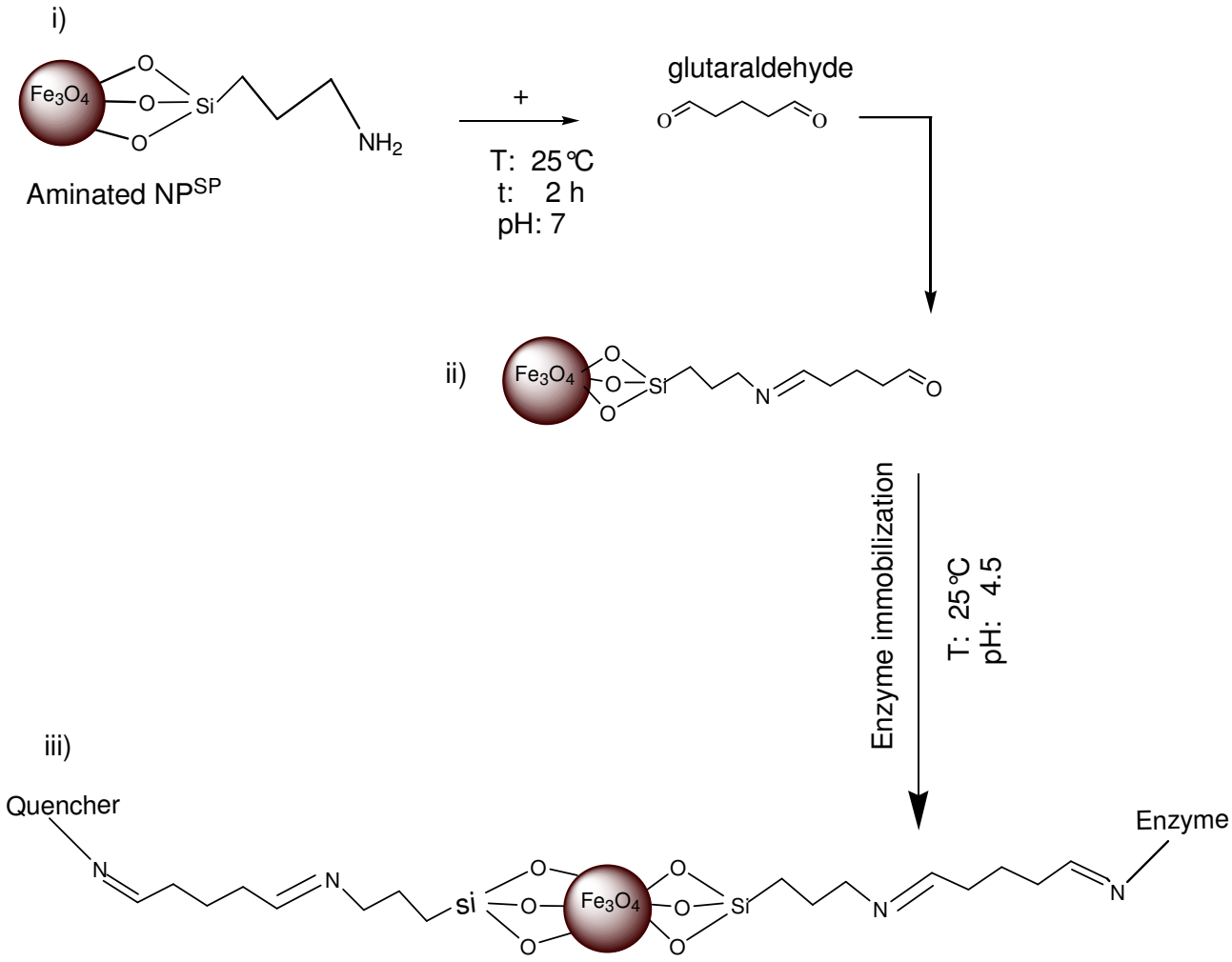

Figure 2: Schematic representation of: i) aminated NP^{SP} and covalent immobilization of glutaraldehyde, ii) NP^{SP} with terminal aldehyde iii) the covalent immobilization of enzymes on the glutaraldehyde activated NP^{SP} to form the Enz^{SP} and quenching of the excess glutaraldehyde with 1 M glycine.

All enzyme immobilizations were performed using glutaraldehyde as a crosslinker. A 2.4 mg of aminated NP^{SP} suspension in sodium acetate buffer 100 mM; pH 4.5 was washed three times

with deionized water before mixing with 0.8 mL of a 25% aqueous glutaraldehyde solution and stirring for 2 h at room temperature to introduce a terminal aldehyde functional group to the NP^{SP}. Non-reacted glutaraldehyde was removed by washing the particles with distilled water.

The aldehyde derivatized NP^{SP} were then mixed with different concentrations of polygalacturonase (EC232-885-6) dissolved in a sodium acetate buffer (pH 4.5, optimal for pectinase). Out of preliminary experiments, an immobilization time of 10 h was found to keep immobilized activity at maximum level.

The polygalacturonase concentration ranges from 0.009 mg/mL to 10 mg/mL in a 1.2 mL reaction volume. The enzyme and the NP^{SP} were reacted for 10 h at room temperature on a custom-made mechanical rotator to form biocatalytic superparamagnetic nanoparticles with immobilized pectinase ($Pect^{SP}$). The reaction was quenched with (1 mL; 1 M) glycine to block the excess activated aldehyde groups on the Enz^{SP} [26] (Figure 2).

For endo-β-1-4-D-xylanase, 1.2 mL of xylanase dissolved in sodium acetate buffer (pH 5, optimal for xylanase), was incubated with 2.4 mg of aldehyde derivatized NP^{SP} to form biocatalytic superparamagnetic nanoparticles with immobilized xylanase (Xyl^{SP}). The approximate initial concentration of the enzyme (measured with the BCA protein quantification kit) was about 10/mg mL. The reaction was quenched with (1 mL of 1 M glycine) to block the excess of active aldehyde groups on the Enz^{SP} [26].

Both $Pect^{SP}$ and Xyl^{SP} were then decanted using a permanent magnet to separate them from unreacted enzyme solution. Before storing them at 4°C in their respective buffers, none systematically attached enzymes were removed by washing the particles with their respective buffers. Post-coupling supernatant and pre-coupling enzyme solutions were kept in a refrigerator at 4°C to determine the coupling efficiency, according to the BCA protein quantification kit method (Sigma Aldrich) using BSA as standard.

4.3.5. Enzyme activity assay

4.3.5.1. *Polygalacturonase activity*

Native pectinase and $Pect^{SP}$ activities were assayed as reduced ends (galacturonic acid) forming activity by the 2-cyanoacetamide method [27]. The method is based on the Knoevenagel condensation reaction between an active methylene group of cyanoacetamide and the aldehyde group of the galacturonic acid to form an ultraviolet absorbing product [28]. Similar amounts of the coupled and free enzymes were incubated in 5 mL of 4 mg/mL pectin at 37°C and pH 4.5

under constant shaking for 1 h. A 2-Cynaoacetamide (1%, 1 mL) was added to 1 mL of hydrolysate that was magnetically decanted from the Enz^{SP} in 2 mL; 100 mM cold borate buffer of pH 9 and vortex mixed. The cold borate buffer helped for instantaneous termination of the enzymatic reaction. The mixture was then heated to 100°C for 10 min. After cooling down to room temperature, the absorbance at 274 nm was measured on a Shimadzu 1650PC spectrophotometer against distilled water. The concentration of galacturonic acid was calculated from the standard curve obtained by using galacturonic acid solutions at different concentration dissolved in the buffer 0.1-2 µM. Enzyme activity was defined as the amount of product obtained per unit time ($\mu M .h^{-1}$) at 40°C and pH 4.5.

4.3.5.2. *Xylanase activity*

The hydrolysis activity of both free xylanase and Xyl^{SP} was determined by using the colorimetric xylazyme method (Megazyme, Ireland). After 10 min pre-incubation of the enzyme at 40°C, a tablet consisting of azurine cross-linked arabinoxylan substrate was added. After 10 min incubation, the reaction was terminated by adding 10 mL of Tris base solution 1% w/v and instantaneous filtration through a 0.2 µm filter paper. The absorbance of the filtrate was measured in a Shimadzu spectrophotometer at 590 nm against distilled water.

4.3.5.3. *Enzyme reuse*

In order to assay the repeated use stability of the Enz^{SP}, a shaking flask experiment of $Pect^{SP}$ was performed with the following experimental conditions: substrate concentration 0.3 mg/mL, substrate volume 5 mL, reaction temperature 37°C, reaction duration 1 h and shaking speed 150 rpm. A $Pect^{SP}$ activated with 2.34 mg/ml of initial enzyme concentration was employed. Subsequent to incubation, the reaction mixture was magnetically decanted from the $Pect^{SP}$. The $Pect^{SP}$ were ready for the next incubation with fresh substrate after thorough washing with the working buffer to remove residues. These steps were repeated over ten consecutive cycles. The amount of galacturonic acid in the magnetically decanted supernatant was measured after each cycle according to the method described earlier.

4.3.6. Superparamagnetic biocatalytic membrane reactor (BMR^{SP})

4.3.6.1. *Experimental setup*

The M^{SP} prepared from 0.33 w/w % NP^{SP} (highest flux and lowest fouling propensity: results found from preliminary characterization was selected for the BMR^{SP} application. The Enz^{SP} were

confined on the surface of M^{SP} using a permanent magnet located at a certain distance below the membrane (outside the filtration cell). As a control, inert NP^{SP}, i.e. without immobilized enzyme, were dispersed on a similar membrane in a parallel experiment.

The system was operated in a continuous mode (See Figure 3) at a constant reactor volume of 500 mL and feed concentration of 0.3 mg/mL on 0.0078 m^2 membrane area. Due to mechanical limitations the maximum TMP our system can withstand is 150 mbar. Preliminary screening of different flux values indicated that 20 $L/m^2.h$ is the maximum flux, in which the system can be continuously operated for 8 h without exceeding 150 mbar, when 1 g/m^2 $Pect^{SP}$ is deposited.

As a proof-of-concept, it is of interest to operate the system under accelerated fouling conditions, presuming a worst case scenario. Therefore, taking the mechanical limitation and the desire to provide worst case scenario into consideration, the flux is fixed at 17 $L/m^2.h$, which is well above the critical flux 10 $L/m^2.h$. Permeate recirculation was avoided deliberately to prevent product inhibition of the enzyme [29]. All substrates were dissolved in their respective working buffers. Whenever elevated temperatures were desired, a heating coil was located 1 cm above the membrane surface to heat the feed continuously. Fouling resistance, manifested as a rise in TMP, was used to evaluate the system efficiency. In addition, permeates were sampled, and later analyzed to assay the activity of the enzyme. In between operation, the Enz^{SP} were detached from the membrane by simply manually removing the permanent magnet followed by gentle mixing. The NP^{SP} or the Enz^{SP} were thus freed from the M^{SP} surface, ready for use in a next experiment. In addition, any alteration in the membrane hydraulic resistance was further controlled by measuring pure water permeability before and after the filtration.

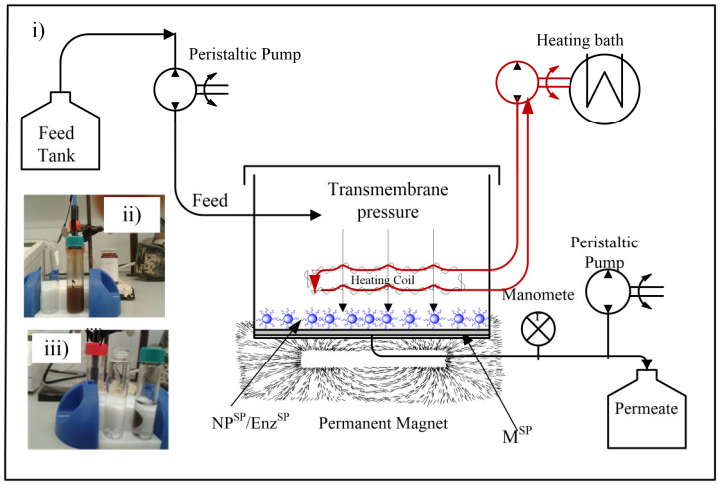

Figure 3: i) Schematic representation of a biocatalytic membrane reactor (BMR) using enzymes immobilized on superparamagnetic nanoparticles (Enz^{SP}) and a superparamagnetic mixed matrix membrane (M^{SP}) and inset Figure: ii) Solution containing Enz^{SP} dispersion in the absence of magnetic field and iii) permeate of BMR^{SP} and dispersion of Enz^{SP} in the presence of magnet showing the magnetic responsiveness of the Enz^{SP} and clear permeate solution due to the complete retention of the Enz^{SP} by the M^{SP}.

4.3.6.2. *Effect of temperature and immobilized enzyme loading*

The effects of reaction temperature and enzyme loading were tested for the arabinoxylan/Xyl^{SP} and pectin/$Pect^{SP}$ systems, respectively. For the former, the Xyl^{SP} loading was 8.4 mg of xylanase on 9.6 mg of NP^{SP}, operated at 40°C or 25°C using an arabinoxylan feed concentration of 0.3 mg/mL. For the latter, the $Pect^{SP}$ loadings were 8.4 and 16.8 mg of pectinase on 9.6 and 19.2 mg NP^{SP} (twice the concentration of xylanase to obtain equal activity), operated at 40 °C with a feed pectin concentration of 0.3 mg/mL.

4.3.6.3. *Long-term stability*

To evaluate the long-term stability of the proposed system, filtration tests comprising 5 consecutive cycles (each lasting 8 h) were carried out. For the pectin/$Pect^{SP}$ system, the pectin feed concentration and $Pect^{SP}$ loading were 0.3 mg/mL and 8.4 mg pectinase on 9.6 mg NP^{SP} at 40°C, respectively. For the arabinoxylan/Xyl^{SP} system, the wheat arabinoxylan concentration, temperature, and Xyl^{SP} loading were 0.3 mg/mL, 25°C and 8.4 mg respectively. For both substrate/Enz^{SP} systems, subsequent to each cycle, the systems were relaxed overnight with the

Enz^{SP} on the membrane at room temperature. This is presumed to help in degrading the oversaturated foulants and make the Enz^{SP} free for the subsequent cycle.

4.3.6.4. *Mixed substrate/foulants*

The possibility of using the novel concept to treat more complex systems, typically wastewaters containing different types of foulants was evaluated using a mixture of two different Enz^{SP}. Thus, 9.6 mg and 19.2 mg of Enz^{SP} containing 8.4 mg of xylanase and 16.8 mg of pectinase, respectively were uniformly dispersed on a fresh M^{SP}. The system was fed with 0.3 mg/mL of wheat arabinoxylan and pectin mixed in an equal ratio at 40°C.

4.4. Results and discussion

4.4.1. Membrane characterization

4.4.1.1. SEM images and EDX spectra

Both surface and cross-sectional SEM images of a PVDF/PP reference membrane (a) and a MMM with 0.33 w/w % NP^{SP} loading (b) were recorded on three different membrane samples at several spots (Figure 4). Both membranes exhibited good membrane integrity showing a typical asymmetric cross-sectional morphology with a denser top layer [30]. Upon inclusion of the nanoparticles, no significant changes in the membrane structure could be observed.

By comparing the EDX spectra (Figure 4c) of the reference and the 0.33 w/w % loaded M^{SP}, the M^{SP} however showed a prominent iron peak, arising from the inclusion of the NP^{SP} in the polymer matrix. The observed EDX spectrum matches well with the EDX spectrum of bare NP^{SP} reported in literature [31]. The resulting Fe/C ratio from the EDX elemental analysis also systematically increased with increasing NP^{SP} loading (0.77, 0.81, 1.03, 1.05, and 1.14 for 0.08, 0.17, 0.25, 0.33 and 0.5 w/w % NP^{SP} loading, respectively).

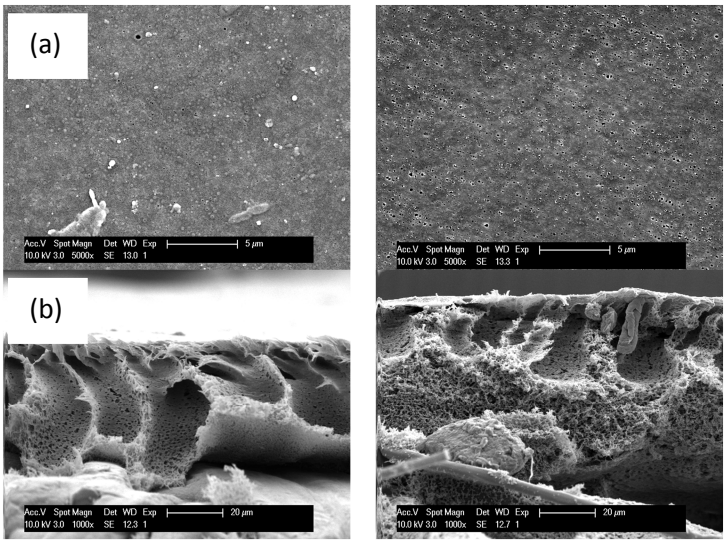

(c) Reference

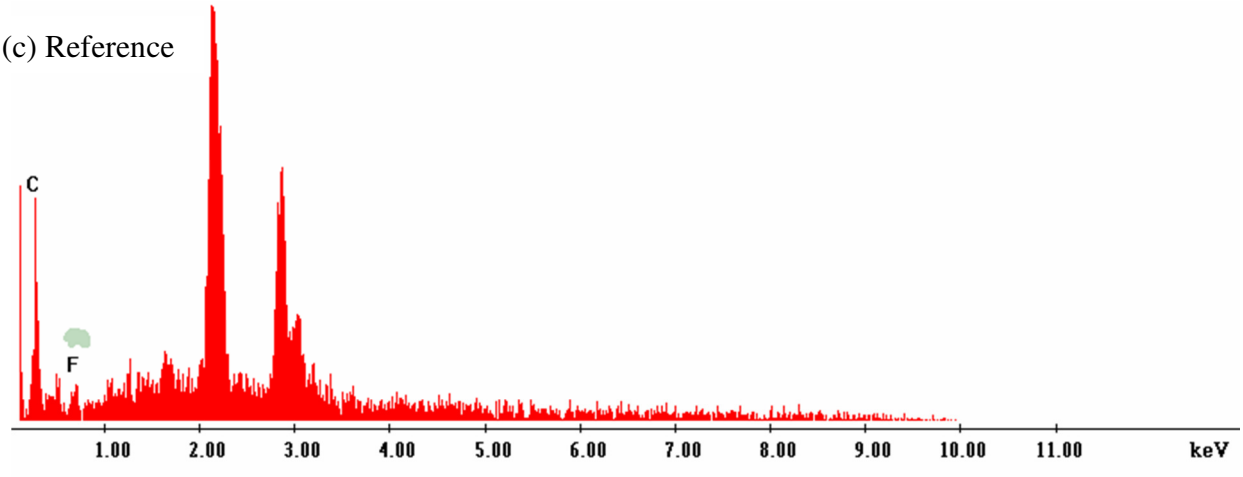

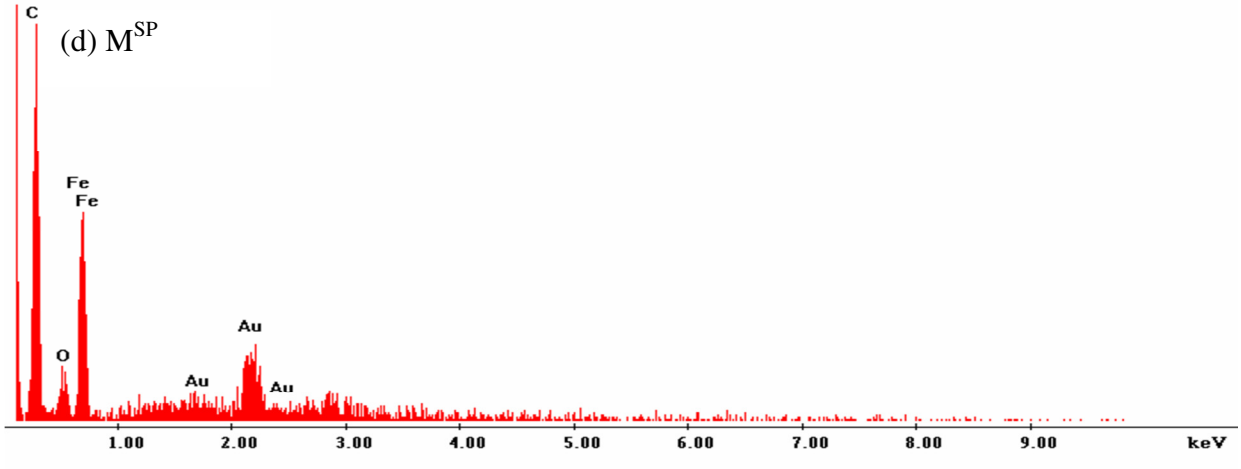

Figure 4: Surface (a) and cross-sectional (b) SEM morphology of reference (left) and M^{SP} (right) membrane, showing absence of a significant change in the membrane morphological structure due to presence of NP^{SP} layer in the polymer matrix and (c) EDX spectra of reference and d) EDX spectra of 0.33 w/w % M^{SP} indicating inclusion of ferric particles in the polymer matrix resulted in a prominent peak related that is related to Fe.

4.4.1.2. Clean water permeability, pectin retention and critical flux

Despite the similar morphologies observed in SEM, the reference and the O/I hybrid membrane behaved differently in filtration, reflecting the different kinetics and thermodynamics of the phase inversion process induced by the presence of the NP^{SP} during the membrane formation process. Pectin retention by the M^{SP} increased progressively from 57% to 90% when increasing the NP^{SP} loading in the membrane, while the pure water permeability of the O/I hybrid membrane somewhat lowered (see Table 4.1). A similar reduction in water permeability was also observed by Daraei et al. when preparing Fe_3O_4/PES O/I hybrid membrane [6]. Nonetheless, the permeability of a 0.3 mg/mL pectin solution in a stirred dead-end filtration cell measured at 0.5 bar increased from 150 L/m^2.h.bar for the reference membrane to 348 L/m^2.h.bar for the M^{SP} (0.5 w/w % NP^{SP} loading). This can possibly be ascribed to better antifouling properties of the M^{SP} in turn attributed to the presence of PEG coated NP^{SP} that changed surface chemistry of the M^{SP}. Moreover, inclusion of the PEG coated NP^{SP} lowered the membrane pore size from 0.4 µm to 0.2 µm (SEM image analysis). This might also reduced the amount of pectin that could

penetrate through the porous structure to cause internal fouling (see increased pectin retention in Table 4.1). Overall, the inclusion of the NP^{SP} in the polymer matrix thus served an additional, even though untargeted, purpose of enhanced antifouling.

Table 4.1: Characterization of PVDF membranes with different amount of nanoparticle loading using pure water permeability, pectin containing simulated wastewater permeability and pectin retention.

NP^{SP} loading (wt %)	**$L_{p,w}$ ($kg/m^2.h.bar$)**	**$L_{p,v}$ ($kg/m^2.h.bar$)**	**Pectin retention (%)**
0	3733	150	57
0.17	2680	-	92
0.33	2179	323	82
0.50	-	348	90

The pure water permeability reported here are without any prior compaction.
$L_{p,w}$: water permeability and $L_{p,v}$: pectin containing solution permeability measured at 0.5 bar once the linearity between applied TMP and water flux was confirmed in the range of 0.25 to 5 bar.

Results of a typical flux stepping experiment revealed a J_c value of 10 $L/m^2.h$ for M^{SP} with 0.33 w/w % loading in both configuration represented in Figure 1b and Figure 3. Beyond this flux, severe membrane fouling occurred, as manifested by a dramatic rise in TMP (Figure 5).

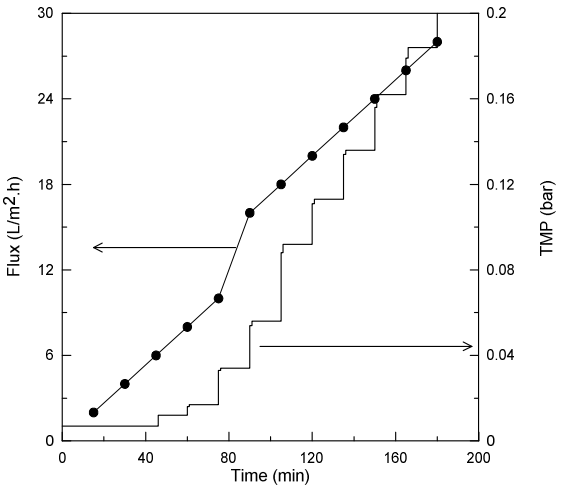

Figure 5: Critical flux determination of the M^{SP} (0.33 % loading) by using an initial flux of 2 L/m^2.h, a step height of 2 L/m^2.h and a step duration of 15 minutes at constant feed concentration of 0.3 mg/mL and at constant feed volume.

4.4.2. Enzyme immobilization on the NP^{SP}

4.4.2.1. Effect of enzyme/NP^{SP} ratio

The enzymes were covalently linked to the NP^{SP} in a two-step process involving glutaraldehyde activation and enzyme immobilization (Figure 2). Figure 6a shows the activity of the $Pect^{SP}$ as a function of initial mass of enzyme per mg of NP^{SP} used to form a range of $Pect^{SP}$ in a 1.2 mL reaction mixture. The assay indicated that the activity of covalently attached enzyme (Pec^{SP}) increased with an increased amount of immobilized pectinase per milligram of NP^{SP} (Figure 6a). The covalently linked pectinase retained roughly 60% of the activity of similar amount of free enzyme, as measured using a 5 mL of 4 mg/mL pectin solution at 37°C. Such loss in activity could arise from over estimation of the amount of enzyme immobilized on the NP^{SP}. Apart from this, loss in enzyme activity after covalent bonding is common since covalent immobilization mostly causes 3-D conformational distortion of the enzyme due to the high glutaraldehyde reactivity [32].

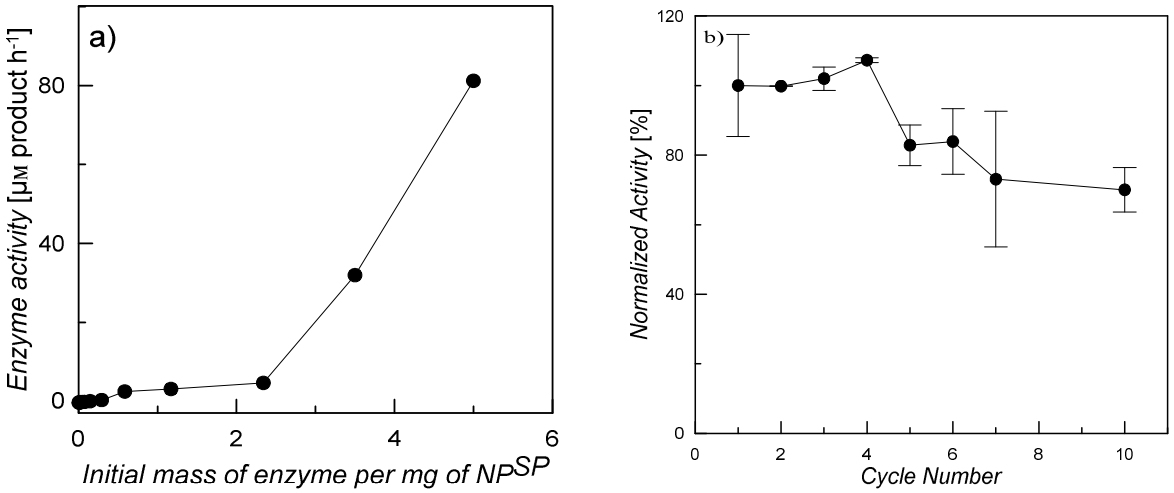

Figure 6: a) Activity at 37°C of immobilized enzyme incubated with a range of initial enzyme concentrations on 2.4 mg NP^{SP} in a 10 mL reaction flask tested using a 5mL and 4 mg/mL pectin solution under constant shaking at 150 rpm, b) reuse stability of the $Pect^{SP}$ on 2.4 mg NP^{SP} activated with 1.2 mL a 2.34 mg/mL enzyme solution. The $Pect^{SP}$ was incubated with 4 mg/mL pectin solution at 37°C for one hour under constant shaking at 150 rpm for 10 consecutive cycles with intermediate magnetic isolation of the reaction product and washing to avoid residual effect to the subsequent cycle

4.4.2.2. Repeated use stability

Since the ability to retain the enzyme activity and to reuse the immobilized enzyme over several cycles is an essential and critical feature of immobilized enzymes, the stability of the immobilized enzyme was studied in batch with a very easy magnetic isolation in between each batch, realized by simply contacting an external permanent magnet with the wall of the flask (see inset of Figure 3). The residual activity of the $Pect^{SP}$ (Figure 6b) after each cycle was normalized to the initial value. As anticipated, the superparamagnetic properties and the enhanced stability of the immobilised enzyme were in favour of efficient multiple cycles of magnetic isolation and reuse. Although the activity of $Pect^{SP}$ started to decrease after the 4^{th} cycle, more than 65% of its initial catalytic activity was still retained after 10 consecutive cycles. According to Johnson et al., [33]., immobilizing enzymes on highly curved surfaces, such as the present NP^{SP}, helps to maintain stability due to prevention of protein-protein lateral interactions which would otherwise lead to denaturation. The slightly decreased activity after 10 cycles may be caused by various reasons, such as aggregation of particles, enzyme denaturation and loss of some particles during

the multiple step washing or magnetic isolation [34].

4.4.3. BMR^{SP} for membrane surface cleansing

4.4.3.1. Effect of enzyme concentration

An important feature of the developed hybrid system is the reduction of filtration resistance through *in-situ* degradation of deposited foulants by the dynamic layer of Enz^{SP} and its effects on creating a membrane with a self-cleaning capacity. This phenomena avoids or at least reduces the frequency of harsh chemical membrane cleanings which are expensive, decrease the membrane lifetime and lead to significant downtime of the filtration process [35-36].

Figure 6 exhibits the TMP trend of a continuous filtration that went on for 8 h in a pectin/Pect^{SP} system. Due to a continuously growing filtration resistance by the pectin that is convectionally transported towards the membrane surface, the TMP over the control system containing a 1 g/m^2 non-functionalized NP^{SP} layer reached 0.165 bar at the end of the filtration. In contrast, owing to the *in-situ* degradation of the pectin by the immobilized enzyme and simultaneous separation of its hydrolysis product, the TMP of the BMR^{SP} containing a 1 g/m^2 Pect^{SP} layer was restricted to 0.102 bar at the end of filtration. By doubling the amount of Pect^{SP} (2 g/m^2) present on the membrane surface, the TMP at the end of filtration could be significantly further reduced (0.044 bar). The increased thickness of the Pect^{SP} layer may act as a dynamic membrane, thus increasing the filtration resistance to some extent, as indicated by the slightly higher initial TMP of the system with high Pect^{SP} loadings. Nevertheless, filtration under such circumstances still clearly reduced fouling once the enzymatic action got fully started.

In membrane operation, in general, the necessity to fix flux well below the critical flux in order to limit fouling might make processes economically not viable [25]. In the present system however, due to the effective *in-situ* foulant degrading capacity of the Pect^{SP}, and the simultaneous permeation of hydrolysis product through the membrane pores to avoid enzyme-product inhibition [29, 37], it was possible to operate the system at 17 L/m^2.h, which was well above the measured critical flux of 10 L/m^2.h without facing severe filtration resistance.

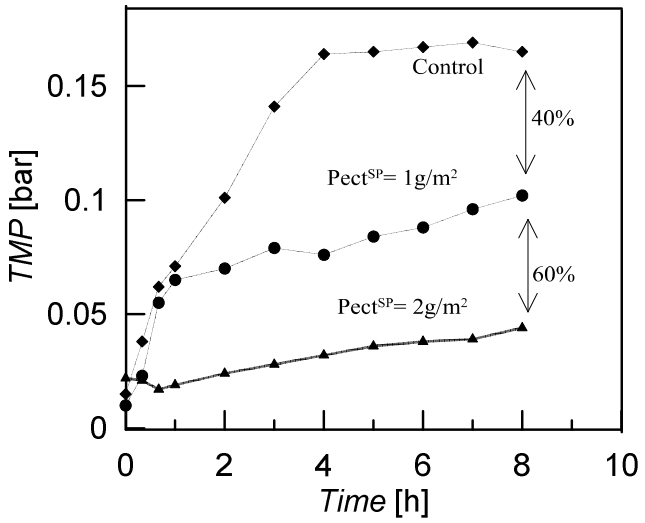

Figure 7: Evolution of TMP during the filtration of 0.3 mg/mL pectin through a layer of 1 g/m^2 neautral NP^{SP} layer as a control and a BMR^{SP} containing 1 g/m^2 or 2 g/m^2 Pect^{SP} layer at 40°C, pH 4.5 and a fixed flux of 17 L/m^2.h.

4.4.3.2. Effect of temperature

Enzymatic hydrolysis of cellulosic material to generate fermentable reducing sugars has huge potential in meeting global food and energy demand via biological routes. Especially combination of this biocatalysis with membrane separation would definitely benefit from simultaneous production, purification and concentration of the sugars. Xylanases are one of these potential enzymes that are typically involved in the hydrolysis of lignocellulosic biomass as a pre-treatment in the production of biofuels [38]. Thus the performance of the system was evaluated further in a xylan/xylanase system, extending the proof of principle of the BMR^{SP} beyond the above illustration of membrane fouling reduction during wastewater treatment.

Therefore, 9.6 mg of NP^{SP} loaded with 8.4 mg xylanase was applied during a filtration experiment to form an arabinoxylan/Xyl^{SP} system. Figure 8a-b shows the performance of the system at 25°C and 40°C while keeping feed volume and concentration constant. Due to *in-situ* degradation of the high-molecular weight arabinoxylan into easily permeable sizes, the system showed a 75% reduction in membrane filtration resistance at 40°C (Figure 8a). In contrast, it took about 4 h before the enzyme had sufficiently hydrolyzed the foulants into permeable sizes at 25°C due to the much reduced activity of the enzyme at this temperature. Nevertheless, a substantial reduction in filtration resistance of 40% was observed at the end of the filtration at

25°C compared to the control experiment (Figure 8b). The reactor productivity from analysis of the total permeable sugar in the permeate was 9.35 g/m^2.h.

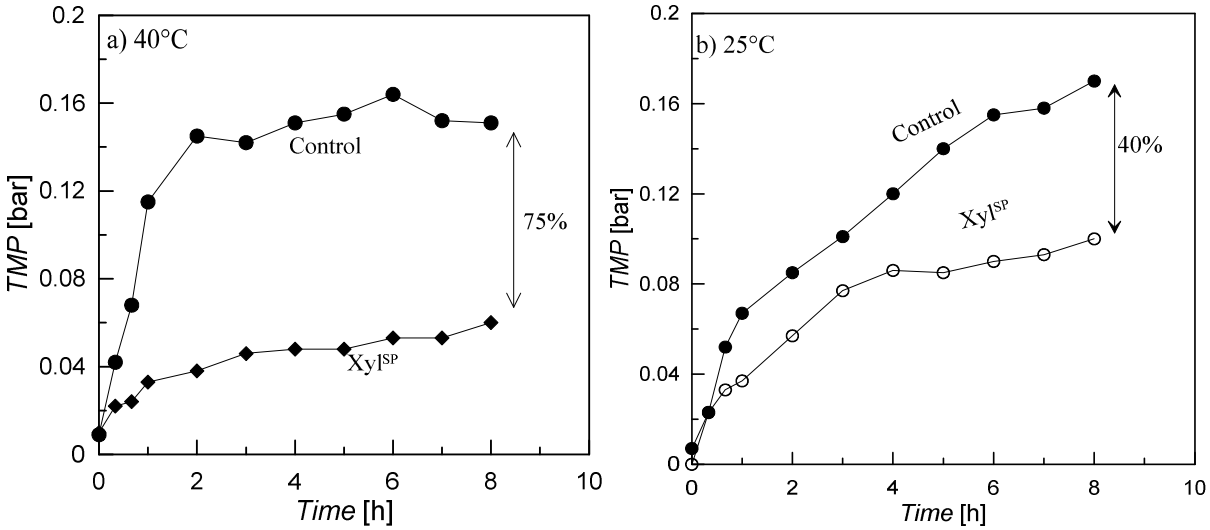

Figure 8: Effect of presence of Xyl^{SP} on TMP during the filtration of 0.3 mg/mL wheat arabinoxylan at a constant flux of 17 L/m^2.h, compared to a system operated without enzyme: a) at 40°C and b) at 25°C.

4.4.3.3. Long term stability of the BMR^{SP}

The cycling stability of the Xyl^{SP} during continuous filtration of 0.3 mg/mL arabinoxylan at 25°C is exhibited in Figure 9a. Results showed that the TMP after 8 h of continuous filtration and foulant deposition was limited to 0.1 bar during the 1st and 2nd cycle filtration. However, a slight and progressive performance loss was also observed cycle after cycle. This increase in TMP with increasing cycle number could be correlated to the occurrence of local structural changes in the immobilized enzyme, resulting in a regional collapse and compaction of the Enz^{SP} layer [39]. Moreover, the system is operated in the supercritical flux regime, where mass transfer rate might prevail over reaction rate. Consequently, the enzymes might get oversaturated with foulants and might become isolated from newly arriving foulants. Hence, the enzymes are "deactivated" in appearance giving TMP hysteresis over the five cycles. Yet, the observed TMP was low enough to enable an 8 h continuous filtration over 4 consecutive cycles without a major hurdle.

For the Pect^{SP} system operated at 40°C (Figure 9b), an extensive reduction in filtration resistance was observed in the first cycle. This significant performance improvement over the control

system however was followed by a sudden rise in the TMP in the subsequent cycles. This may be mainly attributed to enzyme deactivation due to extended exposure to higher temperatures, as further explained in the supplementary information.

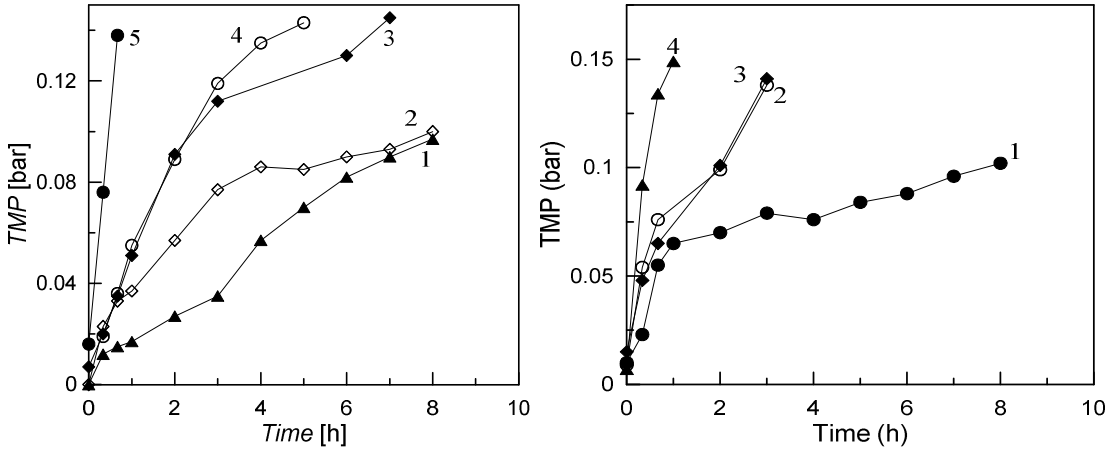

(a) (b)

Figure 9: Operational stability of a) Xyl^{SP} (0.3 mg/mL wheat arabinoxylan feed, 17 L/m^2.h flux at 25°C) and b) $Pcet^{SP}$ (0.3 mg/mL pectin, 17 L/m^2.h flux at 40°C). Numbers on the Figure represent the cycle number.

4.4.3.4. Mixed substrates/foulants

A blend of Xyl^{SP} and $Pect^{SP}$ was magnetically attracted to the membrane surface as a representative example of a mixture of an enzyme system treating a more complex feed. Effecting multiple enzymatic reactions in a single stage BMR by using a blend of different Enz^{SP} could actually facilitate process intensification by avoiding the need for multistage BMRs e.g. to treat fouling of mixed wastewaters, to enzymatically hydrolyze complex sugars [40-41], to enhance the efficiency of an enzyme by the *in-situ* generation of its substrate, to remove undesired by-products of an enzymatic reaction etc [9]. Figure 10a represents the TMP dynamics while feeding a mixture of pectin and arabinoxylan at 40°C. Here again, the TMP curve of the mixed BMR^{SP} loaded with mixtures of Xyl^{SP} and $Pect^{SP}$ magnetically attracted to the M^{SP} surface laid well below that of a parallel M^{SP} control system due to the excellent membrane cleansing potential of the enzyme blend. The proposed BMR^{SP} concept thus also proved successful in tackling complex foulant mixtures.

In addition, a two step filtration experiment of the mixed substrate system was conducted by

using a bare M^{SP} (i.e. without forming a dynamic layer) for the first 3 h, followed by dispersion of an Enz^{SP} layer on the formed foulant layer. After arriving at a TMP of 0.12 bar during the first 3 h, the mixture of $Pect^{SP}$ and Xyl^{SP} was thus dispersed in the reactor and adhered to the fouled membrane by bringing the external magnet underneath the membrane module. The filtration of the mixed substrate was then extended on the same membrane for another 8 h (Figure 10b). In such configuration, the idle part of the attached enzymes in direct contact with the M^{SP}, hence normally not facing any substrate, would now work its way downward through the layer of the already existing foulants, while the immobilized enzyme facing the feed side will act on the newly depositing foulants. Figure 10b showed that the rate of fouling (based on the slopes of the corresponding fitted lines) in the first 3 h while filtering the mixed foulant over the bare M^{SP} (0.015 bar/h) was much greater than the rate of fouling while filtering the mixed foulant on the dynamic layer (0.032 bar/h). This improvement in the rate of fouling was owing to the upward and downward degradation of foulants by the enzymatically active NP^{SP} layer (5-11 h).

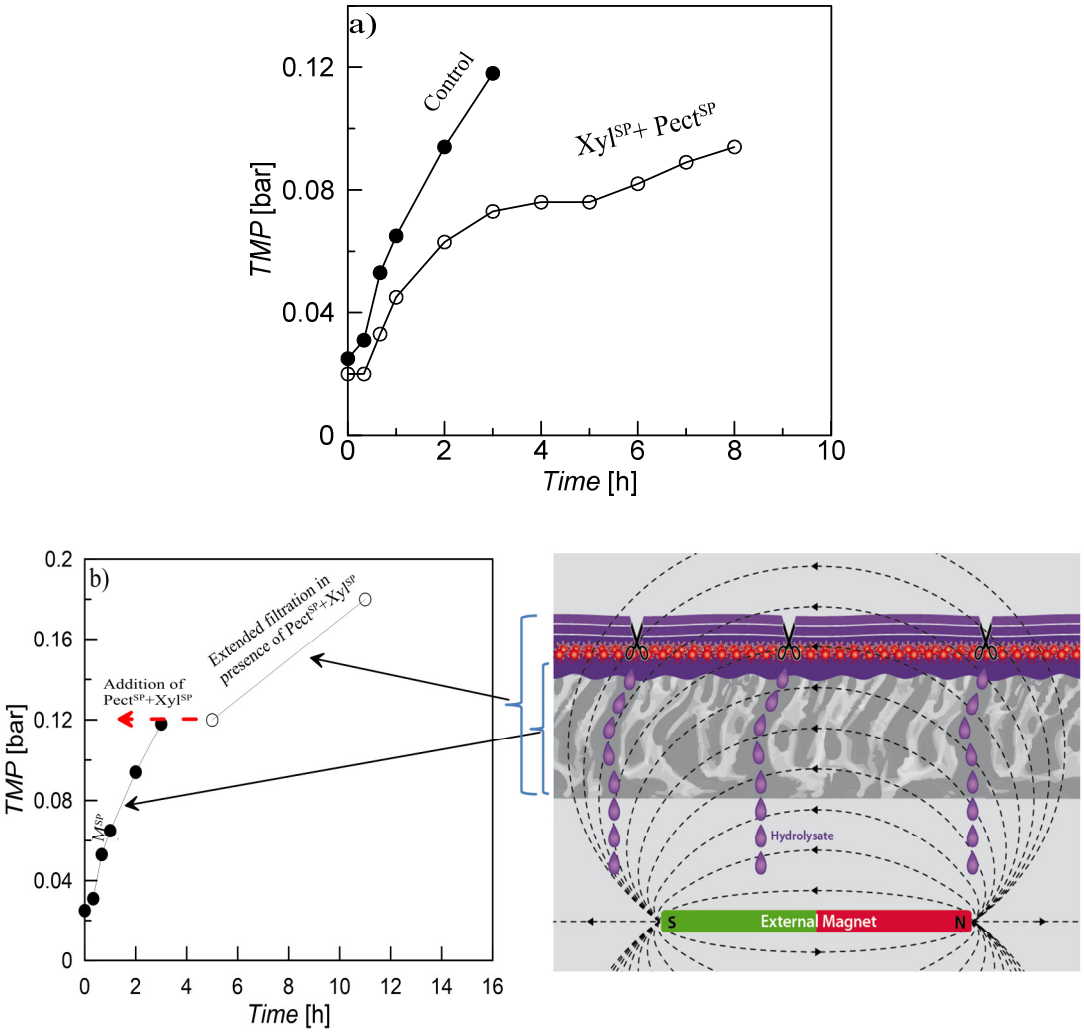

Figure 10: Effectiveness of using enzyme blend (Xyl^{SP} and $Pect^{SP}$ mixtures) on degrading mixed pectin and arabinoxylan fouling layers (feed containing 0.3 mg/mL wheat arabinoxylan and 0.3 mg/mL pectin mixed in equal ratio, 17 $L/m^2.h$ flux at 40°C. (a) Filtration on a dynamic layer formed from a Xyl^{SP} and $Pect^{SP}$ mixture, (b) two step filtration, involving a first step on bare M^{SP} (during first 3 h), followed by dispersion of a mixture of Xyl^{SP} and $Pect^{SP}$ recovered from part (a) on the pre-fouled M^{SP} and subsequent filtration (3-11 h).

4.5. Broader context and perspectives

Membranes with either physically or covalently attached enzymes have long been investigated but still face many problems [22]. Enzyme immobilization via physical adsorption on the membrane surface requires retentive surfaces in order to avoid enzyme leakage through membrane pores [42]. Such required enzyme retention lowers the degrees of freedom to optimize

the membrane performance with respect to creating high fluxes and the passage of desired components. Immobilizing enzymes on larger retainable carrier particles, such as alginate beads, also poses serious problems of isolating and recovering them from other retained components with possibly similar particle size. Covalent immobilization on the membrane is not conceptually attractive, since enzyme denaturation and loss of system performance is inevitable. The ultimate fate of such membranes would then be disposal, since detaching the inactivated enzyme to regenerate the membrane would be difficult, if not impossible. With the here proposed novel BMR^{SP}, the procedure to disperse the Enz^{SP} and to recover them from the membrane at any time becomes straightforward. Moreover, when the enzyme gets denatured or oversaturated, the membrane remains intact, as both denaturation and oversaturation effects are mostly restricted to the dynamic Enz^{SP}/NP^{SP} layer. Therefore, physical localization on a nanoscale of Enz^{SP} on the M^{SP} surface in a reversible superparamagnetic way can out-compete currently employed approaches in BMRs. Remarkably, no leaked Enz^{SP} was detected at all in the permeate (see inset of Figure 3). The 8 nm Enz^{SP} were thus completely retained by the M^{SP} having a much larger average pore size of 0.2 µm, owing to the superparamagnetic properties of both the M^{SP} and Enz^{SP} (Figure 11). This offers an important additional flexibility to the proposed membrane-cleaning strategy, since it does not require retentive surfaces and can then even be operated with highly porous membrane surfaces allowing sustainable operation at higher fluxes.

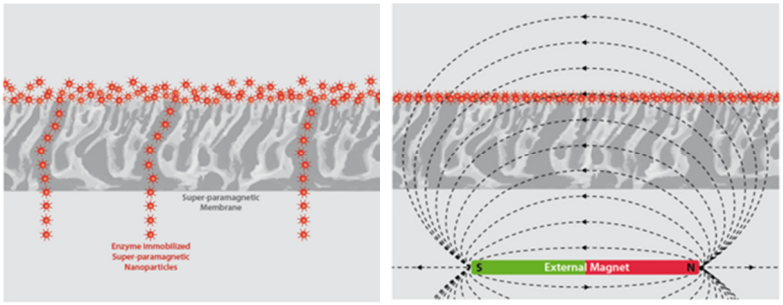

Figure 11: Permeation of an 8 nm NP^{SP} through 0.2 µm diameter pores of an M^{SP} (a) in the absence of an external magnet and (b) in the presence of an external magnet.

In addition to reducing fouling propensity, both Enz^{SP} and NP^{SP} dynamic layers prevent direct membrane-foulant interaction, hence serving as an additional anti-fouling coating on the membrane which re-disperses a possibly formed cake layer at the moment the Enz^{SP} or NP^{SP} are being redispersed. The observed immobilized enzyme and membrane stability, together with the high reusability suggests an estimated wide use of this BMR^{SP} in the production of bulk

chemicals, pharmaceuticals, bio-based commodities and biodiesel in near feature [9, 11].

The BMR^{SP} concept as a whole can be employed to "re-engineer" not only membranes, but also any fouling prone surface, such as in medical appliances, pipelines, reservoirs, bathroom equipment to discourage fouling or as biofilm inhibitor [43] by simply incorporating NP^{SP} in the respective surfaces. With respect to membrane applications, retrofitting the superparamagnetic approach in an existing process would involve replacement of the current membranes by membranes containing small amounts of the very cheap NP^{SP}. Since this addition hardly changes the membrane properties (even with an apparent bonus in anti-fouling properties), industrial membrane manufacturing hardly needs to be re-designed.

The possibility to mix different enzymes either coated as an enzyme mixture per nanoparticle or combined as a mixture of single enzyme NPs for consolidated bioprocessing, also offers ample opportunities.

4.6. Conclusions

The novel BMR^{SP} system described here resulted in up to 75% reduction in membrane filtration resistance through the membrane surface cleaning action of the Enz^{SP}. The BMR^{SP} has a great potential for broader applications in diverse areas due to its flexibility, stability, absence of shear initiated activity loss of enzymes during recycling, and possibility to use enzyme cocktails. Both immobilized enzyme and membrane gave a stable performance over multiple cycles. This stability paves a potential breakthrough towards successful commercialization of BMRs for continuous operations. Compared to direct immobilization of enzymes on membranes by adsorption or covalent bonding, the bio-inspired NP^{SP} are easily scalable, hence, have a broad potential to intensify the numerous membrane biocatalytic reactions reported in literature. It also opens a new horizon for bio-inspired NP^{SP} applications in localized biocatalysis to enhance performance in industrial production, processing, environmental remediation or bio-energy generation. Moreover, the process is not limited to membrane technology and can be exploited to prevent any enzymatically cleavable fouling on any surface.

4.7. References

[1] L. Cao, Immobilised enzymes: science or art?, Current Opinion in Chemical Biology, 9 (2005) 217-226.

[2] C.G.C.M. Netto, H.E. Toma, L.H. Andrade, Superparamagnetic nanoparticles as versatile carriers and supporting materials for enzymes, Journal of Molecular Catalysis B: Enzymatic, 85–86 (2013) 71-92.
[3] E. Duguet, S. Vasseur, S. Mornet, J.-M. Devoisselle, Magnetic nanoparticles and their applications in medicine, Nanomedicine, 1 (2006) 157-168.
[4] M.H. Kumar, N. Mathews, P.P. Boix, K. Nonomura, S. Powar, L.Y. Ming, M. Graetzel, S.G. Mhaisalkar, Decoupling light absorption and charge transport properties in near IR-sensitized Fe2O3 regenerative cells, Energy & Environmental Science, (2013).
[5] J. Lee, Y. Lee, J.K. Youn, H.B. Na, T. Yu, H. Kim, S.-M. Lee, Y.-M. Koo, J.H. Kwak, H.G. Park, H.N. Chang, M. Hwang, J.-G. Park, J. Kim, T. Hyeon, Simple Synthesis of Functionalized Superparamagnetic Magnetite/Silica Core/Shell Nanoparticles and their Application as Magnetically Separable High-Performance Biocatalysts, Small, 4 (2008) 143-152.
[6] P. Daraei, S.S. Madaeni, N. Ghaemi, M.A. Khadivi, B. Astinchap, R. Moradian, Fouling resistant mixed matrix polyethersulfone membranes blended with magnetic nanoparticles: Study of magnetic field induced casting, Separation and Purification Technology, 109 (2013) 111-121.
[7] K. Boodhoo, A. Harvey, Process Intensification: An overview of principles and practice, in: K. Boodhoo, A. Harvey (Eds.) Process Intensification for green chemistry, John Wiley & Sons.Ltd, 2013.
[8] L. Giorno, E. Drioli, Biocatalytic membrane reactors: applications and perspectives, Trends in Biotechnology, 18 (2000) 339-349.
[9] M.C.R. Franssen, P. Steunenberg, E.L. Scott, H. Zuilhof, J.P.M. Sanders, Immobilised enzymes in biorenewables production, Chemical Society Reviews, 42 (2013) 6491-6533.
[10] P. Lutze, D.K. Babi, J.M. Woodley, R. Gani, Phenomena Based Methodology for Process Synthesis Incorporating Process Intensification, Industrial & Engineering Chemistry Research, 52 (2013) 7127-7144.
[11] Z. Xiao-Ming, I.W. Wainer, On-line determination of lipase activity and enantioselectivity using an immobilized enzyme reactor coupled to a chiral stationary phase, Tetrahedron Letters, 34 (1993) 4731-4734.
[12] K. Abe, M. Goto, F. Nakashio, Novel Optical Resolution of Phenylalanine Racemate Utilizing Enzyme Reaction and Membrane Extraction, Separation Science and Technology, 32 (1997) 1921-1935.
[13] A. Machsun, M. Gozan, M. Nasikin, S. Setyahadi, Y. Yoo, Membrane microreactor in biocatalytic transesterification of triolein for biodiesel production, Biotechnology and Bioprocess Engineering, 15 (2010) 911-916.
[14] R. Mazzei, E. Drioli, L. Giorno, Enzyme membrane reactor with heterogenized β-glucosidase to obtain phytotherapic compound: Optimization study, Journal of Membrane Science, 390–391 (2012) 121-129.
[15] Dong-Hyun Kim, Elena A. Rozhkova, Ilya V. Ulasov, Samuel D. Bader, Tijana Rajh, M.S. Lesniak, V. Novosad, Biofunctionalized magnetic-vortex microdiscs for targeted cancer-cell destruction, Nat Mater, 9 (2010) 165-171.

[16] T.-H. Bae, J.R. Long, CO2/N2 separations with mixed-matrix membranes containing Mg2(dobdc) nanocrystals, Energy & Environmental Science, (2013).
[17] Q.K. Beg, M. Kapoor, L. Mahajan, G.S. Hoondal, Microbial xylanases and their industrial applications: a review, Applied microbiology and biotechnology, 56 (2001) 326-338.
[18] N. Miguel-Sancho, O. Bomati-Miguel, A.G. Roca, G. Martinez, M. Arruebo, J. Santamaria, Synthesis of Magnetic Nanocrystals by Thermal Decomposition in Glycol Media: Effect of Process Variables and Mechanistic Study, Industrial & Engineering Chemistry Research, 51 (2012) 8348-8357.
[19] W. Brullot, N.K. Reddy, J. Wouters, V.K. Valev, B. Goderis, J. Vermant, T. Verbiest, Versatile ferrofluids based on polyethylene glycol coated iron oxide nanoparticles, Journal of Magnetism and Magnetic Materials, 324 (2012) 1919-1925.
[20] N. Blumenkrantz, G. Asboe-Hansen, New method for quantitative determination of uronic acids, Analytical Biochemistry, 54 (1973) 484-489.
[21] A.E.R. Ahmed, J.M. Labavitch, A simplified method for accurate determination of cell wall uronide content, Journal of Food Biochemistry, 1 (1978) 361-365.
[22] A.Y. Gebreyohannes, R. Mazzei, E. Curcio, T. Poerio, E. Drioli, L. Giorno, Study on the in Situ Enzymatic Self-Cleansing of Microfiltration Membrane for Valorization of Olive Mill Wastewater, Industrial & Engineering Chemistry Research, 52 (2013) 10396-10405.
[23] H.N. Englyst, J.H. Cummings, Simplified method for the measurement of total non-starch polysaccharides by gas-liquid chromatography of constituent sugars as alditol acetates, Analyst, 109 (1984) 937-942.
[24] P. Le Clech, B. Jefferson, I.S. Chang, S.J. Judd, Critical flux determination by the flux-step method in a submerged membrane bioreactor, Journal of Membrane Science, 227 (2003) 81-93.
[25] H.K. Vyas, R.J. Bennett, A.D. Marshall, Performance of crossflow microfiltration during constant transmembrane pressure and constant flux operations, International Dairy Journal, 12 (2002) 473-479.
[26] Y. Li, X. Xu, C. Deng, P. Yang, X. Zhang, Immobilization of Trypsin on Superparamagnetic Nanoparticles for Rapid and Effective Proteolysis, Journal of Proteome Research, 6 (2007) 3849-3855.
[27] K.C. Gross, A rapid and sensitive spectrophotometric method for assaying polygalacturonase using 2-cyanoacetamide [Tomato, fruit softening, HortScience, (1982).
[28] E. Bach, E. Schollmeyer, An ultraviolet-spectrophotometric method with 2-cyanoacetamide for the determination of the enzymatic degradation of reducing polysaccharides, Analytical Biochemistry, 203 (1992) 335-339.
[29] K. Bélafi-Bakó, M. Eszterle, K. Kiss, N. Nemestóthy, L. Gubicza, Hydrolysis of pectin by Aspergillus niger polygalacturonase in a membrane bioreactor, Journal of Food Engineering, 78 (2007) 438-442.
[30] V. Vatanpour, S.S. Madaeni, L. Rajabi, S. Zinadini, A.A. Derakhshan, Boehmite nanoparticles as a new nanofiller for preparation of antifouling mixed matrix membranes, Journal of Membrane Science, 401–402 (2012) 132-143.

[31] Z. Lei, N. Ren, Y. Li, N. Li, B. Mu, Fe3O4/SiO2-g-PSStNa Polymer Nanocomposite Microspheres (PNCMs) from a Surface-Initiated Atom Transfer Radical Polymerization (SI-ATRP) Approach for Pectinase Immobilization, Journal of Agricultural and Food Chemistry, 57 (2009) 1544-1549.
[32] A.A. Mendes, R.C. Giordano, R.d.L.C. Giordano, H.F. de Castro, Immobilization and stabilization of microbial lipases by multipoint covalent attachment on aldehyde-resin affinity: Application of the biocatalysts in biodiesel synthesis, Journal of Molecular Catalysis B: Enzymatic, 68 (2011) 109-115.
[33] A. Johnson, A. Zawadzka, L. Deobald, R. Crawford, A. Paszczynski, Novel method for immobilization of enzymes to magnetic nanoparticles, J Nanopart Res, 10 (2008) 1009-1025.
[34] Y. Ren, J. Rivera, L. He, H. Kulkarni, D.-K. Lee, P. Messersmith, Facile, high efficiency immobilization of lipase enzyme on magnetic iron oxide nanoparticles via a biomimetic coating, BMC Biotechnology, 11 (2011) 63.
[35] E. Arkhangelsky, D. Kuzmenko, V. Gitis, Impact of chemical cleaning on properties and functioning of polyethersulfone membranes, Journal of Membrane Science, 305 (2007) 176-184.
[36] A. Levine, Chapter 3 - Industrial waters, in: S. Judd, B. Jefferson (Eds.) Membranes for Industrial Wastewater Recovery and Re-use, Elsevier Science, Amsterdam, 2003, pp. 75-101.
[37] J.M. Rodríguez-Nogales, N. Ortega, M. Perez-Mateos, M.D. Busto, Operational Stability and Kinetic Study of a Membrane Reactor with Pectinases from Aspergillus niger, Journal of Food Science, 70 (2005) E104-E108.
[38] J.C. Serrano-Ruiz, J.A. Dumesic, Catalytic routes for the conversion of biomass into liquid hydrocarbon transportation fuels, Energy & Environmental Science, 4 (2011) 83-99.
[39] J. Chen, L. Wang, Z. Zhu, Preparation of enzyme immobilized membranes and their self-cleaning and anti-fouling abilities in protein separations, Desalination, 86 (1992) 301-315.
[40] R. Xue, J.M. Woodley, Process technology for multi-enzymatic reaction systems, Bioresource Technology, 115 (2012) 183-195.
[41] S. Brethauer, M.H. Studer, Consolidated bioprocessing of lignocellulose by a microbial consortium, Energy & Environmental Science, (2014).
[42] J.M. Rodriguez-Nogales, N. Ortega, M. Perez-Mateos, M.D. Busto, Pectin hydrolysis in a free enzyme membrane reactor: An approach to the wine and juice clarification, Food Chemistry, 107 (2008) 112-119.
[43] P.B. Messersmith, M. Textor, Nanomaterials: Enzymes on nanotubes thwart fouling, Nat Nano, 2 (2007) 138-139

Chapter 5: Effect of operational parameters on the efficiency of magnetic responsive biocatalytic membrane reactor

5.1. Abstract

In this work the catalytic performance of BMR^{SP} under different operational conditions is investigated. The feed concentrations, flow rates across the bed, temperature and amount of biocatalytic bead were varied to probe the flow-dependent transport and kinetic properties of the reaction in the BMR^{SP}. When varying the feed concentration from 0.01 to upto 300 times higher values, the degree of conversions decreased from 76% to 20%. The average bed porosity estimated using Ergun equation for laminar flow is 0.8. A comparison of the kinetic parameters with those obtained using solution-phase enzymatic reactions shows decrease in enzyme activity after immobilized. Apparent v_{max} of the flow BMR^{SP} was 58% higher than an immobilized enzyme that was used in stirred tank reactor (STR). The better performance exhibited by the reactive filtration compared to STR is attributed to enhanced mass transfer rate by the convective transport and absence of enzyme-product inhibition.

Analysis of flowrate dependent rate of reaction indicated that the system is kinetically controlled. The rate of fouling for the BMR^{SP} was always lower than a parallel control system. The maximum pressure after two weeks of continuous filtration at 25°C was limited to 0.76 bar. Product assay in the permeate stream also gave constant value in the entire duration, meaning no enzymatic activity decay owing to stable enzyme immobilization and no leakage through the pores of the membrane owing to the synergistic magnetic interaction between the magnetic membrane and bionanocomposites.

The obtained stability over a broad range of operational parameters and sustainable performance over long period gives a high prospect to the newly developed BMR^{SP} to be utilized in continuous biocatalysis and separation, thereby significantly improved process efficiency.

This chapter is based a manuscript under preparation: **Gebreyohannes A. Y**, L.Giorno, T. Verbiest, I.F.J. Vankelecom, P. Aimar. Hybrid magnetic responsive enzyme membrane reactor for tailoring physical immobilization of enzyme: an optimization study.

5.2. Introduction

An immobilized enzyme membrane reactor provides the platform for a continuous reactor operation without the need for secondary step for enzyme recovery [1-2]. Using this strategy, in the previous chapter, we have fabricated an O/I hybrid stimuli-responsive biocatalytic membrane reactor that can immobilize enzyme by effective switching off vs on of an external magnet.
However both mass transfer resistance and enzyme activity loss may negatively affect the reactor yield [3]. Both parameters have similar effect, but the mechanism to control their effect is very different [4]. So adjusting process parameter such as feed flowrate, feed and enzyme concentration, and reaction temperature is crucial [5]. More particularly, careful consideration of parameters that have a tradeoff effect on the reactor performance need to be analyzed very well. Thus in this chapter, detailed investigation of the effect of different operational parameters on the efficiency of the newly developed BMR^{SP} is carried out. The different operational parameters considered includes: flux to control residence time and mass transfer rate, temperature, feed concentration and enzyme concentration. The fundamental characteristics of a continuous flow immobilized enzyme membrane reactor can be quantified through kinetic measurement. Hence the kinetic parameters for the batch and continuous flow reactor are also evaluated.

5.2.1. Kinetics of heterogeneously catalyzed reactions

In heterogeneous catalysis, surface-specific reaction rate comprise three steps: adsorption, desorption and reaction. Often the rate of adsorption and desorption are much greater than the rate of reaction. In addition, there is need to consider both external and internal mass transfer limitations. Despite this difference from homogeneous catalysis, it is still possible to apply the design equations that are often used (e.g. those used in chapter 3). But for the heterogeneous catalysis, it is imperative to take the reduced "empty volume" of the reactor (ε) into account. To recall the equation used in chapter 3, initial reaction rate (V_0) was calculated based on the following mass balance equation [3]:

$$\text{IN - OUT + PROD = ACC} \qquad 1$$

$$\frac{dV}{dt} = (FC)_{in} - (FC)_{out} + \nu_r V \qquad 2$$

Where F is the feed flowrate, C is concentration, v_r is the volumetric reaction rate and V is the reactor volume. At steady state the accumulation term is zero. In addition for STR, the flow term is zero. Therefore the equation can be simplified as:

For STR:

$$\nu_r = \frac{dC}{dt} \qquad 3$$

For flow-through:

$$\nu_r = \frac{F(C_f - C_p)}{V} \qquad 4$$

Where C_f substrate concentration in the feed and C_p is substrate concentration in permeate. Since the BMR^{SP} is made of beads of catalytic bed supported by a flatsheet membrane, it can be assumed as packed bed reactor (PBR). PBR is essentially a plug flow reactor (PFR) and hence can be designed with plug flow reactor design equations [3, 6]. However, since the catalytic bed is porous to allow fluid flow, the reactor volume needs to be corrected by the void fraction (ε). The fraction of the reactor volume that is not filled with catalyst is:

$$V = V_T * \varepsilon \qquad 5$$

Where V is reactor volume free of catalyst, V_T is total reactor volume and ε is the bed porosity. The total volume of the reactor is calculated as:

$$V_T = m_p / \rho_p \qquad 6$$

For the sake of simplification, the following assumptions are made during the formulation of equation 6 or equation 8:

1. The particle is solid; hence its density is equal to the density of ferrous iron (5.15 g/cm^3).
2. There is no particle agglomeration
3. The particle have a spherical shape

Where m_p, total mass of Enz^{SP} (4.8 mg) deposited on the membrane and ρ_p is the density of ferrous particles. But the actual reactor volume is the total volume minus the voidage of the bead (ε). The value of the bed porosity (ε) was estimated as:

$$\varepsilon = 1 - \frac{\rho_b}{\rho_p} \qquad 7$$

Where ρ_b is the bulk density (1.008 g/cm^3), calculated by weighting the mass of 1 mL of NP^{SP} containing suspension.

The actual reactor volume actively engaged in the biocatalysis is:

$$V_a = V_T * (1-\varepsilon) \qquad 8$$

For PBR, Ergun Equation, an empirical relation, is most often used to calculate the pressure drop along the catalytic bed length [7]. For a fluid flowrate of 23.8 mL/h after magnetically depositing 4.8 mg of nanoparticles on 0.0016 m^2, the measured pressure drop was 0.087 bar. In order to use the Ergun equation, the assumptions stated earlier are taken into consideration. Given all the measured parameters and the pressure drop, equation 9 was also used to calculate the bed porosity:

$$\frac{\Delta P_c}{L} = 150\frac{\mu u_0 (1-\varepsilon)^2}{d^2{}_p \varepsilon^3} + 1.75\frac{\rho_f u^2{}_0 (1-\varepsilon)}{d\varepsilon^3} \qquad 9$$

Where ΔP_c is the pressure drop, d_p is the particle diameter, ρ_f is fluid density and u_0 is the fluid velocity. In this case, since the flowrate was measured after the formation of the catalytic bed, there is no need to correct for change of the fluid velocity due to the presence of the beads. Since the Reynolds number at $4.13*10^{-6}$ m/s crossflow velocity is much less than 1 i.e. laminar flow, equation 8 can be simplified according to the Kozney-Carmann Equation:

$$\frac{\Delta P}{L} = 150\frac{\mu u_0 (1-\varepsilon)^2}{d^2{}_p \varepsilon^3} \qquad 10$$

5.3. Material and methods

5.3.1. Materials

The lists of materials used in this study are described in the material section (section 4.1) of chapter 4.

5.3.2. Method

Membrane and NP^{SP} preparation and characterization and enzyme immobilization are provided in method section of chapter 4.

5.3.2.1. Experimental condition

Reactions of Enz^{SP} with model pectin solution were carried out at 40 ± 3°C in stirred tank reactor (STR; batch) and convective modes (continuous). During batch operation, the feed concentration was varied from 0.1 to 0.5 mg/mL at pH 4.5, while the volume was fixed at 60 mL. Sample probes were collected at different times for further analysis. For the convective mode experiments, the membrane with an area of 0.0016 m^2 was mounted in 50 mL Amicon filtration cell, and the feed solution, was supplied continuously using syringe pump (PHD 2000 Syringe, Harvard instruments). The separation characteristics of the selected membrane permit total rejection of pectin and zero rejection of galacturonic acid (GalA). This bench scale reactor, situated inside a water bath for temperature control, is equipped with continuous on-line measuring of temperature and transmembrane pressure using LEO 2 micro-processor controlled pressure gauge equipped with digital display. A circular permanent magnet with a diameter of 5 cm, which helps to form dynamic layer Enz^{SP} on the membrane, was located underneath the filtration cell. Permeate was collected continuously from the bottom of the filtration unit and stored at -20°C until further analysis. The product (GalA) was determined according to the method detailed in chapter 4, section 4.3.5.1. In order to change the permeate flow rate through the membrane, the pumping rate was varied from 4.8 to 71.5 mL/min. Table 5.1 depicts the different parameters and their range of values considered in this study.

Table 5.1: Operational parameters and their range varied while studying their effect on the efficiency of BMR^{SP}.

Parameters	Feed concentration (mg/mL)	Flux ($L/m^2.h$)	Enz^{SP} concentration (g of NP^{SP}/ m^2)	T (°C)
Range	0.01 – 3	5 - 45	1 - 9	25 - 40

5.3.2.2. Long term stability

The BMR^{SP} was continuously operated over many days to measure the rate of enzyme deactivation, leakage and long term operability. The experimental conditions were: flux; 5 $L/m^2.h$, feed concentration; 0.3 mg/mL, amount of Enz^{SP} per membrane area; 3 g/m^2 and filtration temperature 25 and 40°C.

5.4. Results and discussion

5.4.1. Kinetics of Enz^{SP} in STR

Evaluation of catalytic properties of the enzyme hetroginized on magnetic nanoparticles and measurement of kinetic parameters (K_m, V_{max}) was conducted in batch (STR) operational mode at 40°C. The degree of conversion after 30 minutes of incubation at 0.3 mg/mL feed concentration was 44±4.8%. The K_m and V_{max} estimated from the Lineweaver-Burk plot were 0.98 M and 0.02 M/h respectively.

5.4.2. Estimations of Peclet no and bed porosity

The diffusion resistance encountered by the product molecules can sometimes cause the product to accumulate near the dynamic layer of particles to an undesirably high level, leading to enzyme-product inhibition. Thus, ideally the dynamic layer should have enough porosity so that there is no hindrance to the passage of product molecules in and out of the dynamic layer. Besides, the dynamic layer should allow the free mobility of the substrate inside the matrix to

some level inorder for the enzyme immobilized on the spherical particle can stay engaged in the biocatalysis.

The total reactor volume estimate from equation 6 was $9.3*10^{-7}$ L, while the bead porosity estimated using equation 7 was 0.8. After accounting for the catalytic bed porosity, the actual reactor volume (V_a) according to equation 8 was $1.86*10^{-7}$ L.

Pure water was filtered through a catalytic bed containing 4.8 mg of NP^{SP} at a flowrate of $4.16*10^{-6}$ m/s. At steady state, the measured pressure drop (ΔP) was 0.085 bar. The bed porosity estimated according to Ergun equation at this pressure was 0.99. One of the reasons that caused 19% difference between estimated values of porosity using equation 7 and 9 can be accounted for any presence of porosity in the particle itself. In addition, presence of agglomeration or uneven distribution of particles could be another cause.

Besides, in a continuously operated packed bed reactor (PBR), back-mixing processes are involved. They originate in molecular diffusion of components as well as in the hydrodynamic characteristics of the solvent flow that eventually causes axial dispersion [6]. In this reactor, evaluating presence of back-mixing of hydrolysis product (GalA) is important as this may also affect the reactor performance. An empirical relation between the rates of convective transport of product in the flow direction balanced by its diffusive transport normal to the surface by the Peclet (Pe) number was used:

$$Pe = \frac{Lu_o}{D} \qquad 11$$

Where D is the diffusion coefficient of GalA ($5*10^{-6}$ cm^2/s), u_0 is the superficial velocity (m/s) calculated from permeate flux and L is the effective diffusion length. Since none stirred dead-end filtration cell is used, the effective diffusion length (L) is defined as the length of the filtration cell (60 mm). The Pe numbers at different flowrate corresponding to different transmembrane flux are depicted in Table 5.2. Results exhibited a much greater than 1 Pe number for all tested flux rates, implying high convective transport than diffusive back diffusion. Hence, the reactor can be operated under any of the given flux values ranging from 1 to 45 $L/m^2.h$ and above without the risk that an enzyme may get contaminated with a back-diffused GalA. Moreover pragmatically, since the rate of convection is faster than back-diffusion, the entire GalA should be found in permeate. Therefore, measuring the GalA in permeate alone can allow us to calculate a reliable degree of conversion or rate of reaction.

Table 5.2: Relation between flux and ratio of convective and diffusive transport of GalA.

J ($L/m^2.h$)	u ($x10^{-6}$ m/s)	Pe
5	1.38	167
15	4.16	500
30	8.33	1000
45	12.5	1500

5.4.3. Effect of Feed flowrate (flux)

We characterize the stability of the reactor by the rate of TMP change over time, often called "rate of fouling". An optimum operating condition for the BMR would be that it can operate at zero "rate of fouling". Figure 1a-b represents the effect of transmembrane flux on the rate of fouling and degree of conversion. The TMP trend of a BMR^{SP} and a parallel control system at 5 and 45 $L/m^2.h$ is shown in Figure 1-a. Owing to the *in-situ* degradation of foulants by the dynamic layer of Enz^{SP}, an 80% performance difference between control and BMR^{SP} was obtained at both flow rates. However, the high flux value implies a mass transfer prevailing situation where enzyme gets over saturated with substrate and subsequent increased filtration resistance. For example, the last TMP reading after 6 h of continuous filtration for the BMR^{SP} was as high as 1.92 bar. This is about 80 times more than the last reading taken for 5 $L/m^2.h$ (0.024 bar).

Figure 1-b shows the effect of feed flowrate on the rate of fouling for a BMR^{SP} and a parallel control system. The rate of fouling was highly dependent on the filtration flux. As expected the BMR^{SP} efficiency in terms of controlling the TMP was always higher than a corresponding control system. The difference between the rate of fouling of control and BMR^{SP} systems was larger at higher flux than at lower flux. This suggests that regardless of the fast foulant deposition at higher flux, the overall reactor productivity increased with increased transmembrane flux.

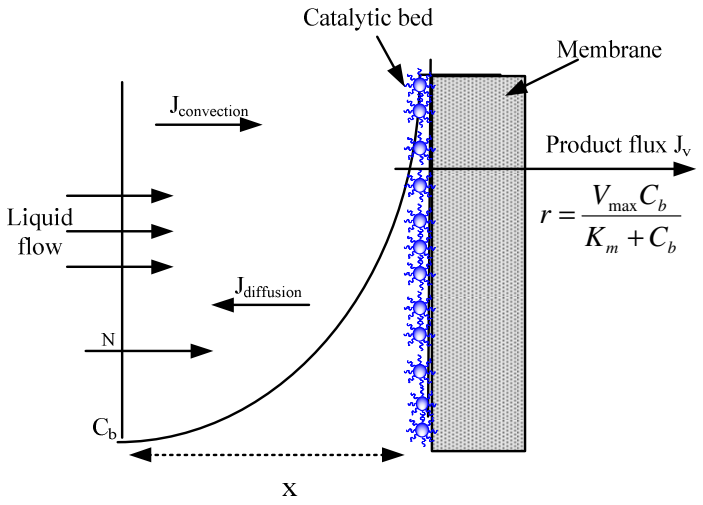

Schematic representation of the boundary layer conditions for BMR^{SP}.

The rate of fouling for the control experiment in Figure 1b shows a straight line. It has a positive Y- intercept which would correspond to either a natural deposit by settling or to an adsorption of pectin, which may happen even in the absence of transmembrane flux. Assuming a classical resistance-in-series model for the flux versus transmembrane pressure relationship and a cake layer formation to simulate the fouling resistance, one would predict that the rate of fouling considered in the present work would vary as a quadratic function of the permeate flux, which was not what one observed in any of our experiments. Accordingly, a more complex fouling mechanism, whose deciphering was beyond the scope of the present project, was probably at work during our experiments. The BMR^{SP} experiment shows a straight line as well, but with 27.6% lower slope and a negative Y-intercept, corresponding to the rate of fouling material degradation by the enzymes.

The difference between the intercepts gives an indication of the rate of pectin degradation by the biocatalytic effect of the enzyme in BMR^{SP}. The estimated rate of reaction based on this assumption is 0.057 h^{-1}.

Moreover, the X-intercept of the BMR^{SP} line gives the flux J^* which would theoretically give no fouling at this bulk concentration. Finally, it is possible to use the graph in Figure 1b to withdraw more practical information. If one can determine the level of rate of fouling that is acceptable in a process, then the maximum constant flux (let's call it J_s for "sustainable flux") that can be applied can be read from the straight line (BMR^{SP}). As for an example in this graph if one accepts a 0.1 bar/h rate of fouling, then a sustainable flux of 8 $L/m^2.h$ could be chosen.

The challenge here would be, by increasing the enzymatic efficiency, to increase the absolute value of the initial offset, which would in turn increase J_s for a given acceptable rate of fouling. Assay of GalA in the permeate stream for each flux gave constant value meaning no enzyme activity loss or leakage. As a general rule high superficial velocity reduces the external mass transfer resistance. Hence the reactor productivity increased with increased transmembrane flux (Figure 1-b). However, this increased productivity came along with larger pressure drop inorder to achieve the high superficial velocity. In most immobilized enzyme membrane reactors, flux defines the residence time there by the degree of conversion. Contrary to this, in this experiment equal level of conversion for all flux values were obtained. Therefore, the average degree of conversion at 5, 15, 30 and 45 L/m^2.h were 27.5, 31, 28 and 33.5 ± 5.2% respectively (Figure 1-b).

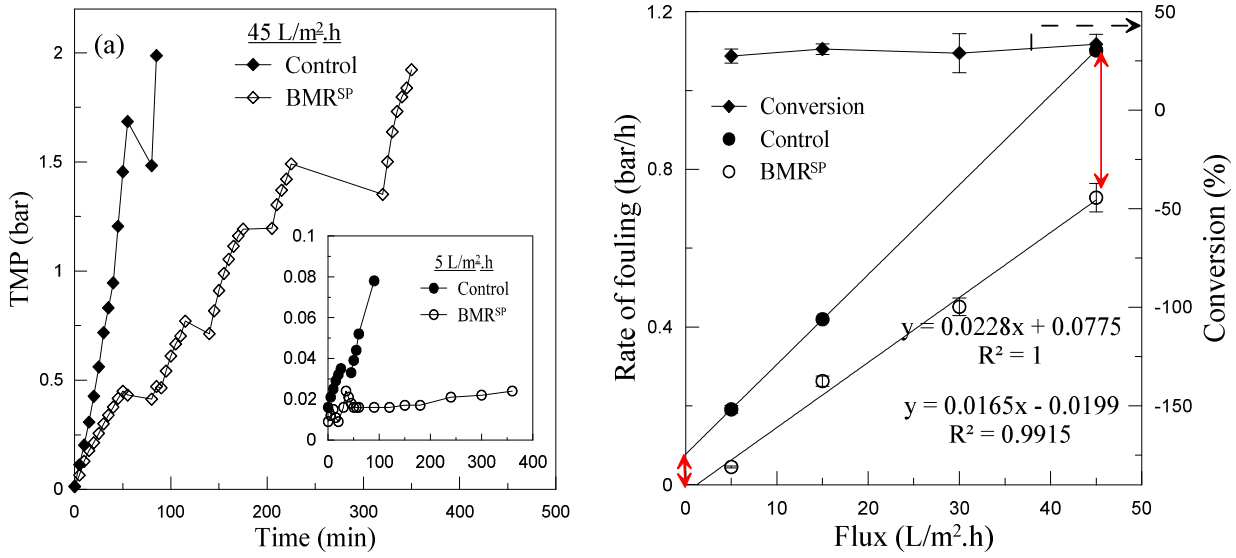

Figure 1: a) The TMP profile of BMR^{SP} and a parallel control system at 5 and 45 L/m^2.h and b) relation between flux, rate of fouling and degree of conversion at 0.3 mg/mL feed concentration, 40°C and pH 4.5.

5.4.4. Effect of Temperature

The thermal stability of the BMR^{SP} was studied in the range of (25-40°C) as shown in Figure 2. The 25°C is room temperature while the 40°C is the optimum temperature on which the pectinase works fast. The enzymatic activity increases with greater temperature due to the greater kinetic energy possessed by molecules, thereby increasing the possibilities of collision between the immobilized enzyme and the foulant. As a result, the rate of fouling at 40°C was significantly

lower than at 25°C. However**,** the concentration of the GalA assayed in the permeate of both streams were almost similar (see Figure 5-b).

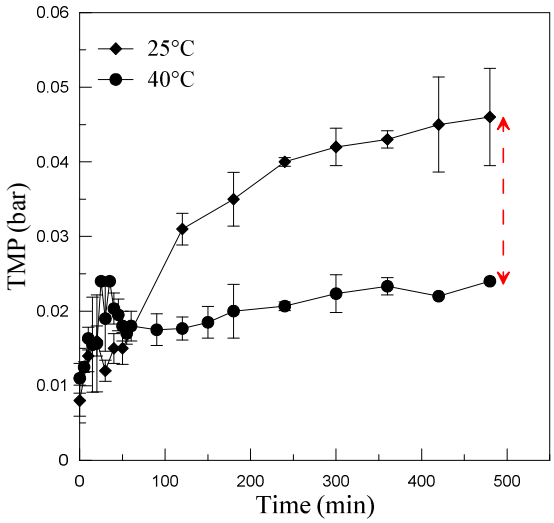

Figure 2: Effect of temperature on the transmembrane pressure development: 0.3 mg/mL feed concentration, 15 L/m^2.h flux, the TMP in the y-axis is normalized by the viscosity of the feed solution at 25 and 40°C.

5.4.5. Effect of feed concentration

To evaluate the kinetic parameter, the feed concentration was varied over a broad range (0.01, 0.1, 0.3, 1 and 3 mg/mL), at 40°C, 15 L/m^2.h flux and 3 g/m^2 (11 µm) Enz^{SP}.

Figure 3a shows that at 3 mg/mL feed concentration, the TMP rises linearly. On the contrary, at low feed concentration especially at 0.1 and 0.01 mg/mL feed concentration the TMP arrives at a steady state after certain time. That means it is possible to operate the reactor under these concentrations and a reasonable flux of 15 L/m^2.h without facing sever membrane fouling.

The apparent Michaels-Menten constant $K^{app}{}_m$ and the maximum reaction velocity v_{max} obtained by Lineweaver-Burk plot were 0.066 M/h and 1 M respectively (Table 5.3). The $K^{app}{}_m$ value is significantly higher than the K_m obtained for free enzyme (0.51 M). But the v_{max} obtained here is close enough to the value obtained for free enzyme in chapter 3 (0.07 M/h). Of course the results of the fee enzyme reactor were obtained in the presence of enzyme-product inhibition with an inhibition constant of 0.31 mg/mL. Given the absence of enzyme-product inhibition in the present reactor, better catalytic efficiency could have been obtained. However, due to possible conformational distortion of the enzyme after immobilization, an almost equal

level of catalytic efficiency and 50% higher affinity towards substrate was obtained for the BMR^{SP} as compared to the free enzyme that suffered from enzyme-product inhibition. Nevertheless, the ν_{max} value obtained here is about 57.6% higher than the value obtained when the Enz^{SP} was used in STR (Table 5.3). In section 5.4.3., the rate of reaction was estimated based on the fitted lines to the rate of fouling obtained for BMR^{SP} and a parallel control system at different transmembrane flux. The obtained value of reaction rate was 0.057, which is close to the ν_{max} value obtained here (0.066). This similarity between the actual and the maximum attainable reaction rate can thus be the overlying reason for the observed independency of the enzyme activity on the residence time. Hence, the reactor was operated at its maximal efficiency for the given enzyme concentration i.e. the rate of reaction was the rate limiting step.

Table 5.3: Kinetic parameters derived for Enz^{SP} in STR (batch) and in BMR^{SP} (continuous) operation at 40°C and pH 4.5.

Kinetic parameters	STR	BMR^{SP}
ν_{max} (M/h)	0.028	0.066
K_m (M)	0.98	0.97

Hence, the optimum reactor performance is a factor of feed concentration and transmembrane flux.

The BMR^{SP} productivity, q, is the amount of GalA acid generated at different transmembrane flux:

$$q = C_p * J \qquad 12$$

Where J is flux, C_p is permeate concentration.

The feed concentration in pectin (C_f) is correlated with the permeate concentration in GalA (C_p) with a factor *x* i.e. degree of conversion as:

$$C_p = x * C_f \qquad 13$$

For a given membrane area (A), the productivity is:

$$JC_p = J * x * C_f$$

Given the form of equation 12, which by implicit contained effect of feed concentration and TMP, the productivity is a constant term say γ, if the conversion is a constant, which is related to the flux as:

$$J * C_f = \gamma \qquad 14$$

Hence the optimum flux (J_{opt}) for a given feed concentration is:

$$J_{opt} = \frac{\gamma}{C_f} \qquad 15$$

Under the light of this correlation, an optimum flux for the present study is a flux at which zero rate of fouling can be attained ($J_{opt} \sim J^*$).

In Figure 1b, at 0.3 mg/mL feed concentration, the flux J^*, at which ~zero rate of fouling can occur was 5 L/m^2.h. If one assumes that the flux is maintained constant because the enzymatic degradation of pectin exactly compensates its convection JC_f, (the productivity) then γ=1.5 g/m^2/h. However, when J^* was set to 15 L/m^2.h, the feed concentration at which zero rate of fouling occurred was found to be 0.1 mg/mL (Figure 3b), in other words γ had again the same value of 1.5 g/m^2/h.. Accordingly, if the value of J^* were fixed at 45 L/m^2.h, one would need to reduce the feed concentration to 0.01 mg/mL to attain zero rate of fouling. The challenge here again is the importance of modifying the concentration of the Enz^{SP} in order to boost the BMR^{SP}`s biocatalytic performance.

Practical application of this model (equation 15), especially flux and feed concentration correlated by the constant factor γ, is to predict the flux needed for a certain feed concentration in order to get an optimum degree of conversion (x). This may further be used to automate and control online mass transfer and reaction rate during continuous operation. Example, when a reactor is operated continuously, one can install an inline sensor that adjust feed flowrate for a given feed concentration in order to keep the reactor performance at the optimum degree of conversion without facing sever fouling.

A conclusion of this section seems to be that a BMR^{SP} reactor is characterized by a specific capacity to digest a given load of pectin (here 1.5 g/m^2/h).

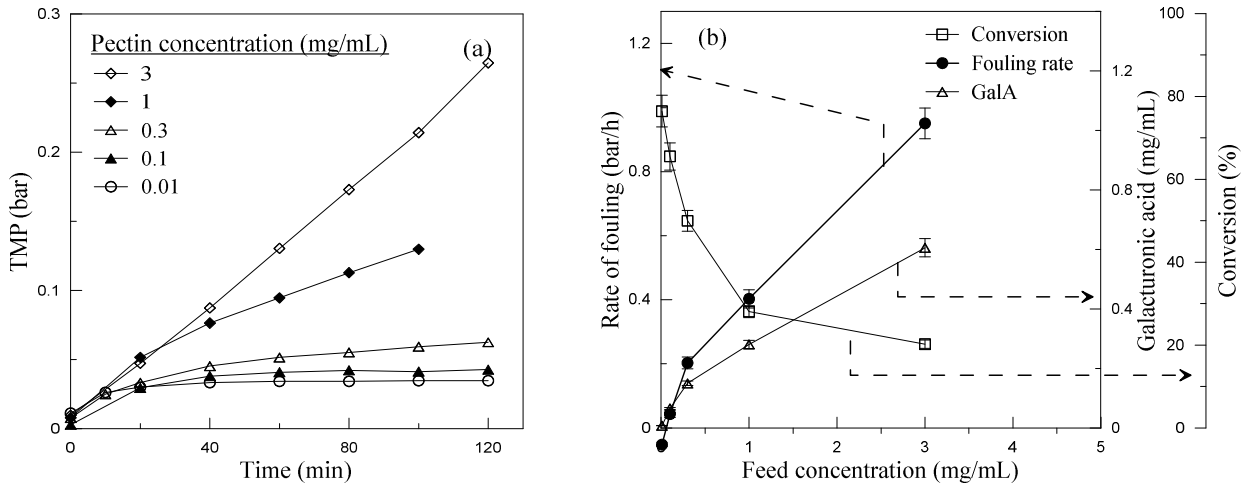

Figure 3: Relation between a) feed concentration and TMP and b) feed concentration, degree of conversion, rate of fouling and amount of GalA produced at 15 L/m^2.h, 40°C, pH 4.5.

5.4.5. Effect of enzyme concentration

Figure 4 shows the effect of enzyme concentration on BMR^{SP} at fixed transmembrane flux of 15 L/m^2.h, 0.3 mg/mL feed concentration and 40°C. The amount of Enz^{SP} deposited per given membrane area was varied from 1 to 9 g/m^2. In fact, these Enz^{SP} are mainly micrometers in length and several hundreds of nanometers in diameter. Before conducting the experiment, hampered flow of product due to increased resistance to the flow by the increased layer of Enz^{SP} was expected. Despite this expectation, the degree of conversion in Figure 3 indicated a linearly increased value when the Enz^{SP} layer was progressively increased from 1 g/m^2 (3.67 µm) to 3 g/m^2 (11 µm) and further to 9 g/m^2 (33 µm). Hence the whole biocatalytic bed was active in the pectin degradation along its length. This is in good agreement with the obtained 0.8 bead porosity e.g., at 11µm bed height. Meaning the biocatalytic bed is composed of thick but porous layer of bed that allowed easy passage of prodcut. The observed decrease in rate of fouling with increased Enz^{SP} revealed a second order relation with the deposited Enz^{SP} layer. An increase in the efficiency of the reactor (γ) can thus be obtained by increasing the enzyme concentration over the surface of the membrane: higher loads ($J.C_f$) can then be taken while keeping a low if not zero increase in TMP over time at constant flux.

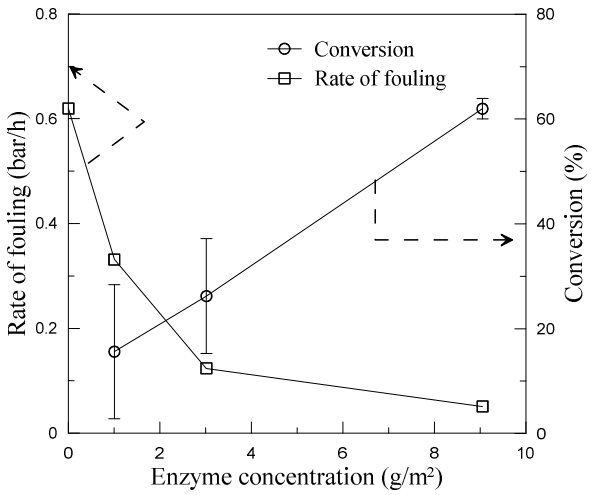

Figure 4: Effect of amount of Enz^{SP} deposited per membrane area on the rate of fouling and degree of conversion. The transmembrane flux was fixed at 15 L/m^2.h, temperature 40°C and pH 4.5.

5.4.6. Long-term stability

One of the main limitations of an enzyme membrane reactor is the loss of enzyme activity and leakage through the pores that eventually limit their long term operability. The developed system showed an interesting performance over a broad range of operational conditions. It is thus important to verify its time stability by conducting filtration over long periods. In chapter 4, it was shown that when the system was operated over five cycles comprising an 8 h continuous filtration at 17 L/m^2.h, step-by-step decrease in the performance was observed. It is thus crucial to verify the long term stability of the developed system, when it is operated at low transmembrane flux.

Figure 5a-b exhibit the trend of TMP and enzyme activity when the system was continuously operated at 5 L/m^2.h for two weeks both at 25 and 40°C and pH 4.5. In order to account for viscosity change due to temperature difference, the reported TMP was normalized by the corresponding viscosity values. As shown in Figure 5-a, there is a unique difference in the rate of fouling between the system operated at 25 and 40°C. This is accounted for lowered enzyme activity at lower temperature according to Arrhenius law [8]. It is worth noting that the rate of TMP rise in both cases was very slow, particularly for the first six days. Subsequently, the TMP of the system operated at 25°C started to rise faster arriving at 0.725 bar after 224 h of continuous filtration, while the TMP at 40°C was limited to only 0.448 bar after 178 h.

The catalytic activity did not show any significantly visible decay in the entire duration (Figure 5-b). The constant concentration of GalA at each temperature indicates constant performance of the continuous (time in variant) reactor system. Results also showed that a 33% degree of conversion was reached at both temperatures.

All in all the observed possibility of operating the system continuously for long time without significant loss in enzyme activity as well as limited rate of fouling is an immense improvement over the direct covalent immobilization of enzyme in chapter 3 which only allowed us to operate the system for 24 h before completely losing its performance.

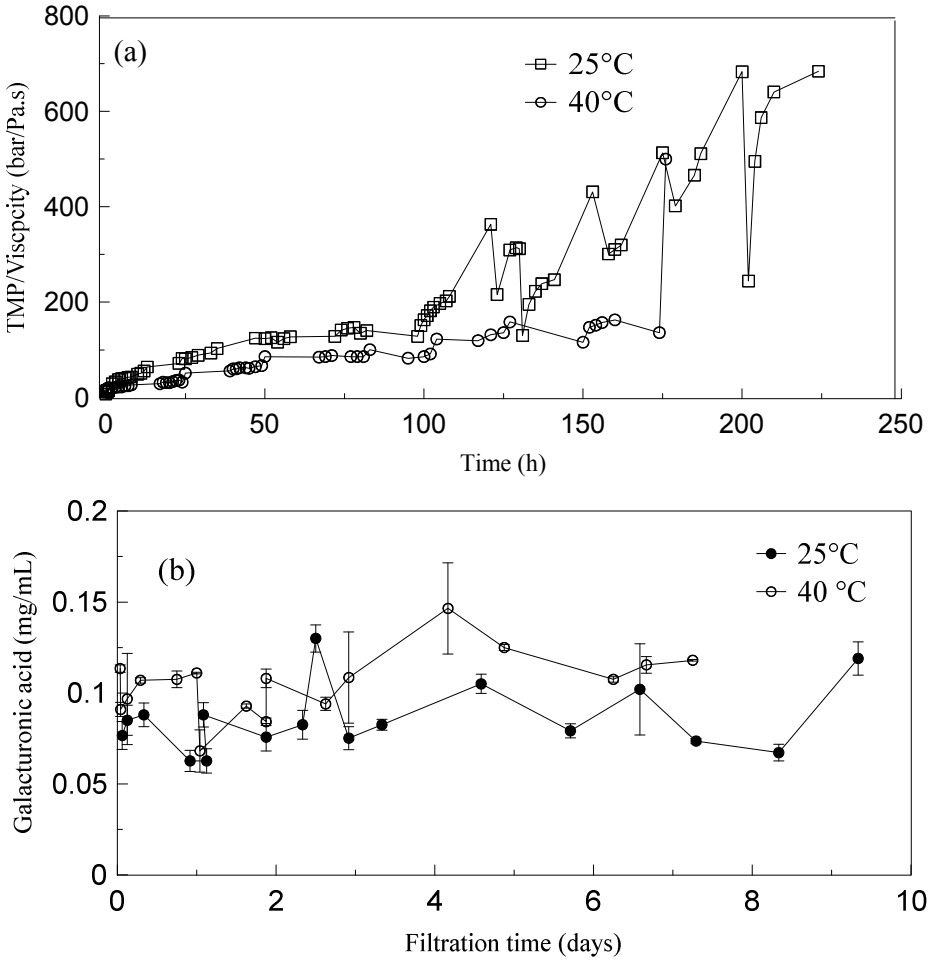

Figure 5: Operational stability of BMR^{SP} operated at 0.3 mg/mL, 5 L/m^2.h and 3 g/m^2 (11µm) Enz^{SP}, opertaed contineoulsy for two weeks: a) TMP trend at 25 and 40°C, b) enzyme activity at 25 and 40°C.

5.4.7. Pure water permeability before and after filtration

According to Table 5.4, the water permeability loss after using the NP^{SP}, either neutral or biocatalytically active, falls within a narrow range (~50%). This loss can thus be attributed to the presence of foulants which are too small to be retained by the membrane but too large to easily permeate through the pores. Hence they were trapped inside the pore structure resulting in the observed approximately 50% loss of the membranes' original performance.

Table 5.4 also exhibits the concentration of GalA measured in the retentate streams of BMR^{SP} at different transmembrane flux. Absence of sufficiently large concentration of GalA allows to say that there is no back-diffusion of the hydrolysate to the bulk stream. These results are also in good agreement with the estimated Pe number in section 5.4.2, that has suggested absence of possible back diffusion of the products to the bulk stream over a wide range of flux values. The retentate of the blank or control experiments with no enzymatic preparation were also assayed for the GalA content. As shown in Table 5.4, at the lowest flux, the value was negative while at highest flux, the value was rather high. This lateral increase is attributed to fouling modified rejection layer of the membrane and the neutral NP^{SP} bed.

Table 5.4: Summary of the difference in percentage of pure water permeability measured before and after use of BMR^{SP} or a control system that only contains neutral NP^{SP} deposited on the membrane. In addition concentration of GalA measured in the retentate under different operating conditions is depicted.

Process	Enz^{SP} deposited per membrane area (g/m^2)	Pure water permeability before and after (%)	Retentate GalA (mg/mL)
5 LMH-control	3	52	-0.038
5 LMH-BMR^{SP}	3	55	0
15 LMH- BMR^{SP}	3	36	0.012
15 LMH- BMR^{SP}	1	-	0.012
15 LMH- BMRSP	9	-	0.012
30 LMH- BMR^{SP}	3	26.8	0.0025
45 LMH- BMR^{SP}	3	48.5	0.0002
45 LMH- control	3	50.5	0.028

5.5. Conclusion

The operability and stability of the BMR^{SP} has been investigated over a wide range of operational parameters. The system integrates reaction and separation zone inside one device, complemented by continuous on-line substrate feeding at constant flow rate and *in-situ* enzymatic degradation of major foulant to maintain separation efficiency.

When the feed concentration varied by a factor of 300 (0.01 to 3 mg/mL), the rate of fouling varied only by a factor of 8 owing to the efficient biocatalytic *in-situ* foulant degrading capacity of the magnetically formed dynamic layer of Enz^{SP}. Results also showed simultaneous increase in productivity and rate of fouling of BMR^{SP} when flux was varied from 5 to 45 $L/m^2.h$.

The enzyme activity at different flux was constant, meaning the kinetics was independent of the flow rate through the catalytic bed. Comparison between kinetic parameters obtained from L-B plot and fitted parameters of rate fouling of BMR^{SP} and a parallel control system gave an indication that reaction rate was the rate limiting step. This has thus been taken as possible reason for the observed residence time independent kinetic performance of the reactor. Indeed, residence time played an important role in determining the rate of fouling.

More importantly, the system when run in optimized conditions showed no performance loss, activity decay or enzyme leakage when operated continuously over two weeks both at 25 and 40°C and 0.3 mg/mL feed concentration.

A cake layer model used to describe the reactor failed to represent the transient state of the BMR^{SP}. However, an empirical model equation used to correlate mass transfer and reaction rate and the subsequent rate of fouling correlated the flux and feed concentration to a constant factor. Hence the BMR^{SP} reactor is characterized by a specific capacity to digest a given load of pectin (here 1.5 $g/m^2/h$). We could then found conditions to operate a BMR at zero or very low increase in TMP, provided that the flux and feed substrate concentration properly correlated. Such predictive model based on the experimental results can further be utilized for an easy process automatization.

5.6. References

[1] P. Jochems, Y. Satyawali, L. Diels, W. Dejonghe, Enzyme immobilization on/in polymeric membranes: status, challenges and perspectives in biocatalytic membrane reactors (BMRs), Green Chemistry, 13 (2011) 1609-1623.

[2] L. Giorno, E. Drioli, Biocatalytic membrane reactors: applications and perspectives, Trends in Biotechnology, 18 (2000) 339-349.
[3] O. Levenspiel, Chemical Reaction Engineering, 3rd ed., John Wiley & Sons Inc, New York, 1999.
[4] E. Nagy, E. Kulcsár, Mass transport through biocatalytic membrane reactor, Desalination, 245 (2009) 422-436.
[5] J.M. Rodríguez-Nogales, N. Ortega, M. Perez-Mateos, M.D. Busto, Operational Stability and Kinetic Study of a Membrane Reactor with Pectinases from Aspergillus niger, Journal of Food Science, 70 (2005) E104-E108.
[6] M.F. Chaplin, C.Bucke, Enzyme technology, Cambridge University Press, 1990.
[7] I.F. Macdonald, M.S. El-Sayed, K. Mow, F.A.L. Dullien, Flow through Porous Media-the Ergun Equation Revisited, Industrial & Engineering Chemistry Fundamentals, 18 (1979) 199-208.
[8] J.E. Bailey, D.F. Ollis, Biochemical Engineering Fundamentals, McGraw-Hill, New York, 1986.

Chapter 6: Challenging the chemical stability of magnetic responsive organic-inorganic hybrid membrane during cleaning

6.1. Abstract

The chemical cleaning stability of PVDF based organic-inorganic hybrid membrane, containing superparamagnetic nanoparticles (NP^{SP}) as inorganic filler is studied under accelerated ageing in combination with and without fouling conditions. These membranes have gained great attention to treat wastewater due to possibility to introduce smart features such as magnetic responsiveness, increased permselectivity and improved antifouling property.

Complimentary data from simultaneous microscopic and macroscopic characterization of membrane under accelerated ageing are used to evaluate the effect of different parameters (hypochlorite concentration, exposure duration and pH). The ageing caused change in the physico-chemical characteristics of the membrane, fouling propensity, increased hydraulic resistance and hampered operating lifetime. ATR FTIR, EDX and SEM results correlated these changes with step-by-step degradation of the polymeric coating layer of used magnetic nanoparticles. A unique membrane densification is also observed when membrane is aged for 12 h in 800 and 2000 ppm NaOCl solution. Mobilization (plasticization) of the polymeric constituent of the NP^{SP} coating layer from incomplete oxidation reaction that partially covered the membrane surface is assumed as the main cause. The pores are also observed to open up gradually with extended exposure, presumably after complete mineralization of the polymer.

After careful consideration of both physico-chemical and hydraulic variations during accelerated ageing, a 400 ppm solution of hypochlorite at pH 12 is found satisfying a good compromise between satisfactory maintenance cleaning and membrane preservation under the given experimental conditions.

This chapter is based on manuscript to be submitted to Journal of Membrane Science as:
Gebreyohannes A. Y, C.Causserand, I.F.J. Vankelecom, L. Giorno, P. Aimar. Challenging the chemical stability of magnetic responsive hybrid membrane during cleaning.

6.2. Introduction

The research on organic-inorganic (O/I) hybrid membranes with incorporated superparamagnetic nanoparticles (NP^{SP}) is an emerging field that holds numerous unexplored interesting avenues [1-2]. The membrane benefits from the combination of both polymeric and inorganic materials. It leads to stimuli-responsive "smart" polymeric membrane with properties that can be modulated in a reversible manner. For example, recently magnetic responsive micro-mixing nanofiltration membrane is developed. The membrane was prepared by grafting magnetic responsive nanolayers consisting hydrophilic poly(2-hydroxyethyl methacrylate) (polyHEMA) flexible polymer chains with NP^{SP} attached to the chain ends. The chain oscillates in an oscillating magnetic field, induced mixing at the membrane-fluid interface that maximized the disruption of concentration polarization layer [3].

NP^{SP} has also been used as inorganic nanofillers in a PVDF membrane to impart desired surface functionality [4]. The hybrid membrane has controlled porosity, texture and chemical composition that can provide real prospect to an efficient membrane filtration. Presence of the NP^{SP} also induces magnetic property in the membrane that can be controlled by an external magnetic field through remote on-off switches [1, 5]. This responsive behavior, for example is useful to manipulate the deposition of magnetic nanoparticle on the membrane surface to prevent direct membrane-foulant interaction (see chapter 4&5). In addition to inducing magnetic properties, inclusion of the NP^{SP} is reported to enhance the membranes' hydrophilicity, mechanical strength, compaction-resistance, improved permselectivity and antifouling property [1, 4]. Therefore, this membrane can have broad function ranging from environmental remediation to smart product manufacturing. Particularly, the synergistic antifouling property and improved permselectivity gives the membrane a big prospect to be utilized in wastewater purification. NP^{SP} coated membranes for example have been used for effective removal of natural organic matter [6], arsenic [7] and copper [8] during water treatment.

In chapter 4, this membrane is used to treat wastewater coming from food processing industries rich in hydrocolloids such as pectins and arabinoxylan. During dead-end filtration of a wastewater containing 0.3 mg/mL pectin at 0.5 bar and pH 4.5, permeability increased from 150

kg m^{-2} h^{-1} bar^{-1} for unmodified membrane to 348 kg m^{-2} h^{-1} bar^{-1} for hybrid membrane with 0.33 w/w % NP^{SP} loading, while solute rejection capacity increased from 57% to 90%.

However, when quality and quantity of permeate reduces to a critical level due to fouling, applying both maintenance and recovery cleaning is inevitable.

Both organic and inorganic irreversible fouling caused by adsorption or chemical interaction during membrane filtration can only be removed through chemical cleaning. In principle, three strategies are employed; applying 200-2000 ppm of hypochlorite to oxidize organic compounds on the membrane, adjust pH of cleaning solution with 150-4000 ppm NaOH to dissolve organic compounds, and decreasing pH with acids to dissolve inorganic scale formation [9]. The cleaning step comprises transport of the cleaning agents through fouling layers and membrane surface reactions to detach the foulants from the membrane surface [10]. Among these, long or short term oxidative cleaning by hypochlorite are commonly employed to effect off-line and in-place chemical cleaning of organic foulants [11]. It is mostly preferred because of its availability, reasonable price, and its well demonstrated successful sanitizing capacity [12].

However, hypochlorite also makes fast and nonselective progressive reaction with a wide array of organic substance. As a result, it may cause damage to the oxidation sensitive polymeric materials constitutive of the membrane [13]. Several studies have already shown the presence of hypochlorite induced damage to different types of membranes. The negative effect is mostly correlated to modification of the polymer resulting in enlarged membrane pore size [14], change in membrane hydrophilicity [12], deteriorated mechanical strength [11], increased electronegativity [14] and enhanced protein retention [10]. For example, Arkhangelsky et al. [14] showed effective removal of foulants from PES membrane surface after cleaning with hypochlorite followed by profound fouling due to changed membrane properties. The authors ascribed the changed behaviour to chain scission of the polymer leading to the formation of phenyl sulfonate, increased electronegativity and loss of overall membrane integrity. Suggested possible mechanism of hypochlorite induced damage to the membrane indicates that solution chemistry plays a leading role on the membrane degradation.

When chlorine as hypochlorite (ClO^-) is introduced into water, it rapidly undergoes hydrolysis [15]. The hydrolysis may end up releasing hydroxyl ($^{\bullet}OH$) or chlorine monoxide ($ClO^{\bullet}$) radicals depending on solution pH [16]. For some polymeric membrane materials, presence of these radicals is reported to facilitate the membrane degradation. Causserand *et al.*, [16] for example

have demonstrated polymer chain breakage after ageing in hypochlorite solution of UF membrane made of polysulfone (PSf) and polyvinylpyrrolidone (PVP). They also observed a more significant chain breakage in the pH range where the solution chemistry allows the formation of the $^{\bullet}OH$ radicals.

The exhaustive research efforts made so far helped to understand the role of hypochlorite cleaning to recover membrane flux of most polymeric membranes. The researched results have also revealed the subsequent membrane performance deterioration due to the oxidative damage induced by routine hypochlorite. Yet no vital damage to the chemical structure of PVDF due to hypochlorite cleaning is reported [12, 17]. Nevertheless, additives included in the polymer matrix such as to enhance its hydrophilicity are found prone to the oxidative degradation [18].

A study by Abdellah and Berubé [18] attributed the observed changes after hypochlorite treatment of PVDF based blended membrane to the oxidative removal of the hydrophilizing additives (HA). When the membrane is exposed to a constant concentration of 3600 ppm hypochlorite pH 10, the size of the dominant peak of the major functional group of the HA decreased as the exposure dose to sodium hypochlorite increased. In another study, Puspitasari *et al.*, [17] observed removal of the surface modification substance used in PVDF membrane manufacturing during cleaning due to the oxidative ageing effect of NaOCl. Hypochlorite induced ageing process is also demonstrated by the decrease in the hydraulic resistance and increased hydrophilicity. They also have reported that the ageing effect is much faster at high temperature than at low temperature.

As an emerging field of research, the knowledge regarding the hypochlorite cleaning effect on organic-inorganic hybrid membrane properties is insufficient. Especially for magnetic responsive membranes, most ferric particles are coated with different polymers to induce various features [19-21]. In addition, polymers like polyethylene glycol (PEG) or polyvinylpyrolidone (PVP) are used as an additive or pore former during preparation of NP^{SP} containing mixed matrix membrane [4]. Daraei et al [1] for example used 1 w/w % PVP to prepare PES based Fe_3O_4 containing fouling resistant mixed matrix membrane. Thus, verifying the chemical cleaning stability of the presented NP^{SP}-PVDF membrane which also have polymer coated magnetic nanoparticles as nanofillers is crucial.

Therefore, this study focuses on comprehensively quantifying the effects of hypochlorite exposure on changes in the physico-chemical characteristics, hydraulic permeability and fouling

propensity of magnetic responsive NP^{SP}-PVDF hybrid membranes. An extensive study regarding the hypochlorite cleaning stability of the embedded NP^{SP} and the ageing effect of NaOCl at various concentrations, pH and soaking duration has been examined.

The membranes have been characterized based on chemical composition (FTIR and EDX), antifouling property (pectin filtration), pore density (scanning electron microscopy), and hydraulic resistance (clean water permeability). The main mechanism(s) responsible for the observed changes is also identified. The ultimate outcome of the research is the development of cleaning protocols under a given experimental condition that is effective at controlling fouling and less detrimental to the overall membrane integrity.

6.3. Material and methods

6.3.1. Solutions

Citrus pectin 25-30% degree of esterification and acetic acid 99% purity are acquired from Sigma Aldrich, France. Buffer: sodium acetate is a commonly utilized buffer to dissolve pectin. Hence it is used here also as a working buffer. A 100 mM sodium acetate buffer is prepared by dissolving 3.05 g of glacial acetic acid in 1 L ultrapure water. A 0.5 M NaOH solution is used to adjust the pH to 4.5.

To represent an effluent rich in hydrocolloids e.g., effluents of olive oil extraction or fruit juice clarification [22], pectin dissolved in the working buffer (0.3 mg/mL) is used as a model foulant.

The total free chlorine concentrations in the bath before and after ageing are measured using a HACH 2400 spectrophotometer with a specific reagent (DPD free chlorine reagent HACH 14070–14099 Pk/100). The lamp is operated at a wavelength of 530 nm. Solutions are prepared from sodium hypochlorite (Oxena, 36° in chlorine) diluted in ultrapure water. A 1 M NaOH was used to adjust pH.

6.3.2. NP^{SP} and membrane preparation

Method used to prepare the NP^{SP} utilized as nanofillers during membrane preparation as well as the membrane preparation procedure are described in chapter 4 sections 4.3.2 and 4.3.3 respectively.

6.3.3. Filtration set-up

Filtration experiments are performed in 50 mL stirred dead end cell (Model 8050, Amicon) equipped with a 45 mm diameter membrane, a magnetic stirrer at 300 rpm, a backpressure TMP controller, a 3 L feed tank and constant N_2 pressure sources. The TMP is set with a precision regulator and the value is recorded with a LEO 2 micro-processor controlled pressure gauge equipped with digital display (chapter 4, section 4.3.3.2., Figure 1-a).

Preliminary characterization of the membranes with different NP^{SP} loading indicated that membrane with 0.33 w/w % NP^{SP} has the best pectin permselectivity (chapter 4, section 4.4.1.2). Hence this membrane is selected for this particular study. Before the experiment, each piece of pre-ethanol wetted membrane was compacted at 2 bar for a period sufficient to reach a stable flux using ultrapure water. Subsequently, the water permeability at room temperature is determined by filtering the working buffer at 1 bar. Use of the buffer is preferred over water in order to avoid change in the deposit (foulant) structure that could have arisen from foulant interaction with different solvents in the subsequent fouling studies. The model foulant used to measure the membranes' permselectivity (anti-fouling property) is pectin with high degree of esterification dissolved in the working buffer. Previous works well demonstrated that the ageing effect by hypochlorite is much faster at high temperature than at low temperature [17]. Hence to exclude any special effect induced by temperature variation, in the present case, all the ageing and cleaning experiments are conducted at room temperature. Unless otherwise stated, the pH of the soaking solution is also kept at its natural value.

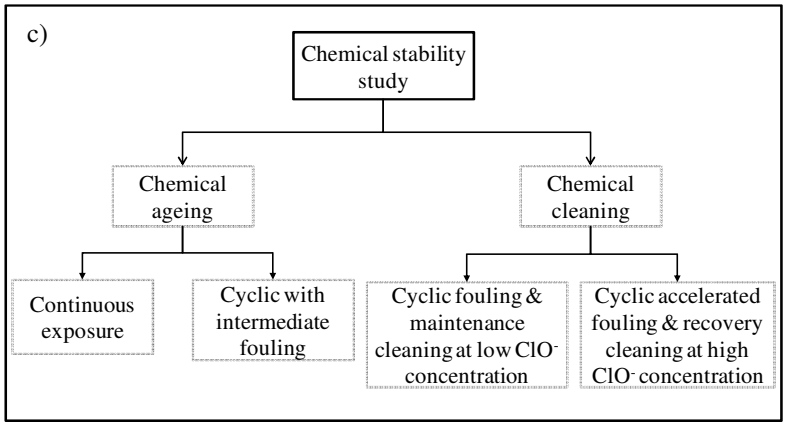

Figure 1: schematic representation of the strategical chemical ageing and chemical cleaning studies.

6.3.4. Chemical ageing

The concept of accelerated ageing suggests that ageing generated by a high concentration during a short time equals to the one attributed to a low concentration during a long time [23]. It serves as a base line for a quick understanding of the chemical stability of the membrane. In this study, during ageing experiments, the membrane is kept in contact with different concentrations of NaOCl under static condition. The tested NaOCl concentrations are on a scale focused on its industrial concentration (400 ppm) and accelerated ageing condition (800 or 2000 ppm). The continuous exposure durations are varied from 3 h to 210 h in Pyrex tubes protected from light at room temperature. The bathing solution is kept at its natural pH or adjusted to 12 using 1M NaOH. The natural pH of 400, 800 and 2000 ppm solutions were 8.04, 8.47 and 9.02 respectively. In order to keep the concentration of NaOCl constant, bathing solution is changed every 24 h. Subsequent to rinsing with water, permeability and fouling propensity of aged membranes is measured using the working buffer and 0.3 mg/mL pectin solution as feed respectively. Alternative to continuous exposure, membrane were subjected to a 12 h lasting ageing in 2000 ppm solution pH natural and an intermediate 2 h lasting fouling at 0.25 bar.

6.3.5. Membrane fouling and cleaning

6.3.5.1. Maintenance cleaning

In wastewater treatment, maintenance cleaning is employed to avoid long term development of membrane fouling. Here also a suitable maintenance cleaning strategy at low NaOCl concentration is studied under a given operational condition. Previous studies have shown that hypochlorite induced changed membrane property is not obvious in the first instance, while it becomes more apparent after several episodes of fouling and cleaning [12]. The maintenance cleaning study in the present case is thus comprised of multi-step fouling and cleaning.

Irreversibly fouled membrane is obtained by filtering 0.3 mg/mL pectin solution dissolved in the working buffer at a TMP of 2 bar for 4 h. Subsequent to rinsing with buffer and manual brush to remove reversible fouling, the membrane is kept in contact with 400 ppm NaOCl solution at pH 12 for one hour in light protected Pyrex tube. This cleaning condition is set after careful examination of ATR-FTIR spectra of membrane aged for 12 h under these conditions has given similar absorbance with a virgin membrane. To evaluate the hydraulic cleaning efficiency,

permeability is measured using the working buffer. Equation 1 shows the hydraulic cleaning efficiency evaluated as ratio of membrane resistance before and after chemical cleaning:

$$\text{Hydraulic cleaning efficiency} = \frac{R_{cleaned}}{R_{Virgin}} * 100 \quad (1)$$

Where $R_{cleaned}$ is the resistance of chemically cleaned membrane, and R_{virgin} is the resistance of virgin membrane. The total membrane resistance is calculated according to Darcy's law (Equation 2):

$$R = \frac{TMP}{\mu * J_v} \quad (2)$$

Where TMP is the transmembrane pressure, J_v the working buffer flux and μ the viscosity of the buffer at ambient temperature.

6.3.5.2. Recovery cleaning

To achieve severely fouled membrane in short duration, multi-cycle accelerated fouling tests are run. This is achieved by immersing the membrane potted on opposite side of a porous spacer in a bath containing 0.3 mg/mL pectin solution. The immersed membrane is connected to a peristaltic pump to achieve constant permeate flux (chapter 4, Figure 1-b). This helps to have well established membrane fouling protocol that can serve as a baseline for proper evaluation of the efficiency of the recovery cleaning. Moreover, in addition to enhanced foulant formation in short duration, setting the flux well above the critical flux is important to avoid formation of reversible fouling.

In a preliminary experiment, the critical flux for each membrane is determined according to the method proposed by Le Clech *et al*, 2003 [24]. Taking a step height of 2 L/m^2.h and step duration of 15 minute, the critical flux is 6 and 10 L/m^2.h for the particle free and O/I hybrid membrane respectively. So during the accelerated fouling test, the flux is set at 25 kg/m^2.h, well above these critical flux.

To get a fully developed fouling, each experiment was subjected to last six hours. However, due to mechanical limitations in the experimental system, the maximum TMP that the system can withstand is 0.150 bar. Thus, depending on the rate of fouling, filtration has also been terminated before 6 h. Subsequently, all the membranes are *ex-situ* cleaned by soaking in 2000 ppm NaOCl

at room temperature for 1 h. This concentration is chosen to overcome mass transfer barrier and to maintain reasonable reaction rate during cleaning [10].

6.3.6. Membrane characterization

Any physical or chemical change in the membrane induced during the cleaning or the ageing is further evaluated through EDX, ATR-FTIR, TEM and SEM analyses. Inclusion of NP^{SP} in the polymer matrix was examined by a transmission electron microscope (JEOL JEM-2010F). The microstructures of virgin, fouled & cleaned or chemically aged membranes are carefully examined by scanning electron microscope (SEM) (Carl ZEISS LEO 435VP with an EDX - INCA Oxford Instruments) after air drying and gold coating. In addition to qualitative interpretations such as pore enlargement, quantitative evaluation of the SEM pictures are also realized through analysis of porosity and pore density by processing the SEM microstructures with an open access image analyzing software (Image J, version 1.47). The results are compared with the results of the virgin membrane. The presence of NP^{SP} in the membrane is further analyzed through energy dispersive X-ray spectroscopy (EDX, integrated within the SEM apparatus). To obtain an accurate representation of the results, three to four measurements on three separate membranes (set of 9 to 12 measurements) are carried out for each type of analysis and treatment condition. ATR-FTIR spectrum of the membranes was realized by the attenuated total reflectance (ATR) technique on Thermo Nicolet Nexus 670 fitted with DTGS detector and diamond ATR crystal, where 16 scans at 4 cm^{-1} resolution are averaged. Results are mean intensities of six different measurements. All data acquisition, baseline corrections and image construction is done using OMNIC^s software.

In addition, ATR-FTIR map of the chemical composition of the membrane surface was composed by measuring the IR spectrum in a narrow frequency band with FTIR microscopy while the focal spot is moved across the surface. This method is very suitable to provide with a quick, easy and reproducible mechanism to evaluate the structural integrity of functional groups going beyond identification of specific surface functional groups [25]. In this work, parts of these functional groups are attributed by the polymeric coating layer of the NP^{SP}. Hence the mapping could also serve as an easy way of measuring the homogeneous dispersion of the used NP^{SP} and applied hypochlorite treatment over a given membrane area. Thus, membranes ATR-FTIR mapping over an area spanning from 3 mm by 3 mm to 7 mm by 15 mm is employed before and

after ageing using Iniomx thermo scientific FTIR unit with Germanium ATR crystal at a resolution of 8 cm^{-1}. The overall approach is based on normalization of the signal correlated to oxidative damage by that of a specific band considered to be invariant during the membrane degradation (1185 cm^{-1}). ATR-FTIR analysis of the membrane indicated that the virgin membrane contains bands belonging to both PVDF and and NP^{SP} used as a nano-filler during organic-inorganic hybrid membrane preparation (Figure 2). Table 6.1 depicts the different bands identified from Figure 2. The specific signals in FTIR-ATR are bands located at 880 due to C-H bending and 2845 cm^{-1} due to C-H stretch linked to octylamine and bands at 2920 and 3020 cm^{-1} due to C-H stretch linked to bonded PEG silane [19]. The band at 1069 cm^{-1} is PVDF fingerprint [17] and the strong absorption bands from 1000-1280 cm^{-1} is fluorocarbon stretching frequencies from PVDF [25]. The visible band at 838 cm^{-1} presents CH out of plane and deformations & CH_2 rocking from either PEG or octylamine groups. Hence, the band intensity analysis consists the normalization of the H height by H_{1185} leading to the H_x/H_{1185} ratio, where x is the band at 880, 2845, 2920 and 3020 cm^{-1}. In order to measure the height H of bands, the line measured between 3025 cm^{-1} and 1160 cm^{-1} is used as a baseline since this is a range where non-specific, nevertheless non-zero absorbance of the membrane occurs. This ratio is then used for the direct quantification of the different bands under different treatment condition.

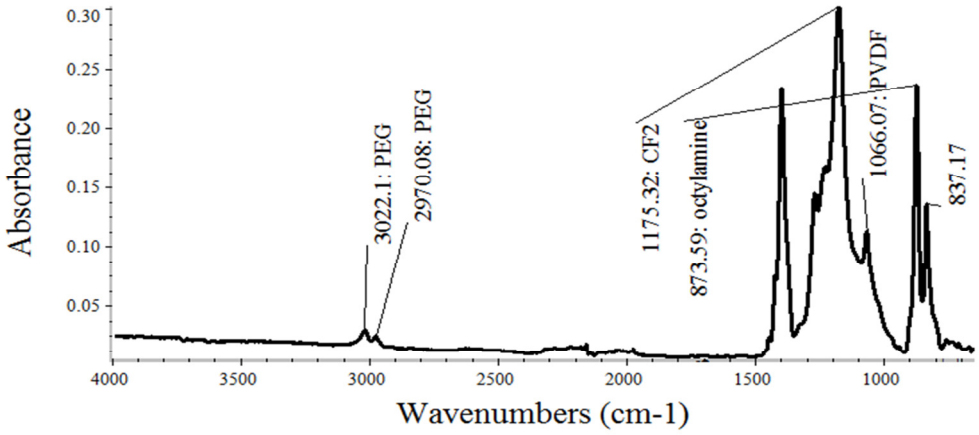

Figure 2: ATR-FTIR spectra of NP^{SP}-PVDF hybrid membrane.

Table 6.1: Identification of the main bands from FTIR spectrum obtained in Figure 2.

Wave number (cm^{-1})	Type of vibration	Sources
838	CH out of plane & CH_2 rocking	PEG or octylamine groups
880	C-H bending	octylamine
2845	C-H stretch	octylamine
2920	C-H stretch	PEG silane
3020	C-H stretch	PEG silane
1069	C-F	PVDF fingerprint
1000-1280	fluorocarbon stretching	from PVDF

Most preferred neutral macromolecules (e.g., PEG or dextran), used to determine selectivity curve of membrane, have much lower particle size as compared to the membrane pore size (0.2 µm). Hence, it was not possible to assess presence of any type of hypochlorite induced change in the membrane rejection capacity. Testing the pectin rejection capacity of membrane is also avoided since the permeation of particles may reduce due to adsorption of particle on the membrane instead of hypochlorite induced membrane surface modification [10].

6.4. Results and discussion

6.4.1. General effect of hypochlorite treatment

There are many debates about the use of accelerated ageing test as a predictive tool especially due to lack of adequate results to transpose lab-scale accelerated ageing to natural ageing phenomena [26]. Yet the method is useful for example to assess the dynamics of the membrane over time [27]. The accelerated ageing study in this paper is thus used as a quick strategy to understand chemical stability of the newly introduced NP^{SP}-PVDF membrane.

ATR-FTIR analysis after accelerated ageing showed that all the parameters (concentration of the NaOCl, exposure time and pH) altered the membrane surface chemistry. As shown in Figure 3, for a fixed NaOCl concentration (2000 ppm), significantly visible new bands that were not observed in the virgin membrane appeared at 2920 cm^{-1} and 2845 cm^{-1}. These bands, corresponding to C-H stretch, can possibly be attributed to residual octylamine layer that was left on the NP^{SP} surface after silanization with PEG during its preparation [19]. Moreover, the

intensity of these new bands increased by an order of magnitude after 210 h of exposure while the band at 3020 cm^{-1}, belonging to PEG, disappeared completely (see inset of Figure 3).

In agreement with most other PVDF based ageing studies, band at 1069 cm^{-1} ascribed as PVDF fingerprint remained intact under any circumstance due to chemical stability of C-F bonds [17-18]. During preparation and characterization of the PEG coated NP^{SP}, Brullot *et al.* [19] ascribed bands at 587 cm^{-1} to Fe-O lattice vibration. They also stated that after modification of the particles with PEG silane, there is possible contribution from Fe-O-Si lattice vibration in this region. However, in this paper, restricted by the lowest detection limit of the ATR-FTIR machine used, it was not possible to examine the status of bands in this region. Thus, the discussion regarding changes in the membrane characteristics were restricted mostly to the polymeric coating layer of the NP^{SP}.

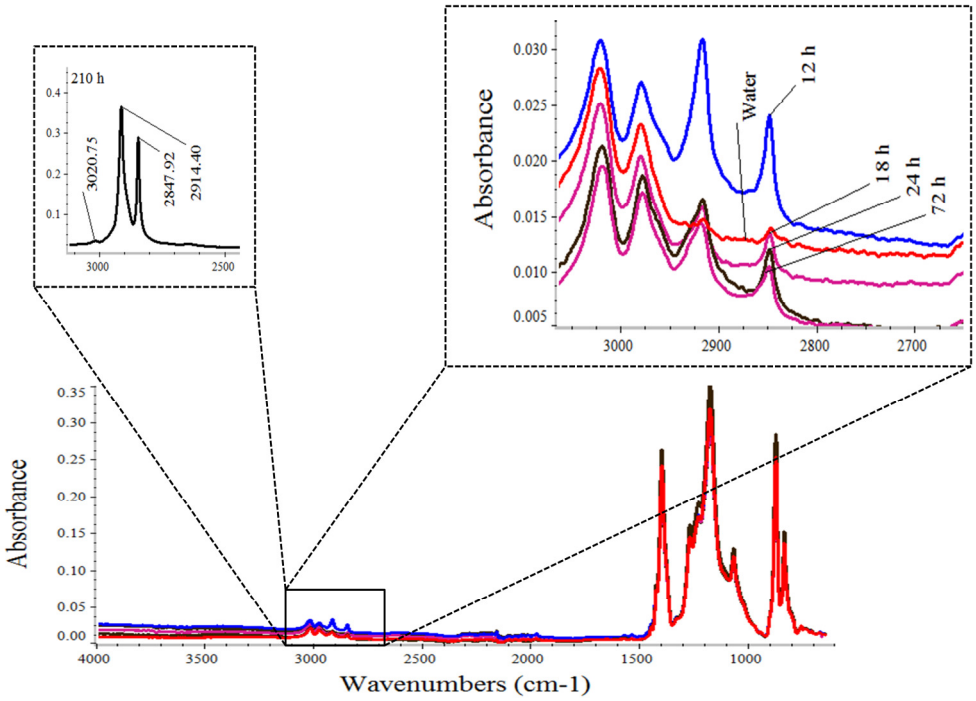

Figure 3: Effect of soaking duration at a fixed 2000 ppm solution without pH adjustment.

Prior to pH adjustment, both 400 and 2000 ppm NaOCl solutions caused comparative oxidative damage to the membrane (Figure 4-a). However, after adjusting pH of both solutions to 12, 2000 ppm has persistently the same effect as at pH 9 (Figure 4-b). In contrast, 400 ppm has a negligible effect at pH 12 as indicated by the absence of bands belonging to octylamine layer (Figure 4-c).

During ageing studies of PSf membrane, an $^{\bullet}OH$ governed oxidation reaction is suggested as the cause for facilitated ageing at low pH [11]. A similar $^{\bullet}OH$ governed reaction mechanism can also be hypothesized for the observed pH dependent facilitated oxidative damage to the membrane.

For the $^{\bullet}OH$ to be formed, the pH of the solution needs to allow presence of both HOCl and ClO^- (pH: 6 to 9) or at least HOCl (pH: 3 to 5). However at pH 12, since the only free chlorine available is ClO^-, there is limited probability of $^{\bullet}OH$ formation.

Prior to pH adjustment, since 400 ppm solution has pH 8, it allows presence of both HOCl and ClO^-, there by production of significant amount of $^{\bullet}OH$. This could explain the equal extent of oxidative damage induced by both 400 and 2000 ppm solutions, regardless of the three fold difference in the total free chlorine concentration (Figure 4-a). Subsequent to adjusting the pH of both solutions to 12, the 2000 ppm solution has consistently similar effect since it still contains considerable amount of ClO^- (Figure 4-b). In contrast, due to absence of $^{\bullet}OH$ formation at high pH [11] and presence of low concentration of ClO^-, 400 ppm solution at pH 12 exhibited limited oxidative damage to the membrane (Figure 4-c).

Several past works pointed out that PVDF is vulnerable to caustic environment (e.g., 12 M NaOH at 80°C) [28-29]. In the present case 0.5 M NaOH was used to adjust pH of the soaking solutions. Contrary to what has been suggested, no significantly visible change in the region of CF_2 fingerprint (1280-1000 cm^{-1}) and hydrocarbon deformations between 1350-1450 before and after treatment was observed.

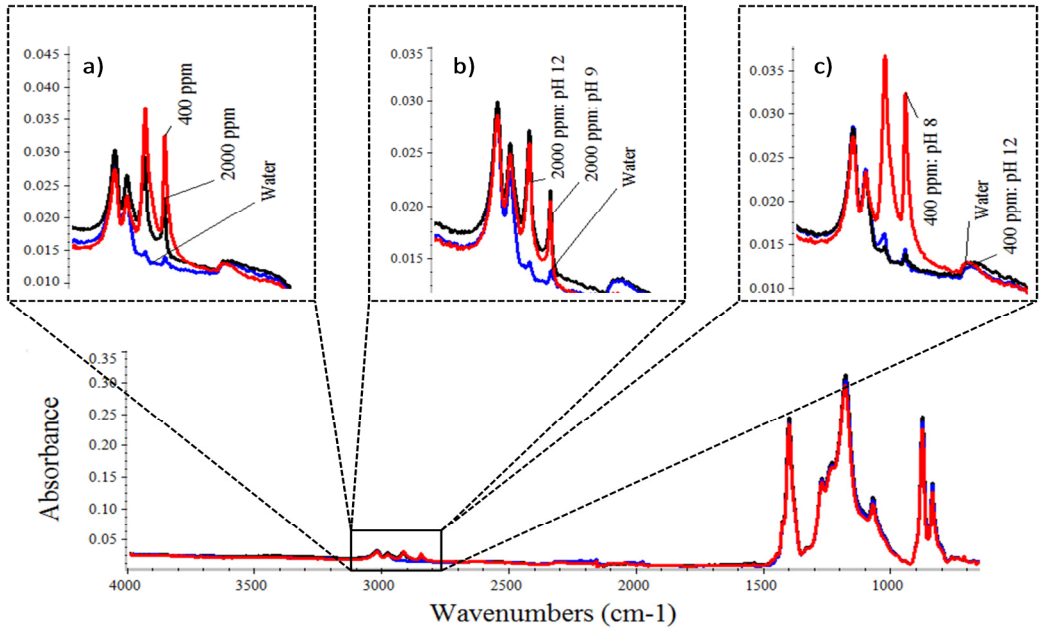

Figure 4: ATR-FTIR analysis of a) effect of NaOCl concentration for 12 h fixed exposure duration at pH natural, b) effect of soaking solution pH for membrane aged in 2000 ppm solution for 12 h and c) effect of soaking solution pH for membrane aged in 400 ppm solution for 12 h.

6.4.2. ATR-FTIR mapping

Figure 5a-d shows IR mapping results for H_{2850}/H_{1185}, H_{2920}/H_{1185} and H_{880}/H_{1185} ratio. The results include IR maps of virgin membrane and membranes aged in 400, 800 and 2000 ppm NaOCl solutions at pH 12 or pH natural (8-9) for 12 h. The absorbance intensities of ATR-FTIR spectral maps are proportional to color changes given as blue, green, yellow and red in increasing order of concentration. 2D images were used in order to visualize the ratio between the signal of surface functional groups and the background. But 2D projections with scaled intensity can be ambiguous when analysis of the roughness of the intensities is desired. To avoid this ambiguity in addition to 2D images, examples of 3D projections are shown.

Figure 5a-b shows 3D and 2D ATR-FTIR spectral map of membranes for H_{2850}/H_{1185} ratio, which belongs to the relative octylamine absorbance. For virgin membrane, uniformly dispersed blue color was obtained over an area of 1.05 cm^2. In the false color images produced, the blue color indicates a domain of low concentration. The color uniformity together with absence of projections in the vertical direction (see the 3D projections) are good indicators of presence of the NP^{SP} all over the membrane surface. Treatment of the membrane with NaOCl under different conditions induced gradual color evolution. These variations are correlated with gradual

appearance of octylamine, after removal of the primary PEG layer. However, combination of different colors appeared on a membrane with a specific treatment condition. Example, at 2000 ppm pH natural, the color combination was dominated by green and yellow and at 400 ppm pH natural the colors were mostly green and blue.

The NP^{SP} are embedded in the polymer matrix. As a result some of the particles are easily accessible to NaOCl while others might be covered by an overlying polymeric constituent of the membrane (PVDF). This can thus be one of the underlying reasons for the presence of different colors (2D projections) and various IR intensities (3D projections). Furthermore, the high concentration NaOCl was dominated by yellow and green (domain of high concentration) while the low concentration was dominated by blue and green (domain of low concentration). The intensities of the bands (IR intensity roughness) as shown in the 3D projections are more visible for 2000 ppm and 400 ppm at pH natural than 400 ppm at pH 12.

During preparation of the O/I hybrid membrane, both mechanical rotation and sonication were applied to mix and disperse the NP^{SP} in the casting solution. Nevertheless, TEM image (see appendix: Figure A1) revealed the inevitability of random particle agglomeration. So the color variation could partly be attributed to presence of these agglomerations.

For H_{2920}/H_{1185}, membrane surface aged in 2000 ppm solution at both pH 9 and pH 12 and 400 ppm at pH 8 were mostly green and yellow i.e. high concentration (Figure 5c). Contrary to this, 400 ppm solution at pH 12 was mostly dominated by low concentration domain (blue). In section 3.1, Figure 4 indicated that at natural pH both 400 and 2000 ppm solutions gave equal extend of oxidative damage while 400 ppm pH 12 did not. This is in good agreement with the observed IR spectral color variation in Figure 5c and intensity roughness in Figure 5a. In Figure 5d IR spectral map of membrane aged in 800 ppm (pH 8.47) and 2000 ppm (pH 9) NaOCl solutions illustrated no obvious difference.

The ATR-FTIR results shown in the previous section allowed an easy and rapid quantification of the surface chemical composition. But ATR-FTIR mapping went beyond from simple detection of specific functional groups to detection of variations in composition over a given surface. Hence it helped to verify the evenness of the NP^{SP} presence and the hypochlorite treatment over a given membrane area. It is worth noting that the observed trends in both simple ATR-FTIR and mapping analyses were coherent.

Treatment condition	Virgin	400 ppm	2000 ppm
pH natural	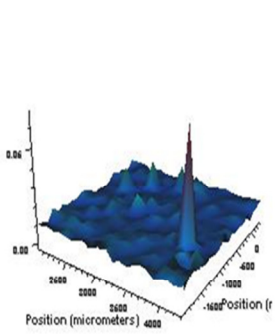	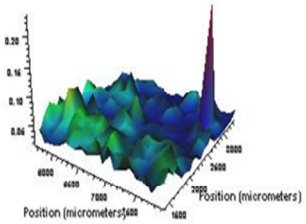	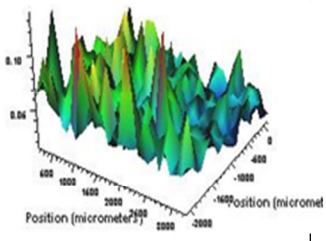
pH 12		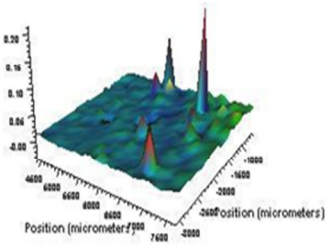	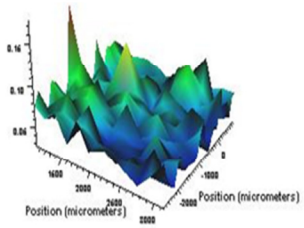

(a): H_{2850}/H_{1185}

Treatment condition	Virgin	400 ppm	2000 ppm
pH natural	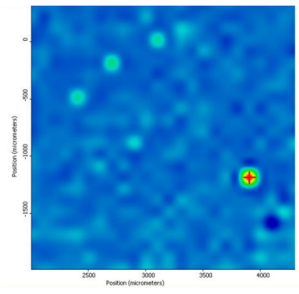	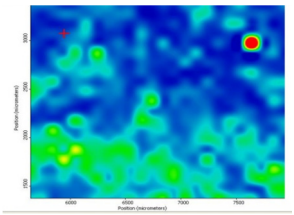	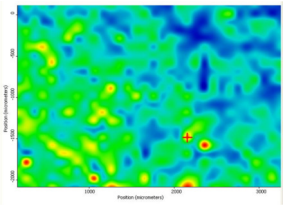
pH 12		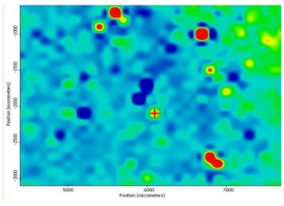	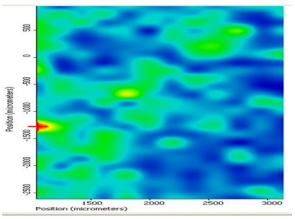

(b): H_{2850}/H_{1185}

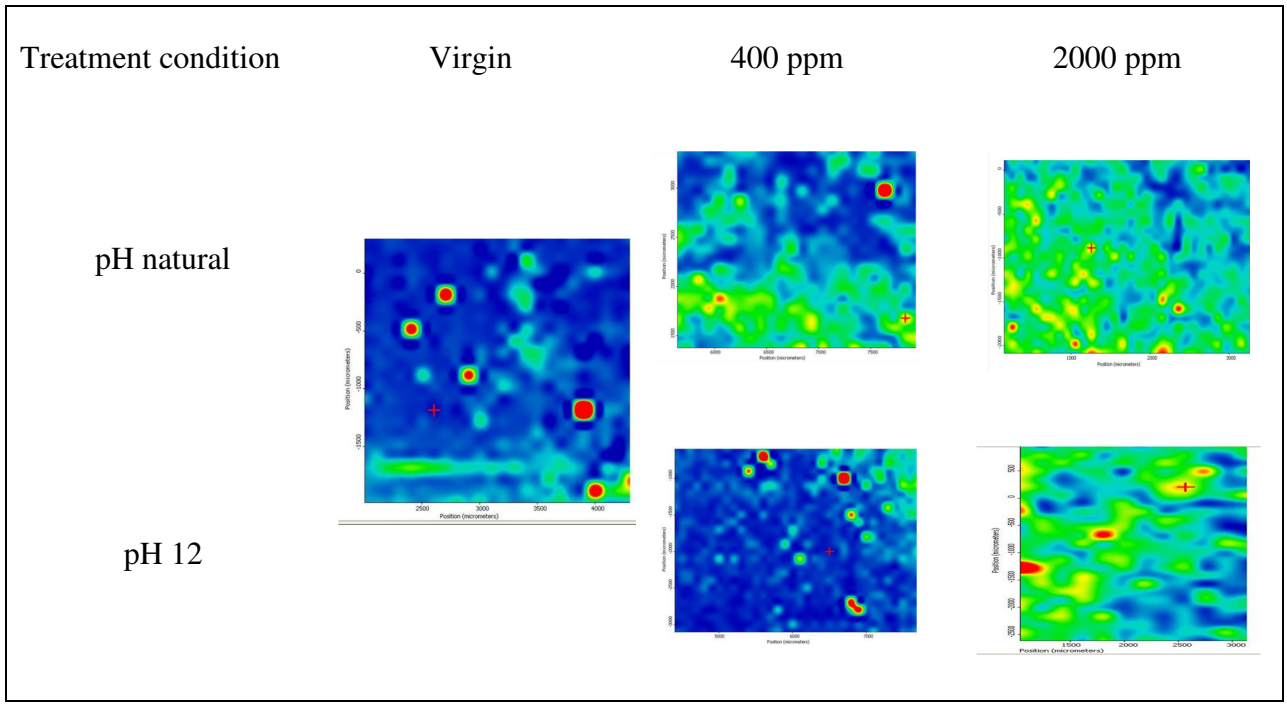

(c): H_{2920}/H_{1185}

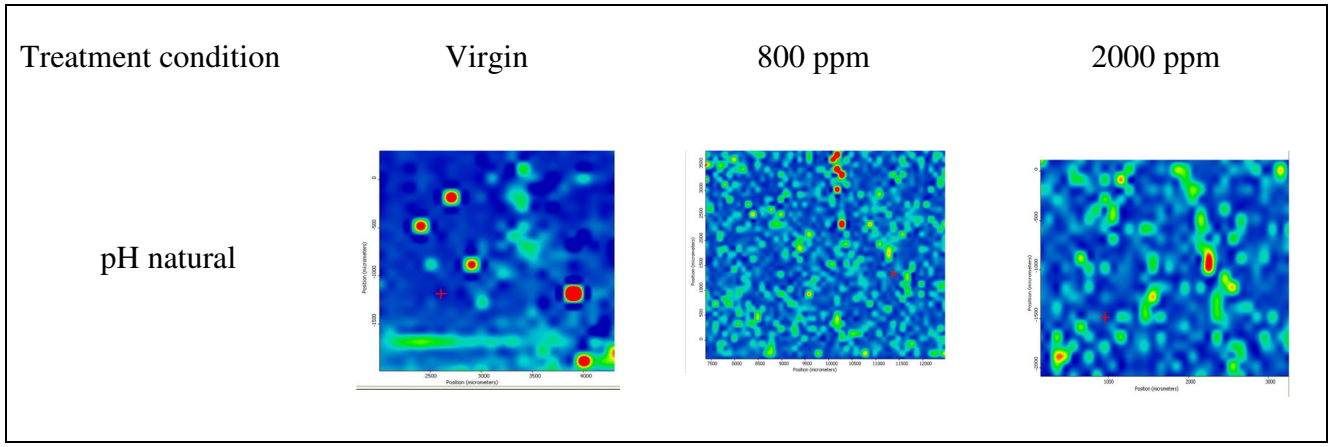

(d): H_{880}/H_{1185}

Figure 5: ATR-FTIR spectral mapping of O/I hybrid membrane aged in 400, 800 and 2000 ppm NaOCl solutions. The colors are relative intensities of bands: a) H_{2850}/H_{1185} 3D projections, b) H_{2850}/H_{1185}, c) H_{2920}/H_{1185} and d) H_{880}/H_{1185}. The treatments were applied at pH 12 or the natural pH of each concentration.

6.4.3.Elemental analysis

The ATR-FTIR analysis was used for an easy and rapid determination of the presence of specific functional groups. However, detection limit in the FTIR analysis did not show the status of Fe,

responsible for the magnetic responsiveness of the membrane. Thus, further elemental analysis of the membrane using EDX was conducted for relative quantification of Fe and C. results showed similar amount of relative Fe with slight variation for all the membranes (Table 6.2). This is an indirect way of ensuring absence of fluctuation in the magnetic property of the membrane that could have arisen from Fe instability during hypochlorite ageing or cleaning.

On the other hand, several studies on advanced oxidation processes have shown that transition metal ions such as Fe^{2+}, present in solution, effectively catalyzes reduction of HClO to release the polymer degrading $^{\bullet}OH$ in a "Fenton like" reactions [11]. For example a polyamide reverse osmosis membrane showed accelerated chlorination in the presence of ferrous iron [15]. The authors hypothesize that $OH^{\bullet}$ radicals produced during the Fe(II)/HOCl redox reaction attack the N-H bond on the membrane amide group, thereby lowering the activation energy for chlorination of the *m*-phenylenediamine ring. Causserand et al, [16] have also shown severe mechanical degradation of PES/PVP membrane in the presence of this ion. Both studies correlated the facilitated degradation to the strong catalytic effect of iron ($Fe^{2+} + HClO \rightarrow Fe^{3+} + {}^{\bullet}OH + Cl^{-}$) without being consumed in the overall reaction. In the present case the catalytic site for such reaction is initially inaccessible since the NP^{SP} are coated with polymer. But verifying the possible involvement of the Fe in a self catalyzed 'Fenton like' degradation of the membrane once the polymer coating layer is oxidized could also be important.

Table 6.2: Summary of Fe and C content from EDX elemental analysis.

Soaking condition	C (% mass)	Fe (% mass)
Virgin	48 ±7	0.27 ± 0.043
0 ppm 12 h	36± 7	0.25 ± 0.014
400 ppm 12 h	38 ± 6	0.28 ± 0.021
24 h 2000 ppm	40 ± 8	0.19 ± 0.021
72 h 2000 ppm	38 ± 7	0.27 ±0.063

6.4.4. Chemical ageing

6.4.4.1. Continuous ageing

Accelerated ageing through continuous exposure to chemical cleaning agent has become the new strategy to quickly understand membrane chemical stability. Subsequently, single step fouling is conducted to assess ageing induced membrane fouling behavior.

Table 6.3 depicts the total membrane resistance calculated according to equation 2, for membranes aged in 2000 ppm NaOCl solution under different soaking duration. The membrane aged for 12 h revealed a threefold higher resistance than virgin membrane. The value increased further by a factor of seven after 210 h of ageing. Nevertheless, the values were also observed to decrease after 24 and 36 h of ageing compared to the value obtained after 12 h.

Table 6.3: total membrane resistance of virgin membrane, membrane aged in 2000 ppm solution for several hours and fouled membrane.

Soaking duration	$R_{after\ ageing}$ ($x10^{11}$ m^{-1})	$R_{after\ fouling}$ ($x10^{11}$ m^{-1})
0	3.9±2.48	-
12	12.4±0.06	13.8±0.18
24	5.2±0.80	8.4±0.04
36	7.3±0.01	16.3±0.48
72	13.3±0.3	25.7±0.54
210	27.7±0.08	-

Even if effect of ageing was evaluated on macroscopic scale by measuring permeability and modified antifouling property, quantifying the effect at a microscopic scale is also interesting. Hence, SEM micrographs were further processed using Image J to quantify the modified pore size and porosity due to chemical ageing. Figure 6-b represents calculated membrane pore densities and measured steady state pectin flux for virgin, 6, 12, 18, 24, 72 and 210 h aged membranes. The standard deviation out of set of 9 to 12 measurements for each treatment conditions ranged between 0.3 to $2.1*10^{12}$ m^{-2}. For membranes aged from 6 to 24 h, both pore density and steady state pectin flux evolved in the same direction. An opposing trend however was obtained when membrane was aged further to 210 h (Figure 6-b). SEM micrograph shows

that membrane aged for 72 h have more open structure with enlarged pore size than virgin membrane (Figure 7-c). However, both pore density and steady state flux of the 72 h aged membrane were half of the value obtained for virgin membrane (Figure 6a-b). These alterations could be perfectly correlated to the elimination of the NP^{SP} polymeric coating layers, which were an added value to the membrane`s improved antifouling property. Regardless of the C-F stable bonds of PVDF membrane, changed behaviors due to modification of surface modifiers in many other commercial or home-made PVDF based membranes is well reported in literature [17-18]. For instance, a similar pore size enlargement as a result of surface modifier elimination was observed by Abdullah and Bérubé, 2013 [18]. By ageing the membrane further to 210 h however, the pore density increased by a factor of e.g, 3 compared to membrane aged only for 24 h while the steady state pectin flux reduced by a factor of 2. Such performance loss regardless of the gain in pore density is in good agreement with the complete disappearance of bands at 3020 and 2920 cm^{-1}, belonging to PEG (see inset of Figure 3 in section 3.1). Since PEG is one of the components that gave the membrane an antifouling property, its gradual removal will eventually leave the PVDF membrane with its intrinsic fouling sensitive nature.

The progressive membrane densification after 6 and 12 h of ageing (Figure 7-c) was also in good agreement with the significantly reduced pore density and steady state pectin flux (Figure 6-b). The cause for this reduction is assumed to be polymer plasticization. This refers to hypochlorite induced change in the thermal behavior that transforms a high-Tg polymer into a rubbery state [30]. When the Tg is reduced to below ambient temperature, molecules are mobilized. This molecule mobilization particularly of PEG could best explain the observed membrane densification in the transient process of chemical ageing.

The steady state fluxes of membranes aged for 18 and 24 h were slightly higher than membrane exposed for 72 h regardless of their lower pore densities. This may be due to the presence of the surface modifiers from incomplete oxidation reaction that still gives the membrane an antifouling property. Nevertheless, owing to its open structure, the 72 h exposed membrane revealed a 15% higher initial flux compared the flux obtained for 18 or 24 h aged membranes followed by rapid decline until it stabilize after about 40 minutes of filtration (Figure 6-a: ◊).

Figure 7-a shows SEM micrograph of membrane aged in 400, 800 and 2000 ppm solution for 12 h. The membrane pore densities were $9.98\pm0.42*10^{12}$, $1.88\pm0.30*10^{12}$ and $2.49\pm0.72*10^{12}$ m^{-2} respectively. Figure 7b shows SEM image of membrane aged in 400 and 2000 ppm solution for

12 h with and without pH adjustment. The pore density of membrane aged in 400 ppm pH 12 ($11.38\pm0.33*10^{12}$ m^{-2}) was similar to the pore density of virgin membrane ($11.25\pm0.29*10^{12}$ m^{-2}) while the value reduced for membrane aged at its natural pH 8 ($9.98\pm0.42*10^{12}$ m^{-2}). In contrast, the pore density of membrane aged in 2000 ppm solution, controlled pH at 12 ($3.41\pm0.77*10^{12}$ m^{-2}) and natural pH at 9 ($2.49\pm0.72*10^{12}$ m^{-2}) were significantly lower than the virgin membrane. In summary, chemical ageing caused membranes' altered hydraulic resistance, morphology and antifouling property. All these changes are perfectly correlated to the modification of the used NP^{SP}. The different types of changes with respect to exposure conditions were coherent with the observed altered surface chemistry during ATR-FTIR analysis. Example in Figure 5d, IR spectral map of membrane aged in 800 ppm (pH 8.47) and 2000 ppm (pH 9) NaOCl solutions showed no noticeable difference. Parallel to this, the membrane pore densities calculated for both conditions were similar.

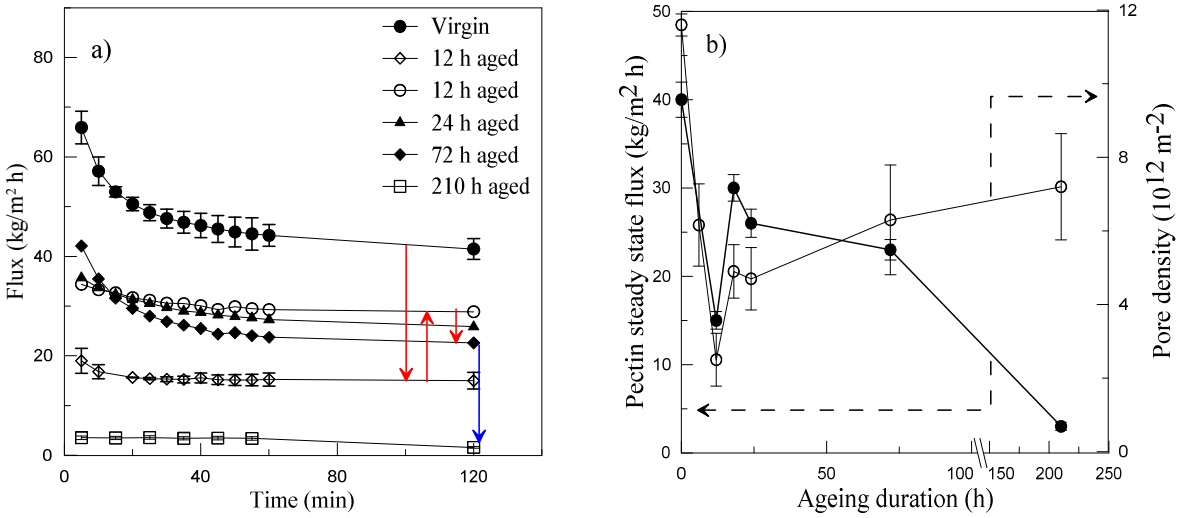

Figure 6: Transmembrane flux of membrane aged in 2000 ppm solution while filtering 0.3 mg/mL pectin at 0.25 bar and b) the steady state pectin flux measured at 0.25 bar from (a) and membrane pore density estimated based on SEM image analysis using Image J.

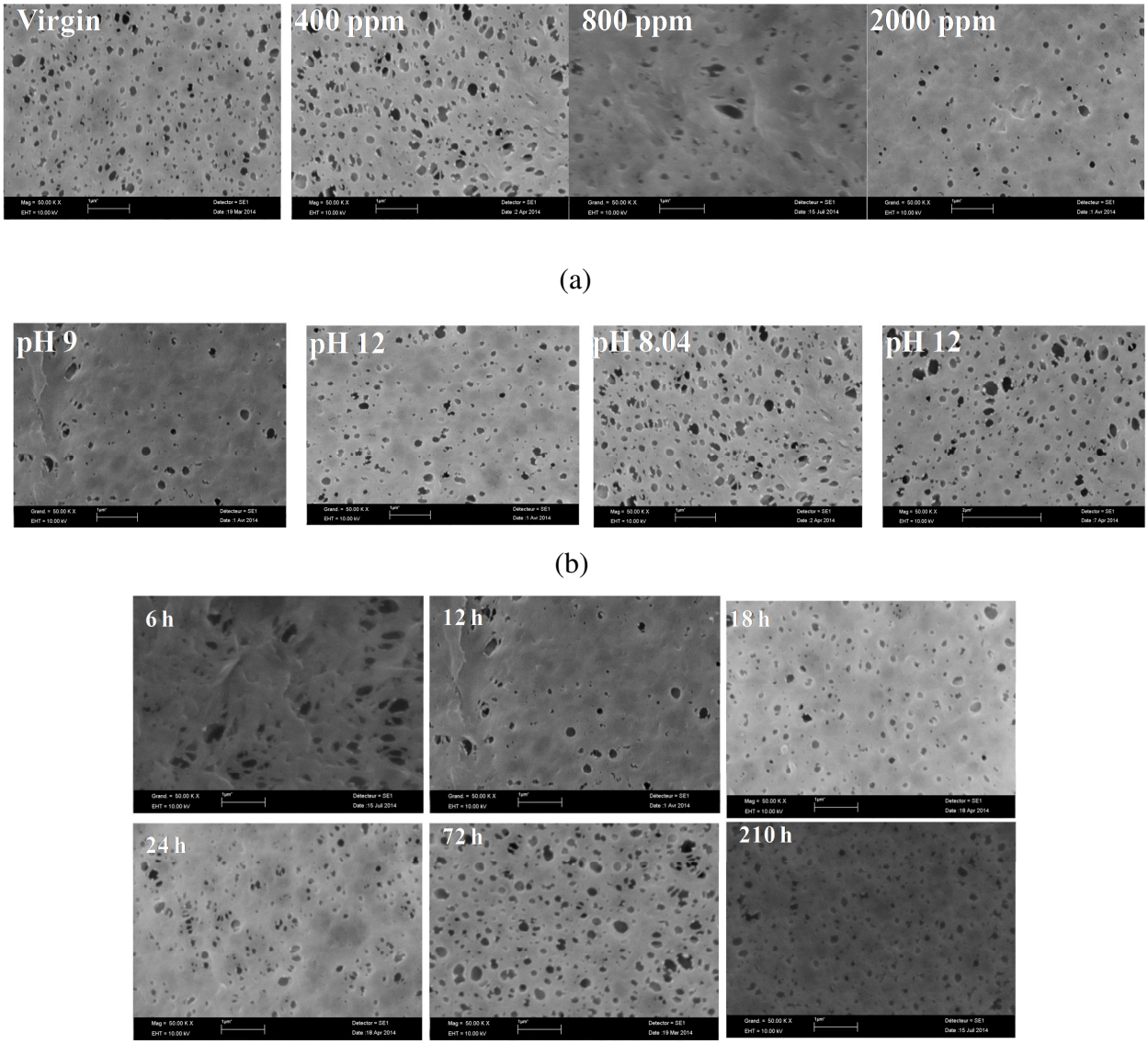

Figure 7: SEM micrograph of membrane a) treated with different concentrations of NaOCl for 12 h without prior pH adjustment, b) treated with 2000 at pH 9 and 12 and 400 ppm at pH 8 and 12 and c) treated with 2000 ppm at pH 9 for 12, 24, 72 and 210 hours.

6.4.4.2. Cycling ageing and an intermediate fouling

In addition to continuous exposure, membranes were subjected to many episodes of ageing accompanied with intermediate fouling. This approach is supposed to represents the actual situation where cleaning is employed among many episode of fouling. Figure 8 shows the flux trend of membrane exposed to sequential accelerated ageing and an intermediate fouling. Virgin

membrane is aged for 12 h in 2000 ppm solution without a prior compaction. The steady state flux through this 1st cycle aged membrane was 15 kg/m^2.h at 0.25 bar while filtering 0.3 mg/mL pectin. By exposing the membrane to 2nd cycle ageing, 50% of the steady state flux obtained after 1st cycle ageing was lost. However, oxidative ageing of the membrane also resulted in an 18% enhanced flux after 4th cycle ageing compared to the value obtained after 3rd cycle ageing, possibly due to enlarged pore size. But the 4th cycle improved flux also became a profound base for a severe fouling that resulted in a significant performance loss in the 5th cycle.

Compared to a continuously aged and subsequently fouled membrane (Figure 6-a), those with an intermediate 2 h fouling after each 12 h ageing duration (Figure 8) seems to have delayed impact of the exposure to NaOCl. This is attributed to hindrance in the extent of hypochlorite induced damage to the membrane by the presence of adsorbed foulant layer. Nevertheless, the observed similar flux between first cycle of Figure 6-a and Figure 8 confirm the reproducibility of the unique densification observed after 12 h of ageing.

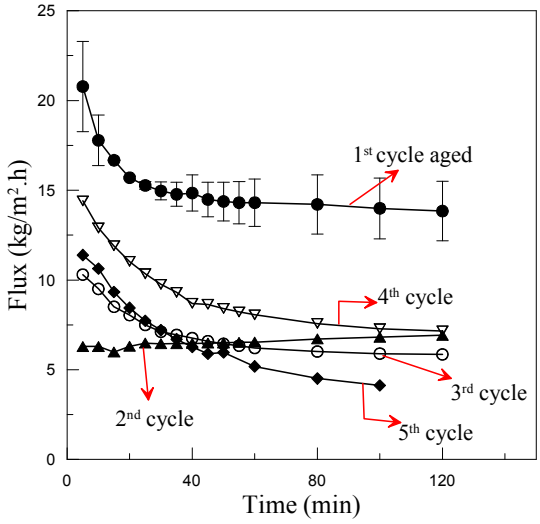

Figure 8: the membrane is subjected to a multi-cyclic ageing of the membrane in 2000 ppm solution at pH 12 with intermediate fouling using 0.3 mg/mL pectin. The flux in this figure therefore represents the flux obtained during a 2 h lasting pectin filtration at 0.25 bar.

6.4.5. Chemical cleaning

6.4.5.1. Recovery cleaning

Figure 9 represents the TMP trend over five consecutive cycles for membranes with zero, 0.25 and 0.33 w/w % NP^{SP} loadings immersed in 0.3 mg/mL pectin. The immersed membrane was

connected to a peristaltic pump to attain a constant supercritical flux of 25 kg/m^2.h for an accelerated fouling. For recovery cleaning, usually higher concentrations of cleaning reagents are applied. Hence, after each cycle the membranes were soaked in 2000 ppm NaOCl solution under static condition for 1h.

Looking at Figure 9, the NP^{SP} free membrane gave the worst performance under any circumstance due to sensitivity of plain PVDF to fouling (Figure 9-a). In contrast, both types of hybrid membranes allowed an extended filtration period owing to the NP^{SP} induced antifouling property of these membranes. And for the hybrid membranes, 0.33 w/w% NP^{SP} gave greater performance than 0.25 w/w % NP^{SP} loading. Moreover, the average membrane pore size for the particle free and both O/I hybrid membranes were 0.4 µm and 0.2 µm respectively. Hence, in addition to fouling sensitivity of pure PVDF membrane, part of the performance difference can be attributed by larger pores being more easily plugged.

The main target of hypochlorite cleaning of membrane is to restore initial membrane performance but not to gain increase over initial values [10]. In this case however, strictly linked to NaOCl induced changes in the membranes structure, 1st and 2nd cycle post-cleaned hybrid membranes gave an extended filtration time over virgin membrane. Nevertheless, this early stage NaOCl related performance improvements also became a profound base for a proliferated fouling in the later stages. Hence, 3rd and 4th cycle NaOCl cleanings were able neither to increase nor restore the original membrane performance.

Previous studies have shown that initial stage performance improvements of post cleaned membrane over virgin membrane is caused by enlarged pore size caused by polymer chain breakage, increase hydrophilicity or weak mechanical strength [8, 14]. In the present case, the initial stage enhanced permeability could be attributed to pore size enlargement after the oxidative action of NaOCl removed part of the NP^{SP} coating layer that partially filled the membrane pores as shown in the SEM micrograph. And the later stage enhanced fouling propensity is linked to the partial or complete removal of the NP^{SP} polymeric constituents that had given the membrane an antifouling property.

Furthermore, during continuous ageing, a significant reduction in membrane pore density occurred after 6 and 12 h of exposure to 2000 ppm hypochlorite at pH natural. Looking at the trend in Figure 9, the timing at which performance loss occurred (4th cycle) was after 5 h of intermittent exposure i.e. close to the 6 h continuous exposure. Hence, the performance loss at

the 4th cycle could also be caused by reduced membrane pore densities due to the same plasticization effect.

While comparing effects of continuous and cyclic ageing in Figure 6b and 8, possible delayed effect of hypochlorite on the membrane was reported. In Figure 9 however, delaying effect due to presence of foulants on the possible plasticization effect was not obvious. This could emanate from difference in the applied TMP between the two systems. While the TMP in Figure 8 was 2 bar, the maximum TMP in Figure 9 was 0.15 bar for the same range of transmembrane flux. The loose bound between foulant and membrane at lower TMP in the later case could be the major reason for the absence of delayed impact of hypochlorite on the membrane.

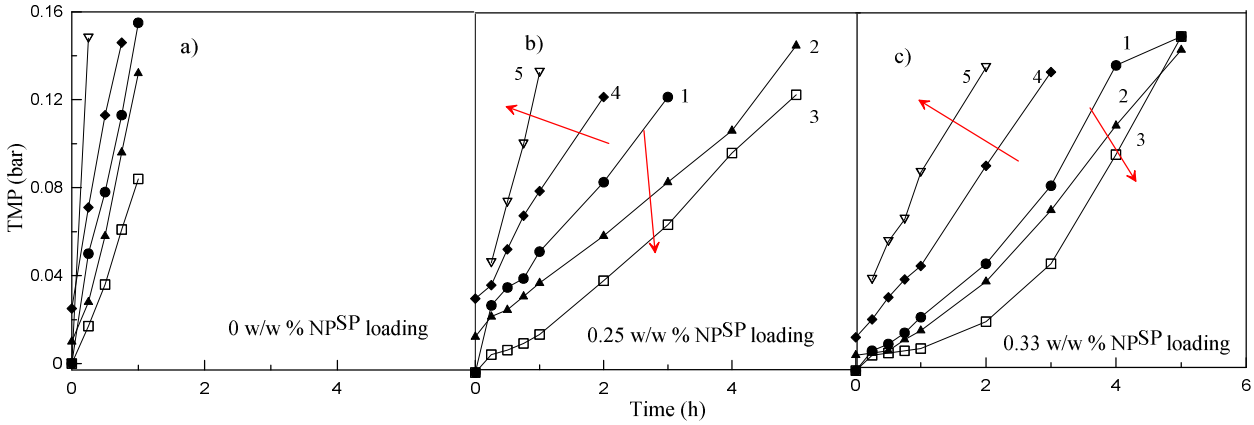

Figure 9: Accelerated fouling experiments at constant flux over five different cycles using particle free membrane and hybrid membranes containing 0.25 and 0.33 w/w % NP^{SP} (feed: 0.3 mg/mL pectin solution: flux: at 25 kg/m^2.h). Y-axis represents rise in transmembrane pressure caused by foulant deposition inorder to keep the flux constant. The numbers on the graphs represent filtration cycle. Each cycle proceeded until the maximum TMP arrives at 0.15 bar. In between the cycles, membrane was cleaned by soaking in 2000 ppm hypochlorite solution at pH natural and ambient temperature.

6.4.5.2. Maintenance cleaning

While defining cleaning protocols, distinction between maintenance and recovery cleaning is made. Maintenance cleaning is commonly used to reduce long-term fouling developments, where cleaning agents are applied at low concentrations. Effective application of maintenance cleaning helps to limit the frequency of recovery cleaning. This in turn reduces operation and maintenance routines that directly impact the plant production capacity. Hence identification of

suitable cleaning condition that is less detrimental to the membrane integrity and the resulting hydraulic cleaning efficiency was also carried out.

Membrane fouled with 0.3 mg/mL of pectin at 2 bar for 4 h were cleaned by keeping in contact with 400 ppm solution at pH 12 for 1 h. This cleaning condition is selected after ATR-FTIR analysis of membrane aged under these conditions for 12 h showed absence of NaOCl led oxidative damage to the membrane. As shown in Figure 10a, compared to virgin membrane, the flux through chemically cleaned membrane was much smaller. Since stirring of the feed solution at high speed (300 rpm) is supposed to reduce concentration polarization effectively [31], the decrease in flux is mainly coming from irreversible fouling. Figure 10b shows the hydraulic resistance of virgin, fouled, manually brushed and chemically cleaned membrane calculated using equation 2. The resistance was measured by filtering sodium acetate buffer before and after chemical cleaning at 1 bar. In agreement with the flux trend, an initial stage fast irreversible membrane fouling even with an immediate chemical cleaning resulted in a 59% increased R value. Nevertheless, the cleaning was strong enough to keep track of a stable performance in the subsequent three cycles giving an average R value of $6.8 \pm 1.2*10^{11}$ m^{-1}. Even so, the possibility of recovering a previous step membrane performance through manual brush was lost gradually.

Flux and membrane resistance are the most commonly utilized tools for quantitative evaluation of the cleaning efficiency of membrane cleaning protocol [23]. Hence, ratio of 'R' before and after chemical cleaning is used here to quantify the hydraulic cleaning efficiency of the chemical cleaning (equation 1). The maximally achievable hydraulic cleaning efficiency after the 1^{st} cycle fouling and cleaning was only 59%. However, the applied chemical cleaning in the subsequent three cycles easily restored more than 95% of the permeability in the preceding cycle.

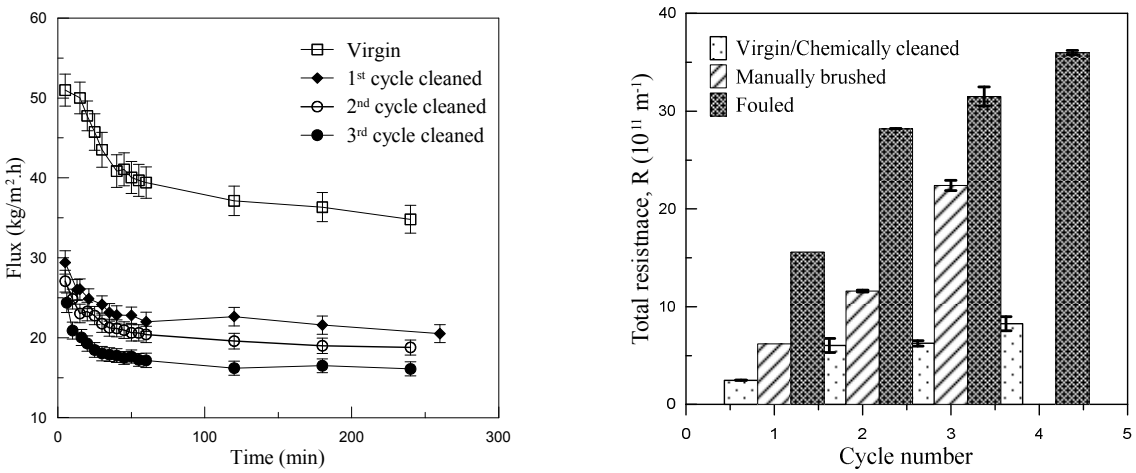

Figure 10: Flux trend of a membrane while filtering 0.3 mg/mL pectin with intermediate static cleaning in 400 ppm NaOCl at pH 12 for 1 h, and b) total resistance of virgin, fouled, manually brushed and chemically cleaned membrane estimated with Equation 2. The resistance was measured by filtering sodium acetate buffer before and after chemical cleaning at 1 bar.

In addition to hydraulic performance, the surface chemistry of fouled and chemically cleaned membranes was further examined. The ATR-FTIR spectra in Figure 11 shows that after pectin adsorption, broad peak appeared between 3692 cm^{-1} and 2985 cm^{-1} attributed as O-H stretch from pectin and at 1710-1502 cm^{-1} due to presence of C=O bond stretching in carboxylic acid groups [25]. These bands are similar to the characteristic bands of foulant scrapped from the surface of the membrane. In addition, minor peaks at 1088 cm^{-1}, 1014 cm^{-1} were also observed in the fouled membrane resembling characteristics peaks observed for the scrapped foulant. All the bands related to fouling are completely absent from the virgin membrane. More importantly, except for a residual effect, the band intensities have also disappeared from the chemically cleaned membrane. This further suggests that the applied cleaning strategy was sufficient to remove membrane surface foulants. As a result, it was possible to keep flux value of about 20 $kg/m^2.h$ in the 2^{nd}, 3^{rd} and 4^{th} cycles once 59% of the original performance was lost after 1^{st} cycle pectin filtration and chemical cleaning. This 59% performance loss can therefore be attributed to the presence of foulants trapped inside the pore structure that could not be cleaned by simply keeping the membrane in contact with NaOCl.

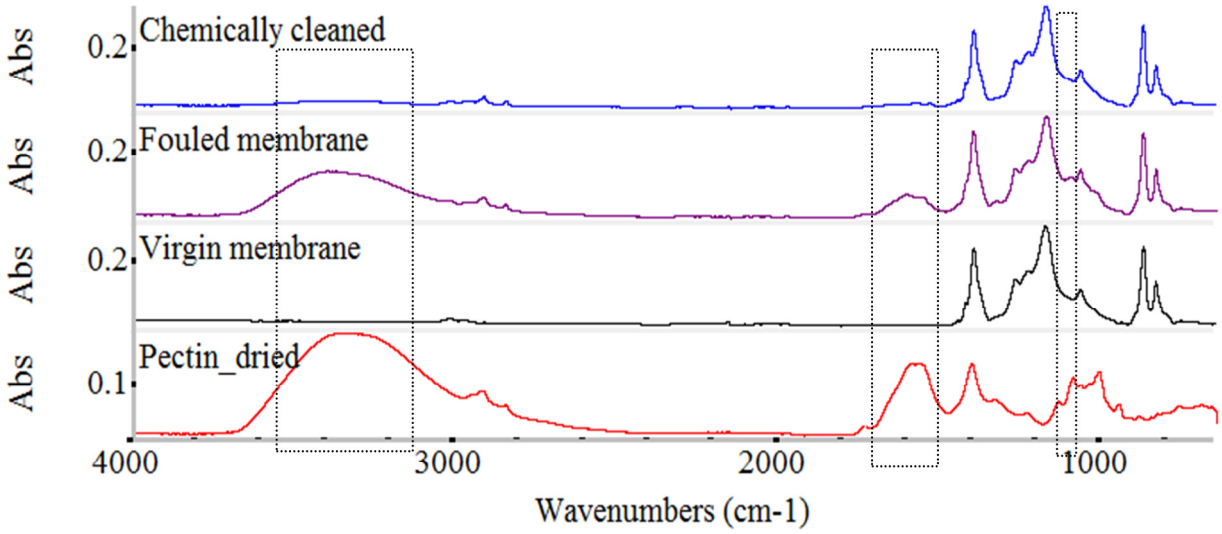

Figure 11: cross-sectional veiw of a) virgin membrane, b) chemically cleaned membrane and c) ATR-FTIR spectra of virgin, fouled, chemically cleaned membrane and foulants scrapped from the membrane surface. These bands aare average of ATR-FTIR analysis taken at three different spots of a membrane.

6.5. Conclusion

This chapter presented results of an extensive study regarding the ageing effect and cleaning efficiency of NaOCl on a newly introduced NP^{SP}-PVDF magnetic responsive membrane.

Both accelerated ageing under static condition and accelerated fouling studies revealed changed behavior after NaOCl treatment of the membrane. PEG used as NP^{SP} coating layer accounts for less than 0.33 w/w % in the membrane matrix. Detailed characterization of the membrane however linked the damage to the hypochlorite induced oxidation sensitivity of this molecule. The accelerated ageing study also showed progressive initial stage densification followed by gradually increased pore size as compared to virgin membrane. Paradoxically, a seven fold increased hydraulic resistance was obtained after 210 h of ageing at 2000 ppm solution regardless of the observed pore size enlargement. In order to limit the observed damage to the NP^{SP}-PVDF magnetic responsive membrane, it may therefore be important to consider the use of a more chemically stable polymeric coating layer during the NP^{SP} preparation.

EDX elemental analysis indicated that Fe responsible for the magnetic responsive behavior of the membrane was stable under any circumstance. The observed macroscopic and microscopic changes with ageing were consistent with one another. After careful consideration of ATR-FTIR

analysis, 400 ppm solution at pH 12 was found effective to keep reasonable flux of 20 kg/m^2.h during multi-cycle fouling and cleaning.

Overall, regardless of the stability of PVDF, close consideration should be given to exposure condition (pH, hypochlorite concentration and exposure duration) to attain best cleaning efficiency in a less detrimental way. In addition, a paradigm shift from post damage chemical cleaning to utilizing preventive action e.g., taking the magnetic responsiveness of the membrane as an advantage to modulate foulant deposition could also be interesting.

Appendix

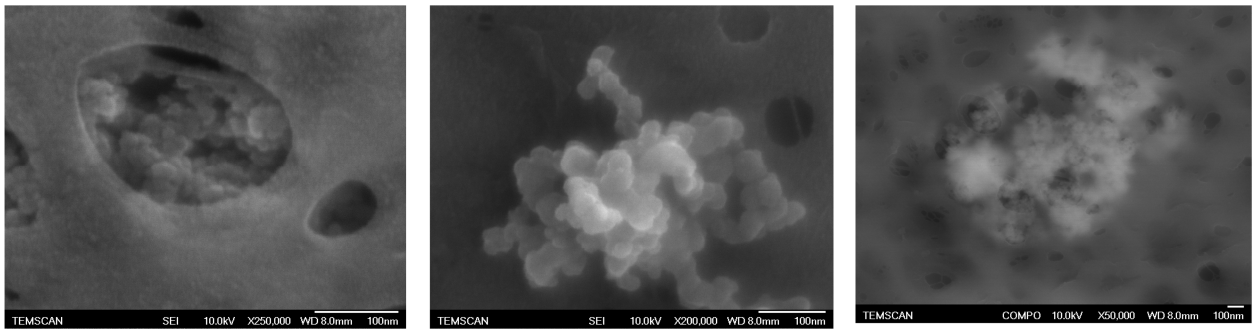

Figure A1: TEM scan showing the presence of the NP^{SP} integrated within the polymer matrix. Big size agglomerates of particles are observed inside a 100 nm membrane pore size.

6.6. References

[1] P. Daraei, S.S. Madaeni, N. Ghaemi, M.A. Khadivi, B. Astinchap, R. Moradian, Fouling resistant mixed matrix polyethersulfone membranes blended with magnetic nanoparticles: Study of magnetic field induced casting, Separation and Purification Technology, 109 (2013) 111-121.

[2] C. Sanchez, P. Belleville, M. Popall, L. Nicole, Applications of advanced hybrid organic-inorganic nanomaterials: from laboratory to market, Chemical Society Reviews, 40 (2011) 696-753.

[3] H.H. Himstedt, Q. Yang, L.P. Dasi, X. Qian, S.R. Wickramasinghe, M. Ulbricht, Magnetically Activated Micromixers for Separation Membranes, Langmuir, 27 (2011) 5574-5581.

[4] Z.-Q. Huang, F. Zheng, Z. Zhang, H.-T. Xu, K.-M. Zhou, The performance of the PVDF-Fe3O4 ultrafiltration membrane and the effect of a parallel magnetic field used during the membrane formation, Desalination, 292 (2012) 64-72.

[5] J. Thevenot, H. Oliveira, O. Sandre, S. Lecommandoux, Magnetic responsive polymer composite materials, Chemical Society Reviews, 42 (2013) 7099-7116.

[6] P. Yao, K.H. Choo, M.H. Kim, A hybridized photocatalysis-microfiltration system with iron oxide-coated membranes for the removal of natural organic matter in water treatment: effects of iron oxide layers and colloids, Water Res, 43 (2009) 4238-4248.

[7] P. Sabbatini, F. Yrazu, F. Rossi, G. Thern, A. Marajofsky, M.M. Fidalgo de Cortalezzi, Fabrication and characterization of iron oxide ceramic membranes for arsenic removal, Water Research, 44 (2010) 5702-5712.
[8] P. Daraei, S.S. Madaeni, N. Ghaemi, E. Salehi, M.A. Khadivi, R. Moradian, B. Astinchap, Novel polyethersulfone nanocomposite membrane prepared by PANI/Fe3O4 nanoparticles with enhanced performance for Cu(II) removal from water, Journal of Membrane Science, 415–416 (2012) 250-259.
[9] R.W. Baker, Reverse Osmosis, in: Membrane Technology and Applications, John Wiley & Sons, Ltd, 2004, pp. 191-235.
[10] I. Levitsky, A. Duek, E. Arkhangelsky, D. Pinchev, T. Kadoshian, H. Shetrit, R. Naim, V. Gitis, Understanding the oxidative cleaning of UF membranes, Journal of Membrane Science, 377 (2011) 206-213.
[11] C. Causserand, S. Rouaix, J.-P. Lafaille, P. Aimar, Degradation of polysulfone membranes due to contact with bleaching solution, Desalination, 199 (2006) 70-72.
[12] P. Wang, Z. Wang, Z. Wu, Q. Zhou, D. Yang, Effect of hypochlorite cleaning on the physiochemical characteristics of polyvinylidene fluoride membranes, Chemical Engineering Journal, 162 (2010) 1050-1056.
[13] C. Regula, E. Carretier, Y. Wyart, M. Sergent, G. Gésan-Guiziou, D. Ferry, A. Vincent, D. Boudot, P. Moulin, Ageing of ultrafiltration membranes in contact with sodium hypochlorite and commercial oxidant: Experimental designs as a new ageing protocol, Separation and Purification Technology, 103 (2013) 119-138.
[14] E. Arkhangelsky, D. Kuzmenko, V. Gitis, Impact of chemical cleaning on properties and functioning of polyethersulfone membranes, Journal of Membrane Science, 305 (2007) 176-184.
[15] C.J. Gabelich, J.C. Frankin, F.W. Gerringer, K.P. Ishida, I.H. Suffet, Enhanced oxidation of polyamide membranes using monochloramine and ferrous iron, Journal of Membrane Science, 258 (2005) 64-70.
[16] C. Causserand, S. Rouaix, J.-P. Lafaille, P. Aimar, Ageing of polysulfone membranes in contact with bleach solution: Role of radical oxidation and of some dissolved metal ions, Chemical Engineering and Processing: Process Intensification, 47 (2008) 48-56.
[17] V. Puspitasari, A. Granville, P. Le-Clech, V. Chen, Cleaning and ageing effect of sodium hypochlorite on polyvinylidene fluoride (PVDF) membrane, Separation and Purification Technology, 72 (2010) 301-308.
[18] S.Z. Abdullah, P.R. Bérubé, Assessing the effects of sodium hypochlorite exposure on the characteristics of PVDF based membranes, Water Research, 47 (2013) 5392-5399.
[19] W. Brullot, N.K. Reddy, J. Wouters, V.K. Valev, B. Goderis, J. Vermant, T. Verbiest, Versatile ferrofluids based on polyethylene glycol coated iron oxide nanoparticles, Journal of Magnetism and Magnetic Materials, 324 (2012) 1919-1925.
[20] N.A.D. Burke, H.D.H. Stöver, F.P. Dawson, Magnetic Nanocomposites: Preparation and Characterization of Polymer-Coated Iron Nanoparticles, Chemistry of Materials, 14 (2002) 4752-4761.

[21] H. Lee, E. Lee, D.K. Kim, N.K. Jang, Y.Y. Jeong, S. Jon, Antibiofouling Polymer-Coated Superparamagnetic Iron Oxide Nanoparticles as Potential Magnetic Resonance Contrast Agents for in Vivo Cancer Imaging, Journal of the American Chemical Society, 128 (2006) 7383-7389.
[22] A.Y. Gebreyohannes, R. Mazzei, E. Curcio, T. Poerio, E. Drioli, L. Giorno, Study on the in Situ Enzymatic Self-Cleansing of Microfiltration Membrane for Valorization of Olive Mill Wastewater, Industrial & Engineering Chemistry Research, 52 (2013) 10396-10405.
[23] C. Regula, E. Carretier, Y. Wyart, G. Gésan-Guiziou, A. Vincent, D. Boudot, P. Moulin, Chemical cleaning/disinfection and ageing of organic UF membranes: A review, Water Research, 56 (2014) 325-365.
[24] P. Le Clech, B. Jefferson, I.S. Chang, S.J. Judd, Critical flux determination by the flux-step method in a submerged membrane bioreactor, Journal of Membrane Science, 227 (2003) 81-93.
[25] V. Smuleac, L. Bachas, D. Bhattacharyya, Aqueous-phase synthesis of PAA in PVDF membrane pores for nanoparticle synthesis and dichlorobiphenyl degradation, Journal of Membrane Science, 346 (2010) 310-317.
[26] I. Batterham, R.R.R. Rai, A comparison of artificial ageing with 27 years of natural ageing.
[27] S.H. Mohammadian, D. Aït-Kadi, F. Routhier, Quantitative accelerated degradation testing: Practical approaches, Reliability Engineering & System Safety, 95 (2010) 149-159.
[28] G.J. Ross, J.F. Watts, M.P. Hill, P. Morrissey, Surface modification of poly(vinylidene fluoride) by alkaline treatment1. The degradation mechanism, Polymer, 41 (2000) 1685-1696.
[29] N. Awanis Hashim, Y. Liu, K. Li, Stability of PVDF hollow fibre membranes in sodium hydroxide aqueous solution, Chemical Engineering Science, 66 (2011) 1565-1575.
[30] I. Edmund H, M. Herman F, Principles of Plasticization, in: <bold>Plasticization</bold> and Plasticizer Processes, AMERICAN CHEMICAL SOCIETY, 1965, pp. 1-26.
[31] L. Wang, Y.-l. Su, L. Zheng, W. Chen, Z. Jiang, Highly efficient antifouling ultrafiltration membranes incorporating zwitterionic poly([3-(methacryloylamino)propyl]-dimethyl(3-sulfopropyl) ammonium hydroxide), Journal of Membrane Science, 340 (2009) 164-170.

Chapter 7: Treatment of Olive Mill wastewater using Forward Osmosis process

7.1. Abstract

Olive millings are known to periodically release huge volume of environmentally detrimental wastewater. In this work, Forward Osmosis (FO) is applied to concentrate Olive Mill Wastewater (OMWW). Single-step FO at 3.7 molal $MgCl_2$ draw solution and 6 cm/s crossflow velocity resulted in 71% reduced volume, complete decolorization and more than 98% rejection to all components of OMWW including biophenols and mono- or multi-valent ions. The significantly reduced volume lowers the larger area required for storage, transportation to treatment facilities or the difficulty to handle large volume during the recovery of biophenols

The single step complete rejection is also more attractive than mostly practiced multi-staged step-by-step removal of pollutants that may even comprise energy intensive centrifugation and adsorbent utilization.

Cleaning cycle based on osmotic back-flushing, after continuous OMWW dehydration for over 200 h, helped to remove 6µm thick foulant layer and permitted to restore upto 95% pure water permeability of CTA membranes.

Reclaiming good quality water through appropriate integration of FO with draw solution regeneration and recovery of biophenols from the concentrated stream may short circuit the natural water cycle to access clean water. Therefore, FO may hold significant potential for the valorization of OMWW within the logic of Zero Liquid Discharge.

This chapter is based on paper submitted to Journal of Water Research as: **Gebreyohannes A. Y.**, E. Curcio, T. Poerio, R. Mazzei, G. Di Profio, E. Drioli and L. Giorno, Treatment of Olive Mill wastewater using Forward Osmosis process.

7.2. Introduction

Discharging heavily polluted wastewater generated during the extraction of olive oil has posed serious economical and environmental concern worldwide. The situation is particularly sever in Mediterranean region where more than 75% of the world olive oil is produced [1]. The amount of Olive Mill Wastewater (OMWW) generated is about 5 m^3 per ton of produced olive oil with as high as 220 g/L COD [2-4] . The high variability of feed composition and, in particular, the presence of antibacterial phenolic compounds makes OMWW difficult to treat [3, 5]. Environmental impact due to the toxic load of OMWW is estimated to be more severe than municipal sewage. Rise and expansion in the problem is foreseen due to the health driven production increase by up to 30% in the last 15 years and the emerging of new producers like US, Argentina and South Africa [2, 6].

Although different management options focusing on the destruction of polyphenols have been implemented, recently integrated membrane operation for combined OMWW reclamation and extraction of biophenols have got great interest [2, 4-5, 7-12]. The motivation for treating and reclaiming OMWW arises from legislation which constrains its illegal discharge to the environment [1]. More pragmatically, reclaiming good quality water from OMWW also helps to short-circuit the natural flow of water used for drinking or industrial activity and limit the need for fresh water supply [13]. While good quality water reclamation from OMWW is of interest in industrial applications, the biophenolic fractions have antibacterial properties and hold a wide range of antioxidant, cardio-protective and cancer-preventive activities [9, 14-16]. Biophenolic exhausted concentrate may also be transformed into syngas for the production of methanol, ammonia and synthetic fuel [17].

So far, occurrence of severe membrane fouling has restricted the applicability on large scale of conventional membrane operations [9, 18]. Irreversible membrane damage resulted in 57% permeability loss when treating OMWW with 2kDa polyethersulfone Ultrafiltration (UF) membrane, and in 60% permeability loss using 0.4 µm polyethylene Microfiltration (MF) membranes [18-19]. Despite the significant efforts made to restore the original membrane performance by chemical cleaning, results obtained are still unsatisfactory [18]. In general, severe fouling affects the investment costs as a result of reduced membrane lifetime and increased chemical cost. The sever membrane fouling is augmented by periodic discharge of

huge volume of wastewater [20]. These combined problems arises the need for huge storage facilities and environmental deterioration and insect proliferation due to long term storage. Moreover, longer storage period causes oxidative loss of the most useful biophenolic compounds that can potentially be recovered from OMWW.

Recently, Forward Osmosis (FO) has re-emerged as a low-energy demanding membrane operation for dehydration of aqueous solution [21]. FO is a membrane process that uses an osmotic pressure gradient as a driving force to transport water across an ideally semi-permeable membrane [22]. FO has been investigated for sea water desalination [23], wastewater treatment and concentration of diluted streams [24], food processing [25], removal of trace organic matter [26] and for use in membrane bioreactor [27]. Interestingly, several studies have shown that fouling occurring in FO is in most part reversible due to negligibility of foulant compaction by hydraulic pressure gradient. It therefore holds a great potential to treat wastewater [28]. As a consequence, FO is potentially attractive for the treatment of OMWW, characterized by low osmotic pressure, high fouling propensity [29] and periodic discharge of large volume [20].

The aim of this work is to investigate the effect of operational parameters on FO performance for the treatment of OMWW. Single-step FO performance was evaluated in terms of rejection to individual ions, total phenolics, total organic carbon (TOC), total inorganic carbon (TIC) and total suspended solids (TSS), sensitivity to fouling and effectiveness of cleaning procedures. Detailed analysis of FO flux performance with respect to applied osmotic pressure and dilutive internal concentration polarization is provided. Ultimately, the possibility of integrating FO with different pressure driven membrane operations to recover biophenolic compounds is explored.

7.3. Materials and Methods

7.3.1. Materials

OMWW (TSS = 4.13%, pectin = 0.3-0.46 mg/mL, pH 4.2) is taken from three-phase local olive oil producer (Olearia San Giorgio, Calabria - Italy).

$MgCl_2 \bullet 6H_2O$ (Fischer Scientific, Italy) is used to prepare DS; Gallic acid, Folin-Ciocalteau reagents are purchased from Sigma Aldrich (Italy).

7.3.2. OMWW characterization

- Total Solids (TS): 1 g of OMWW is dried at 100°C in a thermo-balance (Ohus S.r.l Milan, Italy) until arriving at steady-state weight.
- Total Dissolved Solids (TDS): 1 g of OMWW is filtered through a 0.45µm membrane and the filtrate is dried in a thermo-balance at 105°C until steady-state weight. TSS is evaluated as difference between TS and TDS.
- Total Phenolic content: is determined based on phenolic substances oxidation by the Folin-Ciocalteau reagent which contains a mixture of phosphotungstic acid and phosphomolybdic acid [30]. The partly reduced reagent produces molybden-tungsten blue complex, which is measured spectrophotometrically at 756 nm with UV/VIS spectrophotometer (Perkin Elmer, Lambda EZ201). Calibration curve is prepared using standard solutions of gallic acid (0-100 mg/l).
- Ionic compositions: determined using inductively coupled plasma optical emission spectrometry (Optima2100 DV, Perkin Elmer).
- Viscosity (µ) of feed and DS: measured at 25°C by using Brookfield viscometer.
- TOC) and Total Carbon (TC) are analyzed by a TOC analyzer (Shimadzu TOC-V). TIC is evaluated as difference between TOC and TC.

7.3.3. OMWW pre-treatment

Three pre- treatment methods are used: (1) raw OMWW that is sequentially pre-filtered through 35 µm and 15 µm pore size stainless steel wire mesh, resulting in 99.3% total solid reduction (from 14 g/kg to 0.1 g/kg); (2) MF through 0.4 µm permanently hydrophilic polyethylene (PE) membrane after method 1; (3) MF on Polyethylene membrane with immobilized pectinase to degrade macrofoulnats as explained elsewhere [18].

7.3.4. Draw solution

High solubility, reduced molecular weight, reduced back-diffusion through membranes are some of desirable features of good draw solute [23]. Solutes containing scale precursor ions (mainly Ca^{2+} and SO_4^{2-}) show the risk of accidental precipitation of sparingly water-soluble minerals such as $BaSO_4$, $CaCO_3$, $CaSO_4$ [31]. In the present study, due to the complex ion matrix of the OMWW, $MgCl_2$ is chosen as the draw solution (DS). This salt has limited back-diffusion

tendency to the feed side and scale forming potential at the pH of OMWW (4.5). DS is prepared within a concentration range from 1.8 to 7.5 molal. The osmotic potential (mOsm/kg H_2O) of $MgCl_2$ at different concentration and feed OMWW is measured using Fiske® 210 Micro-Sample Osmometer (Analytical control De Mori S.r.l, Milan - Italy).

7.3.5. FO Membrane

Flat sheet cellulose triacetate (CTA) membranes (Hydration Technology Inc., US) is used for FO tests. A cross-sectional SEM micrograph (Figure 1) shows thick polyester mesh embedded within the polymeric matrix as a mechanical support. The total membrane thickness varies between 50 µm and 85 µm [23]. The membrane structural parameter (S), defined as the ratio of membrane thickness (t) x tortuosity (ζ) over membrane porosity (ε), is 481µm [32]. Prior to use, membranes are soaked in ultrapure water for 30 minutes to remove preservatives.

Water and OMWW contact angle measurements were done with the sessile drop method using a VCA video contact angle system CAM 200. Images of water and OMWW droplets on the membrane surfaces are depicted in Figure 1b-c. The water and OMWW contact angles were 52° and 36.5° respectively indicating a higher hydrophilicity. ATR-FTIR spectrum of the membranes is realized by the attenuated total reflectance (ATR) technique on Thermo Nicolet Nexus 670 fitted with DTGS detector and diamond ATR crystal, where 32 scans at 4 cm^{-1} resolution. All data acquisition, baseline corrections and image construction are done using OMNIC^s software.

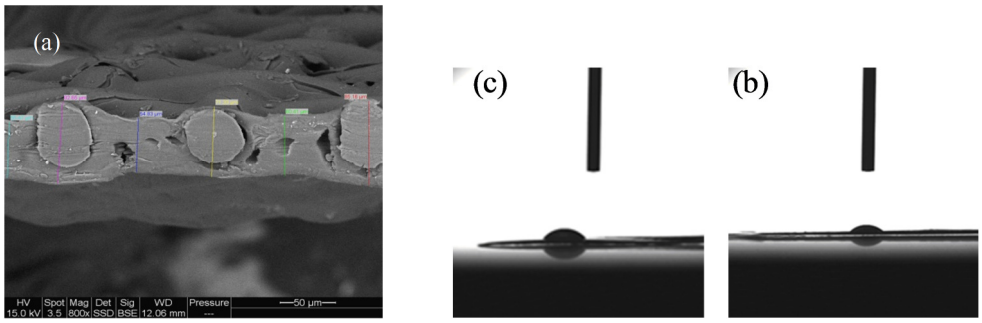

Figure 1: a) Cross-sectional SEM image of used FO membrane (Hydration Technology Inc., US; thickness ~ 50µm): a polyester mesh is embedded within the polymer material as a mechanical support, b) image of water droplet on membrane and c) image of OMWW droplet on membrane.

7.3.6. FO bench-scale setup

The lab-scale FO apparatus is depicted in Figure 2**.** Flat CTA membrane with 0.02 m^2 effective surface area is installed in a homemade crossflow cell (200mm L x 50mm H x 6mm W). Peristaltic pumps General Control S.p.A (Milan, Italy) are used to recirculate the feed and DS in co-current flow. The operation mode feed solution facing the active layer is used in order to limit membrane clogging. Crossflow velocity of both feed and DS are varied in the range of 2-8.6 cm/s.

The tests are carried out in batch mode, with DS getting progressively diluted while feed solution getting concentrated. The transmembrane flux is determined by weighing the DS tank placed on an electronic balance (Gibertini S.r.l, Milan, Italy) interfaced to a personal computer. During the FO operation, the extent of reverse salt flux (J_s) is determined by measuring the feed conductivity over time by conductivity meter YSI 3200 (Conductivity Instrument, US).

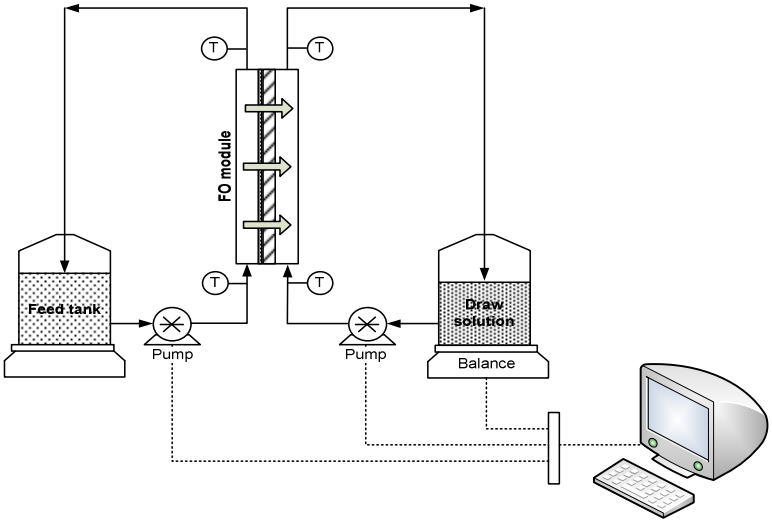

Figure 2: Flow-sheet of the lab-scale FO setup.

7.3.7. Long-term stability

In batch operational mode, volume of both feed and DS have a direct impact on the overall osmotic driving force. Hence, prior to long term experiment, different combinations of feed and DS volumes are examined. Based on these, every day 3 L of fresh OMWW is supplied while setting the cross flow velocity at 6 cm/s. For the draw solution, the exact quantity needed to correct the volume and concentration to 4 L and 3.7 molal is added to the previous day diluted draw solution. For the first 4 days the membrane is subjected to either water rinse or water rinse

followed by osmotic back-flush, when the flux was reduced to about 50% of the value obtained at the start of each experiment. From day 6 to 8, cleaning is applied only after 80% of the initial flux is lost (after 71 hours of continuous dehydration). The cleaning is conducted as detailed in section 7.3.8.

7.3.8. FO membrane cleaning procedure

Subsequent to each test, the membrane is subjected to the following cleaning protocol:

1. flushing out both feed and DS;
2. recirculating deionized water at 1.55 L/min on both side of the membrane;
3. measure pure water flux using deionized water as feed and DS of 3.7 molal ($\Delta\pi_b^0$ = 103 bar) $MgCl_2$ at 6 cm/s crossflow velocity;
4. If the water flux is below 80% of the original value, an osmotic back-flush is additionally conducted: the feed side is filled with 3.7 molal DS while the support side is filled with pure water. The system runs in this configuration for 30 minutes, and then is flushed for 10 minutes with deionized water.

7.3.9. Theoretical considerations

Figure 3 illustrates the operational principle of FO process, with emphasis on the difference among effective/membrane/bulk osmotic pressure gradient. The water flux through FO membrane is defined as [22]:

$$J_w = L_p\left(\sigma\Delta\pi - \Delta P\right) \qquad 1$$

where J_w is water flux, L_p hydraulic permeability, σ reflection coefficient, $\Delta\pi$ the osmotic pressure gradient between feed and draw solution, and ΔP the applied hydrostatic pressure (null in FO). L_p is calculated from pure water filtration tests at different ΔP.

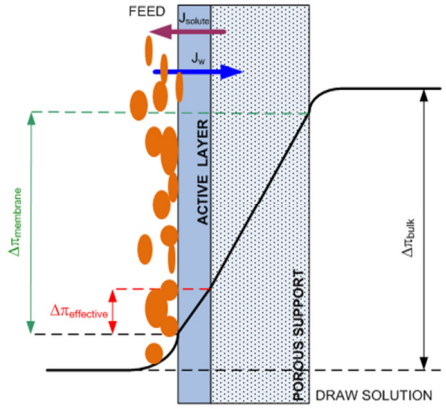

Figure 3: Schematic representation of FO concept.

The water flux predicted by equation 1 is unreachable due to concentration polarization phenomenon. The polarization can be internal (ICP) occurring inside the substructure of porous support layer [22]. ICP due to hindered diffusion of solutes within the membrane support layer is inherent to FO. The extent of ICP is correlated to the solute diffusivity resistance (K) into the porous substructure, defined in terms of the membrane structural parameter (S):

$$S = \frac{t \cdot \tau}{\varepsilon} \qquad 2.a$$

$$K = \frac{S}{D_s} \qquad 2.b$$

where D_s is the draw solute diffusion coefficient. Diffusion coefficients for $MgCl_2$ are deduced from data of Miller *et al.* (1984) [33].

In addition to ICP, occurrence of external concentration polarization (ECP) in the boundary adjacent to the surface of both active and porous support layer is inevitable. Thus flux by itself cannot give adequate information regarding the factors that affect the performance of FO. Inorder to account for the effect of both ICP and ECP, two main approaches are used to describe the FO flux performance.

The first is use of apparent FO water permeability**,** based on normalizing the FO flux (J_w) by the bulk osmotic driving force ($\pi_{ds} - \pi_{fs}$):

$$L_p = \frac{J_w}{\pi_{ds} - \pi_{fs}} \qquad 3$$

Where L_p is overall water permeability coefficient of the membrane, J_w is average of the last three flux values obtained at the end of a 4 h lasting continuous FO OMWW concentration. Since there is change in the overall osmotic driving force, $\pi_{ds} - \pi_{fs}$ is estimated based on measured osmolality of both feed and DS at the end of the FO processes. When complete salt rejection by the membrane is assumed, the value of σ becomes 1.

The second approach is based on flux-efficiency analysis as proposed by Lay et al. [34]. The method uses an equation that accounts for both fouling and ICP derived based on resistance-in-series model [8]. This approach is claimed to have practical relevance since it takes recovery (φ) into consideration. Recovery is an important system parameter that provides information regarding the total output and the volume of concentrated stream that needs further handling. The general equation that relates flux with recovery when feed solution faces the active layer is [34]:

$$J_w = L_p \cdot [(\pi_{ds} - \frac{B}{L_p}) \cdot e^{-\left(\frac{J_w}{K_m}\right)} - (\pi_{fs} + \frac{B}{L_p}) \cdot (\frac{1}{1-\varphi}) e^{-\left(\frac{J_w}{k_{CECP}}\right)}] \quad 4$$

Where B is the overall salt permeability coefficient of the membrane, π_{ds} and π_{fs} are the DS and feed solution osmotic pressures respectively, K_m is the mass transfer coefficient that accounts for the diffusive phenomena through the porous support layer of the membrane which plays a major role in ICP. It is inverse of solute transport resistivity (K) defined in Equation 2b and φ is recovery defined as the ratio of permeate volume to feed volume, hence 1/(1-φ) is volumetric concentration factor (VCF), when the membranes' rejection coefficient is assumed 1.

In addition, very high concentration of solute may occur on the membrane surface due to hindered solute transport within the fouling layer. This phenomenon is called cake enhanced concentration polarization (CECP). It has dominant performance diminishing effect on FO system particularly when it is augmented by high solute back diffusion. Thus k_{CECP} is the mass transfer coefficient that accounts for the diffusive phenomena through the cake layer which plays a major role in describing CECP.

Equation 4 is a quantitative method that may be applied to assess the FO flux performance. For this, a reference condition is defined by assuming complete pollutant rejection, absence of draw solute back-diffusion (B/L_p =0), fouling and concentration polarization (k_{CECP}=0) while keeping membrane and operating conditions similar to the real situation:

$$J_w = L_p \cdot [(\pi_{ds}) \cdot e^{-\left(\frac{J_w}{K_m}\right)} - (\pi_{fs}) \cdot (\frac{1}{1-\varphi})] \quad 5$$

Since flux and recovery have tradeoff effect, reference curve plotted according to equation 5 gives the maximum attainable flux for a given recovery. Based on this a flux efficiency factor is defined as:

$$\text{Flux efficiency factor} = \left(\frac{J_{w,obs}}{J_{w,ref}}\right)_{\varphi_{obs}=\varphi_{ref}} \quad 6$$

Where $J_{w,obs}$ and $J_{w,ref}$ are the observed and refernce FO water flux at equal φ values.

7.3.10. Recovery of polyphenols

The concentrated stream from FO is further treated to purify and fractionate the biophenolic compounds. The feed water composition is a 50% concentrated OMWW by FO with 6.3, 0.01 and 1.9 g/L TOC, TIC, and total phenols respectively and a 1.7% TSS. The performance differences of two types of commercially available membranes, permanently hydrophilic flat sheet polysulfone (Nadyr GmbH, Germany) and a tubular ceramic membrane (Membraflow GmbH, Germany) are examined as a case study. Details of the membranes and experimental conditions are provided in Table 7.1.

In an alternative case, the 50% FO concentrate is first treated with enzyme pectinase (corresponding to optimal enzyme to substrate ratio of 23:1). The mixture is incubated at 40°C for 1 h to hydrolyze pectins, which are major foulants [18]. The hydrolysate is then filtered through the PSH UF membrane at 40°C together with a control experiment (without enzymatic treatment) at 40°C. Both UF and NF membrane are cleaned by filtering deionized water at 40°C and 250 L/h. The flux recovery is calculated as the ratio of pure water flux before OMWW filtration and after cleaning.

Table 7.1: Used membranes and experimental conditions during pre-treatment before FO and polyphenol recovery after FO process.

Membrane	Pore size	Configuration	Crossflow rate (L/h)	TMP (bar)	Inner diameter/ Length (mm)
PE	0.4 µm	HF	60	0.1	0.6/110
PE-biocatalytic	0.4 µm	HF	60	0.1	“
NF-ceramic	10 nm	Tubular	200	7	7/100
PSH UF	100 kDa	FS	100	3	

The biophenols collected in the permeate stream of the PSH UF membrane is further concentrated using FO at 3.7 molal ($\Delta\pi_b^0$=103 bar) draw solution and 6 cm/s.

7.3.11. UF/NF experimental set-up

The UF process consists of circular plate and frame cross-flow module made of stainless steel. Inside an 8 cm flatsheet UF membrane, a support and a spacer plates are stacked together. A gear pump (Techma GPM S.r.l, Milan) equipped with magnetic drive and an electrical motor (Supply voltage: 230 /400V; Power: 0.37 Kw) is used to circulate the feed along the membrane. Feed tank is kept in a thermostatic water bath. A valve located along the retentate line is used to adjust the TMP. Two manometers are installed at the inlet and outlet of the module to measure TMP. Permeate flux is measured by placing the permeate tank on a laboratory scale balance (Gilbertini S.r.l, Milan). The same experimental set-up is also used for the NF process. However, the flatsheet module is replaced by a tubular module made of stainless steel to accommodate the tubular ceramic NF membrane. UF and NF are operated under different operating conditions. To account for this, flux is normalized by the corresponding feed flowrate and TMP:

$$¥= \frac{\text{Flux}}{\text{TMP}*\text{Feed Flowrate}} \qquad 7$$

7.4. Results and Discussion

7.4.1. Water/$MgCl_2$ FO tests

The bulk osmotic pressure was evaluated on the basis of experimentally measured osmolality:

$$\pi = \Theta \cdot RT \qquad 8$$

Where Θ is osmolality (osmol/kg), R is the universal gas constant (0.0821 L bar/mol K), and T the absolute temperature. In addition, equation 9 was used to calculate the osmotic pressure using the osmotic coefficient (γ) obtained from slope of osmolality plotted against molality:

$$\pi = \gamma cRT \qquad 9$$

Where c is the molar concentration of the solute.

These experimentally determined data were also compared with predictions using the van't Hoff equation ($\pi = \iota cRT$) and the equation proposed by Wilson and Stewart ($\pi = 24.5\Theta \cdot \rho$) [35].

The Van`t Hoff coefficient (ι) assumes complete ion dissociation while γ takes possible osmotic potential loss at high concentration due to inverse ion pairing [35].

According to Figure 4, at low DS concentration, there is a good agreement between experimentally measured and theoretically predicted values. With increased molal concentration however, the method of Wilson and Stewart overestimates osmotic pressure, while Van't Hoff equation diverges exponentially for a molality greater than 4.

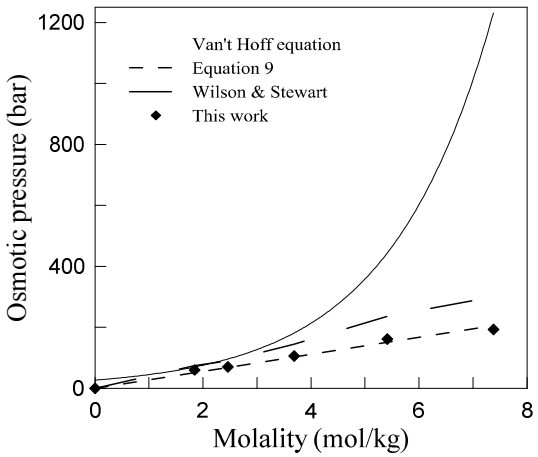

Figure 4: Osmotic pressure of the DS ($MgCl_2$) evaluated at different molal concentration.

Baseline FO tests were carried out using pure water as feed and aqueous $MgCl_2$ as DS prepared at different concentrations. According to Figure 5a, flux trend against applied osmotic pressure gradient at 6 cm/s crossflow velocity appeared almost linear up to ~100 bar bulk osmotic pressure. In order to explain the existence of a plateau at higher concentration, we have listed solute diffusivity resistance (K) and diffusion coefficient of $MgCl_2$ (D_s) in Table 7.2 at different DS concentration. Below 3.7 molal, both D_s and K showed reduced sensitivity to $MgCl_2$ concentration. At higher molality, the solute diffusivity resistance increases drastically, reaching a value of $86 \cdot 10^5$ s/m for a two fold increase in concentration (7.4 molal). Since flux and mass transfer resistivity (K) have an exponential relation (see equation 5), high K value implies the occurrence of severe dilutive ICP acting against the osmotic driving force that prevent an appreciable increase of the permeate flux.

When the crossflow velocity was increased from 2 to 7 cm/s, flux was enhanced by 70% (from 2.2 to 7.9 $kg/m^2.h$) (Figure 5b). This is due to improved hydrodynamic mixing that mitigated the effect of dilutive ECP. However, the effect came to saturation at higher crossflow velocity. Hence, an optimum crossflow rate of 6 cm/s can be identified for the system.

The detected amount of $MgCl_2$ that back-diffused from draw to feed side after 8-hours lasting FO tests were 0.0028, 0.011 and 0.011 mol/kg for DS concentrations of 1.8, 3.7 and 7.4 molal,

respectively. These results are coherent with the claimed good rejection capacity of the used CTA membrane [23].

Table 7.2: Physico-chemical characteristic of draw solution.

Concentration (mol/kg)	μ ($x10^{-3}$ kg/m·s)	K* ($x10^{5}$ s/m)	Density (kg/m^3)	D** ($x10^{-9}$ m^2/s)	K_m ($x10^{-5}$ m/s)
1.8	1.6	4.0	1183	1.2	0.25
2.5	1.8	4.3	1228	1.1	0.23
3.7	2.1	5.7	1307	0.85	0.16
5.4	3.3	12.4	1399	0.39	0.08
7.4	4.7	86.1	1490	0.06	0.01

* Solute diffusivity resistance calculated from equation 2b, ** Diffusion coefficient deduced from data of Miller *et al.* (1984) [33] and K_m is solute mass transfer coefficient i.e. 1/K.

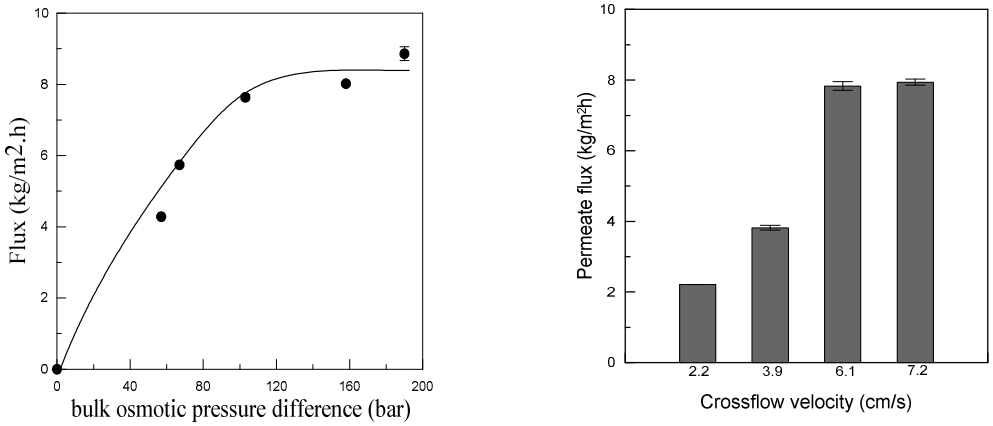

Figure 5: Effect of a) osmotic pressure gradient (feed: pure water; crossflow velocity: 6 cm/s) and b) crossflow velocity (feed: pure water; $\Delta\pi_b^0$=103 bar).

7.4.2. Olive Mill Wastewater FO tests

7.4.2.1. Effect of osmotic pressure

Figure 6a shows dynamics of permeates flux against VCF at different initial osmotic pressure gradient ($\Delta\pi_b^0$) during FO concentration of OMWW. The figure shows that, the higher is $\Delta\pi_b^0$, the higher the initial flux. However, high initial flux was always accompanied by fast flux decline compared to low initial flux. The difference between initial and final flux values at $\Delta\pi_b^0$

of 57, 67, 103 and 158 bar were 23, 29, 33 and 52% respectively. Regardless of the different initial flux values, the curve of 158 and 103 bar collapsed to the same region after 2 h of operation**.** This performance loss can be attributed to the combined effects of loss in driving force due to change of feed and DS volumes over time, dilutive ICP and membrane fouling.

In order to split these overlapping effects, experimental data in Figure 6a were further treated. Correction for the loss in driving force was done by taking the VCF value into consideration. These corrected values were further treated according to the method proposed by Mi and Elimelech (2008) [36] to account for the effect of dilutive ICP. The FO flux data from OMWW experiments were corrected by a normalization factor obtained from corresponding FO tests on pure water as feed.

Therefore, referring to data reported in Figure 6b, for $\Delta\pi_b^0$ of 158 bar, 30% of flux decline is due to loss in driving force while 22% is attributed by dilutive ICP. The effect of membrane fouling was therefore limited. At $\Delta\pi_b^0$ of 57 bar however, presence of low flux limited the extent of feed and DS volume changes. In addition, lower molality corresponds to low viscosity and high diffusion coefficient, hence limited dilutive ICP.

Table 7.3: FO flux analysis using the method of flux-efficiency factor.

$\Delta\pi_b^0$ (bar)	VCF* (%)	$J_{w,obs}$ (kg/m^2 h) ‡	$J_{w,ref}$ at VCF (kg/m^2 h)	Flux-efficiency factor†
57	33.8	2.6	3.3	0.77
67	53.1	2.8	3.8	0.74
103	63.3	3.4	4.7	0.73
158	70.6	4.5	6.3	0.71

*FO tests lasting 4 hours, ‡means values are corrected for the effect of feed and DS volume change in time, †Calculated from equation 6.

Further insight towards FO flux performance was provided by calculating FO flux efficiency factor. The difference between $J_{w,obs}$ and $J_{w,\ ref}$ was more evident at higher $\Delta\pi_b^0$ values (Table 7.3). The flux-efficiency factor however lied in a narrow range (0.71-0.77) irrespective of the different $\Delta\pi_b^0$ values. This trend is strictly correlated to the changes in transport properties of the DS (Table 7.2). Increased $\Delta\pi_b^0$ corresponds to high DS viscosity, low diffusion coefficient and

hence low mass transfer coefficient. Hence, the high flux observed at higher $\Delta\pi_b^0$ value was a profound base for severe dilutive ICP. Nevertheless, the obtained VCF (33-71%) regardless of the severe dilutive ICP was satisfactory. A theoretical analysis by Lay et al. [34] suggests that operating FO system at low flux would limit the extent of dilutive ICP. In agreement with this, stable flux was obtained when a low value of $\Delta\pi_b^0$ was applied (Figure 6a).

Figure 6c shows that the FO water permeability L_p decreased exponentially while increasing $\Delta\pi_b^0$. This is theoretically explained by the increasing prominence of **t**he dilutive ICP modulus: (e^{-J_w/K_m}) in equation 5, which is significantly affected by the decreased value of K_m (Table 7.2). This trend is in good agreement with the dilutive ICP driven flux decline observed in Figure 6b.

The maximum attainable recovery, φ_{max} estimated according to equation 5 at 57, 67, 103 and 158 bar were 95%, 96%, 97.5 and 98.4% respectively. This convergence of φ_{max} values at different $\Delta\pi_b^0$ can be explained by considering equation 5. Since the OMWW used, already contained considerable amount of various salts (Table 7.6) and low molecular weight compounds, high recovery will imply up-concentration of these components. As a result π_{fs} of OMWW will increase significantly, while π_{ds} of DS decreases. Since the measured B is less than 1%, B/L_p is assumed zero and the term J_w/K_m is negligible compared to the high osmotic pressure values of the feed and DS. Hence, equation 5 will be dominated by $L_p\pi_{ds}$ and $L_p\pi_{fs}$ [37]. The equation also implies that, at high recovery the feed water osmotic pressure will be raised by a factor of φ. As a result, all streams at high recovery will eventually exhibit similar osmotic driving force.

Chou *et al*. [37] also provided a further discussion about the convergence behavior of FO flux at high feed and DS concentrations based on mass transfer resistance of the skin and the porous support layer. Accordingly, at low feed and DS concentration, the extent of dilutive ICP is limited hence the rate limiting step is the skin layer resistance to water permeation. In contrast, at high feed and DS concentration, the support layer resistance is very important. Thus, the recovery is only determined by the membrane structural parameter (S), π_{ds} and π_{fs}. So in our case the high recovery corresponds to the regime where S is the rate limiting step. This could

also be another explanation for the convergence of the different φ_{max} values at high recovery since single membrane corresponding to a unique S value was used.

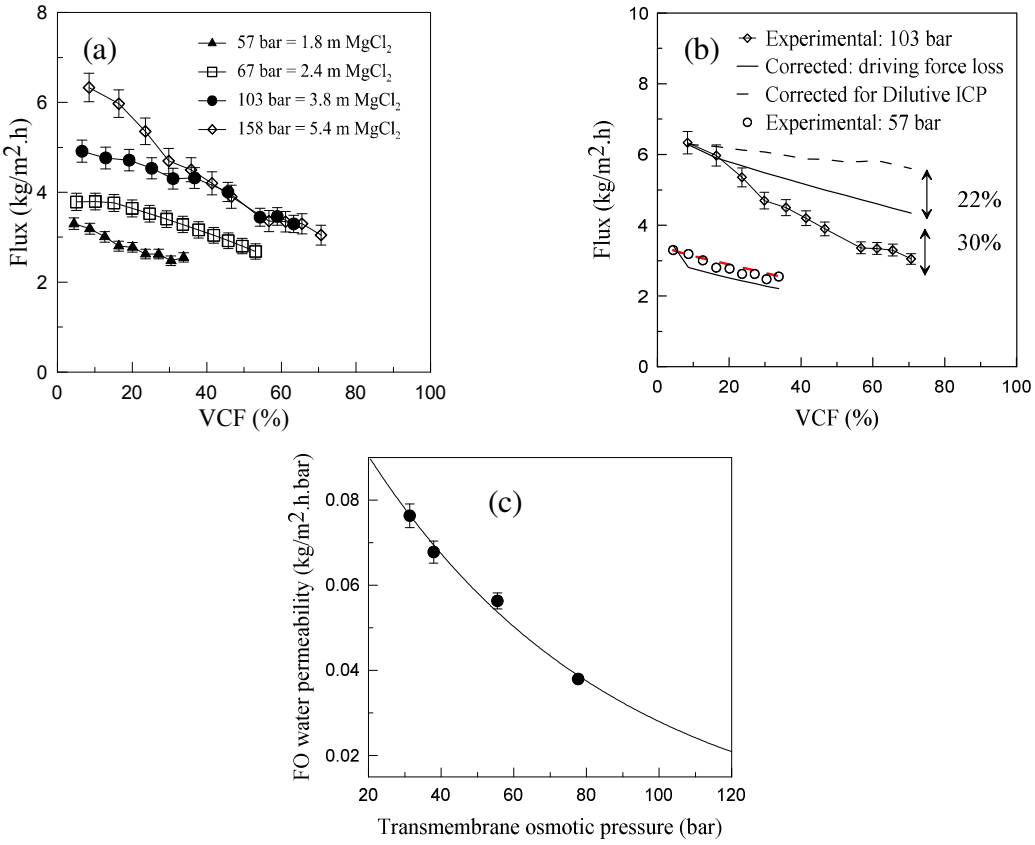

Figure 6: Permeate flux measured at $\Delta\pi_b^0$ of 57 to 158 bar a) before and b) after correcting for the effect of dilutive ICP and c) apparent FO water permeability according to equation 3 (feed: OMWW; crossflow velocity: 6 cm/s).

7.4.2.2. Effect of crossflow velocity

Based on result of FO characterization with pure water as feed, $\Delta\pi_b^0$ of 103 bar was selected to characterize the influence of varying crossflow velocity on flux during concentration of OMWW. While ICP in the porous substructure is highly determined by physico-chemical properties like diffusivity, viscosity or ion/molecular size [38], ECP is mostly determined by hydrodynamic condition. The extent of ECP is evaluated by boundary layer film theory, where the mass transfer coefficient (k) is calculated as:

$$k = \frac{Sh \cdot D_s}{d_h} \qquad 10$$

Where d_h the hydraulic diameter (0.023 m^2) and Sh is the dimensionless Sherwood number for laminar flow defined as:

$$Sh= 1.85*(Re*Sc*d_h/L)^{0.33} \quad (11)$$

By increasing the crossflow velocity, the feed side mass transfer coefficient (equation 10) increased progressively from 1.74 to $2.26*10^9$ m/s (Table 7.4) reducing the effect of ECP. Hence, the final flux obtained at 8.4 cm/s (6.01 kg/m^2.h) was 20% higher than the flux obtained at 4 cm/s (4.8 kg/m^2.h). By moving the crossflow velocity from 4 to 8.6 cm/s, the VCF was raised from 57 to 70%. Nonetheless, the draw solute mass transfer coefficient relating dilutive ICP with hydrodynamic mixing was almost constant (K_m; 4.92-5.01*10^{-5} m/s). Therefore, the limiting step in this complex mass transfer operation lies in the boundary layer resistance, unlike the effect of osmotic pressure where the limiting step was resistance inside the pore structure.

Table 7.4: Transport parameters of the system operated at fixed $\Delta\pi_b^0$ of 103 bar and 4, 6, 7.4 and 8.6 cm/s crossflow velocity using OMWW as feed.

v (cm/s)		Re = ρvDs/μ	μ (kg/m.s)	Sh	K (x10^5 s/m)	k (x10^9 m/s)
4	Feed side	570•-329••	1.7• -2.9••	75.6		1.74
	Draw side	504•-484••	2.14•-2.09••		4.98 ± 21	
6	Feed side	895•-645••	1.7•-2.35••	87.8		2.04
	Draw side	792•-762••	2.14•-2.09••		5.01 ± 20	
7.4	Feed side	1058•-740••	1.7•-2.43••	92.8		2.14
	Draw side	936•-912••	2.14•-2.09••		4.92 ± 23	
8.6	Feed side	1262•-931••	1.7•-2.5••	98.3		2.26
	Draw side	1116•-1057••	2.14•-2.09••		4.9 ± 23	

D_{fs}=0.3 x10^{-9} m^2/s ; μ_f=2.12+0.51 •10^{-3} kg/m s; μ_{ds}=2.12+0.51 •10^{-3} kg/m s, D_{ds}=0.99-1.06 x10^{-9} m^2/s; •: initial and •• final values.

7.4.2.3. Effect of pre-treatment

In addition to stand-alone unit, three different pre-treatments were considered: (1) pre-filtration through stainless steel; (2) MF after pre-filtration; (3) MF using biocatalytically active membrane (BMR).

FO tests were carried out with 3.7 molal $MgCl_2$ ($\Delta\pi_b^0$=103 bar) at 6 cm/s. The initial bulk osmotic pressure of OMWW was 3 bar. Table 7.6 shows more than 80% unexpected multi-valent ions retention during pre-treatment by MF. This could be attributed to loss of the ions due to complex formation with organics or rejected by a secondary layer on the MF membrane made from foulants.

According to Figure 7, the FO permeate flux fed with microfiltered OMWW (method 2) was about 30% higher than the FO flux fed with simply pre-filtered (method 1). However, the highest initial permeate flux (6.2 kg/m^2.h) and VCF (85%) was attained when feed was pre-treated with BMR (method 3). This is attributed by reduced amount of micro-colloids by the immobilized enzyme. Even so, a significant decrease was also detected after 1 h operation (-23%), and the flux dropped to comparable values with MF pre-treated. Due to hydrolysis of pectin by the immobilized enzyme at the solution-membrane interface, permeate of step (3) is rich in small molecular weight galacturonic acid. Since these compounds increase the feed water osmotic pressure, a reduced overall osmotic driving force as a result of change in the feed water volume could be the cause for the observed fast flux decline.

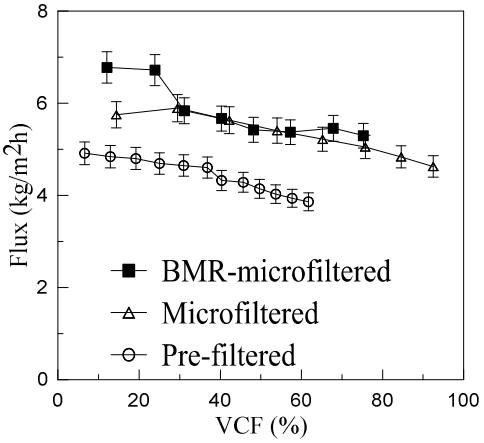

Figure 7: Effect of different pre-treatment methods on FO performance (feed. OMWW; crossflow velocity: 6 cm/s; $\Delta\pi_b^0$: 103 bar).

7.4.3. Long term stability

According to Figure 8, with the renewal of the feed and DS every 24 h, the membrane gave a almost stable performance over 200 h. 70% of the data gave a VRF (70.6 ± 0.45) with maximum VCF (80%) and minimum VCF (45%) occurred at day 5 and day 8 respectively. In addition, a water rinse or sequential water rinse and osmotic back-flush gave an average pure water flux of 8.2 ± 0.77 kg/m^2.h in the entire operational period (Table 7.5).

Although there is no fair basis for comparison, this stable performance over long period and an easily reversible fouling makes FO process strong competitor with the commonly employed pressure driven membrane operations. Owing to the use of large DS volume, there was no significant driving force loss. Hence the ratio of initial to final DS conductivity was close to one (0.93 to 0.97).

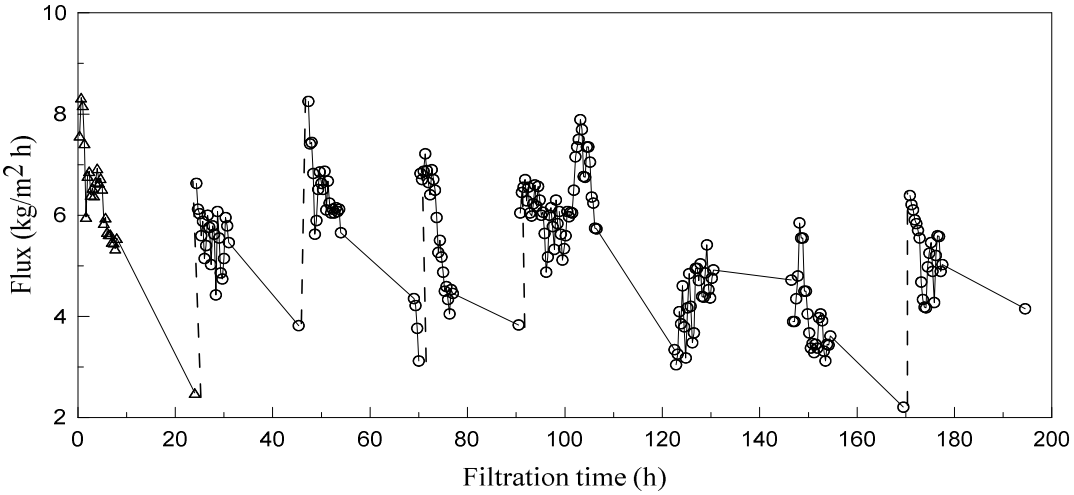

Figure 8: Single step FO performance continuously operated for ten days: OMWW volume; 3 L), DS; 4 L, DS concentration; 3.7 molal $MgCl_2$ at 6 cm/s.

Table 7.5: Parameters measured at the start and end of 24 hours cycle, during a ten day continuous OMWW FO process at 3.7 molal $MgCl_2$, 6 cm/s and 3 L and 4 L of initial feed and DS volume respectively.

Day	VCF (%)	J_w (kg/m^2 h)	$J_{w,i}/J_{w,i+1}$ (kg/m^2 h)	η^f / η^i OMWW	η^f / η^i DS	Cleaning method
0	-	9.8	-	-	-	-
1	71	8.6	88	2.4	0.94	osmotic back flush
2	62.8	8.9	103	5.1	0.93	"
3	68.7	7.2	81	5.9	0.95	"
4	59	7.1	99	4.6	0.95	"
5	70.8	7.8	109	2.0	0.97	Water rinse
6	80	-	-	4.6	0.96	
7	73	-	-	7.3	0.95	
8	45	9.0	94	3.7	0.92	"
9	73	8.5	88	8.2	0.95	osmotic back flush

η: Conductivity

7.5. FO pollutant rejection

The analysis of dried residue showed total phenolic rejection by FO exceeded 98%. The system also gave almost complete decolorization and ion retention, and 96% and 99% TOC and TIC retentions, respectively (see Table 7.6 and Figure 9). Conventionally, the removal of dried OMWW residue is accomplished by combination of multi-stage filtration and energy intensive centrifugation [2, 4, 39]. For instance, seven sequential steps comprising of acidification, centrifugation, MF, UF and RO were used to remove the entire dried residue OMWW by Russo (2007) [4]. Agalias et al.(2007) proposed three successive steps to remove suspended solids followed by series of adsorbent resins for deodorizing and decolorization [2]. In our study, an almost complete removal of the dried residues through single step FO process makes this application promising for the treatment or valorization of OMWW.

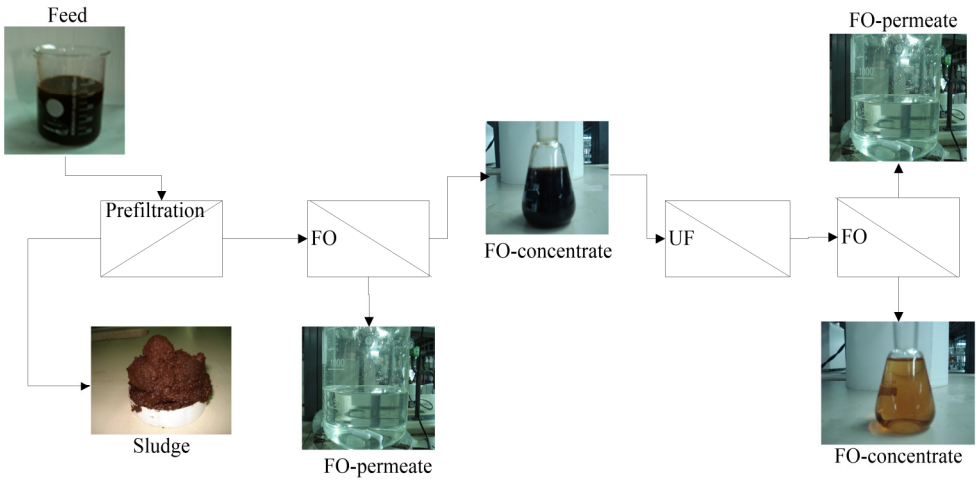

Figure 9: Schematic representation of an FO-UF-FO combined membrane operations used to concentrate OMWW after pre-filtered with sequential 35 µm and 15 µm stainless steel wire meshes.

Table 7.6: Physico-chemical properties of FO process streams.

Parameter	Pre-filtered OMWW	MF OMWW	FO concentrate	FO permeate
Ca^{2+} (mg/L)	560	48	71	n.d.
Mg^{2+} (mg/L)	160	30	97	30800
K^{+} (mg/L)	390	390	710	n.d
Mn^{2+} (mg/L)	99	2	0.5	n.d.
Fe (mg/L)	40	n.d.	n.d.	n.d.
Cu (mg/L)	300	7	5	4.5
Zn^{2+} (mg/L)	34	1.5	n.d.	n.d.
TOC (mg/mL)	4.1	3.8	3.6	0.13
TIC (mg/mL)	0.23	0.19	0.22	0.0016
Pectins (mg/mL)	0.3-0.46	n.d	-	n.d
TS (g/kg)	0.1	n.d	0.27	n.d
Total phenolic (mg/mL)	0.83	0.55	-	0.013

n.d.*: not detectable*

7.6. Fouling and reversibility

Chemical cleaning of membrane causes additional cost for energy consumption, loss in selectivity, short membrane life and cleaning chemicals that needs end-of-pipe treatment. Even so, irreversible membrane damage with extensive chemical or biological cleaning after treating OMWW with conventional pressure driven membrane operation is well reported in literature [4-5, 7-9, 39]. A study using alginate, BSA and AHA as model foulants of CTA-FO membrane suggested that, when foulants have high degree of carboxylic group, Ca^{2+} forms complex even at low concentration (0.5 mM) [36]. Composition of our OMWW shows presence of 14 mM Ca^{2+} and pectin 0.3-0.46 mg/mL (Table 6). Hence, enhanced fouling due to formation of calcium complexes and cross-linked foulants and consequent difficulty in flux recovery was expected. Indeed, absence of foulant compaction by hydraulic pressure in FO process [40] led to significant flux restoration (more than 95%) after short cleaning cycle.

The ATR-FTIR analysis in Figure 10 shows that both OMWW foulant and fouled membrane exhibited a characteristic peak around 1580 cm^{-1}, attributable to C-C stretching occurring in aromatic rings of polyphenols. This signal is absent in both virgin and cleaned membrane, indicating effectiveness of the applied back-washing mechanism. The membrane shows sharp band at 1736 cm^{-1} attributed to C=O stretching in acetate groups of CTA membrane and the bands between 1200 cm^{-1} and 1000 cm^{-1} are attributed to C-O stretching in ester groups of the polyester mesh supporting the CTA membrane.

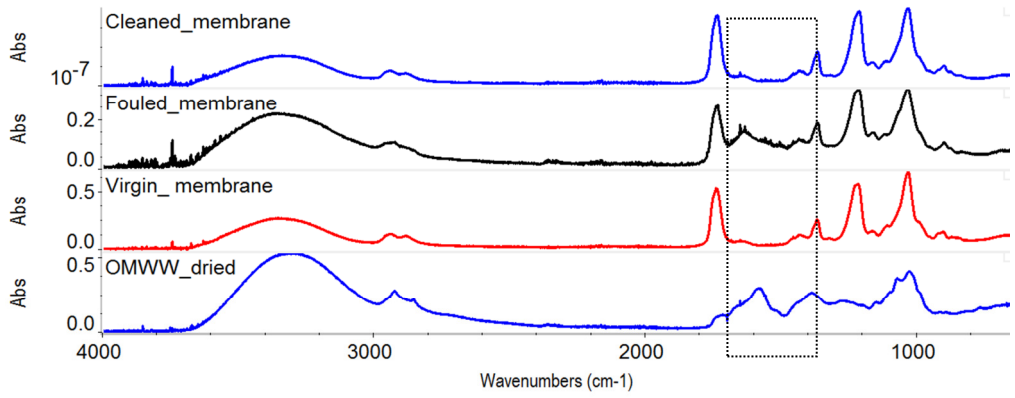

Figure 10: ATR-FTIR spectra of dried OMWW and virgin, fouled and osmotically cleaned membranes after 200 h of continuous use.

Figure 11a-c shows surface SEM images of virgin (a), fouled (b) and osmotically cleaned (c) membranes after a 200 h lasting continuous FO dehydration. The thick layer of membrane surface foulant completely disappeared after cleaning. As a result there was no significant morphological difference between virgin (a) and cleaned (c) membranes. Likewise, cross sectional SEM image of fouled membrane showed a 6µm thick layer of foulant (Figure 11d) on the top of 10 µm membrane skin layer, that completely disappear after cleaning as shown in Figure 11e. Overall, FO membrane resulted in a more stable performance and higher lifetime preservation with respect to conventional membrane filtration [9, 18-19, 41].

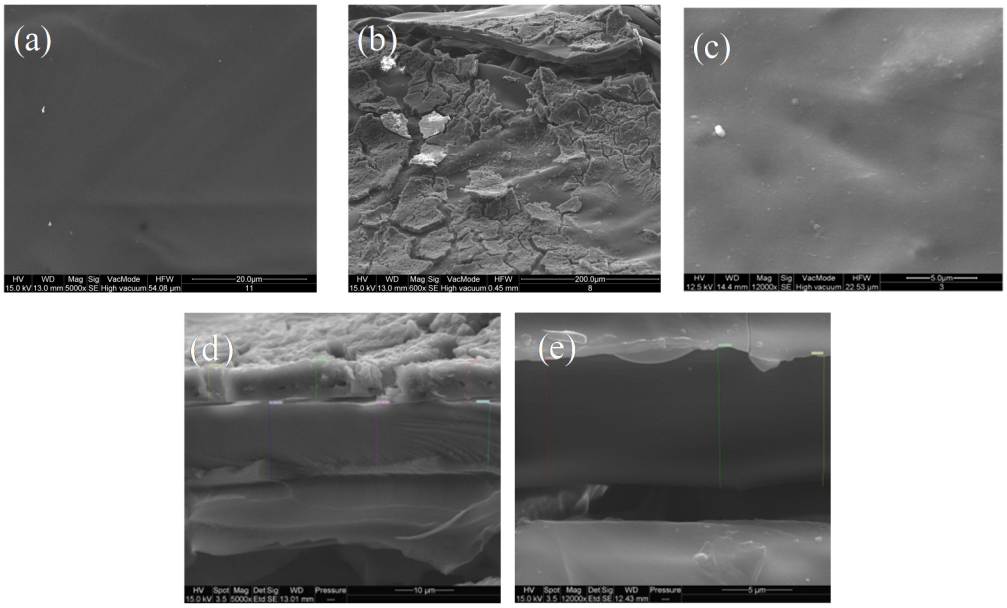

Figure 11: Surface images of a) virgin, b) fouled c) cleaned membrane and cross section images of d) fouled and e) cleaned membrane:

7.7. Recovery of polyphenols

The FO concentrated stream needs further treatment to fractionate high added value compounds such as biophenols. Hence, the performance of two pressure driven membrane operations: 10 nm ceramic NF and 100 kDa polymeric UF membranes were evaluated.

When a 50% FO concentrated stream was supplied in the feed stream, ceramic NF membrane (at 7 bar, 200 L/h with 150 L/m^2.h.bar pure water permeability) gave 27 kg/m^2.h flux, 77% flux recovery, possibly attributed by the high antifouling property that is generally exhibited by ceramic membranes [4]. On the contrary, UF membrane (at 3 bar and 100 L/h with pure water permeability: 70 L/m^2.h.bar) gave 7 kg/m^2 h, small flux recovery after cleaning (24%) and

visually inspected thick layer of adsorbed foulants after cleaning. Therefore, the NF membrane productivity was 35% higher than the UF membrane despite the fivefold higher pore size exhibited by the UF membrane (Figure 12). Nevertheless a 55% improved flux was also obtained for the UF membrane after pre-treating the 50% FO concentrate by enzyme pectinase to degrade foulants (see inset of Figure 12).

Both NF and UF membranes exhibited similar TOC and TIC retentions (54-61%). They also revealed high biophenolic (MW: 100-300 Da) retention coefficient (92 and 83 %, respectively). The high retention for the 100 kDa UF membrane could be explained by presence of thick layer of adsorbed foulants that modified the intrinsic rejection capacity of the membrane [42], as shown in Figure 12.

Permeate of UF, rich in low molecular weight biophenols and containing 6.6 g/L TOC and 1.1 g/L total phenols, was further processed by FO. At 3.7 molal $MgCl_2$ ($\Delta\pi_b^0$=103 bar) and 6 cm/s, 5 kg/m^2.h average FO flux with a VCF of 64% was achieved. During this time, the concentration of TOC and total biophenolic compound in the concentrated streams were 13.9 and 1.9 g/L respectively while the total biophenolic compounds found in FO permeate was limited to 0.01 g/L.

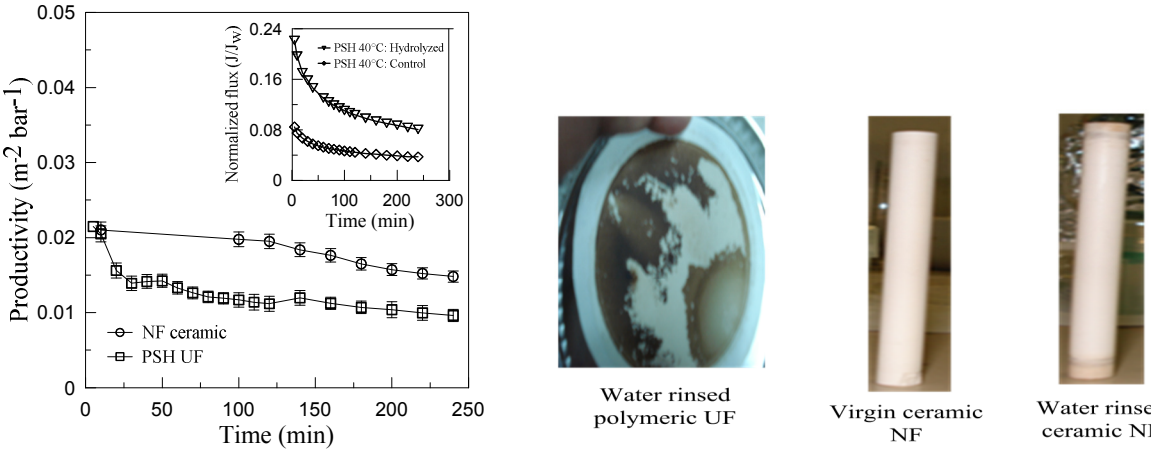

Figure 12: Productivity of 10 nm ceramic NF at 7 bar, 200 L/h and 100kDa PSH UF membrane at 3 bar, 100 L/h and ambient temperature (feed: 50% FO concentrate). Inset: OMWW UF PSH flux trend when 50% FO concentrate is hydrolyzed with pectinase at 40°C for 1 h and control system at 40°C, 100 L/h feed flowrate and 3 bar TMP.

7.8. Conclusion

The present study showed that dehydration by FO represent a plausible alternative for the treatment and valorization of OMWW. Single-step FO resulted in 71% reduced volume, more than 98% dried residue removal and less than 1% w/v of draw solute back-diffused into the feed. The extent of irreversible fouling was significantly low, due to more favorable active layer facing feed water operational mode, hydrophilic and smooth membrane material surface and absence of foulant compaction by hydraulic pressure. Analysis of flux-efficiency factor and FO water permeability however revealed the presence of sever dilutive ICP that was augmented by the high viscosity of the used draw solution. Regardless of this, FO exhibited an interesting performance when it was used for continuous dehydration over 200 h.

Once the total processable volume was effectively reduced by FO, a ceramic NF used to fractionate biophenols from a 50% concentrated stream gave 27 $kg/m^2.h$ flux at 200 L/h flowrate and 7 bar TMP with easy flux restoration. FO used as a final polishing step to obtain a highly concentrated biophenols from permeate of UF also showed an interesting performance.

Overall, the observed single step FO flux performance with complete pollutant rejection irrespective of both concentrative and dilutive concentration polarization phenomena is promising. Both NF and UF were used to illustrate the need for further hybridization of FO with other process. The main weakness of membrane process however is its dependence on feed water concentration. Hence, further optimization of the hybridization is crucial.

It should be envisage that hybridization with other membrane operations or traditional separation mechanisms is highly imperative. Example, combination of FO with membrane distillation (MD) for simultaneous regeneration of DS and reclaiming high quality water from a highly recalcitrant waste stream could be one of the possibilities. This will lead to efficient utilization of FO process for valorisation of OMWW.

7.9. References

[1] A. Roig, M.L. Cayuela, M.A. Sánchez-Monedero, An overview on olive mill wastes and their valorisation methods, Waste Management, 26 (2006) 960-969.

[2] A. Agalias, P. Magiatis, A.-L. Skaltsounis, E. Mikros, A. Tsarbopoulos, E. Gikas, I. Spanos, T. Manios, A New Process for the Management of Olive Oil Mill Waste Water and Recovery of Natural Antioxidants, Journal of Agricultural and Food Chemistry, 55 (2007) 2671-2676.

[3] H. Dhaouadi, B. Marrot, Olive mill wastewater treatment in a membrane bioreactor: Process feasibility and performances, Chemical Engineering Journal, 145 (2008) 225-231.
[4] C. Russo, A new membrane process for the selective fractionation and total recovery of polyphenols, water and organic substances from vegetation waters (VW), Journal of Membrane Science, 288 (2007) 239-246.
[5] C.A. Paraskeva, V.G. Papadakis, E. Tsarouchi, D.G. Kanellopoulou, P.G. Koutsoukos, Membrane processing for olive mill wastewater fractionation, Desalination, 213 (2007) 218-229.
[6] FAOstat2006, http://faostat.fao.org, (Accessed August 2012).
[7] E.O. Akdemir, A. Ozer, Investigation of two ultrafiltration membranes for treatment of olive oil mill wastewater, Desalination, 249 (2009) 660-666.
[8] A. Cassano, C. Conidi, E. Drioli, Comparison of the performance of UF membranes in olive mill wastewaters treatment, Water Research, 45 (2011) 3197-3204.
[9] E. Garcia-Castello, A. Cassano, A. Criscuoli, C. Conidi, E. Drioli, Recovery and concentration of polyphenols from olive mill wastewaters by integrated membrane system, Water Research, 44 (2010) 3883-3892.
[10] M. Pizzichini, C. Russo, Process for recovering the components of olive mill wastewater with membrane technologies, in, Google Patents, 2005.
[11] M. Stoller, Technical optimization of a dual ultrafiltration and nanofiltration pilot plant in batch operation by means of the critical flux theory: A case study, Chemical Engineering and Processing: Process Intensification, 47 (2008) 1165-1170.
[12] A. Zirehpour, M. Jahanshahi, A. Rahimpour, Unique membrane process integration for olive oil mill wastewater purification, Separation and Purification Technology, 96 (2012) 124-131.
[13] S. Judd, B. Jefferson, Membranes for Industrial Wastewater Recovery and Re-use 2003.
[14] G. Bleve, C. Lezzi, M.A. Chiriatti, I. D'Ostuni, M. Tristezza, D.D. Venere, L. Sergio, G. Mita, F. Grieco, Selection of non-conventional yeasts and their use in immobilized form for the bioremediation of olive oil mill wastewaters, Bioresource Technology, 102 (2011) 982-989.
[15] S. Takaç, A. Karakaya, Recovery of phenolic antioxidants from olive mill wastewater, Recent Pat. Chem. Eng, 2 (2009) 230-237.
[16] E. Tsagaraki, H. Lazarides, Fouling Analysis and Performance of Tubular Ultrafiltration on Pretreated Olive Mill Waste Water, Food Bioprocess Technol, 5 (2012) 584-592.
[17] F. Jurado, A. Cano, J. Carpio, Modelling of combined cycle power plants using biomass, Renewable Energy, 28 (2003) 743-753.
[18] A.Y. Gebreyohannes, R. Mazzei, E. Curcio, T. Poerio, E. Drioli, L. Giorno, Study on the in Situ Enzymatic Self-Cleansing of Microfiltration Membrane for Valorization of Olive Mill Wastewater, Industrial & Engineering Chemistry Research, 52 (2013) 10396-10405.
[19] C.M. Galanakis, E. Tornberg, V. Gekas, Clarification of high-added value products from olive mill wastewater, Journal of Food Engineering, 99 (2010) 190-197.

[20] I. Karaouzas, N.T. Skoulikidis, U. Giannakou, T.A. Albanis, Spatial and temporal effects of olive mill wastewaters to stream macroinvertebrates and aquatic ecosystems status, Water Research, 45 (2011) 6334-6346.
[21] C. Klaysom, T.Y. Cath, T. Depuydt, I.F.J. Vankelecom, Forward and pressure retarded osmosis: potential solutions for global challenges in energy and water supply, Chemical Society Reviews, 42 (2013) 6959-6989.
[22] T.Y. Cath, A.E. Childress, M. Elimelech, Forward osmosis: Principles, applications, and recent developments, Journal of Membrane Science, 281 (2006) 70-87.
[23] J.R. McCutcheon, R.L. McGinnis, M. Elimelech, A novel ammonia—carbon dioxide forward (direct) osmosis desalination process, Desalination, 174 (2005) 1-11.
[24] R.W. Holloway, A.E. Childress, K.E. Dennett, T.Y. Cath, Forward osmosis for concentration of anaerobic digester centrate, Water Research, 41 (2007) 4005-4014.
[25] K.B. Petrotos, P. Quantick, H. Petropakis, A study of the direct osmotic concentration of tomato juice in tubular membrane – module configuration. I. The effect of certain basic process parameters on the process performance, Journal of Membrane Science, 150 (1998) 99-110.
[26] J.L. Cartinella, T.Y. Cath, M.T. Flynn, G.C. Miller, K.W. Hunter, A.E. Childress, Removal of Natural Steroid Hormones from Wastewater Using Membrane Contactor Processes†, Environmental Science & Technology, 40 (2006) 7381-7386.
[27] J. Zhang, W.L.C. Loong, S. Chou, C. Tang, R. Wang, A.G. Fane, Membrane biofouling and scaling in forward osmosis membrane bioreactor, Journal of Membrane Science, 403–404 (2012) 8-14.
[28] K. Lutchmiah, A.R.D. Verliefde, K. Roest, L.C. Rietveld, E.R. Cornelissen, Forward osmosis for application in wastewater treatment: A review, Water Research, 58 (2014) 179-197.
[29] A. Cicci, M. Stoller, M. Bravi, Microalgal biomass production by using ultra- and nanofiltration membrane fractions of olive mill wastewater, Water Research, 47 (2013) 4710-4718.
[30] K. Slinkard, V.L. Singleton, Total phenol analysis: automation and comparison with manual methods, American Journal of Enology and Viticulture, 28 (1977) 49-55.
[31] A. Achilli, T.Y. Cath, A.E. Childress, Selection of inorganic-based draw solutions for forward osmosis applications, Journal of Membrane Science, 364 (2010) 233-241.
[32] J.S. Yong, W.A. Phillip, M. Elimelech, Coupled reverse draw solute permeation and water flux in forward osmosis with neutral draw solutes, Journal of Membrane Science, 392–393 (2012) 9-17.
[33] D.G. Miller, J.A. Rard, L.B. Eppstein, J.G. Albright, Mutual diffusion coefficients and ionic transport coefficients lij of magnesium chloride-water at 25. degree. C, The Journal of Physical Chemistry, 88 (1984) 5739-5748.
[34] W.C.L. Lay, J. Zhang, C. Tang, R. Wang, Y. Liu, A.G. Fane, Factors affecting flux performance of forward osmosis systems, Journal of Membrane Science, 394–395 (2012) 151-168.

[35] A.D. Wilson, F.F. Stewart, Deriving osmotic pressures of draw solutes used in osmotically driven membrane processes, Journal of Membrane Science, 431 (2013) 205-211.
[36] B. Mi, M. Elimelech, Chemical and physical aspects of organic fouling of forward osmosis membranes, Journal of Membrane Science, 320 (2008) 292-302.
[37] S. Chou, L. Shi, R. Wang, C.Y. Tang, C. Qiu, A.G. Fane, Characteristics and potential applications of a novel forward osmosis hollow fiber membrane, Desalination, 261 (2010) 365-372.
[38] S. Zhao, L. Zou, Relating solution physicochemical properties to internal concentration polarization in forward osmosis, Journal of Membrane Science, 379 (2011) 459-467.
[39] A. Cassano, C. Conidi, L. Giorno, E. Drioli, Fractionation of olive mill wastewaters by membrane separation techniques, Journal of Hazardous Materials, 248–249 (2013) 185-193.
[40] B. Mi, M. Elimelech, Organic fouling of forward osmosis membranes: Fouling reversibility and cleaning without chemical reagents, Journal of Membrane Science, 348 (2010) 337-345.
[41] A. Cassano, C. Conidi, L. Giorno, E. Drioli, Fractionation of olive mill wastewaters by membrane separation techniques, Journal of Hazardous Materials, 248 (2013) 185-193.
[42] M. Mulder, Basic Principles of Membrane Technology, 1996.

Chapter 8: Comparison between enzyme & chemical cleaning, Summary & Conclusion, New developments and Future research perspectives

Overview: In this thesis work detailed study regarding integrated membrane process for wastewater valorization mainly focusing on developing fouling prevention strategies is presented. This chapter thus provides a general comparison between the employed enzymatic and chemical cleaning and summary and conclusions of the overall work presented in the thesis. Brief summary of significance promoted by this thesis work and few future directions are also provided.

8.1. Comparison of the set enzymatic and chemical cleaning performance

Whilst cleaning is routinely employed to recover some of the flux, the cleaning downtime incurs cost penalty [1]. To limit this, membrane cleaning period can vary from once or twice a year when used as a final polishing in ultrapure water system to monthly or daily for high fouling propensity wastewater. Therefore, the enzymatic *in-situ* degradation will help for continuous daily cleaning as the wastewater under investigation has high fouling propensity.

Figure 1a-b is taken from chapter 4 and chapter 6 respectively to recall the performance of the employed enzymatic and chemical cleaning over multiple cycles while Table 8.1 provides a general comparison between the two approaches.

The enzymatic cleaning is aimed at preventing direct membrane foulant interaction and involve in their *in-situ* degradation. As a results, it gave an interesting performance over a wide range of operational condition (0.01 to 3 mg/mL feed concentration, 5 to 45 $L/m^2.h$ flux, 1 to 9 g/m^2 NP^{SP} dynamic layer and 25°C and 40°C filtration temperature). More pragmatically, it allowed the use of the membrane beyond the enzymes' active period. Example as shown in Figure 1-a, when the superparamagnetic biocatalytic systems' performance is lost after fives repeated cycles of continuous filtration at 17 $L/m^2.h$, the membrane remained useful with fresh enzyme make-up. However, the current knowledge assumes that the dynamic layer of the bionanocomposites may only help with membrane surface cleansing. Hence, the observed water permeability difference before and after biocatalysis (chapter 5) is attributed to the adsorption of low molecular weight foulants inside the pore structure that survived the enzymatic cleaning.

On the other hand, in chapter 6, chemical cleaning using NaOCl was employed to restore the original membrane performance. The major hurdle of this method is, first it allows interaction of the membrane with foulants. So it is a post damage action that even exposes the membrane to a strong chemical for cleaning. To make it worse, the cleaning reagent when employed at low concentration lacked the possibility to fully reverse the performance. As shown in Figure 1-b, applying high concentration of NaOCl for cleaning resulted in undesired early stage performance improvement over original performance followed by complete membrane damage. It is worth noting that unlike the enzymatic cleaning, when the system looses it performance at the end the 5^{th} cycle, the fate of the membrane would be disposal together with large volumes of concentrated cleaning chemical. Thus, the chemical cleaning incurs a cost penalty through: the energy consumption, the loss of tap or ultrapure water for rinsing, the downtime, the use of hazardous chemicals and premature membrane disposal. Contrary to this the enzymatic cleaning allowed continuous filtration over two weeks with no noticeable performance variation. Despite all this, the chemical cleaning also helped to keep a reasonable flux of 20 $kg/m^2.h$, at the conditions found compatible with the membrane and polymeric coating layer of the NP^{SP} used as nanofillers during the organic/inorganic hybrid membrane preparation.

The comparison between employed chemical and enzymatic cleaning shows that, cleaning once fouling of the membrane has become severe is less effective than continuous maintenance cleaning through *in-situ* degradation which prevents incipient fouling. Nevertheless, in many cases no single cleaning reagent will recover the flux entirely, and it is often advantageous to use a combination of cleaning reagents in sequence [2]. In the present case, rough filtration (chapter 3 and 7) and enzymatic cleaning (chapter 3 to 5) are good pre-treatment strategies that are used to prevent irreversible membrane damage due to fouling. These are essential to achieve a long MF membrane life. They are methods developed based on feed water composition and the type of fouling. But pure water permeability loss among different cycles of these pretreatment strategies indicates their need to be backed up by an appropriate cleaning schedule. Thus, one can also envisage on using combination of the set enzymatic and chemical cleaning. In chapter 6, conditions that are less detrimental to the overall membrane integrity were identified. Hence, hypochlorite cleaning under these conditions can be used to give short back-flush, after magnetically removing the immobilized enzyme from the surface of the membrane, in order to periodically remove foulants that are trapped inside the pore structure.

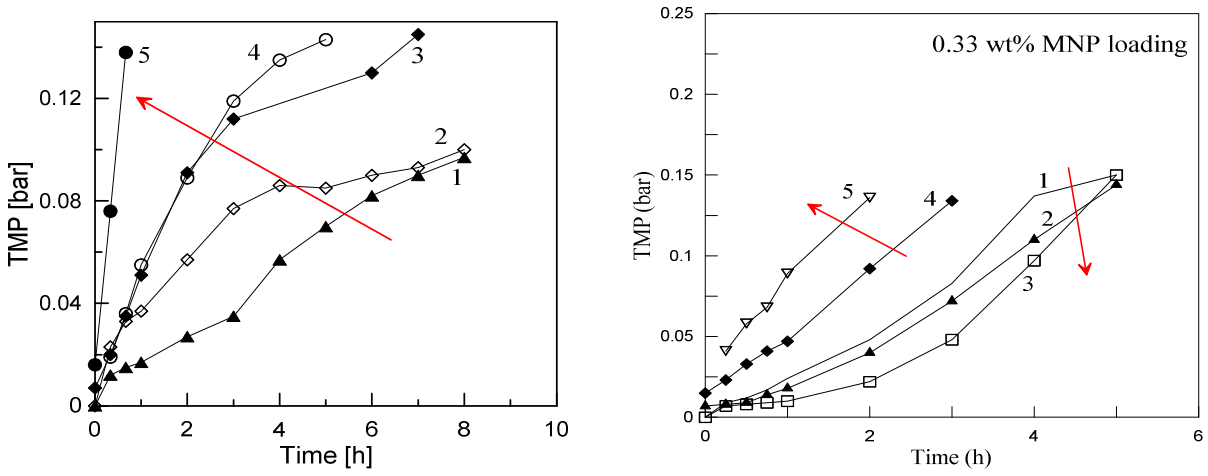

Figure 1: a) accelerated fouling using 0.33 w/w% NP^{SP} loaded O/I hybrid membrane and 1 g/m^2 dynamic layer of biocatalytic particles at 17 kg/m^2.h, and b) accelerated fouling using 0.33 w/w % NP^{SP} loaded O/I hybrid membrane at 25 kg/m^2.h. Feed in both cases is 0.3 mg/mL pectin at room temperature.

Table 8.1: Comparison of membrane cleaning chemically and enzymatically using the dynamic layer of biocatalytically active NP^{SP}.

Chemical cleaning	Enzymatic cleaning
Direct membrane-foulant interaction	Foulant interact with NP^{SP} dynamic layer
Post damage action	Preventive action
Need periodic pause	*In-situ* cleaning
Early stage improved post-cleaned performance becomes a solid based for lateral state intensive fouling.	Damage mostly limited to the dynamic layer, hence the membrane is useful even after deactivation of the enzyme.
At the 5th cycle membrane & concentrated cleaning chemical are subjected for disposal or further end-of-pipe treatment	At the 5th cycle membrane is ready for further use with fresh enzyme make-up

8.2. Possible integrated membrane process based on individual performance

Based on investigation of individual units from chapter 3 to 7, the following integrated membrane schemes are suggested:

1. When the wastewater has high suspended solids as well as high organic content (fouling propensity), rough filtration, biocatalytic MF, NF can be the main integration with FO being used as a final polishing step to obtain highly concentrated biophenols, e.g, from permeate of UF (option 1), or eventually it can also be used subsequent to MF (option 2) of Figure 2.
2. When the wastewaters' macro-pollutant load is limited, FO can precede MF/UF/NF and can also be used as final polishing step to get more concentrated biophenols (Figure 2: option 3).
3. When the feed wastewater has no enough biophenols to encourage recovery, one can envisage on the use of FO to concentrate the stream. This will eventually reduce the total processable volume thereby reducing the need for large onsite and offsite storage facilities and transportation to offsite treatment facilities. Most olive oil production centers are located along the sea side. Since FO process is able to retain more than 98% of all the pollutants, it is possible to use the FO membrane as barrier to retain pollutants while letting the purified water diffuse into the seawater. The seawater will serve as the source of osmotic driving force as shown in option no 4 of Figure 2.

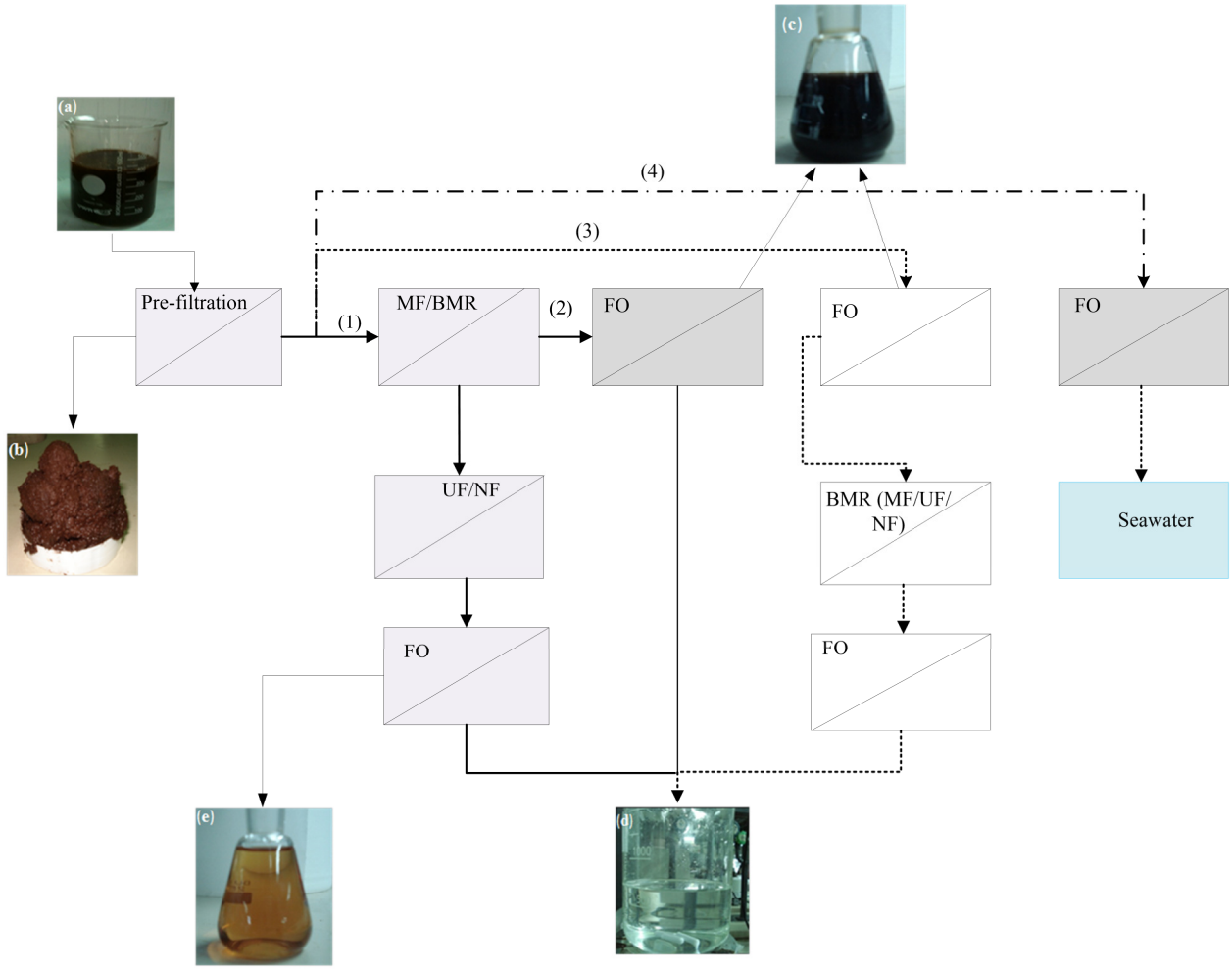

Figure 2: Suggested possible integrated membrane process based on results of individually investigated membrane operations, where a) feed water, b) sludge after screening with 35µm stainless steel wire mesh, c) FO concentrated biophenol and d) permeate of FO.

8.3. Summary and conclusion, New developments and Future perspective

8.3. 1. Summary and conclusion

The research work carried out aimed at developing biohybrid system, based on integration of different membrane operations, enzymes and magnetic nanoparticles for valorization of vegetation wastewater. The main research focus area was development of membrane fouling mitigation/ prevention strategy dictated by the feed water characteristics. This was motivated by identified problem gaps from literatures.

As a result of extensive review of previous works, it was identified that sever membrane fouling and periodic release of huge volume of wastewater are the most important challenges for the

successful commercialization of integrated membrane processes for food based wastewater valorization. Aiming to alleviate these challenges, different individual membrane processes were tested independently with an ultimate goal of developing integrated membrane process. The first problem, fouling, was found to be especially severe during MF. As MF often comes first in the order of integrated membrane process, we conducted detail study with several modifications.

Using OMWW as a case in point, we adapted a new process to handle the problem of fouling during MF. The proposed process is a biocatalytic membrane with covalently immobilized enzyme. It followed an engineered approach that combined both hydrodynamic and kinetic characterization of BMR. The adapted process helped to develop an *in-situ* self-cleansing biocatalytically active membrane that control MF fouling promoted by pectins. Pectinase functionalized MF membrane resulted in 50% higher permeate flux compared to inert membrane. This achievement paved the way to fouling free integrated membrane process for valorization of vegetation wastewater. However, covalent immobilization of enzyme has a major drawback. When the enzyme is denatured, there is no practical means of removing this enzyme to reutilize the membrane beyond the enzymes active life.

To avert the problem of premature membrane replacement, a novel BMR^{SP} system has been developed and evaluated. The system comprised magnetically guided reversible enzyme immobilization. It is based on utilization of the synergistic magnetic responsiveness of superparamagnetic nanoparticles that are embedded inside O/I hybrid membrane and superparamagnetic nanoparticles activated with enzyme (bionanocomposites) that are dispersed in the bulk stream. This approach can be useful to form a dynamic layer of enzyme that can easily be removed from the surface of the membrane whenever needed using an external magnet. Thus it served dual purpose of preventing direct membrane-foulant interaction and *in-situ* degradation of deposited foulant using the bionanocomposites. Both immobilized enzyme and membrane gave a stable performance over multiple cycles. Compared to direct immobilization of enzymes on membranes by covalent bonding, the bio-inspired NP^{SP} allowed using the membrane beyond the enzymes active period. This is due to the fact that the fouling is limited to the dynamic layer.

To further investigate the effect of operational parameters on the BMR^{SP}, detailed experimental analysis was conducted. We found that while the feed concentration, the temperature and the flux were 0.01 mg/mL, 25°C and 15 $L/m^2.h$ respectively, the rate of fouling was 0.12 bar/h.

Furthermore, we investigated the rate of fouling over a wider feed concentration gap i.e. starting from 0.01 mg/mL to upto 300 times more concentration. Within this range, the rate of fouling was observed to increase only by a factor of 8. Moreover, the residence time dictated by the transmembrane flux did not affect the enzyme activity, but the rate of fouling. It is worth noting that the system gave a stable performance when operated continuously over two weeks without visible activity decay or enzyme leakage.

While using enzymatic *in-situ* degradation of foulants to keep sustainable membrane productivity over long-term, there may be a need for periodic chemical flushing. This may be important especially to remove partially permeable hydrolysis products that are trapped inside the membrane pore structure. Therefore, an extensive study regarding the ageing effect and cleaning efficiency of NaOCl on the O/I hybrid magnetic responsive membrane was conducted to investigate the chemical cleaning stability. Accelerated ageing under static condition revealed changed membrane due to cleaning chemical induced gradual damage to the polymeric coating layer of the nano- fillers used. We also confirmed that to attain best cleaning efficiency in a less detrimental way, close consideration should be given to exposure condition (pH, hypochlorite concentration and exposure duration). After careful consideration of the observed membrane changes during accelerated ageing, a suitable cleaning condition that is less damaging to the O/I hybrid membrane is identified.

The other identified problem, which is periodic release of huge volume of wastewater, was also targeted by using FO. We proved, using OMWW as a case study, that dehydration by FO can be an alternative for the treatment and valorization of vegetation wastewater. It was found capable of treating real wastewater that accounts for effects of fouling under actual operating conditions. Single-step FO operated under most favorable conditions resulted in a significant volume reduction of the wastewater with complete rejection of all the pollutants including biophenolic compounds and small ions. This complete rejection facilitated the reclamation of the biophenolic compounds from a significantly reduced volume of wastewater. Moreover, the system revealed a stable performance when operated continuously for over 200 h. After effective reduction of the total processable volume by FO, the possibility of using UF and NF were tested as a post treatment to fractionate and purify the retained biophenols. FO also exhibited a stable performance when it was used as final polishing step to concentrate biophenols recovered in the permeate stream of UF.

Ultimately, based on the results of the detail studies on individual processes, different optional need based new sets of integrated membrane operations have been proposed for the valorization of vegetation wastewater targeting the chronic problems of fouling and huge volume. These possible integrated processes include the unit processes FO, MF with magnetically immobilized enzyme, NF and UF. The integrated system will eventually benefit from the advantages of each membrane process. In addition, this PhD thesis introduced the following advances in wastewater valorization.

The advances promoted in the current work include:

1. Development of biocatalytic MF membrane with covalently immobilized pectinase for *in-situ* degradation of major foulants.
2. Development of an FO process integrated with pressure driven membrane process to reduce total processable volume of vegetation wastewater that basically comes with a challenge of seasonal discharge at high volume.
3. A new method of immobilizing enzyme on the membrane surface was also developed by using the concept of superparamagnetism.
4. A suitable chemical cleaning condition for the newly developed O/I hybrid membrane is established.

8.3.2. Future Perspective

The present thesis work delivered the concepts and groundwork on the development of novel O/I bio-hybrid magnetic responsive BMR^{SP}. The preliminary development of BMR^{SP} and functionality of different individual membrane operations presented in this work have demonstrated the great potential of hybridization to facilitate wastewater valorization. The data in Chapter 4 and 5 showed that magnetically triggered bionanocomposites were better enzyme immobilization technique than direct covalent bonding on the membrane that has been a ground mechanism in the past decades. It also opens a new horizon for bio-inspired NP^{SP} applications in localized biocatalysis to enhance performance in industrial production, processing, environmental remediation or bio-energy generation. Moreover, the process is not limited to membrane technology and can be exploited to prevent any enzymatically cleavable fouling on any surface.

The extensive study made here has also opened the following new research areas that are essential to justify the notion that magnetically controlled bio-hybridization in integrated membrane process are among the potential next-generation wastewater valorization techniques:

- From the detailed hydrodynamic and kinetic characterization of the new BMR^{SP}, there is possibility to develop model equation that can describe the reactor. In addition, based on a developed model equation, it is possible to plot a platform containing different process parameters that can be used to predict the behavior of the reactor under given condition.
- The packing density of NP^{SP} may vary depending on deposition pattern, shape and presence of aggregation. Particularly, presence of agglomeration may change both diameter and shape of the particle, which may further change the bed porosity. In literature, there are a number of guidelines (rule of thumbs) that are designed to provide with the information on the type of packing depending on the shape of the particles. However the surface property of nanoparticles is completely different from a corresponding micro or macro particles. As a result, it is highly difficult to transform the assumptions taken for micro or macro particles to nanoparticles. Therefore, studying the packing pattern and its effect on the hydrodynamic resistance is one direction of future study.
- Driven by the promising performance obtained from individual membrane operations, it is also interesting to integrate individual units and optimize.

8.4. References

[1] A. Levine, Chapter 3 - Industrial waters, in: S. Judd, B. Jefferson (Eds.) Membranes for Industrial Wastewater Recovery and Re-use, Elsevier Science, Amsterdam, 2003, pp. 75-101.

[2] R.W. Baker, Reverse Osmosis, in: Membrane Technology and Applications, John Wiley & Sons, Ltd, 2004, pp. 191-235.

Appendix

Publications

Gebreyohannes A. Y., R. Mazzei, E. Curcio, T. Poerio, E. Drioli and L. Giorno, "Study on the in Situ Enzymatic Self-Cleansing of Microfiltration Membrane for Valorization of Olive Mill Wastewater. *Ind. Eng. Chem. Res.*, **2013**, 52 (31), pp 10396–10405 **DOI:** 10.1021/ie400291w. (2013).

Gebreyohannes A. Y, M. R. Bilad, T.Verbiest, C.Courtin, E.Dorenze, L.Gioro, E.Curcio, I.F.J. Vankelecom. Nanoscale Tuning of Enzyme Localization for Enhanced Reactor Performance in a Novel Magnetic Responsive Biocatalytic Membrane Reactor. (Submitted to journal of membrane science).

Gebreyohannes A. Y., E. Curcio, T. Poerio, R. Mazzei, G. Di Profio, E. Drioli and L. Giorno, Novel use of Forward Osmosis for the treatment of vegetation wastewater: The case of Olive Mill Wastewater valorization (submitted to Journal of Water Research).

Gebreyohannes A. Y, C.Causserand, I.F.J. Vankelecom, L. Giorno, P. Aimar. Challenging the chemical stability of magnetic responsive hybrid membrane during cleaning (to be submitted to Journal of Membrane Science).

Gebreyohannes A. Y, L.Giorno, T. Verbiest, I.F.J. Vankelecom, P. Aimar. Hybrid magnetic responsive enzyme membrane reactor for tailoring physical immobilization of enzyme: an optimization study (under preparation).

Gebreyohannes A.Y., R. Mazzei and L. Giorno, Vegetation wastewater treatment/valorization and challenges, a review article (to be submitted to Journal of Food Chemistry).

Other publications

Hakimhashemi, M., **A. Y. Gebreyohannes,** H. Saveyn, P. Van derMeeren and A. Verliefde, "Combined effects of operational parameters on electro-ultrafiltration process characteristics." Journal of Membrane Science. 403–404(0)(2012): 227-235. DOI: 10.1016/j.memsci.2012.02.054

Honors and Awards

- "Excellent poster presentation" on participating to the 10th international congress on membrane and membrane processes (ICOM2014). Forward Osmosis for the treatment of Olive Mill Wastewater, the 10th international congress on membrane and membrane processes. July 20-25, 2014, Suzhuo, China.
- EMDJ fellowship for Multiple European Union Doctorate in Membrane Engineering, Erasmus Mundus Fellowship grant No FPA 2011-0014.

- Best membrane related thesis of the year 2010 organized by TNAV (Belgian water technology networks).
- Second best master thesis for the Arcelor Mittal Environmental prize.
- VLIR-IUOS scholarship (2008-2010).

Proceedings

- **Gebreyohannes** A.Y., C.Causserand, I.F.J. Vankelecom, L. Giorno, P. Aimar. Challenging the chemical stability of magnetic responsive hybrid membrane during cleaning, International workshop on Membrane Engineering - Joint event of the European programs EM^{3}E and EUDIME, Sept. 2-4, 2014, Montpelier, France.
- **Gebreyohannes** A.Y. , L. Giorno, T. Verbiest, I.F.J. Vankelecom, P. Aimar. Hybrid magnetic responsive enzyme membrane reactor for tailoring physical immobilization of enzyme: an optimization study,International workshop on Membrane Engineering - Joint event of the European programs EM^{3}E and EUDIME, Sept. 2-4, 2014, Montpelier, France.
- **Gebreyohannes A. Y**., E. Curcio, T. Poerio, R. Mazzei, G. Di Profio, E. Drioli and L. Giorno. Forward Osmosis for the treatment of Olive Mill Wastewater, the 10th international congress on membrane and membrane processes, July 20-25, 2014, Suzhuo, China.
- **Gebreyohannes A. Y,** M. R. Bilad, T. Verbiest, C. M. Courtin, E. Dornez, L. Giorno, E. Curcio and I. F. J. Vankelecom, Novel superparamagnetic bioreactors: gate way to enhanced physical localization of enzyme on membrane. The 10th international congress on membrane and membrane processes, July 20-25, 2014, Suzhuo, China.
- **Gebreyohannes A. Y**., E. Curcio, T. Poerio, R. Mazzei, G. Di Profio, E. Drioli and L. Giorno. Investigation of forward osmosis as less energy intensive alternative for concentrating Olive Mill Wastewater, ITM-CNR Seminar Days, December, 2013, Rende (CS), Italy.
- **A.Y. Gebreyohannes**, M. R. Bilad, T.Verbiest, C.Courtin, E.Dorenze, L.Giorno, E.Curcio, I.F.J. Vankelecom: A novel super-paramagnetic nano-supported enzymes for tailored confinement of enzymatic reactions: case studies forin-situ enzymatic cleaning for membrane fouling mitigation and biocatalytic membrane reactor, BMG-Indigo Workshop, Sep 2013, Leuven, Belguim.
- **Gebreyohannes A. Y**., R. Mazzei, E. Curcio, T. Poerio, E. Drioli and L. Giorno. Enzyme membrane reactor: A green tool for developing membranes with self-foul controlling potential for vegetation wastewater treatment. ICCMR11, July 2013, Porto, Portugal.
- **Gebreyohannes A. Y**., R. Mazzei, E. Curcio, T. Poerio, E. Drioli and L. Giorno. Biocataltic membrane reactor combined with Forward osmosis for controlling fouling during Olive Mill wsatewater valorization. Euromembrane 2012, London UK.
- **Gebreyohannes A. Y**., R. Mazzei, E. Curcio, T. Poerio, E. Drioli and L. Giorno. Combination of Pretreatment, Membrane Bioreactor and Forward Osmosis for a Less Fouled Valorization of Olive Mill Wastewater.CNR-ITM seminar days 2012, Rende (CS), Italy.

Oral presentation at international congress

International workshop on Membrane Engineering - Joint event of the European programs EM^{3}E and EUDIME, Sept. 2-4, 2014, Montpelier, France.

The 10th international congress on membrane and membrane processes, July 20-25, 2014, Suzhuo, China.

ITM-CNR Seminar Days, December, 2013, Rende (CS), Italy.

BMG-Indigo Workshop, Sep 2013, Leuven, Belguim.

Euromembrane 2012, Sep 20-26, 2012, London UK.

ITM - CNR seminar days, September 2012, Rende (CS), Italy.

Poster presentation at international congress

International workshop on Membrane Engineering - Joint event of the European programs EM^{3}E and EUDIME, Sept. 2-4, 2014, Montpelier, France.

The 10th international congress on membrane and membrane processes, July 20-25, 2014, Suzhuo, China.

11th International conference on Catalysis and Membrane Reactors, ICCMR11, July 7-11, 2013, Porto, Portugal.

Education and training

Course title	**ECTS**	**Place of attendance**
Introduction to membrane technology	1	ITM-CNR, Italy
Polymeric membrane preparation and characterization (by H. Strathman)	2	ITM-CNR, Italy
EMS summer school	2	Nancy, France
Experimental Design	4	KU Leuven, Belgium
Chemical fundamentals of Membrane Operations (by E. Drioli)	6	UNICAL-Italy